THE INFLUENCE OF NATIVE WHEAT LIPIDS ON THE RHEOLOGICAL PROPERTIES AND MICROSTRUCTURE OF DOUGH AND BREAD

by

SHERRILL LYNE CROPPER

B.S., The Ohio State University, 2006
M.S., The Ohio State University, 2008

AN ABSTRACT OF A DISSERTATION

submitted in partial fulfillment of the requirements for the degree

DOCTOR OF PHILOSOPHY

Department of Grain Science and Industry
College of Agriculture

KANSAS STATE UNIVERSITY
Manhattan, Kansas

2015

Abstract

Bread quality and final crumb grain are reflective of the ability for wheat flour dough to retain and stabilize gas cells during the baking process. The visco-elastic properties of dough allow for the incorporation of air cells and expansion during fermentation and baking. The gluten-starch matrix provides the backbone support. However, following the end of proofing and during the beginning of baking, the structure weakens due to over-extension and expansion and the matrix begins to separate and eventually break down. Native wheat lipids, which are found in small quantities in wheat flour, provide a secondary support for gas cell stabilization because of their amphiphilic characteristics and ability to move to the interface and form condensed monolayers. The objectives of this research were to evaluate the influence of native wheat lipids on the rheological properties of dough and the microstructure of bread.

Native wheat lipids were extracted from straight-grade flour and separated into total, free, bound, nonpolar, glycolipids, and phospholipids using solid-phase extraction (SPE) with polar and nonpolar solvents. Defatted flour was reconstituted using each lipid fraction at a range of levels between 0.2% and 2.8%. Dough and bread were made following AACC Method 10-10.03. Rheological testing of the dough and evaluation of the microstructure of the bread was conducted using small and large deformation testing, C-Cell imaging, and x-ray microtomography analysis to determine changes in visco-elastic properties and gas cell structure and distribution.

Rheological assessment through small amplitude oscillatory measurements demonstrated that nonpolar, phospholipids, and glycolipid fractions had a greater interaction with both proteins and starch in the matrix, creating weaker dough. Nonpolar, phospholipids, and glycolipids, varied in their ability to stabilize gas cells as determined by strain hardening index. C-Cell imaging and x-ray microtomograpy testing found that treatments containing higher concentrations of polar lipids (glycolipids and phospholipids) had a greater effect on overall loaf volume, cell size, and distribution. This illustrates that level and type of native wheat lipids influence the visco-elastic properties of dough and gas cell size, distribution, cell wall thickness, and cell stability in bread.

THE INFLUENCE OF NATIVE WHEAT LIPIDS ON THE RHEOLOGICAL PROPERTIES AND MICROSTRUCTURE OF DOUGH AND BREAD

by

SHERRILL LYNE CROPPER

B.S., The Ohio State University, 2006
M.S., The Ohio State University, 2008

A DISSERTATION

submitted in partial fulfillment of the requirements for the degree

DOCTOR OF PHILOSOPHY

Department of Grain Science and Industry
College of Agriculture

KANSAS STATE UNIVERSITY
Manhattan, Kansas

2015

Approved by:

Co-Major Professor
Jon Faubion

Approved by:

Co-Major Professor
Hulya Dogan

Copyright

Abstract

Bread quality and final crumb grain are reflective of the ability for wheat flour dough to retain and stabilize gas cells during the baking process. The visco-elastic properties of dough allow for the incorporation of air cells and expansion during fermentation and baking. The gluten-starch matrix provides the backbone support. However, following the end of proofing and during the beginning of baking, the structure weakens due to over-extension and expansion and the matrix begins to separate and eventually break down. Native wheat lipids, which are found in small quantities in wheat flour, provide a secondary support for gas cell stabilization because of their amphiphilic characteristics and ability to move to the interface and form condensed monolayers. The objectives of this research were to evaluate the influence of native wheat lipids on the rheological properties of dough and the microstructure of bread.

Native wheat lipids were extracted from straight-grade flour and separated into total, free, bound, nonpolar, glycolipids, and phospholipids using solid-phase extraction (SPE) with polar and nonpolar solvents. Defatted flour was reconstituted using each lipid fraction at a range of levels between 0.2% and 2.8%. Dough and bread were made following AACC Method 10-10.03. Rheological testing of the dough and evaluation of the microstructure of the bread was conducted using small and large deformation testing, C-Cell imaging, and x-ray microtomography analysis to determine changes in visco-elastic properties and gas cell structure and distribution.

Rheological assessment through small amplitude oscillatory measurements demonstrated that nonpolar, phospholipids, and glycolipid fractions had a greater interaction with both proteins and starch in the matrix, creating weaker dough. Nonpolar, phospholipids, and glycolipids, varied in their ability to stabilize gas cells as determined by strain hardening index. C-Cell imaging and x-ray microtomograpy testing found that treatments containing higher concentrations of polar lipids (glycolipids and phospholipids) had a greater effect on overall loaf volume, cell size, and distribution. This illustrates that level and type of native wheat lipids influence the visco-elastic properties of dough and gas cell size, distribution, cell wall thickness, and cell stability in bread.

Table of Contents

List of Figures

List of Tables

Acknowledgements

The author would like to acknowledge and thank Abigail Lape, Carrie Lendon, and Cargill's Global Foods Research group for allowing the usage of their X-ray Microtomograph and for their time, guidance, and advice with the technique, methodology development, and interpretation of the results.

Also, the author would like to thank Mary Roth at the Kansas State University Lipidomics Research Center for her assistance, guidance, and expertise in sample preparation and lipid profiling for this dissertation research.

Special thanks goes to Dr. Greg Aldrich, Dr. Cassie Jones, and Dr. Yong Cheng Shi for the allowed use of their labs and equipment.

Much gratitude goes to Chao-Feng Hsieh for kindly running starch damage analysis on the tested flour samples.

To my advisors, Dr. Jon Faubion and Dr. Hulya Dogan for their countless hours of leadership and guidance, for always taking the time to discuss with me about any topic, and for their endless support throughout this entire process.

Much appreciation goes to Dr. Becky Miller for her assistance with the research, use of her equipment, and advice.

Much gratitude goes to Dr. Kelly Getty for always sharing words of encouragement and support.

A special thanks goes to Dr. Sean Finnie for coming to the aid and rescue with providing endless advice on life, wheat lipid extractions, and technique assistance.

Much appreciation goes to Dr. Chris Miller for assistance with extraction techniques and knowledge on chemical analysis as well as any other help needed.

To Dave Krishock, for always being there to help and assist on anything and everything, for being an endless support and sounding board and for giving me the respect and opportunity to work and teach along side him. Not to forget, the chance to make donuts.

Many thanks goes to Michael Moore for always assisting with any of my research needs via equipment or water, for being a kind ear, and for all the encouragement.

Much appreciation goes to my lab mates, Gabriela Rattin, Andrew Mense, and Reona Oshikiri, for the countless hours of laughter, conversation, and support. My success was only as great as my team.

To Audrey Girard and my Emily's (Emily Jackson and Emily Elliot), for the countless hours of conversation, laughter, research, and Baking Science Lab fun; you truly made my experience a lot brighter.

Much gratitude goes to all the bakery and milling science students, for allowing me the opportunity to teach, mentor, and for making me apart of the Grain Science and Industry family.

Special thanks goes to my OSU family, Dr. Jim Harper and Dr. Nurdan Kocaoglu-Vurma, for seeing potential in me and for the continued support and to Angela Eliardi, Thais de Nardo, and Ruth Luther, for being the three best friends a person could ever ask for.

Much appreciation goes to Anne Rigdon-Huss, Lauren Brewer, Sarah Gutkowski, Carlos and Keyla-Lopez Campabadal, Adrian Martinez-Kawas, and Kyle Probst for all the meals, the laughter, and all the memories.

Many thanks and appreciation to Deanna Scheff, Orelia Dann, Jennifer and Levi Fredrick, Sara Menard, and Cara Dennis for being great friends and support system.

And to my parents, Becky and Harold, brother, Scott, sister-in-law, Carrie, and niece, Clara, for being the foundation for everything that I am and for never faltering in their love, support, and allowing me to go and accomplish my dreams. For that, I am indebted.

Dedication

This dissertation is dedicated to all the dreamers who have undertaken the course to find their own personal greatness and to all those who have been a guiding light on my path to help me achieve my unthinkable.

Chapter 1 - Literature Review

Throughout history, bakery products have been a major part of the diet with much of the popularity being due to their nutritional value and the variety of goods found on the market. Bread was first discovered by the ancient Egyptians and today, it still remains as a widely consumed product that provides energy as well as other essential nutrients (Jacob 1944). In 2009, 194.5 pounds of flour and cereal based foods were consumed per capita with 135 pounds coming from wheat-based goods (U.S. census 2009). During 2012, total U.S. bread sales reached a high of $6260 million dollars and provided 633,000 jobs (American Bakers Association 2010; AIB International 2012). Through scientific advances, research has helped to improve quality and increase shelf-life by providing a better understanding of bread ingredients, dough composition, and final product quality.

1.1 Bread

Bread is defined as "a yeast-leavened dough made from flour or treated flour that is hydrated by the addition of water, milk, eggs, and is leavened by yeast or a yeast by-product" (21CFR136.10). White pan bread can be made from a variety of different cereal grains, however, wheat is preferred as it contains storage proteins that form a continuous gluten network that traps air cells and affects loaf volume (Cauvain 1998). The dough, which is created by the addition of water and mixing, exhibits visco-elastic characteristics. Those extensible and elastic properties allow for easier dough handling and processing (Cauvain 1998). The visco-elastic characteristics of dough promote the incorporation and expansion of air/gas cells into the dough matrix. This influences the expansion of the dough during fermentation and proofing, ultimately affecting the final loaf volume and crumb.

1.1.1. The bread-making process

Mixing serves two principle purposes in breading-making: to form and develop the gluten network and to evenly incorporate and disperse the ingredients throughout the system (Serna-Saldivar 2010). Mixing determines initial size, amount, and distribution of air cells within the dough (Primo-Martin et al 2006). The mixing stage is the main determinant of initial air cell size and viscosity and this is based on the amount of energy applied and the type of mixer being used

(Salt et al 2006). Because of this, the addition of more pressure during mixing ultimately causes an increase in the number of air cells that are integrated into the dough (Mills et al 2003). The increase in air cells in the bread causes a drop in dough density at optimum mixing and "half of the total amount of air possible has been incorporated" (Hoseney 1985).

Water is required for the formation of the dough and the amount is critical for creating optimum dough. The hydration of the gluten proteins results in the morphology of the polymers (Delcour and Hoseney 2010). Water causes these proteins to undergo a glass transition at room temperature, allowing for the conversion of proteins into a rubbery state (Delcour and Hoseney 2010). For this state change to occur, the right environmental temperature and plasticizer (water) concentration is required (Delcour and Hoseney 2010). Dough that is mixed to optimum must have fully hydrated protein and starch. When properly hydrated, this is considered to be at the point where it can produce the best loaf of bread (Hoseney 1985). The addition of too much water results in longer mixing times as there is more water available for absorption and oversaturation of the flour (Stear 1990). Insufficient water reduces the ability for certain fractions of the flour particles to hydrate (Stear 1990; Delcour and Hoseney 2010). Temperature affects dough development and initial ingredient temperatures, mixing, friction, and solubilizing of the molecules all create heat during dough formation (Stear 1990). Temperatures >30°C can increase the ability to hydrate inducing starch granule swelling and causing changes in the physical properties of the dough (Stear 1990). Overall, optimal dough development is influenced by the required mixing time, water absorption, and temperature (Serna-Saldivar 2010).

During the final stages of mixing, gluten proteins unfold due to the shear applied by the mixing pins and bowl (Stear 1990). This facilitates hydrogen and hydrophobic bonding while breaking internal disulfide bonds (Stear 1990; Delcour and Hoseney 2010). An optimal mixed dough can be divided into three different fractions: gluten structure in which starch granules and other compounds are dispersed, fractions that are water soluble and make up the liquid part of the dough, and air cells that were incorporated by mixing (Stear 1990). Once driven past the point of optimal mixing, the dough begins to lose its visco-elastic characteristics due to degradation of disulfide bonds and the connection of thiol groups with carbonyl groups that are present in the dough (Delcour and Hoseney 2010). Over mixing has shown to be influenced by oxidation as well as by the presence of the water-soluble components in the dough (Hoseney 1985).

Following mixing, dough goes through fermentation. This allows the dough to relax in order to develop a network that is able to retain the air cells and for the yeast to become active and start producing CO_2 gas (Belderok 2000). The dough is divided into balls of a predetermined weight and rounded. At this point, some of the gas created by the yeast is forced out of the dough (Belderok 2000). After fermentation, the dough rests for another 15-30 minutes (immediate proofing) and then moulded where it is sheeted and rounded into a cylinder fitted for the bread pan (Belderok 2000). The newly rounded cylinder is proofed one final time allowing for expansion in size to nearly 2X, before being baked (Belderok 2000).

Punching and moulding release some of the carbon dioxide created during fermentation by dividing the existing air cells, creating smaller cells (Serna-Saldivar 2010). During the proofing stage, the dough undergoes changes in height and volume as well as texture and density (Serna-Saldivar 2010). Required proofing time is influenced by flour protein content, time, and desired loaf height (Serna-Saldivar 2010). The last step is baking (200-250°C, 12-45 min) and during the beginning stages, a final increase in volume occurs and the crust sets (Belderok 2000; Serna-Saldivar 2010). The increase in dough volume is created by more active yeast producing CO_2 and the evaporation of water vapor, both resulting in expansion of the existing gas cells (Serna-Saldivar 2010). Also at this time, the starch gelatinizes (55-65°C), takes up most of the available water, and the gluten structure sets (Belderok 2000; Serna-Saldivar 2010). The gas cells continue to expand until the structure sets or until the cell wall begins to fail. At this point, the structure transforms from a foam to a continuous sponge (MacRitchie 2010). The crust also browns due to both chemical reactions of Maillard browning and caramelization (Serna-Salidvar 2010).

1.2 Bread-making components

The components that compose wheat flour provide the scaffolding and strength of the bread structure and are essential for maintaining air cells. Wheat is the only cereal grain that contains the specific gluten-forming proteins that allow for air cell incorporation while resisting coalescence, thus visco-elastic dough is a very important part of bread-making and production. Starch also plays a key part by serving as a filler in the protein matrix. Additionally, native and processed lipids are essential to maintain loaf volume and prevent gas cell coalescence during the

later stages of proofing and baking (Sroan et al 2009). Each component is needed to produce and maintain quality loaves of bread with good loaf volume and crumb grain.

1.2.1. Gluten

Gluten provides the basis, the structural backbone, and it is the gluten proteins specifically that "form the continuous viscoelastic network in the dough" (Singh and MacRitchie 2001). It also serves as the network for which air cells are dispersed and held. In bread-making flours, the gluten protein makes up 80-90% of the total protein (Schofield 1987). Gluten consists of two protein families, glutenins and gliadins, which vary in their composition, but combined in equal proportions, give both viscous and elastic properties to dough (Schofield 1987; Singh and MacRitchie 2001). Gliadins are single chained polypeptides and have very similar molecular weight distributions. The glutenins are created by polymerization of glutenin subunits at a range of molecular weights (Singh and MacRitchie 2001). Both proteins contain disulphide bonds, but the nature of the linkage is different with gliadin having intra-chain linkages, while glutenin has mostly inter-chain linkages (Schofield 1987).

Gliadins and glutenins are not soluble in water, but are plasticized by water. Due to having non-polar amino acid side chains, solvents such as aliphatic alcohol, dilute acids, soaps, or ionic detergents are used as extractants (Schofield 1987; Singh and MacRitchie 2001). The gluten structure is highly dependent on the extent of bonding interactions between the polymers, specifically hydrogen, hydrophobic, and electrostatic interactions (Hamer and Van Vliet 2000). The resulting viscous and elastic properties of dough are important for gas cell incorporation and dough handling properties, both which are essential in bread-making (Schofield 1987). For dough to be elastic, the system must remain strong or have "continuity." This is provided by the glutenin fraction, as it is likely to have more stable entanglements (Delcour and Hoseney 2010).

The mechanism of how gluten creates the dough is not completely understood, but several models exist. One of these theories, the "linear glutenin hypothesis," suggests that extending units of long chain peptides come together in a head-to-tail manner connected by disulphide bonds (Schofield 1987). These connected chain units are thought to be able to extend under an applied strain. Once that strain is removed, they then return to their original confirmation (Schofield 1987). These disulphide bond linked polypeptides contain regions of α-helix and β-turns and during mixing, these bonds are broken and become realigned,

strengthening the dough (Schofield 1987). Both components of the gluten protein have been found to be surface active where the gliadin fraction moves to the gas/liquid surface faster than does the glutenin, thus creating more pressure per area (Gan et al 1995; Primo-Martin et al 2006). Although, both components of gluten have minimal solubility in water, proteins, in general, are best suited for movement to the interface as they can widely spread across its surface allowing for strong interactions between the phases (Primo-Martin et al 2006).

Another model of how gluten functions in dough comes from polymer science and hypothesizes that long protein chains align at the gas liquid interface surface, with loops and tails that extend out into the other phases and then interact with other molecules (Singh and MacRitchie 2001). The glutenins would align at the interface and the extended loops and tails would become "entangled" with other compounds in the structure or form "bridges" with starch (Singh and MacRitchie 2001). The entanglements caused by glutenin would provide more elastic dough properties, due to greater interactions between the proteins, increasing the viscosity of the dough. The gliadin would create a more viscous, liquid like system (Singh and MacRitchie 2001). The nature of the entangled network is highly dependent on size, shape, makeup, and amount of the specific polymers (Hamer and Van Vliet 2000). The "loop and train" model is a third theory of the gluten network. It suggests that the protruding loop or train subunits attached to the main linear chain actually interact with one another through hydrogen bonding. Some of these units will either be bound to one another (called loops) or connected and called trains (Belton 1999). When the loops are extended the proteins are more susceptible to moving over one another, but then can revert back to the loop-train equilibrium, providing elastic behavior (Belton 1999).

1.2.2. Starch

Starch is also a very important component needed for the development of dough and the final bread. Found in the endosperm of the wheat kernel, starch makes up almost 70% of its' mass (Blanshard 1987). When milling wheat flour, the goal is to remove as much of the endosperm as possible while minimizing the amount of starch damage during the process. Starch can be found in granular form as either polygonal or spherical in shape (Delcour and Hoseney 2010). The molecular structure of the starch granules consists of long chains of glucose that are either linear or branched (amylose and amylopectin) (Zobel 1988). Each polymer group consists

of one reducing end (O-H group) with the linear chain of both amylose and amylopectin containing α-1-4 chain linkage (Delcour and Hoseney 2010). However, amylopectin differs from amylose in that it is also branched at some α-1-6 bonds creating a complex branched structure (Delcour and Hoseney 2010). Amylose is thought to exist in the amorphous region of the granule versus amylopectin located in the crystalline regions (BeMiller 2007).

Native starch doesn't swell when mixed with cold water and depending on the starch origin, it undergoes gelatinization or "irreversible swelling" when heated in water to a specific temperature (Schoch 1965). Once the temperature has exceeded the temperature at which starch gelatinizes, the granule swells and takes up water (BeMiller 2007). The water and heat alters the crystalline morphology. The hydrogen bonds between the polymers begin to break and more and more water is absorbed into the swelled structure eventually disrupting the crystalline regions (BeMiller 2007). This change in the granular order of the polymers due to water and heat is described as a "loss of birefringence" and causes irreversible swelling of the granules and the leaching out of amylose (BeMiller 2007). Together, these changes increase the viscosity of starch-water solutions (Primo-Martin et al 2007). External factors that can alter the rate or temperature at which gelatinization occur include salt, pH, sugar and the ratio of water to starch (BeMiller 2007).

Starch interacts with sugar, lipids, proteins, pentosans, and water during the bread-making process, and this is very important for the development of dough (Blanshard 1987). Starch plays a role in the overall bread quality as it affects final product characteristics such as "structure and texture of the final product" (Primo-Martin et al 2007). The changes in texture and structure are heavily influenced by the starch going through the above described transitions (Blanshard 1987). It is suggested that starch acts as "high loading filler" in the dough system (Singh and MacRitchie 2001; Delcour and Hoseney 2010). The functions of starch in bread-making include diluting the amount of gluten so as to adjust the dough consistency, providing fermentable carbohydrates for yeast through the action of amylase, attaching and forming a bond with gluten and increasing the system's elasticity and extensibility during gelatinization in order to allow for flexibility in the gas/air cell film (Hoseney et al 1971). In the crumb, starch creates regions that are amorphous after gelatinization, but as the bread cools and ages it becomes crystalline or retrogrades (Primo-Martin et al 2007).

1.2.3. Lipids

The wheat kernel is composed of approximately 2-4% total lipids that are found within the bran, germ, and endosperm (Pomeranz 1973). Most of the lipids are located in the germ, a fraction (8-15%) of the kernel that is removed during the milling process, followed by the bran and endosperm containing 6% and 8%, respectively (Pomeranz 1973). The germ contains approximately 80% of the total lipids with higher levels of free fatty acids, which are more sensitive to lipid oxidation and promote rancidity (Serna-Saldivar 2010). The total lipid fraction consists of primarily linoleic acid (Carr et al 1992). It makes up roughly 60% of the total lipid fraction and the wheat flour contains roughly 2.5% of total lipids (Carr et al 1992: Eliasson and Larsson 1993). During milling, triglycerides remain in the endosperm and can either be saturated or unsaturated (Sullivan 1940; Carr et al 1992).

In general, the function of lipids in bread-making helps improve textural properties, mouth-feel, dough handling, loaf volume, and increase shelf life (Ponte and Baldwin 1972). Lipids come from both, natural or native lipids in the endosperm and from processed shortenings or liquid oils that are added during production. The lipids in the system act to help stabilize the air cells and prevent coalescence during the growth and expansion of the dough (Chung et al 1978). Bread is considered to be foam and lipids act as "surfactants in stabilizing or destabilizing the foam structure during the expansion of the loaf," thus acting as support and providing more stability to the foam (MacRitchie 1977). The lipids are influential in helping to maintain gas cell stability and loaf volume over time; however, the addition of up to 3% shortening has been shown to help increase final loaf volume and improve crumb softness (Pomeranz 1965; Chung et al 1978).

1.2.4. Native wheat lipids

Although the amount of native lipids that are present in the flour is small, these constituents have a large effect on final bread quality. Lipids in the endosperm of the kernel consist of various fractions that are both functional and nonfunctional in the dough and bread-making processes. Lipids in wheat can be classified as either simple or complex, meaning that they have either one or two structural components (simple) or greater than two structural components (complex) (Chung et al 2009). Further classification of lipids can be done based on the type of extraction used and location within the flour (Chung et al 2009). For classification by

location, lipids can be separated into non-starch lipids, integral starch lipids, and starch surface lipids (Chung et al 2009). Figure 1.1. shows the classification of lipids found in wheat.

From an extraction standpoint, the lipids can be classified in two groups, non-starch lipids or total lipids, which include all the starch lipids and surface starch lipids (Finnie et al 2009). If the extraction process promotes the swelling of starch granules then these lipids fall under the category of total lipids because this includes those lipids that are tightly bound to the internal structure of the starch. However, if the technique doesn't induce granular swelling then the lipids are categorized as being non-starch lipids as these lipids are not linked to the structure of the starch (Finnie et al 2009). The amyloplast is where the development of lipids are thought to originate, particularly, the polar fractions (glycolipids and phospholipids) (Morrison 1988). Lipids that are found inside the starch have been shown to be beneficial against starch degradation as they are inhibitors of enzyme degradation by phosphorylase, α and β-amylase (Morrison 1988). The complexing of amylose with lipids has also shown to slow the rate that degradation occurs (Morrison 1988).

Classification by extraction also divides the non-starch lipids into "free" or "bound" fractions depending on the type of extraction solvent used (Finnie et al 2009). Free lipids are those lipids that can be separated using nonpolar solvents such as petroleum ether, hexane, and dimethyl ether, while the bound lipids are those that can be removed by using polar solvents such as chloroform, methanol, and water-saturated butanol (Hoseney et al 1969; Finnie et al 2009). The amount of free lipids extracted is dependent upon the technique used for the extraction, the temperature of the solvent, and the amount of moisture and particle size of the flour (Chung et al 1977a; Chung et al 1977b; Chung et al 2009). Both the free and starch lipids can further be classified as polar and nonpolar lipids and have the greatest impact on the quality of bread (Ohm and Chung 2002; Chung et al 2009). The removal of the lipids during extraction also has an effect on water absorption as it increases the amount of water needed by the dough (Chung et al 1980c).

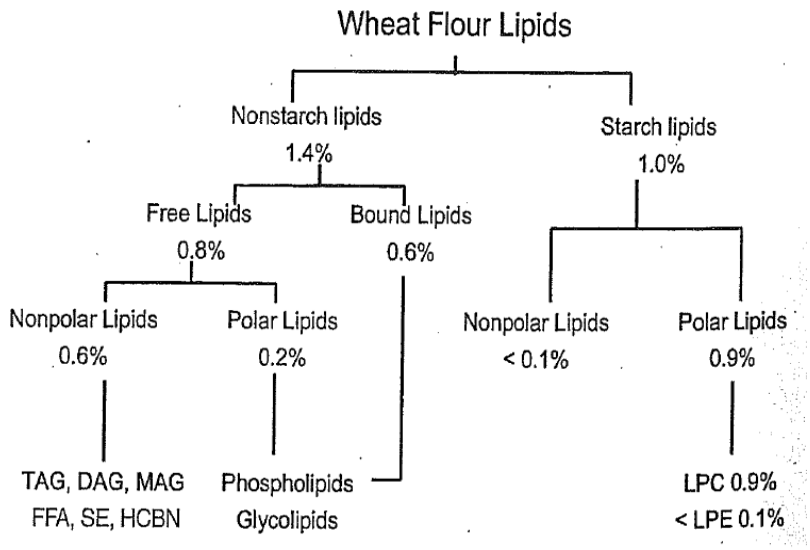

(Chung et al 2009)

Figure 1.1. Wheat lipid classes in flour

1.2.4.1 Free lipids

Free lipid composition consists of 0.8% free lipids of which 0.6% are nonpolar, while 0.2% are polar (Hoseney et al 1970). The nonpolar and polar lipids are defined by their ability to mix with water as some of these lipids have functional groups that are water miscible (Carlson et al 1978). Polar lipids are also more inclined to form "membrane-like" structures, whereas the nonpolar predominantly form drops that are similar to that of oil (Carlson et al 1978). The composition of polar lipids found in flour include: digalactosyldiglycerol (DGDG) monogalactosyldiglycerol (MGDG), N-acyl-phosphatidylethanolamine (NAPE), and phosphohatidylcholine (PC) (Pareyt et al 2011). The nonpolar lipid fraction, consist of triacylglycerols (TAG), diacylglycerols (DAG), monoacylgycerols (MAG), sterols, sterol esters and free fatty acids (Pomeranz 1973; Pareyt et al 2011). The polar lipids are a combination of glycolipids (galactolipids specifically) and phospholipids (Chung et al 1980a). Of the previously listed polar lipids, it is the MGDG and DGDG, which are found in the highest concentration and for the phospholipids, the PC and lysophosphatidylcholine (LPC) are the most common (Chung et al 1980a). Typically, phospholipids contain only one phosphorus group/mole, while the glycolipids contains 1-3 galactoses (Chung et al 1980a).

During the mixing stage, the free lipids become "bound" to other constituents in the dough, thus reducing the amount of extractable free lipids (Chung and Tsen 1975). This decrease

in free lipids is linked to the interaction of protein and lipids or starch and lipids. This causes a reduction of greater than 50% in the free lipids during dough mixing (Chung and Tsen 1975). Early studies of the influence of lipids on the loaf volume and crumb grain through the removal (defatting) and re-addition (reconstitution) of extracted total wheat lipids, found that they do play an important part in maintaining and strengthening the foam structure of the dough (MacRitchie and Gras 1973). The polar lipid fractions had the greatest effect on loaf volume; specifically, the glycolipids having a galactose group attached (Chung et al 1982). These differences can be seen in Figure 1.2. The galactolipids provide the greatest improvement in loaf volume as well as dough development time (Chung et al 1982). However, reduced amounts of polar lipids caused a decrease in loaf volume due to a greater association of protein-protein interactions thereby influencing the air cell distribution and expansion (Chung et al 1980c). The nonpolar lipids have a lower melting point than do the polar lipids and their crystalline state plays a role in maintaining air cell structure as phospholipids are most beneficial when they are in a "liquid-crystalline" form (Pomeranz 1965; Leissner 1988). This phenomenon (improved loaf volume) was seen when polar lipids were added alone and when a combination of nonpolar/polar lipids fractions where added back together (Chung et al 1982).

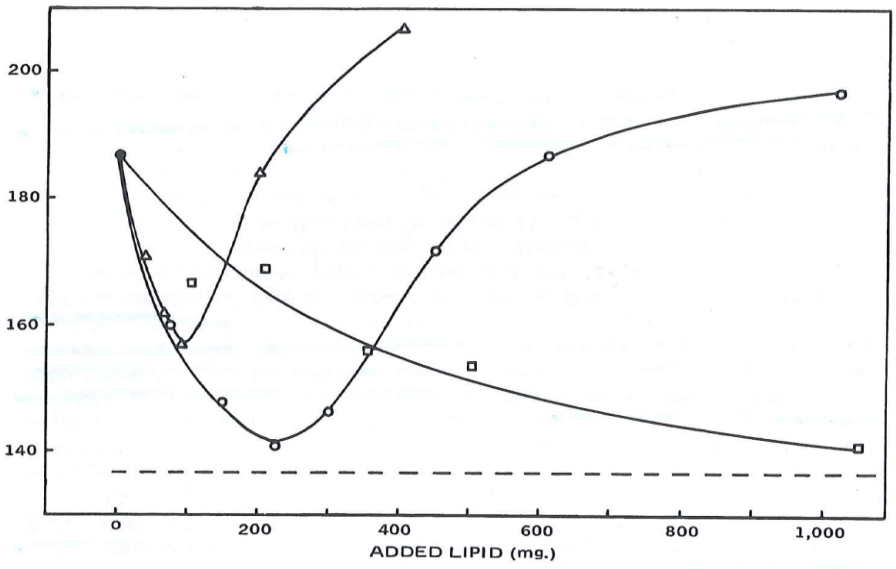

Fig. 3. Effects on loaf volume of additions of polar and nonpolar lipid fractions to defatted flour B. Circles, whole lipid; triangles, polar lipid; squares, nonpolar lipid; dashed line, volume at end of proofing stage.

(MacRitchie and Gras 1973)

Figure 1.2. Loaf volume distribution at varying lipid additions

Extraction studies determined that the glycolipids bind with both gliadin and glutenin through hydrophobic and hydrophilic interactions (Hoseney et al 1970). The glycolipids interact with gliadin by hydrophilic bonding and to glutenin through hydrophobic bonding (Hoseney et al 1970). Due to gliadin playing a bigger role influencing loaf volume, the interactions between the glycolipids and these proteins are more predominant in maintaining structural integrity of the dough (Hoseney et al 1970). From a molecular viewpoint, glutenin has a greater availability of nonpolar side chains that can attach to the lipids (Pomeranz 1973). This allows for more association of lipids with the proteins because of the hydrophobic side chains (Pomeranz 1973). These interactions between lipids and proteins are not limited to hydrophobic bonding, but also include ionic, covalent, hydrogen, and Van der Waals bonding (Pomeranz 1973). During the beginning phase of the mixing process, most of the free lipids become bound and additional mixing time does not influence the amount of lipids that became bound (Chung and Tsen 1975).

The nonpolar components of free lipids are detrimental to loaf volume when they are added back independent of polar lipids or even shortening (Daftary et al 1968). Adding individual subfractions of nonpolar lipids (steryl esters, triglycerides, diglycerides, and fatty acids) back did not improve loaf volume (De Stefanis and Ponte 1976). Loaves made with individual nonpolar fractions were similar to those in which total amounts of nonpolar lipids were added back (De Stefanis and Ponte 1976). Increasing the amount of nonpolar lipids, while maintaining the polar lipid amount constant caused decreases in loaf volumes even with polar lipids present (Daftary et al 1968). However, adding more polar lipids along with increasing amounts of nonpolar lipids reversed the negative effects of the nonpolar lipids (Daftary et al 1968). The addition of free fatty acids decreased the loaf volume even more than did the other nonpolar fraction (De Stefanis and Ponte 1976). Particularly it was linoleic acid, which was the unsaturated fatty acid that had the greatest detrimental effect on loaf volume. De Stefanis and Ponte (1976) hypothesized that the influence of linoleic acid on loaf volume was due to their negative effects on both the gluten fractions and starch.

1.2.4.2. Bound lipids

The non-starch lipids classification also includes 0.6% bound lipids that are made up of primarily polar lipids (Hoseney et al 1970). These groups of bound lipids are those non-starch lipids that are not “free, ” but connected to compounds other than starch (Chung et al 2009).

Following the extraction of the free lipids, non-starch lipids (not associated with starch granules) can be extracted with polar solvents (e.g. water saturated butanol) without requiring heating (MacRitchie and Gras 1973; Chung et al 2009). Starch lipids and starch surface lipids vary among the wheat varieties as lipid content is dependent on the "size and type of starch granule" present (Chung et al 2009). These differences are seen with the variations between A and B starch granule types as well as with fine, course, and intermediate shaped starch granules (Chung et al 2009). Starch lipids also vary in soft versus hard wheat (Finnie et al 2009). Bound polar lipids aren't as effective in maintaining and improving loaf volume as are the free polar lipids (Daftary et al 1968; Hoseney et al 1970).

1.2.4.3. Starch surface lipids

Starch surface lipids are bound lipids attached to the surface of the granule. These lipids are also strongly bound to gluten proteins and are a factor in distinguishing between flours from hard and soft wheat (Chung et al 2009). Typically, starch surface lipids are found in higher concentrations in soft wheat starches (Chung et al 2009). The surface components of the starch influence the rheological properties of the dough, particularly at the lamellar liquid-crystalline phase (Larsson et al 1997). Glycolipids are found in higher concentrations than other lipids on the surface of the starch and the main compounds are DGDG, MGDG, PC, and lysophosphotidylcholine (LPC) (Finnie et al 2009; Finnie et al 2010). During mixing, polar lipids are removed from the surface of starch and incorporated into the gluten matrix (Finnie et al 2010).

1.2.4.4. Starch lipids

Starch lipids are those lipids that are found inside the granules. The abundance of these lipids are often directly and positively correlated to the amount of amylose in the starch (Morrision 1988). Internal starch lipids can only be extracted by solvents (water saturated butanol) that are heated to 95-100°C, which induces starch gelatinization (Morrision 1988). The most common lipid classes here are the phospholipids with LPC and PC being the most prevalent (Galliard and Bowler 1987; Finnie et al 2010). Lipids within starch are often associated with the forming of amylose-lipid complexes (Delcour and Hoseney 2010). This occurs naturally in the starch granule or with unbound free lipids following the initiation of pasting or gelatinization of the starch (Delcour and Hoseney 2010).

The amylose-lipid complex is susceptible to leaching following hydration and heating of starch as it undergoes gelatinization (Morrison 1988). The presence of polar and nonpolar lipids during the gelatinization process influences the pasting properties of the starch during heating (Medcalf et al 1968). The readdition of polar lipids to defatted starch reduced the viscosity during pasting, while the addition of the nonpolar lipids reduced the paste viscosity initially, but resulted in higher peak pasting values than the defatted control (Medcalf et al 1968). The initial reduction in the pasting curve due to the presence of polar lipids was thought to be due to the binding of these lipids with starch, thus reducing the initial hydration of the starch granules (Medcalf et al 1968). Because the water is easily absorbed into the starch granule and nonpolar lipids are less likely to bind with components in starch, the nonpolar lipids cause an increase in the viscosity (Medcalf et al 1968).

1.2.4.5. Lipid interactions

Lipid-glutenin complexes that form during dough making have the greatest effect on mixing tolerance and mixing time especially in the presence of high levels of polar lipids (Chung et al 1980a). Interaction between lipids, proteins, and starch are affected by their polarities (Chung and Tsen 1975). The protein-protein interactions that form following the defatting process change during the reconstitution process as the addition of the lipids cause the intermingling of the polar fractions between the protein-protein bonds (Chung et al 1979). Defatting and reconstitution studies with protein showed that the addition of total lipid as opposed to nonpolar and polar fractions independently had greater interaction with protein, which suggests that the combination of both fractions together had a greater association with the protein (Chung et al 1979).

The increase in lipid-protein binding is influenced by the amount of work or mixing applied to the dough, as a more severe mixing action causes an increase in bound lipids (Daniels et al 1966). However, over-mixing causes a reduction in lipid binding (Pomeranz 1973). Marion et al (1987) also suggested that lipids, specifically phospholipids that bind during mixing, are not actually bound to the gluten phase, but rather these lipids are mixed in and are "physically embedded" in the gluten. The binding is associated with the friabilin or puroindolines, specifically PIN-A, one of the proteins associated with endosperm softness, which is a strong interaction with polar lipids (Dubreil et al 1997; Finnie et al 2010).

1.2.5. Shortening

The addition of shortening to the bread formula improves dough handling characteristics during production, enhances the ease of slicing, loaf volume, texture, crumb structure, and increases the shelf-life (Chung et al 1981). When shortening was added to defatted flour, there were both a positive and negative effect depending on the type of native lipid fractions remaining in the flour (Chung et al 1980c). Polar or total lipids must be present in order for shortening's beneficial effects to be seen in a good quality bread flour (Chung et al 1980b; Chung et al 1980c). On the other hand, dough made from a flour of lower quality or lower protein content, shortening improves overall volume (Chung et al 1980b). In control flours (non-defatted), the addition of up to 3% shortening has shown to increase the overall loaf volume (Chung et al 1980c). As the amount of total lipids were lowered, slight volume increases result from the addition of shortening (Chung et al 1980c). However, shortening only caused a minimal increase in loaf volumes as the greater quantity of total lipids were removed (Chung et al 1980c).

Shortening is functional only up to a specific threshold when a certain amount of total lipids are removed. If nonpolar lipids are only added then there are no benefits from adding shortening (Chung et al 1980c). The polar lipid fraction works synergistically with shortening to help stabilize and maintain the foam structure and bubbles in the dough (Chung et al 1980b). Only small additions of polar lipids are needed in combination with shortening to increase or restore loaves to their original heights (Pomeranz et al 1968). It has been suggested that the addition of shortening in the absence of polar lipids may prevent protein-protein interactions and rather act as blocking agents for these type of interactions (Chung et al 1980b). During the bread production process, shortening promotes continued gas cell expansion at higher temperatures, thus allowing for a longer period of dough extensibility (Junge and Hoseney 1981).

1.2.6. Air cells

The internal crumb structure and loaf volume are highly dependent on the amount of gas cells incorporated into the dough system (Junge et al 1981). Fine grain is associated with many small cells incorporated during mixing (Junge et al 1981). Loaf volume, defined by the dough expansion capacity, is dependent on the air cell network and dough's rheological characteristics following mixing (Gandikota and MacRitchie 2005; Sroan et al 2009). Expansion capacity is described as the maximum amount of growth the air cells can undergo without failing and when

this point is reached the loaf volume stops rising (Sroan et al 2009). This final growth is completed during the end of proofing in doughs made from flours with smaller loaf volume potential and at the start of baking for flours that have large loaf volume potential (Sroan et al 2009). The increase in air cell size, biaxial expansion, and the internal pressure causes a resulting strain on the dough (Sroan et al 2009).

Carbon dioxide produced by the yeast is not capable of creating the cells needed for the crumb. Instead, this happens during the later stages of mixing when the gas cells are incorporated and subdivided to create the bread crumb (Baker and Mize 1941). The rate that air cells are incorporated during mixing is greatest as the dough approaches optimal development (Baker and Mize 1946). Expansion of the dough does not occur until the dough has been fully saturated with gas formed by yeast fermentation. This process is regulated by the temperature and pH of the dough (Delcour and Hoseney 2010). The gas diffuses into the air cells and remains within the aqueous phase due to over saturation of the system caused by the fermentation process (Hoseney 1984). The greater rate in gas production causes an increase in the speed of cell expansion (Hoseney 1984). In order for cells to nucleate (or to be lost) from the system, the internal pressure of the cells must be higher than the surface tension and the viscosity of the dough (Gan et al 1990). The pressure that is created within the newly formed air cell is a result of the radius and the interfacial tension of that particular cell (Hoseney 1984).

For foams, there is little to no effect of surface tension on the incorporation of air cells during mixing (Salt et al 2006). In foam systems, the energy input throughout mixing affects the size distribution of the incorporated bubbles and the resulting rheology (Mills et al 2003). The means to hold and maintain gas cells within a foam system has been described by the formation of a gel-like layer that can support the lamellar phase, which consists of proteins or other surface active groups that provide dough elastic properties (Mills et al 2003). Another mechanism is described best by the Gibbs-Marangoni process in which stabilization comes from surface active constituents such as surfactants or emulsifiers (Mills et al 2003). These surface active components can move from a higher concentration to a lower concentration when the lamellae has broken down. This restores the differences in the lamellar regions that have weakened (Mills et al 2003).

The punching and moulding steps also add no new air cells to the dough. These steps instead increase the number of cells in the dough by dividing and splitting existing cells into

smaller, dispersed bubbles (Baker and Mize 1941; Gan et al 1995). The growth in volume is caused by size expansion of each gas cell and not by the incorporation of more cells (MacRitchie 1977). In some cases, the cells will expand so much that separation is only by a small film layer (Primo-Martin et al 2006). Gas cells are maintained within the dough matrix through the presence of compounds with functional groups that allow them to move to the cell interface (Primo-Martin et al 2006). This phenomenon occurs because these compounds can lessen the potential for air cells to come together, coalesce, or undergo Ostwald ripening, thus stabilizing the cells in the system (Primo-Martin et al 2006). Carbon dioxide produced during fermentation and proofing move into the air cells that were incorporated during mixing. The air cells expand and grow causing internal pressure that inflates the incorporated air bubbles creating a system where the gas can be roughly 75% of the overall volume (Gan et al 1995: Salt et al 2006). During this expansion, cell walls may stretch causing them to be pushed together to a point where the thin wall fails and two gas cells become one (Salt et al 2006).

1.2.7. Aqueous phase of dough

Water influences dough formation as it is needed for the hydration and solubilization of flour as well as for chemical and physical reactions to occur. The addition of varying levels of water can cause the formation of two liquid phases within the dough if the appropriate amount of water is present (MacRitchie 1976a). If there is not enough water then only one liquid phase is created. One of the phases is the liquid phase and this is where chemical and physical changes occur within the dough by fermentation. It also allows for the expansion of air cells during the rest of the baking process (MacRitchie 1976a). It is this phase where the air cells are incorporated and expansion happens due to fermentation (Sahi 1994; Primo-Martin et al 2006). Sahi (1994) described the development of this aqueous phase as when "there is a surplus of water above what is needed to hydrate the dry components (i.e. protein, pentosans, starch, etc) during mixing." At least 35% of the total dough weight of water is required for hydration of the proteins to allow for entrapping air and gas expansion during fermentation within this phase (Gan et al 1995).

Mixing determines the distribution of the ingredients and flavor constituents within this liquid phase (MacRitchie 1976a). MacRitchie (1976a) described the structure and composition of the liquid phase, which is continuous in the dough, as being based on the "equilibrium between

the solutes present in the liquid phase and corresponding solid phase." The make-up of this liquid phase or liquor is comprised of a combination of components including non-starch polysaccharides, lipids and proteins as well as malto-oligosaccharides, and arbinoxylans (Salt et al 2006). The combination of these varying constituents in the liquid phase helps to promote stabilization of air cells and provides much of the dough structure allowing for the growth of the dough during fermentation, proofing, and baking.

1.2.8. Aqueous phase formed by lipids and water

The interaction of polar and nonpolar lipids with water plays an important role in understanding lipid functionality within a complex system such as dough. In this type of a system, polar lipids will more readily bind with water while nonpolar lipids will not (Carlson et al 1978). Looking at the internal phase behavior of wheat lipid-water interactions using x-ray diffraction, Carlson et al (1978) observed the phase behavior of this system and illustrated it using a ternary diagram (Figure 1.3). Both the nonpolar and polar lipid fractions make up the corners of the triangle. For this model, sufficient amounts of water must be present in order to hydrate the lipids and the ratio of nonpolar to polar lipids influence changes in crystalline phase behavior. Several different phases are seen including both an oil phase and a water phase that contained no polar lipids and two phases that consisted of a combination of lipids and water. The lipids + water combinations formed are described as an L2-phase and a liquid-crystalline phase. Depending on the water concentrations when added back with total extractable lipids (containing both polar and nonpolar), an oil phase formed on top and at lower concentrations of water. Two distinctive liquid-crystalline formations were created: hexagonal-liquid crystalline and lamellar-liquid crystalline (Carlson et al 1978).

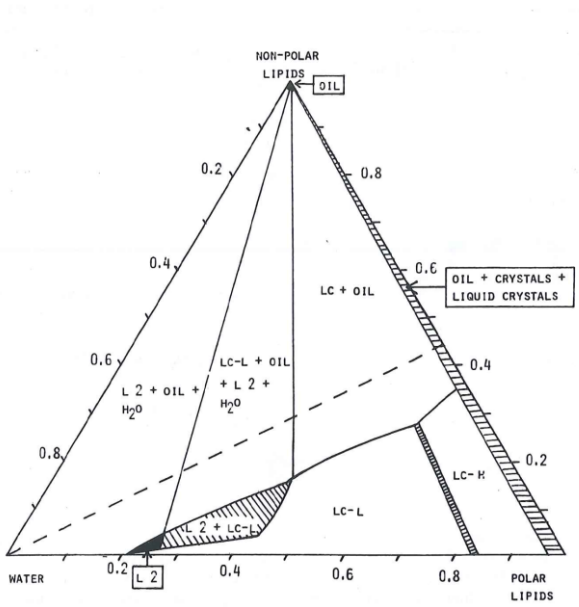

(Carlson et al 1978)

Figure 1.3. Ternary phase diagram of wheat lipids in water

The lamellar liquid crystalline phase is formed with varying compositions of lipids. However, increasing the quantity of water causes a conversion to an L2 phase. These phases (L2 and lamellar-liquid crystalline) are bilayers and the thicknesses of these complexes are dependent on the ratios of nonpolar and polar lipids (Carlson et al 1978). The greater the amount of polar lipids present in the layer causes a reduction in the thickness due to the ability to orient tightly. Nonpolar lipids, which are hydrophobic, must be oriented differently to avoid contact with water (Carlson et al 1978). Also, the varying types of polar lipids will cause or form different liquid-crystalline configurations, hexagonal liquid-crystalline or lamellar liquid-crystalline, with water (Carlson et al 1978). MGDG will form hexagonal configurations while phospholipids and DGDG form lamellar configurations (Carlson et al 1978). The L2 phase that is created by native wheat lipids is unique in that the oil layer is created only when extra water is available (Carlson et al 1978). This layer is made through the melting of the other two crystalline forms (hexagonal and lamellar) by the addition of heat (Carlson et al 1978). The formations of these crystalline phases influence dough rheological properties as the lamellar crystalline phase create “films at the interphase between starch/water, oil/water, and air/water” while the hexagonal phases create “aggregates” (Carlson et al 1978).

Carson et al (1979) studied the interaction and phase behavior of wheat lipids extracted from gluten and water. Similar to the wheat lipid-water ternary diagram determined by Carlson et al (1978), the gluten lipid-water combinations also produced four different phases: oil phase, water phase, L2 phase, and lipid-crystalline phase. Within the liquid-crystalline region, the solubility of the nonpolar lipids were directly correlated with the amount of water added, thus as water content increased, the more nonpolar lipids were dissolved into the system. Also, the addition of salt to the system caused a reduction in the amount of nonpolar lipids dissolved (Carslon et al 1979). The opposite was seen in the wheat lipid-water system for the nonpolar lipids as the water content increased, less nonpolar lipids were dissolved (Carlson et al 1978; Carlson et al 1979). The presence of salt in the gluten-lipid system caused a reduction in thickness of the lamellar liquid-crystalline phase (Carlson et al 1979). The liquid phase (L2) overall was smaller in the gluten-lipid system as compared to the wheat lipid system (Carlson et al 1979).

From the understanding of both of these complex systems (gluten-lipid-water and lipid-water), the lamellar liquid crystalline phase had the greastest effect on the baking characteristics. This was mainly due to surface active constituents that act at the air/water or oil/water interface (Carlson et al 1979). In dough systems, these lipids are able to move to the gas/liquid interface creating a "monolayer," where they expand and stretch, which reduces the overall interfacial tension and promotes the stabilization of the air cell (Gan et al 1995). The lamellar-liquid crystalline phase easily assembles in small groups (liposomes) at the interface following the mixing of water with the flour (Gan et al 1995). The lamellar liquid-crystalline formation, which has a configuration more like shortening or structured lipid, is able to diffuse between the phases easier than the hexagonal liquid-crystalline arrangement (Gan et al 1995). These layers of lipids that are compacted together move to the surface of the gas/liquid layer throughout all stages of the bread development, making it better suited for gas cell stabilization (Gan et al 1995).

1.2.9. Role of native wheat lipids in bread

Sahi (1994) found through electrical conductivity testing, that this film lining the phase of the gluten-starch matrix is a "continuous phase throughout the dough instead of being in discrete droplets." It was confirmed that there is an interface in which both protein and lipids are present and that more protein at the interface, provides more elastic behavior to the dough (Primo-Martin

et al 2006). Gan et al (1990) found, indirectly, that a "liquid film" layer that aligned the air cells and the gluten-starch matrix preventing gas loss or cell coalescences. This layer formed as an independent interface between the air cells and the liquid phase and contained components that were able to align at the interface due to their surface activity. A combination of proteins, lipids, pentosans, and other surface active compounds make up this film and they are able to move to that interface and give it stability over time (Gan et al 1990; Sahi 1994). During the later stages of proofing and baking when cell expansion is the greatest, the network begins to stretch then these surface active agents play the most functional role (Gan et al 1990; Gan et al 1995). Without this film, if breakdown or excessive stretching weakens the network, the gas cells would be more susceptible to migrating towards one another or becoming lost to the environment (Gan et al 1990). The breakdown or separation of the thin liquid film appears to be the cause of the loss of gas cells to the environment during the later stages of proofing (Gan et al 1995). The polar lipids have shown to be able to interact to form a lipid bilayer, which consist of the lamellar liquid-crystalline phase and thus can move to the interface surface creating what is known as a lipid monolayer (Gan et al 1995).

The proteins can stabilize at the air/liquid interface because of their visco-elastic properties and ability to maintain integrity through expansion and movement of air cells (Sahi 1994). Lipids, on the other hand, exhibit or act by a mechanism described as the Gibbs/Marangoni effect that is premised on the amount of lipids initially present (Primo-Martin et al 2006). This effect describes the shifting of the components in the film due to the pressure at the interface, moving them to or from areas where they come into contact with other dispersed droplets (MacRitchie 1976b). This mechanism that lipids use to stabilize the film has a greater surface tension than that produced by the fermentation of CO_2, which allows it to maintain and prevent coalescence of cells (Sahi 1994). The combination of protein and lipid films is the most effective in securing and maintaining gas cells within the network (Sahi 1994). The maintenance of this liquid monolayer is dependent on several factors including "film viscosity, shear resistance, and elasticity" of the dough (Gan et al 1995).

Originally, Gan et al (1990) based the theory of liquid lamellae from SEM images of gluten-starch matrix during the various phases of dough development (1990). Sroan et al (2009) reevaluated this hypothesis and determined that native lipids formed a film that stabilized the air cells and supported the gluten-starch matrix. Using two soft wheat varieties with protein contents

between 9% and 10%, native wheat lipids were extracted and reconstituted back into the flour. The resulting dough and bread were evaluated using C-Cell imaging and biaxial extensional rheology (Sroan et al 2009). The addition of different levels of native lipids produced similar results to those of MacRitchie and Gras (1973), which was a decrease than increase in volume upon lipid type and addition.

It was also found that when flour lipids were added back in varying concentrations, the number of gas cells and their elongation did not vary widely, thus concluding that it is the expansion of the cells rather than the number, which influences loaf volume (Sroan et al 2009). Biaxial extensional rheology testing showed that the addition of the total native wheat lipid in varying amounts to defatted flour did not have any effect on the dough visco-elastic properties even if there was a greater variation between loaf volumes (Sroan et al 2009). This indicated that native wheat lipids did have a stabilizing affect due to their ability to migrate to the interface and that was independent of dough rheology (Sroan et al 2009).

The type of lipid also affects the monolayer created at the interface. This is why the polar lipids are more functional than are the nonpolar lipids in terms of gas cell preservation (Sroan and MacRitchie 2009). The nonpolar lipids consisting of the fatty acids, are more inclined to form expanded monolayers upon the surface, which are more elastic in nature and do not release easily from the monolayer (Sroan and MacRitchie 2009). It is the benefit of the condensed monolayers that are formed by the polar lipids (DGDG) that provide "elastic restoring forces," which help to withstand changes in the liquid lamellae brought about by alterations to the interface caused by expansion or external forces on the dough (Sroan and MacRitchie 2009). The condensed monolayer is a compacted layer of surface active components with the polar groups facing outward towards the water and the nonpolar hydrocarbon groups are protected inside and face the air cells (Sroan and MacRitchie 2009).

Cell elongation helps to determine the durability of the gluten-starch matrix during the expansion of dough (Gandikota and MacRitchie 2005). "The greater elongation is associated with greater tolerance to distortion before rupture" (Gandikota and MacRitchie 2005). Sroan and MacRitchie (2009) saw minimal changes in elongation when the different total lipid concentrations were added, indicating that there was little to no influence on the rheological properties of the gluten-starch matrix by the addition of lipids. The addition of lipids also didn't cause any differences between the biaxial extensional rheology tests providing no evidence that

native wheat lipids affected the rheological properties of the gluten-starch matrix. These results only concluded that the lipids were surface active and form a compressed monolayer at the interface that holds air cells and prevents coalescence (Sroan and MacRitchie 2009).

1.2.10. Solvent extraction of lipids

Defatting and reconstitution studies of native lipids in flour typically are used to provide a better understanding of the native wheat lipids. Factors that influence the extraction of those lipids from flour include: genetic history and composition of the wheat being studied, the flour yield during the milling process, amount of moisture, flour particulate size, and extraction procedures (Chung et al 1982). For optimum extraction the parameters that need to be optimized are "time and temperature of extraction, type of extractor, and solvents used" (Chung et al 1982).

Separation of lipids from flour has been conducted with a variety of different chemicals and varying methods of extraction. However, one of the key evaluation metrics for the extraction technique is the ability to defat and reconstitute the lipids without excessive damage to the flour (i.e. proteins, starch, and lipids). This allows breads to be baked and produce loaves that are comparable to the control, without a solvent effect (MacRitchie and Gras 1973). MacRitchie and Gras (1973) utilized a combination of techniques involving a batch extraction through filters and a soxhlet system to conduct initial extractions of flour. In that study, solvents were allowed to evaporate from the defatted flour while the solvent + lipids underwent evaporation using a rotary evaporator and nitrogen flushing (MacRitchie and Gras 1973). The solvents were compared for effectiveness in extraction and those that were used in the experiment included: petroleum ether, benzene, chloroform, dichloromethane, ether, ethyl acetate, acetonitrile, water saturated n-butanol, acetone, ethanol, and combinations of blended chemicals. All the solvents either reduced loaf volume or increased mixing time, but the authors found that the chloroform and petroleum ether produced loaves that were similar to the controls (MacRitchie and Gras 1973).

Ponte and De Stefanis (1969) also conducted total lipid extractions using an ethanol benzene combination and a batch extraction technique where the solvent and flour were blended three times and filtered through a Büchner funnel. The lipids were further separated into polar and nonpolar fractions using silica gel and diethyl ether. The nonpolar fractions were extracted in silica gel with diethyl ether-petroleum ether (90:10 v/v) and blended with the lipids in a 12:1 (v/w) ratio. Following the elution from the gel, the lipids were dried under nitrogen (Ponte and

De Stefanis 1969). The polar lipids were eluted from the same gel following the nonpolar lipids using methanol and all fractions were nitrogen dried (Ponte and De Stefanis 1969).

Pomeranz et al (1966) used Skellysolve B (hexane) to extact lipids from sixteen different varieties of wheat with a goldfish extractor. Specifically, water saturated n-butanol was blended with the lipids at varying concentrations with a Stein Mill and evaporated with nitrogen Using silica acid column chromatography, the lipids extracted were fractionated into their polar and nonpolar components using a chloroform-methanol solution and then quantified with thin layer chromatography. This technique was able to distinguish between the polar and nonpolar lipid and had good separation between fractions while being able to differentiate between the wheat varieties.

Hoseney et al (1969) determined the influence of solvents on extraction of free and bound lipids. The fractions were characterized by extraction in either nonpolar solvents (petroleum ether) or polar solvents (water saturated-n-butanol). Total lipids were extracted with water saturated n-butanol using a soxhlet system and then blended using a Stein Mill. The nonpolar lipids were separated using silica acid chromatography and the polar lipids underwent two repeated extractions in petroleum ether and then with water saturated n-butanol, followed by differentiation with thin layer chromatography. From this study it was determined, that although water-saturated n-butanol does an effective job in extracting lipids, it is detrimental to loaf volume and characteristics of the bread. This solvent has also been shown to interact with other components in flour, such as the starch binding, breaking down the gliadin component of the gluten, as well as stopping the yeast from producing CO_2 (Hoseney et al 1969).

Further investigation and understanding of extractions techniques for native wheat lipids was conducted by Finney et al (1976) who used a series of solvents to determine their effect on baking quality. Benzene, chloroform, methanol, water saturated-1-butanol, and 95% ethanol were the solvents blended with the flour in a Stein mill at room temperature. After the extraction, lipids were re-dissolved in petroleum ether following the solvent evaporation. Another series of lipids were blended with solvents independently, in petroleum ether, n-hexane, n-heptane, and acetone and then evaporated off using a soxhlet system. Using thin layer chromatography, nonpolar and polar lipids were also fractionated with a chloroform-methanol-water solution. The nonpolar solvents (n-hexane, n-heptane, and petroleum ether) didn't remove as many of the total lipids from the flour as did the more polar solvents (benzene, chloroform, acetone, water

saturated-1-butanol). Methanol and 95% ethanol proved to be the most effective at removing the most polar fractions; however, they didn't remove as many total lipids as the previously mentioned polar solvents did. The nonpolar solvents also weren't as successful in removing the polar lipids (glycolipids and phospholipids) when analyzed with thin layer chromatography. The different solvents did have altering affects on the mixing time and loaf volumes. Solvents typically cause an increase in mixing time and some don't allow for optimal dough development reducing the overall loaf volumes.

Chung et al (1977a) continued to determine the optimum method for extractions using varying apparatus that can remove the solvents from the flour. This research evaluated the differences between two soxhlet systems (a vacuum and a standard system) with different solvents to determine the optimum method for extraction. The soxhlet system utilized a condenser and a boiling flask to evaporate the solvent with a vacuum hooked up to the system, which decreased the pressure within the system. Solvents used in this experiment included hexane (Skelly B), benzene, acetone, and 2-propanol. The solvents were added to the flour (500 grams flour/ 2.8 liters solvent) and this blend was placed in the soxhlet for twenty-four hour extraction and then extractions were repeated on the same sample in order to achieve optimum system extraction for each solvent.

For the soxhlet with the vacuum system attached, a larger quantity (1000 grams) of flour was used and evaporation was conducted at a pressure of 9-10 inches of Hg. It took double the time to extract in the vacuum system than the regular soxhlet system. Following the soxhlet methods, the lipids were extracted in petroleum ether for quantification and fractionated using silica acid chromatography in methanol and chloroform. It was shown that more lipids could be removed from flour by the standard soxhlet method better than the vacuum method and more polar lipids were extracted due to the increase in solubility of the solvent. However, there was an effect of both solvent and system on extraction. It was found that the vacuum soxhlet was able to extract more polar lipids as compared to the increased amount of total lipids that the regular soxhlet system extracted. This shows that the more polar solvent (2-propanol) in the vacuum soxhlet system would be a better system to remove lipids in further studies.

Following the evaluation of soxhlet system, Chung et al (1977b) also asscessed the techniques of extraction, solvent, and temperature on the removal of lipids from flour and their influence on bread making potential in defatted and reconstitution studies. For this study, a water

bath with a connected shaker and compared to a regular soxhlet system. The procedure for the water bath, which only agitated the samples in a horizontal direction, had the samples in a 1:8 (w/v) ratio of flour to solvent and was shaken in the water bath for 2 h. In addition, 3 min shaking by hand step was used every 15 min to accommodate for the horizontal mechanical motion. The solvents that were used again were the same as in the previous study (Chung 1977a) and the temperatures of the water bath was adjusted depending on the solvent, ranging between 30°C and 75°C. Solvents were filtered and removed through a Büchner funnel and evaporated off under pressure and stored frozen. The solvents were also blended with flour and subjected to evaporation using the standard soxhlet system with changing temperatures based by solvent boiling points. These results concluded that solvent solubility, extraction temperature, and method used increased the lipid extractability. The soxhlet appeared to have a better overall extraction for almost all the solvents, except with the hexanes, but it was determined that the shaker method slightly improved crumb grain. However, the soxhlet was more detrimental to flours of better baking quality while using the 2-propanol for extraction. This solvent improved the quality of the breads made from lower quality flours.

Greenblatt et al (1995) conducted a series of extraction on free and bound lipids from starch and flour by doing a hexane extraction of free lipids (1:10 w/v ratio) and using propan-2-ol: water solution (90:10) for the bound lipids. The bound lipids were separated into fractions by a combination solution (4 ml) of hexane, ethyl acetate, and acetic acid (95:5:0.2) and then fractionated using solid-phase extraction (SPE). Noncharged lipids were eluted first followed by glycolipids using a solution (5 ml) of tetrahydrofuran, acetonitrile, and propan-2-ol (35:35:30). Finally, the phospholipids were washed through the SPE cartridge with a 35:65 ratio of acetonitrile and methanol. More recently, Finnie et al (2009) modified this method for the extraction of free and bound lipids to extract surface starch lipids from within the bound fractions. This was conducted by adding 90:10 ratio of isopropanol: water solution to the final stage of the bound lipid extraction technique from starch. Following a vortexing step the samples were heated and centrifuged (4,800 x g) and then the solvent was evaporated off with nitrogen and then placed in chloroform (1 ml).

1.3. Rheology

Rheology is the study and measurement of the change in a material due to the application of an external force (Belton 2005). Typically, a mechanical force is applied and is measured as stress or "force applied per unit of area," and strain, which is the deformation caused by the applied force (Belton 2005). This deformation or strain is already applied at varying rates over time and the results can be used to determine rigidity, viscosity, strength, firmness and durability of a material (Dobraszczyk and Morgenstern 2003). Rheology is used to provide a better understanding of a material's physical properties, molecular structure, and behavior during the processing (Dobraszczyk and Morgenstern 2003). In practice, this type of testing evaluates changes in deformations particularly those associated with compression and tension (Dobraszczyk and Morgenstern 2003).

The factors that influence dough's rheological characteristics include "the properties of the continuous matrix, the volume fractions, the shape of fillers, and the adhesion between filler and matrix" (Larsson and Eliasson1997). The dough components that are most influential on rheological characteristics are also important for maintaining the structural network of the dough (Primo-Martin et al 2006). Through the blending and hydration of ingredients and incorporation of air, a visco-elastic matrix is formed. Certain rheological testing techniques such as those that evaluate large deformation or extensibility provide a better understanding of the dough's baking properties (Dobraszczyk and Salmanowicz 2008). Differences in extensional properties of dough typically have been evaluated using the Kieffer dough testing rig while strain response evaluation has been done utilizing bubble inflation testing (Dobraszczyk and Salmanowicz 2008). From these tests, strain hardening and bubble failure were the most important factors for evaluating baking and expansion properties of dough.

The expansion of dough will apply both stress and strain on the gluten air cell walls (Sroan et al 2009). There is an initial strain that occurs due to the internal pressures of air cells expansion and causes the cell walls to thin in varying directions (Sroan et al 2009). If the stress is greater in the thinner cell wall areas than is the strain, the thinner cell wall area will stop expanding and this, in-turn, will cause thinning towards the thicker sections of the internal cell walls (MacRitchie 2010). This response is strain hardening and can be described as "a localized increase in stress in response to the strain; resisting the failure of the gas cell walls" (MacRitchie 2010). Breakdown of cell walls in dough are resisted by the "elongation or strain hardening and

this property can be measured under large deformation biaxial extension" (Dobraszczyk 2004). The balance between the stress and strain during the expansion process helps to maintain gas cells and structural integrity, which is essential for loaf volume (Sroan et al 2009). Strain hardening is influenced by many characteristics of the dough, external energy, and the degree to which it is applied (MacRitchie 2010). Finally, strain hardening provides an estimate of cell expansion by providing information on the highest amount of inflation that can occur without breakdown (Sroan et al 2009).

1.4. X-ray Microtomography (XMT)

The importance of the cellular structure in bread lies with the incorporation and distribtuon of air cells. It is the microstructure, which "qualifies the size and the morphology of the arrangement of the solid and gaseous phases in a cellular material" (Maire et al 2003). X-ray microtomography (XMT) is a non-invasive technique that allows the visualization of cellular microstructure, even dense solids, by the reconstruction of 3-D images of a material (Babin et al 2006). The technique utilizes an x-ray source that sends x-rays through a sample that has been placed in the path of the beam and the energy is either absorbed or transmitted through the specimen (Salvo et al 2010).

The energy that is transmitted is collected by a camera and used to create projections of the sample. Typically, many projections are accumulated as the sample is rotated 180-360° in the beam. These projections, also known as scans, are used to build the image. Contrasts in the image are based on how the x-ray is absorbed at those various locations. To obtain a good 3D image, there must be sufficient transmission, a large enough number of projections, and the background noise must be corrected by first imaging a flat field without a sample being present (Salvo et al 2010). Common measurement determined from 3D imaging include, global density, air cell size distribution, and cell wall thickness (Maire et al 2003).

This technique has been used to evaluate the microstructural properties of bread crumb to determine the relationship between air incorporation, expansion, and cell structure. Babin et al (2006) looked at the changes in gas cell expansion during proofing. XMT images were taken every 10 min over 2 to 3 hours. It was determined that during the initial stages of the proofing, air cell growth was unrestricted, cells expanded freely, and average cell wall thickness was relatively similar throughout the dough (Babin et al 2006). As proofing continued, cells begin to

be closer to one another, making them more susceptible to integration and coalescence creating larger cells. During the later stages of proofing, as the cells become more enlarged, cell wall thickness changed at different rates (Babin et al 2006).

Tubin-Orger et al (2012) also evaluated dough with varying ingredients and different water levels during the last phase of proofing to determine changes in the internal dough structure. The ingredients and water resulted in differences in the amount and size of the bubbles during proofing (minimum of 157 min). At this stage, gas cell shape was not spherical due to what was believed to be steric hindrance. These results also found that bubbles at the end of proofing were more than 75% of the volume within the dough and the voids were linked to one another with a cell wall thickness of <5μm. The authors were unable to determine if the surface active liquid lamellae separated the cells as they estimated the size of the layer to be smaller than the sensitivity of the XMT (<5μm).

Wang and Bell (2011) utilized microCT XMT scanning to follow the changes that occur within the linkages of the dough network over time and how those changes affected characteristics of the bread. They found that the breadcrumbs were connected and this connection was influenced by a series of single cells that were within the dough matrix and were either considered to be opened or closed. Lampignano et al (2013) utilized XMT to look at the physical properties of bread made with durum wheat and the impact of yeast content on this process. This study observed that yeast was very influential on development and expansion of air cell in bread. This follows the idea that cells were either concave in shape based on the "total pore structure" signifying connections or convex, which had divided linkage between one another (Lampignano et al 2013). The results from these test samples were concave with more separated film structures creating thinner cell walls. These authors also correlated cell size to bread textural properties and found that smaller cell size required a greater force needed to compress the bread slice resulting in bread that was slightly denser in texture. Another study showed changes in bread texture following production using XMTand this showed how the air cell structure changed over time (Besbes et al 2013). These authors also found that the cell walls begin to get thinner as the cells grew during fermentation until they finally ruptured. Baking temperatures were more influential on the final air cell size (diameter) rather than the walls (Besbes et al 2013).

1.5 Scope of the Study

The influence of native wheat lipids on final baked product performance has been shown to be very important for stabilizing gas cells, structural support within the dough, and overall loaf volume. The incorporation of air cells during mixing and expansion of these cells during fermentation and proofing are critical for quality as they provide the characteristic mouthfeel, texture, and crumb grain to the loaf. It has been thoroughly studied and recognized that the gluten-starch matrix is the main backbone and structural support of the dough. However, during the later stages of proofing and the beginning of baking, the dough extends leaving gaps where gas cells can migrate towards one another, making larger cells. Previous research has determined that amphiphilic compounds such as polar lipids are able to move to the interface and stabilize gas cells where the gluten-starch matrix has broken down. The molecular structure of polar lipids can be oriented to form compressed monolayers, which allow for alignment between the gas cells and the interface. However, the influence of polar lipids on dough rheological properties and changes in gas cell size, stability, and distribution are not fully understood.

1.5.1. Objectives

To better understand lipid functionality, the objectives of this study were to evaluate the influence of total and fractionated varieties of native wheat lipids and concentration on the rheological properties of dough and on the microstructure of bread. Testing was conducted using total nonstarch native wheat lipids and total nonstarch lipids that were fractionated into nonpolar and polar groups. In addition, free and bound lipid fractions (containing combinations of both nonpolar and polar lipids) were also evaluated. Lipids were added back in at the level in which they were extracted or at varying concentrations.

1.5.2. Chapter 2-Extraction and Fractionation of Native Wheat Lipids

Chapter 2 describes the methodology that was used to conduct the extraction and fractionation of native wheat lipids from straight grade flour. In addition, it explains the analysis procedure and quantitive results for the type and concentrations of lipids found within each fractionated group extracted.

1.5.3. Chapter 3-The Influence of Native Wheat Lipid Fractions on the Rheological Properties of Dough and Gas Cell Structure and Distribution in Bread

In Chapter 3, the effects of native wheat lipids on the rheological properties of dough and the gas cell size and distribution of bread were tested. The visco-elastic properties of dough were evaluated by small and large deformation testing on flours containing nonpolar and polar lipids fraction or total nonstarch lipids. In addition, bread microstructure was assessed through C-Cell imaging and by x-ray microtomography (XMT), which was performed at two different levels (macro-whole loaf and micro-center section) (Figure 1.4). For XMT testing, nonpolar lipids were either added back to flour at the same concentration as they were extracted or at varying concentrations based on a predetermined standard. Polar lipids were added to flour either as fractionated glycolipids or phospholipids based on the intial level found naturally in the flour or as unfractionated polar lipids at different concentrations based on a preset amount. Table 1.1 shows an overview of the research for Chapters 3 and 4. For more specifics on the experimental design please refer to each chapter.

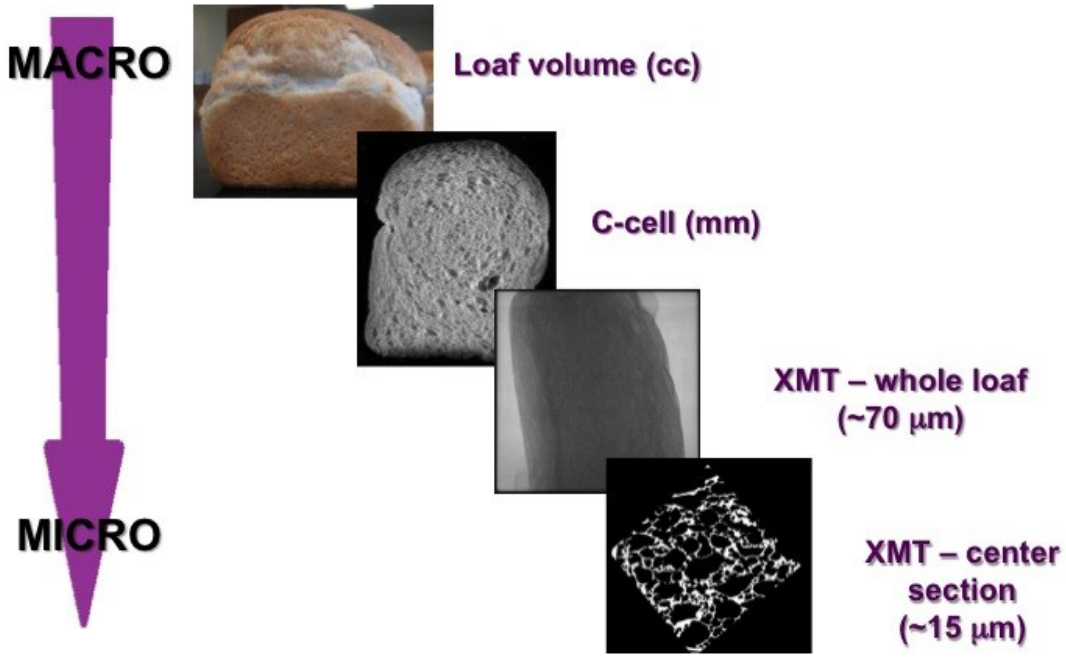

Figure 1.4. Multi-scale analysis of the microstructure of bread

1.5.4. Chapter 4-The Effects of Varying Concentrations of Wheat Lipids Fractions on the Microstructure of Bread

In chapter 4, total nonstarch lipids (reconstituted), free, bound, nonpolar, and polar lipids were extracted and added back to flour at increased levels based on predetermined standards of each lipid type. The microstructure, specifically, changes in volume, gas cell size, and distribution were evaluated using the C-Cell and XMT (micro) to determine how the varying lipid concentrations influenced changes in the bread.

Table 1.1. Experimental approach for Chapters 3 and 4

Section	Variation	Lipid Type	Dough development		Rheology		Analytical baking	C-Cell	X-ray Microtomography	
			Mixograph	Mixolab	Small	Large			Macro	Micro
Chapter 3	Type	Control	x	x	x	x	x	x	x	x
		Defatted	x	x	x	x	x	x		x
		Total lipids		x						
		Nonpolar			x	x	x	x	x	
		Glycolipids			x	x	x	x	x	
		Phospholipids			x	x	x	x	x	
		Nonpolar 0.6%-2.5%					x	x		x
		Polar 0.2%-0.6%					x	x		x
Chapter 4	Amount	Control	x				x	x		x
		Defatted	x				x	x		x
		Reconstituted 1.4%, 2.8%					x	x		x
		Free 0.8%-2.5%					x	x		x
		Bound 0.6%-2.5%					x	x		x
		Nonpolar 0.6%-2.5%					x	x		x
		Polar 0.2%-0.6%					x	x		x

1.6. References

Babin, P., Della Valle, G., Chiron, H., Cloetens, P., Hoszowska, J., Pernot, P., Réquerre, L., Salvo, L., and Dendievel, R. 2006. Fast X-ray tomography analysis of bubble growth and foam setting during breadmaking. J Cereal Sci. 43: 393-397.

Baker J.C. 1941. The structure of the gas cell in bread dough. Cereal Chem. 18: 34-41.

Baker, J.C. and Mize, M.D. 1941. The origin of gas cells in bread dough. Cereal Chem. 18: 19-34.

Baker, J.C. and Mize, M.D. 1946. Gas occlusion during dough mixing. Cereal Chem. 23: 39-51.

Belderok, B. 2000. Part One: Developments in bread-making process. Pages. 42-43 in: Bread-making Quality of Wheat A Century of Breeding in Europe. D.A. Donner, ed. Kluwer Academic Publishers: Dordrecht.

Belton, P.S. 1999. Mini review: on the elasticity of wheat gluten. J. Cereal Sci. 29:103-107.

Belton, P.S. 2005. New approaches to study molecular basis of the mechanical properties of gluten. J Cereal Sci. 41: 203-2011.

BeMiller, J.N. 2007. Carbohydrate Chemistry for Food Scientist. AACC International, Inc.: St. Paul.

Besbes E., Jury, V., Monteau, J.-Y., and Le Bail, A. 2013. Characterizing the cellular structure of bread crumb and crust affected by heating rate using X-ray microtomography. J Food Eng. 115: 415-423.

Blanshard, J.M.V. 1987. The significance of structure and function of the starch granules in baked products. Page 1 in: Chemistry and Physics of Baking. J.M.V. Blanshard, P.J. Frazier, and T. Galliard, eds. Royal Society of Chemistry: London.

Carlson, T., Larsson, K., and Miezis, Y. 1978. Phase equilibria and structures in the aqueous system of wheat lipids. Cereal Chem. 55: 168-179.

Carlson, T.L-G., Larsson, K., Miezis, Y., and Poovarodom, S. 1979. Phase equilibria in aqueous system of wheat gluten lipids and in the aqueous salt system of wheat lipids. Cereal Chem. 56: 417-419.

Carr, N.O., Daniels, N.W.R., and Frazier, P.J. 1992. Lipid interactions in breadmaking. Cr Rev Food Sci. 31: 237-258.

Cauvain, S.P. 1998. Bread-the product. Pages 1-3 in: Technology of Breadmaking. S.P. Cauvain and L.S. Young, eds. Blackie Academic & Professional: New York.

Chung, O.K., Ohm, J-B., Ram, M.S., and Howitt, C.A. 2009. Wheat Lipids. Pages 363-373 in: Wheat Chemistry and Technology, 4th ed. K. Khan and P.R. Shewry, Eds. AACC International, Inc.: St. Paul.

Chung, O.K., Pomeranz, Y., and Finney, K.F. 1978. Wheat flour lipids in breadmaking. Cereal Chem. 55: 598-618.

Chung, O.K., Pomeranz, Y., and Finney, K.F. 1982. Relation of polar lipid content to mixing requirement and loaf volume potential of hard red winter wheat flours. Cereal Chem. 59: 14-20.

Chung, O.K., Pomeranz, Y., Finney, K.F., Hubbard, J.D., and Shogren, M.D. 1977a. Defatted and reconstituted wheat flours. I. Effects of solvent and soxhlet types on functional (breadmaking) properties. Cereal Chem. 54: 454-465.

Chung, O.K., Pomeranz, Y., Finney, K.F., and Shogren, M.D. 1977b. Defatted and reconstituted wheat flours. II. Effects of solvent type and extracting conditions on flours varying in breadmaking quality. Cereal Chem. 54: 484-495.

Chung, O.K., Pomeranz, Y., Hwang, E.C., and Dikeman, E. 1979. Defatted and reconstituted wheat flours. IV. Effects of flour lipids on protein extractability from flours that vary in bread-making quality. 1979. Cereal Chem. 56: 220-226.

Chung, O.K., Pomeranz, Y., Jacobs, R.M., and Howard, B.G. 1980a. Lipid extraction conditions differentiate among hard red winter wheats that vary in breadmaking. J Food Sci. 45: 1168-1174.

Chung, O.K., Pomeranz, Y., Shogren, M.D., Finney, K.F., and Howard B.G. 1980b. Defatted and reconstituted wheat flours. VI. response to shortening addition and lipid removal in flours that vary in bread-making quality. Cereal Chem. 57: 111-117.

Chung, O.K., Pomeranz, Y., Finney, K.F., Shogren, M.D., and Carville, D. 1980c. Defatted and reconstituted wheat flours. V. bread-making response to shortening of flour differentially defatted by varying solvent and temperature. Cereal Chem. 57: 106-110.

Chung, O.K., Shogren, M.D., Pomeranz, Y., and Finney, K.F. 1981. Defatted and reconstituted wheat flours. VII. the effect of 0-12% shortening (flour basis) in bread making. Cereal Chem. 58: 69-73.

Chung, O.K. and Tsen C.C. 1975. Changes in lipid binding and distribution during dough mixing. Cereal Chem. 52: 533-548.

Daftary R.D., Pomeranz, Y., Shogren, M., and Finney, K.F. 1968. Functional bread-making properties of wheat flour lipids. 2. the role of flour lipid fractions in bread-making. Food Technol. 22: 327-330.

Daniels, N.W.R., Richmond, J.W., Eggitt, P.W.R., and Coppock, J.B.M. 1966. Studies on the lipids of flour. III. lipid binding in breadmaking. J Sci Food Agric. 17: 20-29.

Delcour, J.A. and Hoseney, R.C. 2010. Principles of Cereal Science and Technology, 3rd ed. AACC International, Inc.: St. Paul.

Department of Health and Human Services, Food and Drug Administration. 2013. Requirements for specific standardized bakery products. 21 CFR part 136. Fed. Regist. 63: 40135. 21CFR136.110.

De Stefanis, V.A. and Ponte, Jr., J.G. 1976. Studies on the breadmaking properties of wheat-flour nonpolar lipids. Cereal Chem. 53: 636-642.

Dobraszczyk, B.J. 2004. The physics of baking: rheological and polymer molecular structure-function relationships in breadmaking. J Non-Newtonian Fluid Mech. 124: 61-69.

Dobraszczyk, B.J., and Morgenstern, M.P. 2003. Rheology and the breadmaking process. J Cereal Sci. 38: 229-245.

Dobraszczyk, B.J., and Salmanowicz, B.P. 2008. Comparison of predictions of baking volume using large deformation rheological properties. J Cereal Sci. 47: 292-301.

Dubreil, L., Compoint, J-P., and Marion, D. 1997. Interaction of puroindolines with wheat flour polar lipids determines their foaming properties. J Agric Food Chem. 45: 108-116.

Eliasson, A.-C., and Larsson, K. 1993. Cereals in Breadmaking A Molecular Colloidal Approach. Marcel Dekker, Inc.: New York.

Finnie, S.M., Jeannotte, R., and Faubion, J.M. 2009. Quantitative characterization of polar lipids from wheat whole meal, flour, and starch. Cereal Chem. 86: 637-645.

Finnie, S.M., Jeannotte, R., Morris, C.F., Giroux, M.J., and Faubion, J.M. 2010. Variation in polar lipids located on the surface of wheat starch. J Cereal Sci. 51: 73-80.

Finney, K.F., Pomeranz, Y., and Hoseney, R.C. 1976. Effect of solvent extractions on lipid composition, mixing time, and bread loaf volume. Cereal Chem. 53: 383-388.

Galliard, T., and Bowler, P. 1987. Morphology and composition of starch. Pages 71-72 in: Starch Properties and Potential. T. Galliard, ed. Society of Chemical Industry: Great Britain.

Gan, Z., Angold, R.E., Williams, M.R., Ellis, P.R., Vaughan, J.G., and Galliard, T. 1990. The microstructure and gas retention of bread dough. J Cereal Sci. 12: 15-24.

Gan, Z., Ellis, P.R., and Schofield, J.D. 1995. Gas cell stabilisation and gas retention in wheat bread dough. J Cereal Sci. 21: 215-230.

Gandikota, S., and MacRitchie, F. 2005. Expansion capacity of doughs: methodology and applications. J Cereal Sci. 42: 157-163.

Greenblatt, G.A., Bettge, A.D., and Morris, C.F. 1995. Relationship between endosperm texture and the occurrence of friabilin and bound polar lipids on wheat starch. Cereal Chem. 72: 172-176.

Hamer, R.J., and Van Vliet, T. 2000. Understanding the structure and properties of gluten: an overview. Pages. 127-129 in: Wheat Gluten. P.R. Shewry and A.S. Tatham, eds. Royal Society of Chemistry: Cambridge.

Hoseney, R.C. 1984. Gas retention in bread doughs. Cereal Food World. 29: 305-308.

Hoseney, R.C. 1985. The mixing phenomenon. Cereal Food World. 30: 453-457.

Hoseney, R.C., Finney, K.F., and Pomeranz, Y. 1969. Functional (breadmaking) and biochemical properties of wheat flour components. V. role of total extractable lipids. Cereal Chem. 46: 606-613.

Hoseney, R.C., Finney, K.F., and Pomeranz, Y. 1970. Functional (breadmaking) and biochemical properties of wheat flour components. VI. gliadin-lipid-glutenin interactions in wheat gluten. Cereal Chem. 47: 135-140.

Hoseney R.C., Finney, K.F., Pomeranz, Y., and Shogren, M.D. 1971. Functional and biochemical properties of wheat flour components. VIII. starch. Cereal Chem. 48: 191-201.

Junge, R.C., and Hoseney, R.C. 1981a. A mechanism by which shortening and certain surfactants improve loaf volume in bread. Cereal Chem. 58: 408-412.

Junge, R.C., Hoseney, R.C., and Varriano-Marston, E. 1981b. Effect of surfactants on air incorporation in dough and the crumb grain of bread. Cereal Chem. 58: 338-342.

Lampignano, V., Mastromatteo, L.M., and Del Nobile, M.A. 2013. Microstructural, textural and sensorial properties of durum wheat bread as affected by yeast content. Food Res Int. 50: 369-376.

Larsson, H., and Eliasson, A-C. 1997. Influence of the starch granule surface on the rheological behaviour of wheat flour dough. J Texture Stud. 28: 487-501.

Leissner, O. 1988. A comparison of the effect of different polymorphic forms of lipids in breadmaking. Cereal Chem. 65: 202-207.

MacRitchie, F., and Gras, P.W. 1973. The role of lipids in baking. Cereal Chem. 50: 292-302.

MacRitchie, F. 1976a. The liquid phase of dough and its role in baking. Cereal Chem. 53: 318-326.

MacRitchie, F. 1976b. Monolayer compression barrier in emulsion and foam stability. J Colloid Interf Sci. 56: 53-56.

MacRitchie, F. 1977. Flour lipids and their effects in baking. J Sci Food Agric. 28: 53-58.

MacRitchie F. 2010. Concepts in Cereal Chemistry. Taylor and Francis Group, LLC.: Boca Raton.

Maire, E., Fazekas, A., Salvo, L., Dendievel, R., Youssef, S., Cloetens, P., and Letang, J.M. 2003. X-ray tomography applied to the characterization of cellular materials. Related finite element modeling problems. Compos Sci Technol. 63: 2431-2443.

Marion, D., Le Roux, C., Akoka, S., Tellier, C., and Gallant, D. 1987. Lipid-protein interactions in wheat gluten: a phosphorus nuclear magnetic resonance spectroscopy and freeze-fracture electron microscopy study. J Cereal Sci. 5: 101-115.

Medcalf, D.G., Youngs, V.L., Gilles, K.A. 1968. Wheat Starches. II. effect of polar and nonpolar lipid fractions on pasting characteristics. Cereal Chem. 45: 88-95.

Mills, E.N.C., Wilde, P.J., Salt, L.J., and Skeggs, P. 2003. Bubbles formation and stabilization in bread dough. Food Bioprod Process. 81:189-193.

Morrision, W.R. 1988. Lipids in cereal starches: a review. J Cereal Sci. 8: 1-15.

Ohm, J.B., and Chung, O.K. 2002. Relationship of free lipids with quality factors in hard winter wheat flours. Cereal Chem. 79: 274-278.

Pareyt, B., Finnie, S.M., Putseys, J.A., Delcour, J.A. 2011. Lipids in bread making: sources, interactions, and impact on bread quality. J Cereal Sci. 54: 266-279.

Primo-Martin, C., Hamer, R.J., and H.J. de Jongh, H. 2006. Surface layer properties of dough liquor components: are they key parameters in gas retention in bread dough. Food Biophys. 1: 83-93.

Primo-Martin, C., van Nieuwenhuijzen, N.H., Hamer, R.J., and van Vliet, T. 2007. Crystallinity changes in wheat starch during the bread-making process: starch crystallinity in the bread crust. J Cereal Sci. 45: 219-226.

Pomeranz, Y. 1965. Polar vs. nonpolar wheat flour lipids in bread-making. Food Technol. 120-121.

Pomeranz, Y, Chung, O.K., and Robinson, R.J. 1966. The lipid composition of wheat flours varying widely in bread-making potentialities. J Am Oil Chem Society. 43: 45-48.

Pomeranz, Y. 1973. Interaction between glycolipids and wheat macromolecules in breadmaking. Page 153-188 in: Advances in Food Research Vol. 20. C.O. Chichester, ed. Academic Press, Inc.: New York.

Pomeranz, Y., Shogren, M., and Finney, K.F. 1968. Functional bread-making properties of wheat flour lipids. 1. reconstitution studies and properties of defatted flours. Food Technol. 22: 324-327.

Ponte, Jr., J.G., and De Stefanis, V.A. 1969. Note on separation and baking properties of polar and nonpolar wheat flour lipids. Cereal Chem. 46: 325-329.

Ponte, Jr., J.G., and Baldwin, R.R. 1972. Studies on the lipid system of flour and dough. Bakers Dig. 46: 28-35.

Sahi, S.S. 1994. Interfacial properties of the aqueous phases of wheat flour doughs. J Cereal Sci. 20: 119-127.

Salt, L.J., Wilde, P.J., Georget, D., Wellner, N., Skeggs, P.K., and Mills, E.N.C. 2006. Composition and surface properties of dough liquor. J Cereal Sci. 43: 284-292.

Salvo, L., Suéry, M., Marmottant, A., Limodin, N., Bernard, D. 2010. 3D imaging in material science: applications of x-ray tomography. CR Physique. 11: 641-649.

Schoch, T.J. 1965. Starch in bakery products. Bakers Dig. 39: 48-57.

Schofield, J.D. 1987. Flour protein: structure and functionality in baked products. Page 15 in: Chemistry and Physics of Baking. J.M.V. Blanshard, P.J. Frazier, and T. Galliard, eds. Royal Society of Chemistry: London.

Serna-Saldivar, S.O. 2010. Cereal Grains Properties, Processing, and Nutritional Attributes. Taylor & Francis Group, LLC.: Boca Raton.

Singh, H., and MacRitchie, F. 2001. Applications of polymer science properties of gluten. J Cereal Sci. 33: 231-243.

Sroan, B., Bean, S.R., and MacRitchie, F. 2009. Mechanism of gas cell stabilization in bread making. I. the primary gluten-starch matrix. J Cereal Sci. 49: 32-40.

Sroan B., and MacRitchie, F. 2009. Mechanism of gas cell stabilization in breadmaking. II. The secondary liquid lamellae. J Cereal Sci. 49: 41-46.

Stear, C.A. 1990. Handbook of Breadmaking Technology. Elsevier Science Publishers, LTD.: New York.

Sullivan, B. 1940. The function of the lipids in milling and baking. Cereal Chem. 17: 661- 668.

Turbin-Orger, A., Boller, E., Chaunier, L., Chiron, H., Della Valle, G., Réguerre, A.-L. 2012. Kinetics of bubble growth in wheat flour dough during proofing studied by computed x-ray micro-tomography. J Cereal Sci. 56: 676-683.

Wang, S., Austin, P., Bell, S. 2011. It's a maze: the pore structure of bread crumbs. J Cereal Sci. 54: 203-2010.

Zobel, H.F. 1988. Molecules to granules: a comprehensive starch review. Starch-Stärke. 40: 44-50.

Chapter 2 - Extraction and Fractionation of Native Wheat lipids

2.1 Introduction

Lipids found naturally in wheat make up a very small fraction (2-3%) of the overall composition of the kernel (Chung et al 2009; Finnie et al 2009). Wheat lipids can be divided into various classes based on the extraction solvent polarity or by location within the wheat kernel (germ, aleurone, and endosperm) (Chung et al 2009). For many applications, specifically those related to baking, lipids found in endosperm (flour) that remains after milling, have been shown to play an important role in stabilizing gas cells within the dough and improving loaf volume by providing a secondary support to the gluten-starch matrix (MacRitchie and Gras 1973; Sroan et al 2009). The endosperm lipids can be broken down into either total nonstarch lipids or starch lipids and are differentiated by their linkage to the starch granule (Chung et al 2009). Nonstarch lipids do not require gelatinization of starch for extraction. On the other hand; starch lipids do require granular swelling to be extracted (Chung et al 2009; Finnie et al 2009).

Nonstarch lipids can further be divided into free and bound lipids based on solvent polarity used for extraction (Chung et al 2009). Free lipids can be extracted with nonpolar solvents (hexane, ether) and bound lipids using polar solvents (water-saturated butanol, isopropanol-water, chloroform-methanol) (Chung et al 2009; Finnie et al 2009). The free lipids are separated into either polar (PL) or nonpolar lipids (NPL), which consist of glycolipids and phospholipids or fatty acids, triacylglycerides, and sterol esters, respectively (Chung et al 2009). The bound lipids are predominately glycolipids and phospholipids (Finnie et al 2009). It is well known that the polar lipids offer the most functionality and greatest benefit to bakery products due to their ability to move to the gas cell interface because of their surface-active properties (MacRitchie and Gras 1973; Gan et al 1990). The objective of this work was to extract total nonstarch, free, and bound lipids from flour and to fractionate nonstarch lipids into nonpolar (NPL), glycolipids (GL), and phospholipids (PHL) for lipid classification and use in subsequent dough and baking studies.

2.2. Materials and Methods

2.2.1. Flour

Kansas grown, hard red winter wheat was milled into straight grade flour at the Hal Ross Flour Mill at Kansas State University (Manhattan, KS). The flour was produced at 73% extraction with a protein content of 10.36%, ash of 0.55%, and starch damage of 7.1% (AACCI Method 76-31.01) (AACCI 2014). Following milling, samples were collected into 2.3 kg (50 lb) bags and placed into -18°C freezer storage until utilized for analysis.

2.2.2. Defatting and reconstitution of lipids from flour

The native lipids found in wheat were removed from flour in order to determine functionality during the bread-making process. Using a series of solvents, the lipids were removed and added back at concentrations that were found through previous studies to be the standard amount of lipids found within the wheat flour (Chung et al 2009). By removing and re-adding the lipids to the flour, a better understanding was determined of which fractions are the most beneficial for loaf volume and overall bread quality and what levels have the greatest impact on the bread.

2.2.2.1. Non-starch total lipid extraction

Total lipid extraction was conducted following the method of MacRitchie and Gras (1973). This technique utilized batch extraction of 200 g of flour mixed with 400 mL of chloroform (Fisher Scientific-Pittsburgh, PA) using a stir bar on a stir plate at 950 rpm for 3 min. The samples were filtered through a Büchner funnel with Whatman #1 paper (Fisher Scientific, Pittsburgh, PA) and the procedure was repeated 2X. The resulting lipid/chloroform solution was transferred to a round-bottom flask and the solvent removed by a Rotavaporator (R-114, Buchi Labortechnik AG, Switzerland) at 50°C. Following solvent extraction, the sample was re-suspended in 11 mL of chloroform and transferred to a 16 mL vial. The solvent was evaporated by drying with nitrogen, weighed, and stored under N_2 at -15°C until further testing. Extractions and evaporations were conducted at room temperature (25°C ± 5). The extracted flour was spread onto parchment paper and left overnight at room temperature to allow for any remaining solvent to evaporate.

2.2.2.2. Free lipid extraction

Free lipids were extracted following the method of Greenblatt et al (1995) with a few modifications to accommodate a different sample size. Seventeen gram aliquots of flour were mixed with 170 mL hexanes (1:10 w/v) each (Fisher Scientific, Pittsburgh, PA) in glass centrifuge bottles and gently agitated on a shaker (Shaker 35, Labnet International, Inc., Edison, NJ) at speed 6.5 for 30 min. Samples where then centrifuged (CU-5000, Damon/IEC Division, ThermoFisher Scientific, Waltham, MA) for 5 min at 38000 rpm and filtered through Whatman #1 paper (Fisher Scientific, Pittsburgh, PA) with a Büchner funnel. The lipid/hexanes solution was transferred to a round-bottom flask and the solvent evaporated off at 50°C by a Rotavaporator (R-114, Buchi Labortechnik AG, Switzerland). The samples were re-suspended in 11 mL of chloroform, transferred to a 12 mL vial, and dried using N_2. Samples were frozen under N_2 at -15°C until used for further testing. The flour (which now only contained bound lipids) was allowed to dry overnight at room temperature and then used in the bound lipid extraction.

2.2.2.3. Bound lipid extraction

Bound lipids were removed from the flour following Greenblatt et al (1995) with changes to accommodate differences in sample size. Lipids were removed in a 90:10 2-propanol-water solution (Fisher Scientific, Pittsburgh, PA) at 1:6 ratio of sample to solvent. Seven grams of flour was added to 42 mL of solvent and gently agitated on a shaker (Shaker 35, Labnet International, Inc., Edison, NJ) (speed 6.5) for 15 min then centrifuged (Sorvall Legend X1R, ThermoFisher Scientific, Waltham, MA) for 15 min at 10,000 x g. After centrifugation, solvent-lipid solution (supernatant) was filtered through Whatman #1 paper (Fisher Scientific, Pittsburgh, PA) with a Büchner funnel and the solvent evaporated at 57°C using a Rotavaporator (R-114, Buchi Labortechnik AG, Switzerland). The bound lipids were re-suspended in 11 mL of chloroform and transferred to a 12 mL vial, nitrogen flushed and frozen under N_2 at -15°C until needed for further testing.

2.2.2.4. Lipid fractionation: nonpolar, glycolipids, and phospholipids

Total lipids (see "total lipids extraction") were fractionated into nonpolar, glycolipids, and phospholipids, using solid-phase extractions (SPE) and solvents of different polarities. The method was adapted from Yasui (2012) with changes based on the desired sample size. All lipids

were fractionated using a vacuum manifold (Phenomonex, Torrance, CA) with attached silica based cartridges (2g/12mL) (Phenomenex, Torrance, CA) as the separating medium. The manifold's vacuum pressure was set at 10 inches Hg (± 5 inches Hg). All cartridges were first conditioned with 12 mL of methanol and 2 mL of chloroform and those solvents were discarded.

2.2.2.4.1. Nonpolar lipids (NPL)

Total lipid samples were removed from the freezer and allowed to come to room temperature (15 min) before fractionation. Two milliliters of chloroform was added to each sample and then vortexed (Fisher Vortex Genie 2, Fisher Scientific, Pittsburgh, PA) to re-solubilize the nitrogen-dried lipids. Sample vials (12 mL) were placed under each silica cartridge (4 cartridges for each lipid sample) and the lipid/chloroform solution added to the cartridges in 1 mL increments until all of the lipid-solvent solution had been added. Nonpolar lipids were eluted using 4 mL of chloroform-acetone solution (4:1 v/v) (Fisher Scientific, Pittsburgh, PA) added to each individual cartridge. The glycolipids and phospholipids were retained on the stationary phase. The eluents, which were deep yellow in color, were nitrogen dried and frozen under N_2 at -15°C.

2.2.2.4.2. Glycolipids (GL)

Following nonpolar lipid fractionation, glycolipids were eluted using 4 mL of acetone-methanol solution (9:1 v/v). The eluents were nitrogen dried and frozen under N_2 at -15°C. These samples were lighter yellow in color and contained most of the carotenoids that were in the cartridge.

2.2.2.4.3. Phospholipids (PHL)

Phospholipids remaining on the stationary phase were eluted using 5 mL of methanol with eluents collected into 8 mL vials, nitrogen dried, and frozen under N_2 at -15°C. These samples no longer contained carotenoids and were snowy white when dried.

2.2.3. Lipid Profiling

Compositional analysis of each lipid fraction was analyzed by tandem mass spectroscopy at the Kansas Lipidomics Research Center Analytical Lab at Kansas State University. Polar lipid classification within each lipid fraction was conducted following the procedure by Xiao et al (2010). Each lipid fraction was extracted independently with five replicates of each lipid type

tested. Samples were combined and diluted onsite into a dilution series of: 5-10mg/mL for each sample fraction analyzed.

2.3. Results

The same flour was used for all lipid extractions. A respresentative sample of that flour was separated, not used for the lipid extractions, and was labeled as the "control." Total lipid extraction was performed on the flour to provide "defatted" flour, which contained no nonstarch total lipids. This was used for reconstitution for later studies. Table 2.1 shows the polar lipid composition of each lipid fraction extracted from 200 g of flour that was later used as the defatted flour. The polar lipids quantified in the analysis included: monogalactosyldiglyceride (MGDG), digalactosyldiglyceride (DGDG), phosphatidylglycerols (PG), lysophosphatidylglycerols (LysoPG), lysophosphatidylcholines (LysoPC), lysophosphatidylethanolamines (LysoPE), phosphatidylcholines (PC), phosphatidylethanolamines (PE), phosphatidylinositols (PI), phosphatidylserines (PS), and phosphatidic acid (PA)

The total lipid fraction contained the highest content of total polar lipids (0.24g/200g) (0.12%) followed by GL with 0.06 g/200 g (0.03%). Specifically, the polar lipids, MGDG and DGDG, were found in the highest concentrations across all lipid fractions tested with both total lipids and glycolipid fractions having the highest of both levels of these polar lipids. Because NPL, PHL, and GL were separated initially from the total lipids through SPE, recovery of the polar lipids, MGDG and DGDG, were the highest in both total and GL lipid fractions. MGDG levels were greater than all lipid groups evaluated with the highest recovery for the total lipids (0.12g/200g), followed by bound (0.03g/200g), and then the GL fraction at 0.02g/200g. Both PHL (0.01g/200g) and free (0.01g/200g) had the lowest quantity of MGDG. DGDG was also extracted in large amounts from this flour with the highest concentration being in the total lipid extraction at 0.09g/200g. In the GL fraction, it was found to be at 0.03 g/200g and at 0.01g/200g or less in the other independent lipid fractions extracted. In addition, the phospholipids, particularly PC (0.02g/200g), were present at higher concentrations in the total lipid fraction compared to other phospholipid groups. Overall, the polar lipids within each extracted lipid groups were found in relatively small amounts (levels of thousandths or ten-thousandths of a

gram), but both phospholipids and glycolipids were present within all fractions tested. For further classification of the polar groups found in each fraction refer to Appendix B.

Finnie et al (2009) determined that the galactolipids are predominantly located on the exterior surface of the starch granule and phospholipids are more concencentrated inside the starch granule. Also, polar lipids in the total lipid fraction (combination of both free and bound) are DGDG, MGDG, PC, and LPC (Finnie et al 2009). The starch lipids mainly consist of phospholipids with the most common being LPC, LPE, LPG, with LPC and LPE having the highest abundance (Finnie et al 2009; Pauly et al 2013). Even though the recovery was in much smaller quantities, the results shown here were comparable to those found during lipid profiling conducted by Finnie et al 2009. The process of milling typically causes polar lipids naturally found in the endosperm and nonpolar lipids from the aleurone and germ to be blended into the flour (Pauly et al 2013).

2.4 Conclusion

The procedures conducted in this chapter for lipid extraction were successful in removing and separating total nonstarch lipids, free, bound, NPL, GL, and PHL lipid fractions from the tested flour sample. The recovery of polar lipids in the tested flour was lower for all fractions except in the total nonstarch lipids and the GL lipids fractions in which the highest polar fractions were MGDG and DGDG. Phospholipids were also recovered at lower concentrations than glycolipids in the sample with the highest concentrations of PC. Overall, these extraction techniques recovered polar lipids and provided defatted flour, which was used for baking in the following chapters.

2.5 References

AACC International. Approved Methods of Analysis, 11th Ed. Method 76-31.01. Determination of damaged starch-spectrophotometric method. Approved January 10, 2014. AACC International: St. Paul, MN. http://dx.doi.org/10.1094/AACCIntMethod-76-31.01.

Chung, O.K, Ohm, J-B., Ram, M.S., and Howitt, C.A. 2009. Wheat lipids. Pages 363-373 in: Wheat Chemistry and Technology, 4th Ed. K. Khan and P.R. Shewry, eds. AACC International, Inc.: St. Paul.

Finnie, S.M., Jeannotte, R., and Faubion, J.M. 2009. Quantitative characterization of polar lipids from wheat whole meal, flour, and starch. Cereal Chem. 86: 637-645.

Gan, Z., Angold, R.E., Williams, M.R., Ellis, P.R., Vaughan, J.G., and Galliard, T. 1990. The microstructure and gas retention of bread dough. J Cereal Sci. 12: 15-24.

MacRitchie, F., and Gras, P.W. 1973. The role of flour lipids in baking. Cereal Chem. 50:292-302.

Pauly, A., Pareyt, B., Fierens, E., and Delcour, J.A. 2013. Wheat (*Triticum aestivum L.* and *T. turgidum L.* ssp. *Durum*) Kernel Hardness: I. current views on the role of puroindolines and polar lipids. Compr Rev Food Sci. 12: 413-426.

Sroan, B.S., Bean, S.R., and MacRitchie, F. 2009. Mechanism of gas cell stabilization in bread making. I. the primary gluten-starch matrix. J Cereal Sci. 49: 32-40.

Xiao, S., Gao, W., Chen, Q-F., Chan, S-W., Zheng, S-X., Ma, J., Wang, W., Welti, R., and Chye, M-L. 2010. Overexpression of Arabidopsis Acyl-CoA binding protein ACBP3 promotes starvation-induced and age-dependent leaf senescence. The Plant Cell. 22: 1-20.

Yasui, T. 2012. Pleiotropic increases in free non-polar lipid, glycolipid and phospholipid contents in waxy bread wheat (*Triticum aestivum L.*) grain. J Sci Food Agric. 92: 2002-2007.

Table 2.1 Mean composition and levels of polar lipids found in control flour

Lipid Type[a]	Lipid Fractions									
	Total Lipids		Bound		Free		PHL		GL	
	g/200g[b]	%	g/200g[b]	%	g/200g[b]	%	g/200g[b]	%	g/200g[b]	%
MGDG	1.20E-01	6.00E-02	3.00E-02	1.00E-02	1.00E-02	6.37E-03	1.00E-02	6.5E-03	2.00E-02	1.00E-02
DGDG	9.00E-02	5.00E-02	1.00E-02	5.50E-03	1.00E-02	5.54E-03	1.39E-03	6.95E-04	3.00E-02	2.00E-02
PG	3.98E-04	1.99E-04	9.41E-05	4.71E-05	3. 90E-05	1.95E-05	1.92E-05	9.58E-06	1.20E-05	6.00E-06
LPG	2.03E-04	1.02E-04	7.77E-05	3.88E-05	3.33E-05	1.66E-05	3.79E-06	1.90E-06	1.55E-05	7.76E-06
LPC	1.60E-03	8.00E-04	8.81E-04	4.40E-04	2.31E-04	1.15E-04	6.22E-05	3.11E-05	2.78E-07	1.39E-07
LPE	1.37E-04	6.85E-05	6.32E-05	3.16E-05	1.94E-05	9.71E-06	1.67E-05	8.35E-06	5.47E-07	2.74E-07
PC	2.00E-02	1.00E-02	4.14E-03	2.07E-03	2.38E-03	1.19E-03	2.08E-03	1.04E-03	6.91E-06	3.46E-06
PE	1.35E-03	6.74E-04	3.47E-04	1.73E-04	1.62E-04	8.11E-05	2.00E-04	9.99E-05	9.93E-06	4.97E-06
PI	6.67E-04	3.33E-04	6.60E-04	3.30E-04	1.47E-04	7.36E-05	2.10E-05	1.05E-05	2.41E-05	1.20E-05
PS	2.37E-04	1.18E-04	3.67E-05	1.84E-05	5.27E-05	2.64E-05	4.68E-06	2.34E-06	4.45E-06	2.22E-06
PA	1.97E-03	9.86E-04	5.44E-04	2.72E-04	2.65E-04	1.33E-04	1.33E-05	6.67E-06	4.29E-05	2.14E-05
Total PL Lipids	2.40E-01	1.20E-01	4.00E-02	2.00E-02	3.00E-02	1.00E-02	2.00E-02	1.00E-02	6.00E-02	3.00E-02

[a]Monogalactosyldiglyceride (MGDG), digalactosyldiglyceride (DGDG), phosphatidylglycerols (PG), Lysophosphatidylglycerols (LPG), Lysophosphatidylcholines (LPC), Lysophosphatidylethanolamines (LPE), phosphatidylcholines (PC), phosphatidylethanolamines (PE), phosphatidylinositols (PI), phosphatidylserines (PS), and phosphatidic acid (PA)
[b] Amounts (g) of polar lipids found in each lipid fraction extracted from 200 g of flour (n=25)

Chapter 3 - The Influence of Native Wheat Lipid Fractions on the Rheological Properties of Dough and Gas Cell Structure and Distribution in Bread

3.1. Introduction

The dough network is a very complex system consisting of many components. Together, they allow for the entraptment of air cells during mixing and expansion of these cells during fermentation. Within this system, a combination of proteins and starch form the gluten-starch matrix or the backbone structure, and two other internal phases; a gas phase filled with gas cells and a liquid phase that surrounds these cells (Turbin-Orger et al 2015). Within these phases, smaller molecules such as arabinoxylans, pentosans, and lipids containing surface-active functional groups are able to align around the cells to help maintain their stability over time (Turbin-Orger et al 2015). Because of the expansion and growth of these gas cells, especially during the later stages of proofing and the beginning of baking, the gluten-starch matrix weakens, leaving gaps in the structure where gas cells can migrate towards one another (Gan et al 1990). A secondary support system, liquid lamellae comprised of amphiphilic molecules such as lipids, helps the gas cells to stay in place (Sroan et al 2009; Sroan and MacRitchie 2009). Gas cell stability is very important as it is essential for the development of the dough microstructure, which is the basis for the crumb, texture, and sensorial properties of bread.

The roles of wheat lipids in bread-baking have been thoroughly studied and evaluated as they influence dough and the properties of bread (Hoseney et al 1969; Hoseney et al 1970; Hoseney et al 1972; MacRitchie and Gras 1973; Chung and Tsen 1975; De Stefanis and Ponte, Jr. 1976; Chung et al 1982; Ohm and Chung 2002; Sroan et al 2009; Gerits et al 2014). The classification of wheat endosperm lipids is based on solvent polarity used for extraction (Chung et al 2009). Specifically, nonstarch lipids are those that are not associated with the starch granule and do not require starch gelatinization for extraction (Finnie et al 2009). In contrast, starch lipids are tightly linked to the starch granule. The starch must undergo gelatinization in order to extract them (Finnie et al 2009). The nonstarch lipids can be broken down into free and bound lipids, where both contain a combination of polar and nonpolar lipid types (Chung et al 2009). It

has been recognized that polar lipids have a positive impact on loaf volume as compared to nonpolar lipids, which are damaging (MacRitchie and Gras 1973). Free polar lipids have the greatest effect on the loaf volume and air cell stabilization while a smaller influence is seen with the addition of bound polar lipids (Hoseney et al 1969). Nonpolar lipids have an overall negative effect on bread, causing a decrease in volume and quality of the crumb (Daftary et al 1968; MacRitchie 1977). Nonpolar lipids can be found only in the "bulk phase" of the dough and provide no influence at the interface (Li et al 2004).

Polar lipids, specifically glycolipids and phospholipids, stabilize air/gas cells due to their amphiphilic functional groups (consisting of both water-loving and water-hating components). Their structure can be oriented into a compressed monolayer at the interface (Sroan and MacRitchie 2009). This provides the additional layer, or lamella, that helps to control and prevent gas cell migration due to the loss or deterioration of the backbone structure (Sroan et al 2009; Gerits et al 2014). Once some of the gluten matrix is displaced due to continued expansion, polar lipids are able to move into the interface and provide support even when there are high internal pressures in the dough during development (Paternotte et al 1994). The polar lipids are the most beneficial in improving and maintaining loaf volumes because of their higher melting points and their ability to withstand higher pressures without breakdown as compared to proteins (Pomeranz et al 1966; MacRitchie and Gras 1973; Keller et al 1997). However, condensed monolayers can be converted into detrimental expanded monolayers by high temperatures, the addition of higher levels of unsaturation to the lipid molecule, and by decreasing the overall chain length (MacRitchie 2010). The level of added polar lipids can also negatively affect loaf volume, as too much or too little can have a competing effect between one another or proteins (MacRitchie 1977).

The visco-elastic wheat flour dough is unique in that it can be extended allowing for gas cell expansion. This is important for final loaf quality and the interior crumb grain (Tronsmo et al 2003: Salvador et al 2006). The dough network's properties are dependent on changes in the structure and orientation on a molecular level and this, in turn, is linked to the macroscopic properties (Jekle and Beker 2015). The connection between the micro and macro structure of dough can provide a better understanding of viscoelastic properties and the internal gas cell size and distribution of dough and bread (Jekle and Beker 2015).

The basis for the rheological properties of dough is the creation of bonds either covalent or noncovalent (Skerritt et al 1999). More specifically, it is the connections between the gluten proteins, gliadin and glutenin, and starch that are the main contributors to dough structure as well as the changes in its viscoelastic properties (Miller and Hoseney 1999; Gómez et al 2011). This interaction is highly dependent on mixing and the hydration of both the proteins and starch granules (Jekle and Beker 2015). During mixing, the high molecular weight proteins contained in the gluten change in concentration and orientation and starch granules become imbedded into the newly formed matrix (Skerritt et al 1999; Tronsmo et al 2003). Mixing causes lipids to bind to the gluten proteins forming "lipoprotein complexes." Specifically lipids containing galactosyl groups (monogalactosyl diglyceride and digalactosyl diglyceride) become linked either by hydrophobic or hydrophilic interactions (Hoseney et al 1970). In the end, the structural basis for dough is a combination of protein-protein, starch-starch, starch-protein, with contributions from minor components such as the water-soluble fractions and lipids (Tronsmo et al 2003).

Sroan et al (2009) evaluated the presence of native wheat lipids as "surface active compounds" and their influence on dough rheology. This work found that the lipids didn't affect the dough's bulk rheological properties, but confirmed their role in the formation of the liquid lamellae and stabilizing air cells over time. Due to the lipid's inability to influence cell elongation and changes in biaxial rheology, the total, polar, and nonpolar fractions had no affect on the overall rheological properties of the gluten-starch matrix (Sroan and MacRitchie 2009). Other researchers found that lipids on the surface of starch affected the interactions between the starch and gluten in wheat dough (Miller and Hoseney 1999).

Many studies have been conducted on the rheological properties of dough and how both small and large deformation affect the dough's visco-elastic characteristics (Smith et al 1970; Dreese et al 1988; Weipert 1990; Campos et al 1997; Miller and Hoseney 1999; Tronsmo et al 2003; Watanabe et al 2003; Agyare et al 2004; Silwinski et al 2004a; Silwinski 2004b; Georgopoulos et al 2006; Salvador et al 2006). Small and large deformation rheological testing measures the changes in both the microstructure and macrostructure of dough (Tronsmo et al 2003). Small deformation tests can provide a better understanding of the interactions between compounds such as starch and protein or protein and protein and how these connections affect the viscous and elastic properties (Tronsmo et al 2003). This testing utilizes the application of small amounts of strain and stress, but is unique in that it maintains the integrity of the sample

(Weipert 1990). Because the development of dough is dependent on moisture, work energy, temperature, flour quality and composition, and ingredients, understanding functionality at the microstructure level is essential (Campos et al 1997). Both the storage (G') and loss modulus (G") can be determined from small deformation testing, providing a better understanding of the elastic and viscous components of dough (Agyare et al 2004). Much work conducted on wheat flour properties have illustrated that for wheat dough the storage modulus (G') is larger than the G" (loss modulus) indicating that dough behavior is more elastic in nature than a flowing liquid (Létang et al 1999).

Large deformation testing shows the changes that occur during the processing steps of dough development reflecting how applied work (energy) affects dough structure (Sliwinski et al 2004). This testing evaluates changes based on dough stretching and elongation as opposed to shear stress and strain (Dobraszczyk and Roberts 1994). The technique provides a better representation of what differences in fermentation and dough processing can do to the structural integrity of dough. These test showed that glutenin exhibits more elastic surface properties than does gliadin (Dobraszczyk and Roberts 1994; Li et al 2004).

Also in larger deformation analysis, measurements of strain hardening helps to provide a better understanding of the dough's ability to hold air cells (MacRitchie 2010). Specifically, strain hardening is thought to occur due to the presence of "entanglements" created from gluten polymers that have specific molecular weight distributions that form secure linkages between one another (Sroan et al 2009). As the gas cells continue to grow and expand, the outer cell wall layer of the structural matrix begin to stretch to the point of excess thinning until a breakdown occurs allowing for gas cell movement (MacRitchie 2010). However, if there is equal change between the stress and the strain of the dough matrix at the thinned point, then this part becomes stabilized and expansion of the gas cells continue around the thicker part of wall (MacRitchie 2010). Strain hardening is influenced by the make-up of the dough and the amount and rate of the force applied (MacRitchie 2010). Glutenin has been shown to be the biggest contributors to strain hardening because it "can form entanglements" as compared to gliadin, demonstrating more viscous behavior (Li et al 2004).

The Mixolab measures mixing, pasting, and enzymatic activity of complex systems under specified temperature constraints and provides a basis for understanding visco-elastic properties of dough (Bonet et al 2006). Water and flour are blended and kneaded together by two mixing

blades and real time torque measurments can be determined at each stage of an applied temperature ramp (Bonet et al 2006). This method helps to provide analysis of chemical and physical changes that occur within the dough (Bonet et al 2006).

In addition to understanding the function of lipid addition on dough properties, the evaluation of how these compounds influence air cell distribution and stability in the final product also is very important. Most techniques used to view the internal structure of a sample are limited to their harsh sample preparation and invasive methodology (Babin et al 2006). C-Cell imaging and x-ray microtomography (non-invasive) are two techniques that can be utilized to determine varying properties of the structure within an aerated system (Trinh et al 2013). C-Cell imaging utilizes two-dimensional (2D) analysis by capturing an image of the sample with a camera and this equipment can provide information on "cell wall thickness, size, position, and elongation of the cells" (Whitworth et al 2005). This view provides measurements of the sample on macro scale. X-ray microtomography can provide a better internal view of the sample through the use of 3-D image analysis (Moreno-Atanasio et al 2010). Samples are scanned into slices through the absorption of x-rays and the image slices are reconstructed into a 3-D image (Moreno-Atanasio et al 2010). This particular technique provides a microscopic view of the interior structure of an aerated product and allows for measurement of gas cell thickness, distribution, and size (Moreno-Atanasio et al 2010). Both of these techniques have been widely used as methods for viewing parameters related to gas cells in aerated food products (Falcone et al 2004; Falcone et al 2005; Babin et al 2006; Lodi and Vodovotz 2008; Alvarez-Jubete et al 2010; Moreno-Atanasio et al 2010; Besbes et al 2013; Cafarelli et al 2014a; Van Dyck et al 2014; Villarino et al 2014).

Native wheat lipids are important for air incorporation and stability, both of which influence dough rheological properties and final product quality (Gertis et al 2014). The preservation of gas cells allows for expansion of the dough and is essential for crumb development and overall loaf volume (Gerits et al 2014). However, the effects of lipids on the rheological properties of dough aren't fully understood. To better understand wheat lipid functionality, especially on dough rheology and microstructure, the objectives of this study were to evaluate the effects of wheat lipid fractions (nonpolar, phospholipids, and glycolipids) on the rheological properties of dough using small deformation (dynamic oscillatory) and large

deformation (Kieffer Rig) testing and on the gas cell structure and distribution of bread through C-Cell imaging and x-ray microtomograhpy.

3.2. Materials and Methods

3.2.1. Flour

Kansas grown, hard red winter wheat was milled into straight grade flour at the Hal Ross Flour Mill at Kansas State University (Manhattan, KS). The flour was produced at 73% extraction with a protein content of 10.36%, ash of 0.55%, and starch damage of 7.1% (AACCI Method 76-31.01) (AACCI 2014). Following milling, samples were collected into 2.3 kg (50 lb) bags and placed into -18°C freezer storage until utilized for analysis.

3.2.2. Defatting and reconstitution of lipids from flour

For the methodology and techniques for the defatting and reconsitituion of the varying lipid types from flour please refer to Chapter 2.

3.2.3. Physical and chemical properties of wheat flour

3.2.3.1. Moisture analysis

Moisture analysis was conducted in triplicate on both control and defatted flours following AACC method 44-15.02 (AACCI 1999).

3.2.3.2. Mixograph

Flour absorption and mix time for the control and defatted flours were determined using the 35 g mixograph (AACCI Method 54-40.02) and Mixosmart software (National Manufacturing, Lincoln, NE) (AACCI 1999). The control flour was measured once at 59%, 60%, 60.5%, and 62% absorption and the defatted flour was assessed once at 59%, 62%, 64%, and 65% absorption (See Appendix A). Based on the mixograph curves, absorption and optimum mix time was evaluated during a practice bake to determine mixing times and water absorptions that would produce the best loaves for each flour treatment. The results from the practice bake were used for the actual treatment baking.

3.2.4. Mixolab

Mixolab (Chopin Technologies, Villeneuve-la-Garenne, France) analysis was conducted on control, defatted, and two reconstituded flours containing level variations (50% and 100%) of total lipid addition added to 100 g and 200 g defatted flour. The Mixolab testing was performed as a one-way statistical treatment structure with 4 levels (control, 0%, 50% and 100%). of lipid treatments. All samples were evaluated without the addition of yeast and four replicates of each tested treatments were evaluated. The procedure followed the Chopin+ protocol consisting of an initial mixing step where flour and water were blended at a constant temperature (30°C) followed by an increasing temperature until 90°C and then cooling to 50°C. The temperature ramp was set at 4°C /min and broken into 4 stages starting with dough development (8 min), protein reduction and starch gelatinization (15 min), combined time for setback (7 min) and starch gelling (10 min), and cooling (5 min). The software analysis was set at a 14% moisture basis and the test was conducted for the control (8.9% moisture content) at 57.8% absorption and the defatted samples (9.3% moisture content) were tested at 57.7% absorption.

3.2.5. Dough development

Dough for rheological testing was made from flour containing various lipid fractions following AACCI method 10-10.03 (AACCI 1999). Modification to the method included the exclusion of shortening and treatment sampling of the dough was done prior to the bake step. Pup-loaves (100 g) were made from control flour containing all native lipids, and from defatted flours consisting of nonpolar, phospholipids, and glycolipids fractions. Flours were based on 14% moisture and flour weights for each treatment loaf were determined following AACCI method 82-23.01(AACCI 1999). Flour absorptions and mixing times were optimized using the mixograph results and during the practice bake prior to doing treatment testing. The dough was fermented and proofed in a fermentation cabinet (National Manufacturing, Lincoln, NE) at 86°F (± 5°F) at a 92-95% relative humidity. The dough was fermented for 90 min with a punching step at 52 min and at 77 min using a double rolled sheeter (National Manufacturing, Lincoln, NE). Following the fermentation, dough was rounded using a moulder (National Manufacturing, Lincoln, NE), panned, and proofed for 39 min.

3.2.6. Dough rheology (small amplitude oscillatory measurements)

The visco-elastic properties of control, defatted, and defatted flour samples containing NPL, GL, and PHL were analyzed using a StressTech HR Rheometer (ATS RheoSystems, Bordentown, NJ) where stress, frequency and temperature sweep testing was performed. Dough samples (100 g) were made following the AACCI method 10-10.03 (Please refer to section 3.2.9 for full procedure) without shortening. The control dough was optimized for absorption and mix time using the mixograph and through a practice bake to determine optimum levels (see section 3.2.5). The control dough contained 60.5% absorption and was mixed for 3 min 30 sec and the defatted dough was mixed at 64% absorption for 4 min. Samples were evaluated "after mixing," which didn't include fermentation or proofing steps. The "proofed" samples underwent fermentation for 90 min followed by panning then proofing for 39 min. Treatments were prepared and had to be transferred to the rheometer. The after mixing samples were carried in a steel bowl covered with aluminum foil and the proofed dough were panned and brought to the rheometer also covered in aluminum foil. Small pieces (2.5 ± 0.5 g) of dough were taken from the larger sample following mixing then pressed biaxially in a pasta press (0.5 cm) (Tipo Lusso Sp 150, Imperia Titania, Torino, Italy). For the proofed dough, loaves were cut 2.5 cm deep using a baker's knife and a 2.5 g (±0.5 g) piece was removed from the center and pressed biaxially using the pasta press. Dough samples were put onto the lower plate of the rheometer, covered with two metal plates to minimize drying, and allowed to equilibrate and relax for 5 min before any testing was conducted. Stress and frequency sweep testing were setup as a completely randomized 5 x 2 factoral design with 5 levels of lipid treatments by 2 processing treatments. The temperature sweep testing was conducted as a one-way statistical treatment structure with 5 levels of lipid treatments.

3.2.6.1. Stress sweep testing -linear visco-elastic region (LVR)

The linear visco-elastic region (LVR) was first determined for all treatments using oscillation stress sweep (RheoExplore Ver 5.0.40.9, Rheologica Instrumentation, Bordentown, NJ) at 25°C. The rheometer was set to a 2 mm gap and the gap zeroed between every sample test. A serrated parallel upper plate apparatus (P-25 serrated plate) was used to conduct all the rheological testing. The system was set for measurement "to gap" reading with a max load force of 2.00E+1 N. The serrated plate was stopped 0.1 mm above the gap setting to trim excess

dough. Following trimming, mineral oil was added to the edges of the dough to prevent moisture loss during the run and the sample was allowed to relax for 900 s before the stress sweep test was performed. The stress sweep frequency was 1 Hz, measurement interval 20 sec, delay time 1 sec, FFT at 512. The stress was applied between 1-100 Pa and 60 data points were recorded per run. The control, defatted, and all lipid treatments were tested to determine the LVR for both after mix and proofed. From the LVR, the optimum stress was determined to be 40 Pa. This was used for the rest of the testing on all samples. Three replications were conducted on each independent dough treatment (n=15).

3.2.6.2. Frequency sweep testing

Utilizing the 40 Pa stress (above), frequency sweep testing (RheoExplore Ver 5.0.40.9, Rheologica Instrumentation, Bordentown, NJ) was performed under constant stress conditions. All dough was prepared in the same way as for the LVR testing and each treatment tested after mixing and proofing. Samples were evaluated at a constant temperature (25°C). The dough was subjected to frequency sweeps between 0.1 and 100 Hz. The load force was set to 2.00E+1 N, measurement interval at 20 sec, delay time at 1 sec, and FFT at 512. Testing recorded 100 points between the set frequencies and each of the dough treatments were analyzed at least in triplicate replications (n=21).

3.2.6.3. Temperature sweep testing

Temperature sweep testing (RheoExplore Ver 5.0.40.9, Rheologica Instrumentation, Bordentown, NJ) was conducted on each treatment sample across a temperature range of 25°C to 95°C. All dough was prepared the same way as for the stress and frequency sweep testing except that samples were evaluated only after mix. The rheometer was set to a 2.5 mm gap and the gap was zeroed between every sample test. A serrated parallel upper plate apparatus (P-25 serrated plate) was used to conduct all the testing and the plate was stopped 0.1 mm above the gap setting to trim excess of the sample. Mineral oil was added to the edges of the dough to prevent moisture loss during the run and the sample relaxed for 900 s before the test. The max load force was set to 2.00E+1 N, frequency 1Hz, 40 Pa stress, and FFT at 512. Testing was conducted over 4440 s with 148 points recorded for each run. A minimum of three replicate runs were conducted on each treatment (n=21).

3.2.7. Dough Rheology (large deformation)

3.2.7.1. Biaxial extension (Kieffer Rig)

Extensional testing of dough was performed using a TAXT-Plus texture analyzer (Texture Technologies, Hamilton, MA) with a Kieffer extensibility rig. This technique evaluated dough extension through uniaxial motion (Dunnewind et al 2004). Nonpolar (4.5 % ± 0.2), phospholipids (0.45 % ± 0.3), and glycolipids (2.5% ± 0.3) fractions were added back to 100 grams of flour and the flour was left to dry overnight to allow solvent evaporation. Flour amounts for each 100-gram dough were determined based off of 14% moisture basis. Absorptions and mix times were the same as for the other rheometer treatments. Samples were mixed in a 100 g pin mixer bowl and dough was stopped 30 secs before reaching optimum mix time (Control- 3 min; defatted and lipid treatments 3.5 min). Following mixing, 10 g of dough was removed from the larger dough ball and gently pulled into a rectangle. The dough was placed on an oiled, plastic mold that contained small grooves were strips of small plastic were laid in each groove. Enough dough was used to cover 5 grooves on the mold that made 5 small strips of dough. A rectangle solid block was put on top of the dough and then the mold was inserted into a metal press. Excess dough was cut off of the edges of the mold following being pressed and allowed to equilibrate for 30 min.

Texture analyzer settings were setup for gluten extensibility testing (Kieffer Rig), using a preset sequence within the TAXT-Plus software (Exponent Stable Microsystems, Version 6, 1, 5, 0, Texture Technologies, Hamilton, MA). The test mode was set for tension, pre-test speed: 5.00 mm/sec, test speed: 3.30 mm/sec, post-test speed: 10.00 mm/sec. The target mode was set for distance: 75 mm, trigger type: Auto (Force), trigger force: 5.0 grams and results were shown as distance (mm), force (gram), and time (sec). Extensibility measurements were taken by placing dough in between two plates while a small hook caught and stretched the dough as it moved upward vertically until the dough had reached its breaking point. Five strips were measured for each dough with 3 independent dough treatments measured from the control and defatted samples and 4 independent dough treatments for all the lipid samples (n = 90). The raw data was collected from each curve and a macro setup in the texture analysis software was used to determine force and distance measurements from each treatment. This testing was designed as a one-way treatment structure with 5 levels of lipid treatments.

3.2.7.2. Strain Hardening

Strain hardening values were calculated from the uniaxial measurements of force and distance raw data obtained from the Kieffer rig testing. Equations and calculations were conducted in accordance with Abang Zaidel et al (2008).

3.2.8. Flour reconstitution for microstructure bread analysis

The lipid fractions were added back to defatted flour based on specific final concentrations (nonpolar (2.3 % ± 0.2), phospholipids (0.23 % ± 0.3), and glycolipids (1.3% ± 0.3) needed for testing. For macro XMT testing (whole loaf), the samples were taken for analysis at Cargill Global Foods Research (Wayzata, MN) and lipids were fractionated into nonpolar, glycolipids, phospholipids. Each fraction was added back at the same levels at which they were isolated. Chloroform (2 mL) was added to each nitrogen-dried vial and was vortexed to re-suspend the lipids (Fisher Vortex Genie 2, Fisher Scientific, Pittsburgh, PA). The resulting chloroform/lipid solution was added directly back into 200 g of defatted flour at the same concentration at which they were extracted then mixed using a pestle. The samples were dried overnight at room temperature and the flour was split into 100 g portions for baking.

For micro XMT (center section) reconstitution testing, lipid addition was based on the concentrations of each lipid fraction established from previous research (Chung et al 2009). Levels were increased to evaluate the full influence of each fraction. Defatted flour contained 0% lipids. Nonpolar lipids were blended in at concentrations of 0.6%, 1.2%, and 2.5% while polar lipids (combination of both glycolipids and phospholipids) were added at 0.2%, 0.4%, and 0.6%. For reconstitution, all samples utilized each bake day were removed from the freezer and allowed to come to room temperature (~1 h). Flour samples were weighed (100 g) and each lipid treatment was re-suspended into 2000 µL of chloroform and vortexed. Amounts were added back based on the desired concentration and taken from the 2000 µL chloroform + lipid samples with 1000 µL or 200 µL pipettes. All samples were mixed into the flour and blended using a pestle. The reconstituted flour was air dried overnight to remove any remaining solvent.

3.2.9. Analytical baking

Flours were baked as 100 g pup-loaves following AACCI method 10-10.03 (AACCI 1995). Modification to the method included the exclusion of shortening in order to fully evaluate the influence of the lipid fractions on final product. Flours were based on 14% moisture and flour

weights for each treatment loaf were determined following AACCI method 82-23.01 (AACCI 1961). Flour absorptions and mixing times were optimized using the mixograph results and during the practice bake prior to doing treatment testing. Loaves were made following a 90-min fermentation using a 4 min baking schedule. The dough was fermented and proofed (National Manufacturing, Lincoln, NE) at 86°F (± 5°F) at 92-95% relative humidity, punched twice at 52 min and 77 min using a double roll sheeter (National Manufacturing, Lincoln, NE). Following fermentation, dough was rounded using a moulder (National Manufacturing, Lincoln, NE), panned, and proofed for 39 min. Loaves were baked for 24 min, then cooled for 2.5 h. Volume displacement was measured in accordance with AACCI method 10-05.01 (AACCI 1995). Following analysis and cooling, each pup-loaf was wrapped in Saran™ wrap, placed in a zip-lock bag and frozen at -18°C until needed for further analysis. For the whole loaf testing, 8 independent, replicate loaves were made for every treatment and for the center section 9 independent, replicate loaves for each of the 7 treatments were baked for evaluation.

3.2.10. Bread macrostructure (C-Cell imaging)

Treatment loaves were evaluated using C-Cell Imaging (Calibre Control International, Ltd, Warrington, UK) by cutting each loaf into 1.3 cm slices (±0.5 cm) with an electrical food slicer (Chef's Choice, Int., Colorado Springs, Co.). Every fifth slice from the base end with the break and shred facing upward was used for evaluation. Images were taken with the break and shred located on the left side of the slice. Three loaves from each treatment were imaged using the system. Images were analyzed using C-Cell imaging software (C-Cell Version 2.0, Campden & Chorleywood Food Research Association Group, Gloucestershire, UK), which accompanied the equipment. Values determined for each treatment included slice area, number of cells, area of cells, area of holes, number of holes, volume of holes, cell wall thickness, and cell wall diameter.

3.2.11. Bread microstructure (x-ray microtomograhpy)

3.2.11.1. Macro testing (whole loaf)

Total lipids extraction was conducted on 100 g samples of flour. Once removed from the flour, lipids were fractionated and quantified as nonpolar (NPL), glycolipids (GL), and phospholipids (PHL). Lipids were added back to flours at the same level at which they were removed. Average recovery of lipid fractions during the extraction process ranged between 0.2-

2.0 g for NPL, 0.45-1.2 g for GL, and 0.1-0.35 g for PHL. Loaves were packaged and frozen in zip-lock bags at -18°C until transported on dry ice to Cargill (Wayzata, MN). Once on site, samples were stored at frozen temperatures (-18°C). The loaves were pre-wrapped in Saran™ wrap to prevent moisture loss during data analysis. Breads were removed from frozen storage overnight and allowed to come to room temperature (25°C ± 5°C) while still being fully wrapped. Samples were evaluated using an IMAGIX X-ray Microtomograph (North Star Imaging, Inc., Rogers, MN). Full pup loaves were placed on a base platform within the x-ray system and taped down to ensure the sample was secure throughout the testing. All sample measurements were taken at 42 kVs, 100 μA, 720 projections per sample, 4 ms delay, and the stage positioning at 52.3 mm (up/down) and 204 mm table magnification. All samples were analyzed at 61.4 μm resolution. Data analysis was conducted with exf-dr software, while excf-cr software (NorthStar Imaging, Rogers, MN) was used for viewing the images. Image reconstruction was done using exf-cf (NorthStar Imaging, Rogers, MN). The evaluation of binary images and data analysis of the reconstructed sample was done with Ctan software (CT Analyzer, Version 1.10.1.0 Skyscan, Bruker MicroCT, Kontich, Belgium) and provided data that included: air cell size, cell wall thickness, air cell distribution, total porosity, volume index (VOI), structure separation distribution, structure thickness distribution, object volume. Six replicate loaves for every treatment were analyzed.

3.2.11.2. Micro testing (center section)

X-ray microtomography (XMT) analysis of the lipid treatments was conducted using Skyscan 1072 Micro-CT x-ray microtomograph (Skyscan, Belgium) for 0.6% NPL, 1.2% NPL, 2.5% NPL and 0.2% PL, 0.4% PL, and 0.6% PL lipid treatment breads. Three independent loaves from every treatment were tested. Each treatment series was removed from the freezer and with the Saran™ wrap still in place, allowed to stand overnight in the retarder (4°C). Before XMT sampling the loaves were removed from the retarder (~40 min) and allowed to come to room temperature (25°C ±5) to reduce the effects of moisture evaporation during scanning. Bread samples were sliced into 1.3 cm slices (±0.5 cm) using an electrical food slicer (Chef's Choice, Int., Colorado Springs, Co.) and every fourth slice was used for testing. From each slice, an 8 mm x 12 mm cube was cut out of the sample and placed in a plastic tube with matching lid to prevent the sample from drying. The center section sample was securely mounted to the XMT base using a 13 mm two-sided foam adhesive disk. Once placed in the microtomograph, all

samples were allowed to equilibrate for 5 min. XMT images were taken at 41 kV, 102 μA, 1.8 sec exposure, 15-16X magnification, stage position at 11.5 mm (±0.5), and 17.5-18.5 μm pixel resolution. Each treatment sample was rotated at 0.90 scan steps for a total of 180° rotation. Sample reconstruction was conducted using NRecon (Version 1.6.3.3 Skyscan, Bruker MicroCT, Kontich, Belgium). The x-ray scans produced 206, 2-D cross-sectional images for each sample, which was used to reconstruct 3-D structures of the each treatment to determine quantitative values for air cell structure and distribution analysis. The assessment of the binary image and data analysis of the reconstructed sample was done with CTan (CT Analyzer, Version 1.10.1.0 Skyscan, Bruker MicroCT, Kontich, Belgium) and provided data that included: air cell size, cell wall thickness, air cell distribution, % total porosity, volume index (VOI), structure separation distribution, structure thickness distribution, and object volume.

3.2.12. Statistical analysis

Multivariate analysis (ANOVA) was conducted using SAS (Version 9.3, SAS Institute Inc., Cary, NC) with comparisons between sample means using Tukey's least significant difference (LSD) testing at a confidence level of 95%.

3.3. Results

3.3.1. Physical and chemical properties of wheat flour samples

The physical and chemical tested parameters for both defatted and control flours (both macro and micro) are shown in Table 3.1. The macro and micro XMT testing was not conducted at the same time, so the physical parameters were evaluated for each different bake. The differences between bakes was due to changes in the environmental storage conditions and the time that it took to prepare the various lipid treatments. The variations between the treatments themselves (control or defatted) were associated with the properties of the flour rather than environmental conditions. For both tests, the moisture content for the defatted flour was lower than that of the control. This was due to lipid removal by chloroform extraction and drying of the flour overnight. Because of the greater moisture loss, the water absorption of the defatted flour was higher for both bakes than for the control. The defatted flour had an increased affinity for water because of the reduction in polar lipid-protein linkages caused by the lipid removal (Papantoniou et al 2004). The mixing time was also 30 seconds shorter for the control flour (3

min 30 sec) than for the defatted (4 min). The optimized mixographs used to help determine the mixing and absorption parameters for the micro XMT test bake are shown in Figure 3.1.

Table 3.1. Physical and chemical characteristics of control and defatted flours

Parameters	Control (macro)	Control (micro)	Defatted (macro)	Defatted (micro)
Moisture content (%)	13.34	12.59	8.78	8.82
Absorption (%)[a]	62.2	60.5	65.1	64.0
Mix Time[a]	4 m	3 m 30 s	3 m 30 s	4 m

[a]Absorption and mix time were determined by mixograph testing and optimized during the baking process

3.3.1 Mixograph

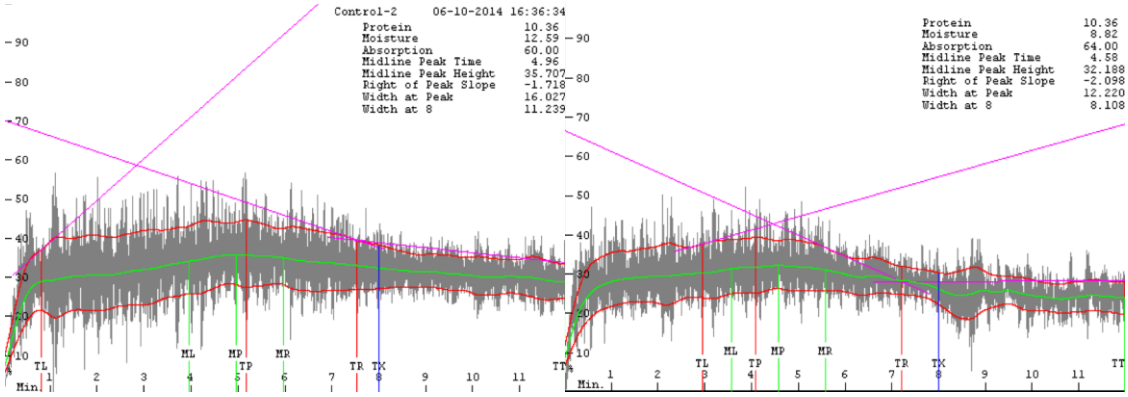

A. Control (60% abs) B. Defatted (64% abs)

Figure 3.1. Optimized mixograph results for sample flours used for testing

3.3.2. Mixolab

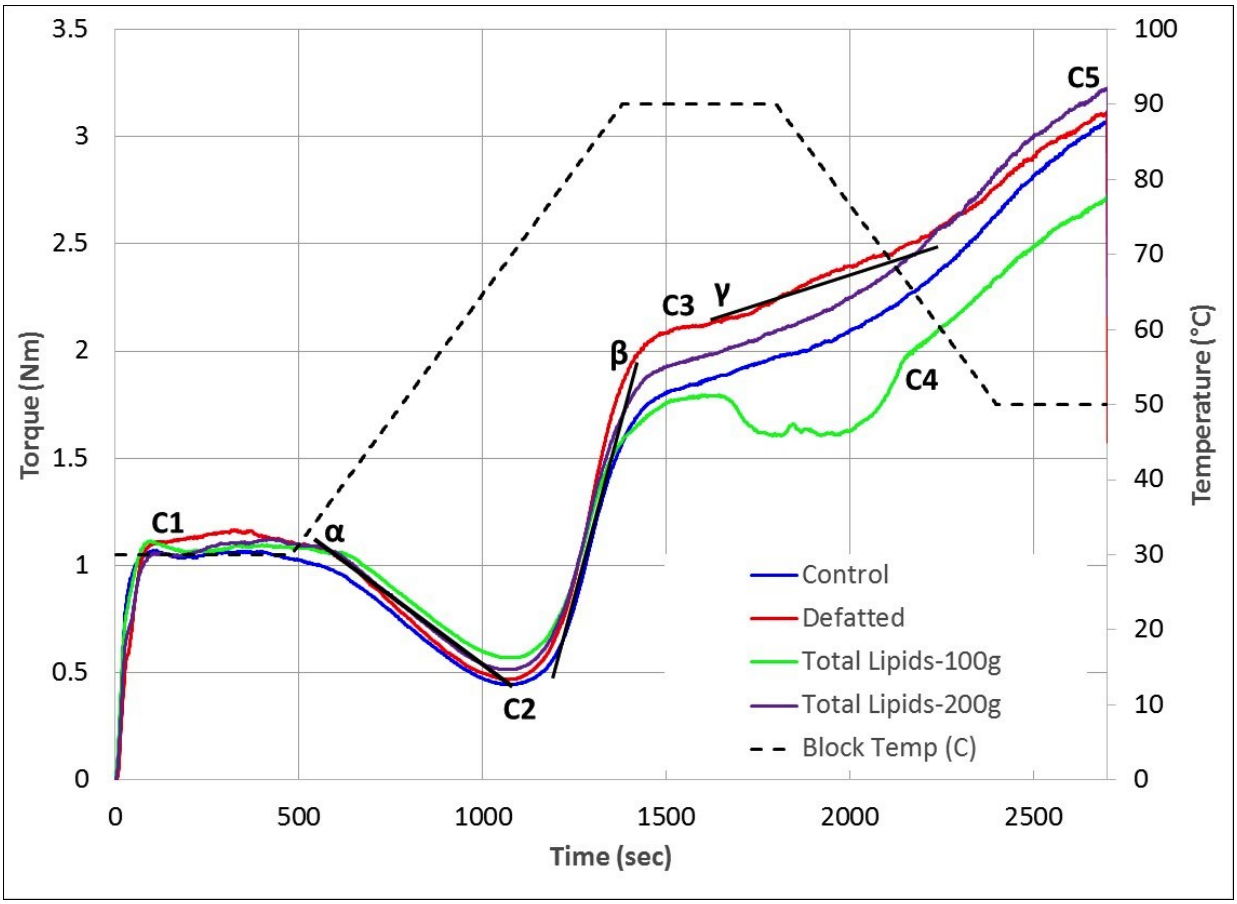

Figure 3.2 Mixolab results for control, defatted (0%), total lipids-100g (50%), and total lipids-200 g (100%)

Table 3.2. Mixolab parameters for control, defatted, and lipid treated flours

Sample[a]	C1 (Nm)	C2 (Nm)	C3 (Nm)	C4 (Nm)	C5 (Nm)	α	β	γ
Control	1.08[a] (0.05)	0.45[a] (0.03)	1.57[a] (0.06)	1.97[a] (0.07)	3.08[a] (0.11)	-0.025[a] (0.01)	0.27[a] (0.03)	0.044[a] (0.02)
Defatted	1.17[b] (0.01)	0.47[ab] (0.04)	2.01[a] (0.32)	2.29[b] (0.11)	3.12[a] (0.14)	-0.047[a] (0.03)	0.22[a] (0.12)	0.013[a] (0.03)
Total Lipids-100g	1.12[ab] (0.03)	0.57[c] (0.01)	1.81[a] (0.03)	1.59[c] (0.02)	2.73[b] (0.01)	-0.044[a] (0.04)	0.24[a] (0.04)	-0.18[b] (0.04)
Total Lipids-200g	1.13[ab] (0.02)	0.51[b] (0.03)	1.94[a] (0.47)	2.22[ab] (0.25)	3.23[a] (0.03)	-0.058[a] (0.02)	0.22[a] (0.11)	0.021[a] (0.03)

[a] Defatted (0% lipid addition), total lipids-100 g (50% lipid reconstitution), and total lipids-200 g (100% lipid reconstitution)
[b]Means in the same column with different letters are significantly different ($p<0.05$)
[c]Values in parenthesis indicate standard deviations
[d] (n=16)

Table 3.3. Mixolab parameters for control, defatted, and lipid treated flours

Sample[a]	Amplitude (Nm)	Stability (min)	Setback (Nm)	Mechanical weakening (Nm)	Thermal weakening (Nm)
Control	0.093[a] (0.01)	10.01[a] (0.18)	1.11 (0.06)	0.053 (0.02)	0.01 (0.01)
Defatted	0.093[a] (0.01)	9.42[b] (0.37)	0.83 (0.14)	0.17 (0.14)	1.07 (0.04)
Total Lipids-100g	0.094[a] (0.01)	10.93[c] (0.10)	1.14 (0.02)	0.020 (0.01)	0.026 (0.01)
Total Lipids-200g	0.090[a] (0.01)	10.13[a] (0.11)	1.01 (0.27)	0.025 (0.00)	0.062 (0.01)

[a] Defatted (0% lipid addition), total lipids-100 g (50% lipid reconstitution), and total lipids-200 g (100% lipid reconstitution)
[b]Means in the same column with different letters are significantly different at ($p<0.05$)
[c]Values in parenthesis indicate standard deviations
[d] (n=16)

The Mixolab helps to provide analysis of chemical and physical changes that occur within the dough (Bonet et al 2006). The phases of the Mixolab results show (C1) mixing, (C2) protein unfolding, starch gelatinization, (C3) setback, (C4) starch gel stability, and (C5) cooling. Figure 3.2 shows the Mixolab results for control, defatted, and total lipid-100 g of flour and total lipids-200 g of flour. No differences were found between test treatments for the mixing stage, protein unfolding/weaking, and the onset of starch gelatinization. However, as the starch started to gelatinize, there was an increase in the height of the curve (increased torque) for both the defatted and total lipids-200 g. Sun et al (2010) determined that defatting flour could delay the onset and speed of gelatinization. Tester and Morrison (1990) also determined that the removal of some of the lipids caused an increase granular swelling while Melvin (1979) observed higher pasting curves in wheat and corn starches with wheat lipids present. Note that the properties of and changes in starch (i.e. crystallinity, amylose and amylopection association, and amount of lipids) in defatted flour was dependent on the experimental conditions such as extraction solvents and temperature (Vasanthan and Hoover 1992).

The curves from total lipid-100 g showed a drop during the starch gelling phase. Takahashi and Seib (1988) determined that adding additional lipids to wheat starch during pasting caused an increase in both the pasting peak and a higher setback peak due to amylose-lipid complexing. The concentration of lipids in this flour was two times the amount found naturally in the wheat. This curve drop was likely due to starch complexing with lipids, particularly forming amylose-lipid complexes (Tang and Copeland 2007). During cooling, more lipids are able to interact with starch causing increased viscosity, but this is dependent on the type of lipids (Takahashi and Seib 1988). Blazek et al (2011) found that long and short chain fatty acids had differing effects on starch properties. The longer chain fatty acids caused a reduction in the formation of tight amylose-lipid complexes and altered the crystallinity and pasting properties of starch. Tang and Copeland (2007) found a dependence on water solubility, concentration, and type of fatty acids that could influence amylose-lipid complexing. Higher concentrations of water and short chain fatty acids prevented linkages to starch, but formed fatty acid micelles.

Other parameters that are determined from the Mixolab curves include: (C1) torque used to determine optimum water absorption, (C2) torque used to determine protein breakdown at high temperatures, (C3) starch gelatinization or cooking stability at 90°C, (C4) starch gel

stability, (C5) starch setback. In addition α (protein weaking caused by applied heat), β (speed of starch gelatinization), γ (setback speed), and amplitude, which is a measure of elasticity of the dough (increased values indicate more elastic dough). Stability is a measure of the dough strength and a longer time indicates a stronger dough. Mechanical weaking and thermal weakening were also calculated for each of the treatments. Sun et al (2010) defined mechanical weaking as the "the torque difference between the maxium torque at 30°C and the torque at the end of the holding time at 30°C" and thermal weaking as the "difference between the holding time at 30°C and the minimum torque." Setback was calculated as the difference between C5 and C4 (Sun et al 2010). Results for these parameters are shown in Table 3.2.

For both 100 g (0.57 Nm) and 200 g (0.51 Nm) samples the addition of total lipids increased the torque needed for protein breakdown compared to both the defatted (0.47 Nm) and the control (0.45) samples. The addition of lipids required more energy for degradation due to lipid protein-binding (Gerits et al 2013). Lipid interactions with gluten proteins are hydrophobic or hydrophilic depending on the polarity of the lipids added (Gerits et al 2013). Gelatinization torque (C3) values were not signicantly different between any of the treatments. These results differ from those of Takahashi and Seib (1988) who observed changes in the pasting curves in the presence of excess water for defatted and lipid containing flours with the amylograph. The starch gel stability (C4) showed the greatest differences between defatted (2.29 Nm) and total lipids 100 g (1.59 Nm). Doubling the amount of lipids caused a change in the consistency of the sample. Again, this was likely related to the types of lipids in the total lipid fractions and the ability for amylose-lipid complexes to be formed (Blazek et al 2011). There was a significant difference between starch cooling torque (C5) values for the total lipids-100 g of flour (2.73 Nm) due to complexing of amylose and lipids. No significant differences were seen between the speed of protein weaking (α) or the starch gelatinization speed (β). However, there was a significant difference in setback (γ) as the total lipid-100 g was lower than all the rest of the treatments.

All the doughs had lower amplitude values, which would indicate the dough exhibited greater viscous properties than elastic characteristics. However, none of the values were significantly different from one another. The total lipids-100 g of flour had the highest overall stabililty (10.93 min) with the defatted (9.42 min) having the lowest. Perhaps because the lipids were removed from the defatted sample this allowed for more protein-protein interactions and reduced lipid-protein interactions causing an increase in denaturation at higher temperatures. The

setback was lowest for defatted flour and highest for total lipids-100 g and these results were comparable to Sun et al (2010) who also determined higher differences between defatted and control samples. The mechanical weaking was lowest for both of the flours containing the lipid treatments and highest for the defatted (0.17 Nm). In this case, the protein-protein interactions appeared to have a strengthening effect on the dough. The control had the lowest thermal weaking measurement (0.01 Nm) while the defatted (1.07), total lipids-100 g flour (0.026 Nm), and total lipids-200 g (0.062 Nm) had a greater effect caused by temperature.

3.3.3. Dough development

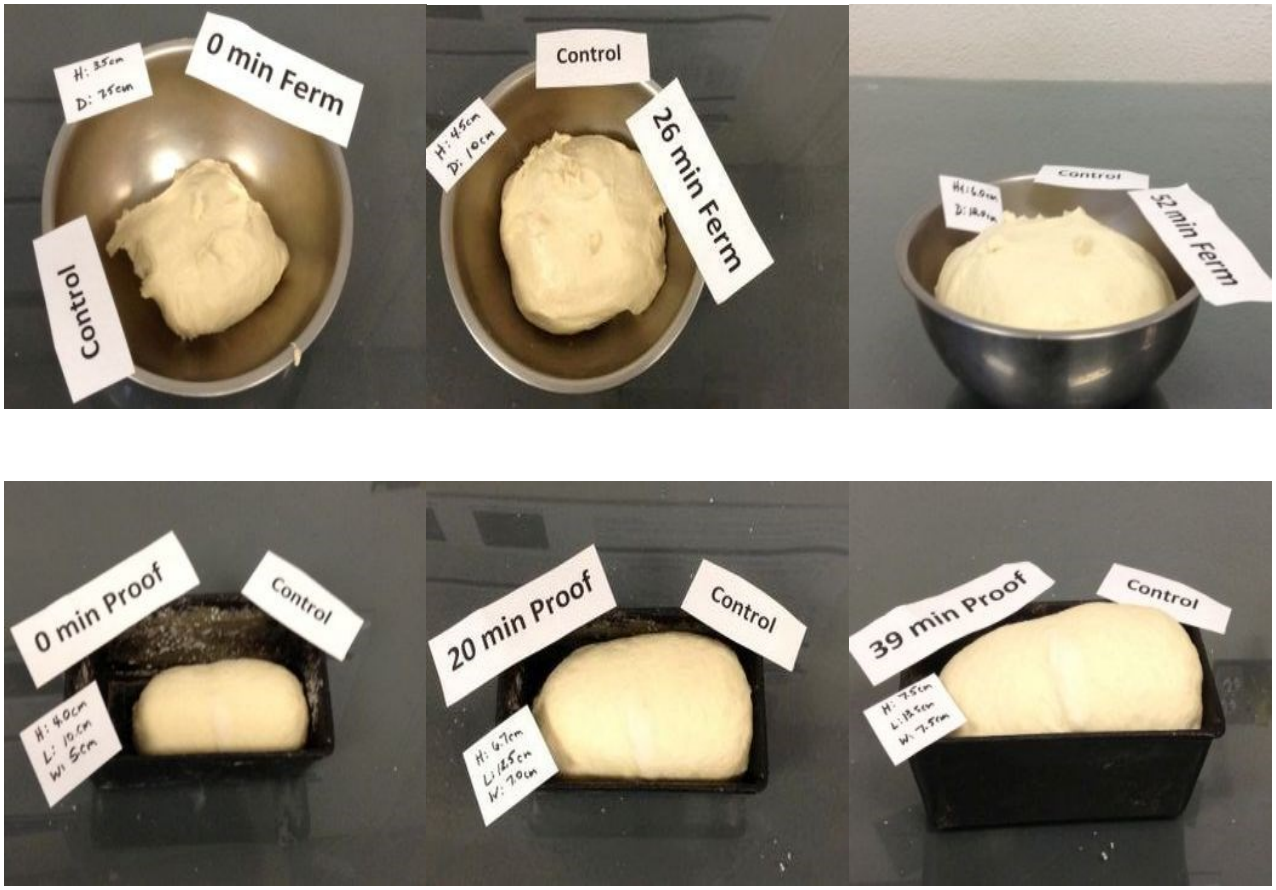

Figure 3.3. Changes in the dough during fermentation and proofing (Control)

Figure 3.4. Changes in the dough during fermentation and proofing (Defatted)

Figures 3.3 and 3.4 illustrate the fermentation and proofing stages of the defatted and control doughs. During fermentation both samples showed an increase in dough size. From 0 min to 52 min the dough diameter and height more than doubled in size. The defatted flour showed a greater increase in height (7.0 cm) than the control (6.0 cm). However, the control diameter (12.8 cm) was wider than the defatted samples (12.0 cm). The defatted dough had more highly cross-linked protein network due to the lipid removal than the control. During proofing, shown at 0 min, 20 min, and 39 min, samples underwent two punching steps and a panning step. This oriented and aligned the cells into two different directions within the dough. Both the defatted and control samples increased in dough volume between 0 min and 20 min, as well as between 20 min and 39 min. Less changes in the dough size and shape were seen during proofing likely due to punching and panning. These steps helped to distribute the gas cells and adjust the cell size.

3.3.2. Dough rheology (small deformation)

3.3.2.1. Stress sweep testing (LVR)

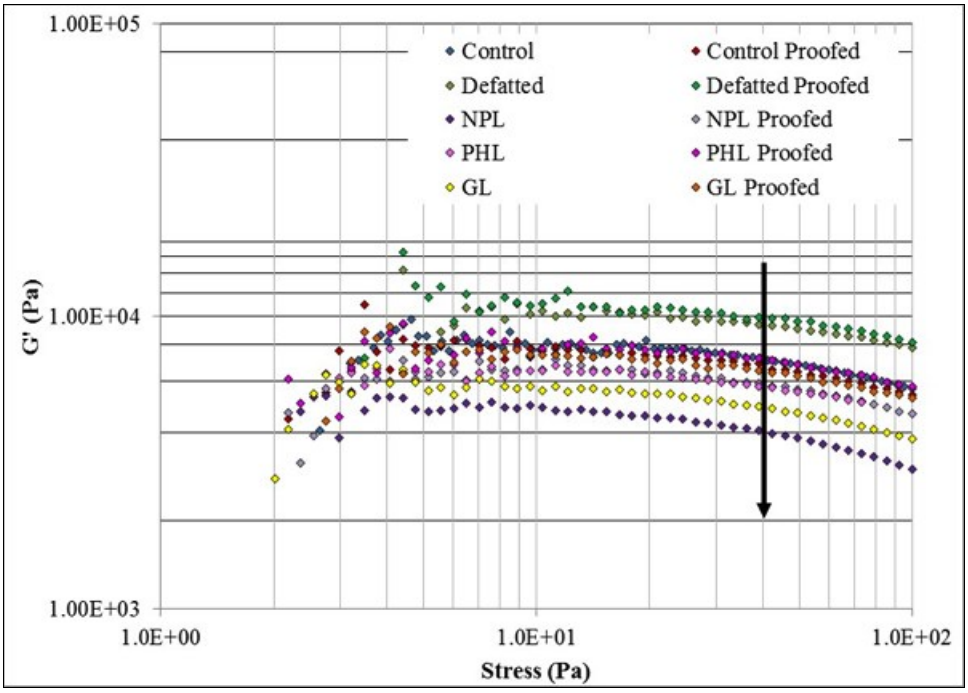

Figure 3.5. Stress sweep results for storage modulus (G') of dough containing lipid treatments tested after mixing and proofing

Because bread exhibits both viscous and elastic characteristics, understanding the changes that occur in these properties during dough formation is important for final product quality. Rheological testing utilizes an applied force or deformation to simulate changes that occur due to small or large extension, compression, and properties based on the flour make-up. As ingredients are blended together during mixing, the applied work causes changes in the dough structure, during fermentation due to gas production, and at moulding and panning (Upadhayay et al 2012). Most of the work conducted on dough is done within its linear viscoelastic region (LVR) or "the region of stress where the strain varies linearly with stress." (Macosko 1994; Campos et al 1997) Beyond this there is a change in the consistency of the sample, making it more challenging to interpret the results. This type of testing doesn't affect the integrity of the dough sample, making the test "non-destructive" (Upadhyay et al 2012).

Figures 3.5 display the changes in the storage modulus (G') as a function of stress between 1 Pa and 100 Pa for both after mixing and after proofing doughs with lipid additions. The LVR region for all treatments fell below 50 Pa (marked with an arrow), so 40 Pa was chosen for subsequent testing to ensure it was within the LVR. In non-yeasted, flour-water dough systems, Autio et al (2001) found the LVR region to be below 1 Pa and Gómez et al (2013) less than 5 Pa. The various wheat flour tested by Hadnađev et al (2013) had LVR ranges between 10 and 15 Pa. In this particular testing the LVR value determined was higher than other previous studies for wheat flour. This could be reflective of other factors including environmental conditions, protein content, and water absorption of the flour.

For both after mix and after proofed stages, there was a decrease in the magnitude of the G' as the applied stress increased for all treatments. Khatkar and Schofield (2002a) and Salvador et al (2006) found similar results where there was a decrease in G' with an increase in the applied stress. The defatted samples exhibited the highest G' values for both the after mix and proofed doughs. The NPL lipid treatments had the lowest values for both after mix and after proof. The PHL, GL, and control fell between these two extremes. At lower levels of stress, interactions are predominately between starch and starch whereas at large deformation the interactions are based on proteins (Song and Zheng 2007).

3.3.2.2. Frequency sweep testing

Frequency sweep testing provides a measure of the strength and the structural characteristics of a sample as it relates to crosslinking within that system (Georgopoulos et al 2006). In the case of dough, the structure is a combination of gluten proteins and starch that fills the spaces between the gluten proteins (Singh and MacRitchie 2001). This combination gives dough the viscous and elastic properties that can be evaluated during frequency sweep testing. The storage modulus (G') measures the solid or elastic behavior of the compound while the loss modulus (G") is indictative of the viscous properties (Khatkar and Schofield 2002a). The ratio of G" to G' is tan δ. This is a measure of the influence of both the viscous and elastic properties on the system (Khatkar and Schofield 2002a). If a material has elastic behavior, G' will be greater than the G" and vice versa if it is more viscous. The tan δ will be less than 1 if it is more elastic and greater than 1 if it is more viscous in nature (Khatkar and Schofield 2002a). Figures 3.6 show storage modulus (G') results for samples tested after mixing, after proofing, and the combination of after mixing and after proofing. Frequencies ranged between 0.1 Hz and 100 Hz

and stress was within the LVR at 40 Pa. The oscillatory rheological testing was conducted with active yeast so the dough underwent fermentation during both testing stages (after mixing and after proof). The fermentation process produces gas that increased the dough bubble size and it has been found that "the shear modulus is inversely proportional to bubble size" (Upadhyay et al 2012). In this case, the results show very small differences between the magnitudes of the treatments between after mixing and after proofing, suggesting there was a limited influence of gas production on the storage modulus compared to those caused by lipid addition during these two phases.

For all treatments, G' increased as a function of frequency. This overall, is an indicator of a weaker dough. The higher magnitude is more associated with weaker doughs that contain larger amounts of starch compared to stronger flour (Khatkar and Schofield 2002b). Masi et al (1998), Khatkar and Schofield (2002b), Salvador et al (2006), Georgopoulous et al (2006), and Singh and Singh (2013) also showed similar increases in G' at higher frequencies. Here the G' suggests that the dough samples containing added lipid at both processing stages behaved more like an elastic-solid rather than a liquid. The defatted flour, both after mixing and proof, had a higher curve magnitude than any other treatments. All the curve magnitudes for G' were lower than after mixing than proof. Georgopoulos et al (2006) found that defatting flour with various solvents caused an increase in the G' frequency dependence and this was associated with higher amounts of friction between the starch granules.

Defatting and reconstitution studies on soft wheat flours found that the starch congregated in "agglomerates and particles" following lipid removal and this caused a layer of protein to surround the starch particles, preventing full hydration of the starch (Papantoniou et al 2004). During after mixing, the G' of the NPL sample was much lower than any of the other treatments. The addition of free fatty acids found in the nonpolar lipids form complexes with themselves or starch and this influences the rheological properties of the dough (Khatkar and Schofield 2002a; Tang and Copeland 2007). Differences between the other lipids treatments and the NPL were lower following proofing.

(a)

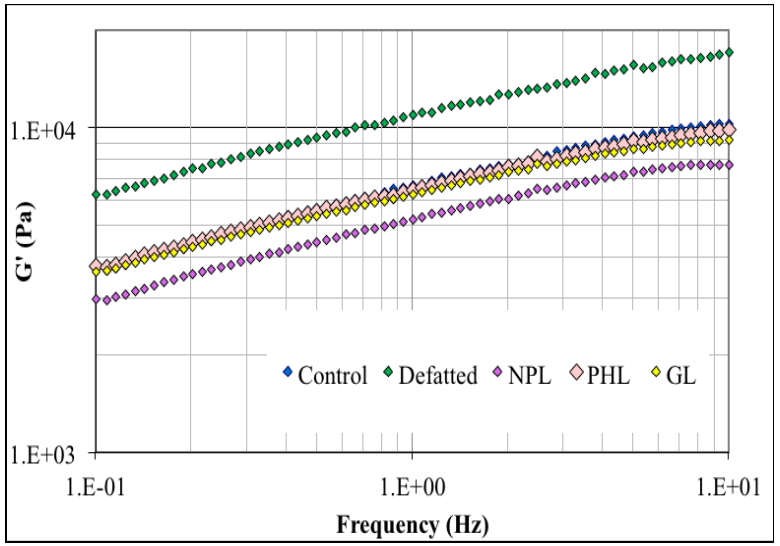

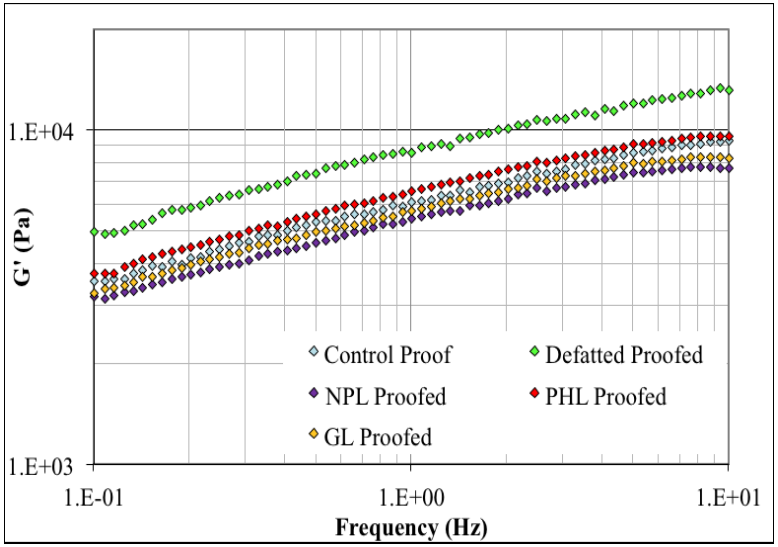

(b)

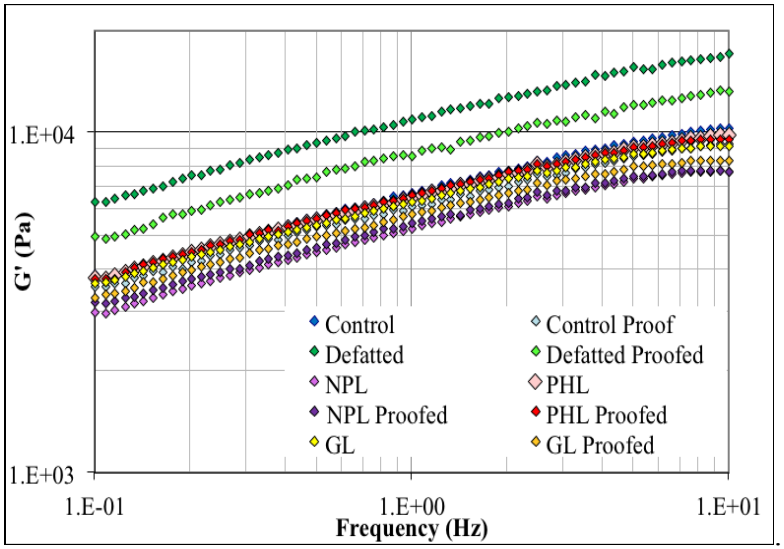

(c)

[a]Nonpolar (NPL), phospholipids (PHL), glycolipids (GL); proofed (after proofing)

Figure 3.6. Dependency of storage modulus (G') on frequency (a) after mixing (b) after proofing and (c) both after mixing and after proofing

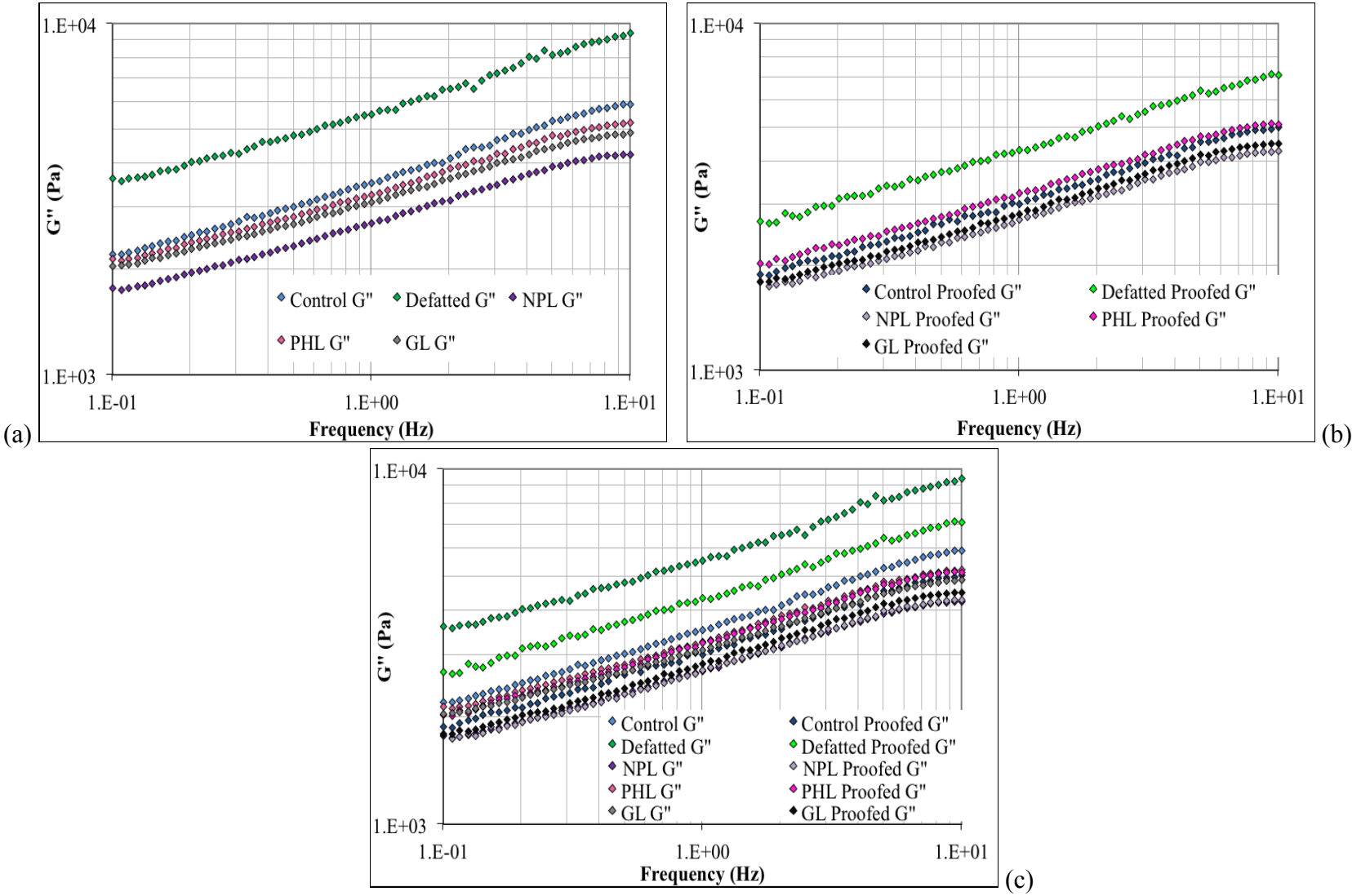

[a]Nonpolar (NPL), phospholipids (PHL), glycolipids (GL); proofed (after proofing)

Figure 3.7. Dependency of loss modulus (G") on frequency (a) after mixing (b) after proofing (c) after mixing and after proofing together

Table 3.4. Slopes of the G' and G" verus frequency values at 1 Hz

Samples[a]	After mixing				After proofing			
	Slope G' (Pa)	Slope G" (Pa)	G' (Pa)	G" (Pa)	Slope G' (Pa)	Slope G" (Pa)	G' (Pa)	G" (Pa)
Control	0.23[a] (0.01)	0.23[a] (0.01)	6683.47[a] (460.10)	3540.70[a] (300.63)	0.22[a] (0.01)	0.22[a] (0.00)	6061.13[a] (403.2)	3055.40[a] (157.64)
Defatted	0.23[a] (0.01)	0.22[ac] (0.01)	10977.87[b] (2158.70)	5607.07[b] (1038.80)	0.22[a] (0.00)	0.22[a] (0.01)	8730.13[b] (1457.50)	4307.53[b] (653.7)
NPL	0.22[a] (0.01)	0.21[bc] (0.01)	5260.98[a] (590.60)	2713.30[a] (254.6)	0.21[a] (0.01)	0.21[a] (0.01)	5425.37[a] (831.90)	2719.40[a] (411.6)
PHL	0.22[a] (0.01)	0.21[bc] (0.01)	6472.90[a] (1259.2)	3272.47[a] (622.00)	0.21[a] (0.01)	0.22[a] (0.01)	6558.40[a] (909.80)	3231.67[a] (435.2)
GL	0.21[a] (0.01)	0.20[b] (0.01)	6265.28[a] (1193.30)	3158.10[a] (617.90)	0.21[a] (0.01)	0.22[a] (0.01)	5753.83[a] (987.90)	2828.60[a] (551.20)

[a] Nonpolar (NPL), phospholipids (PHL), and glycolipids (GL)
[b]Means in the same column with different letters are significantly different at a $p<0.05$
[c]Values in parenthesis indicate standard deviations
[d] (n=21)

(a)

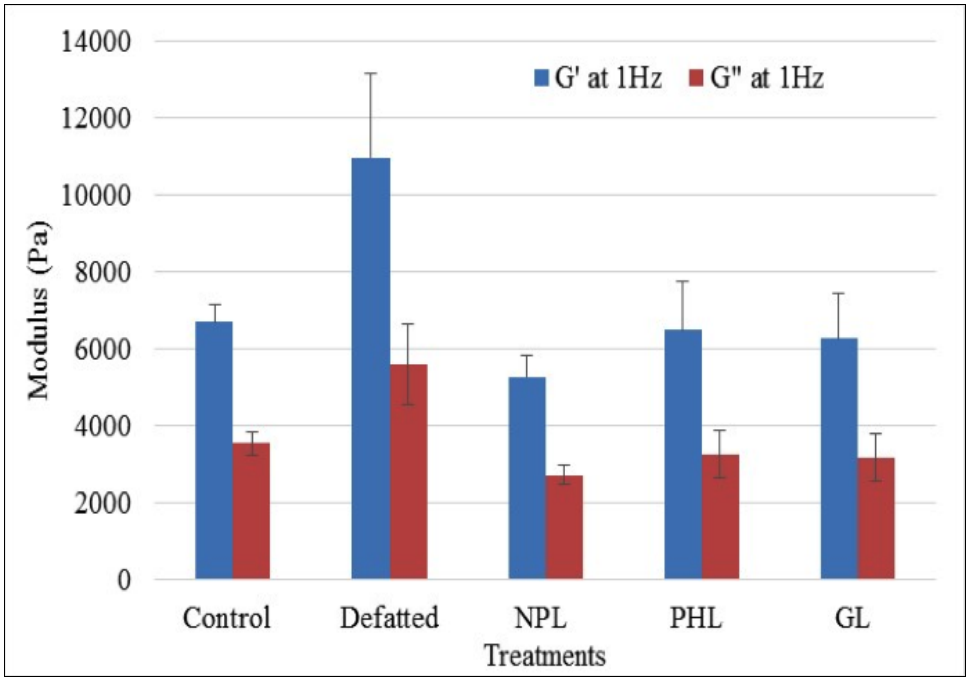

(b)

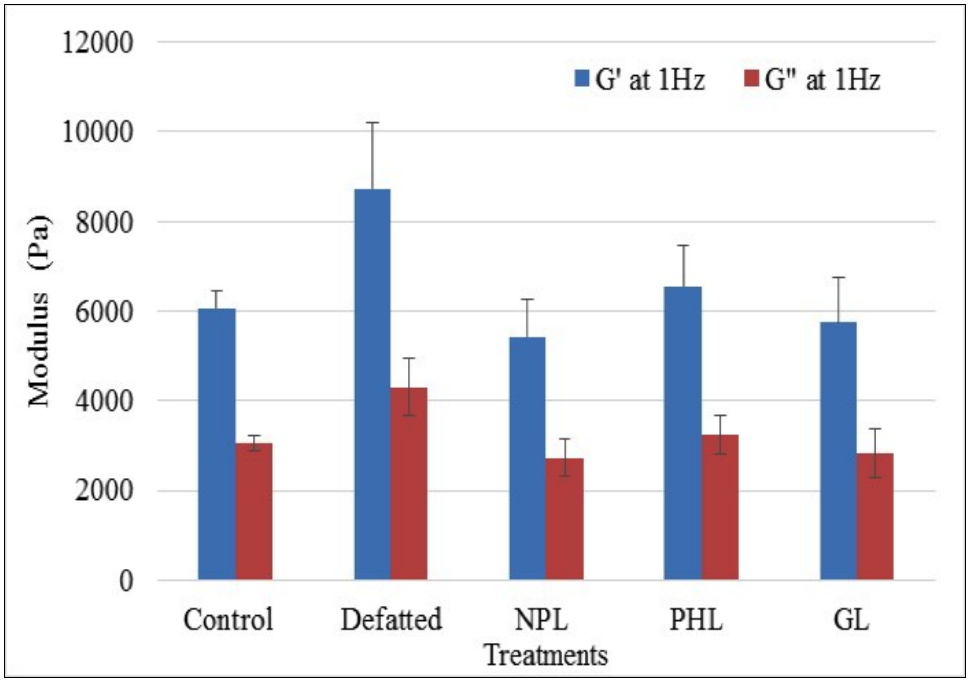

[a] Nonpolar (NPL), phospholipids (PHL), and glycolipids (GL)
[b] Error bars indicate standard deviations

Figure 3.8. G' and G" values at 1 Hz after mixing (a) and after proofing (b)

Changes in the frequency dependency of G" as a function of the lipid presence for after mixing, after proofing, and both are shown in Figure 3.7. These results were similar to the G' results in that there was an increase in G" for both after mixing and after proofing. The G' curves were higher than the G" curves indicating that the dough had more elastic than viscous behavior. Salvador et al (2006) also found similar frequency sweep results for wheat flours tested at both 25°C and 80°C. In the present work, the defatted sample had greater frequency dependence (slope) than did the other samples both after mixing and after proof. Again, the NPL possessed the lowest G" after mixing. The after mixing samples had a greater difference in the G"of the treatments than was the case for the proofed. The same trend was seen for G'. Comparing the G" after mixing and after proofing showed a decrease in the strength of defatted dough following proof. There was no change in the G" or the strength of the dough between the other treatments.

Slopes and G' values at 1 Hz are often determined in order to better understand the behavior of the treatment and control doughs. The slope is often between 0 and 2 and the closer the slope is to 0 the more rubber-like the behavior. While values closer to 2 indicate more liquid behavior. If the system contains a 3-D network, the slope value would be closer to 0 (Upadhyay et al 2012). Table 3.4 presents the G' and G" slope values and the G' values at 1 Hz frequency for all lipid treatments after mixing and proof. Figure 3.8 shows the comparison between the G' and G" value at 1 Hz frequency for both after mixing and following proofing. The after mixing G' values were higher than the G" values and this was also seen following proofing. The defatted samples were always higher for both G' and G" after mixing and proofing than the other treatments. The slopes of all treatment's G' and G" were between 0.20 and 0.23. This suggests that the dough was an elastic solid rather than a viscous liquid and that the dough possessed a 3-D network between its polymeric components. There were no significant differences between slopes of the treatments for G' after mixing, G' after proofing, and G" after proofing. The slope of G" after mixing showed a significant difference between the control (0.23 Pa), the NPL (0.21 Pa), PHL (0.21 Pa), and the GL (0.20 Pa) lipid additions. The G' and G" slopes after mixing were higher than the G' and G" after proofing illustrating less elastic characteristics and frequency dependency at the later stages.

Gandikota and MacRitchie (2005) found that "expansion capacity of dough based on gas cell structure and rheological properties occur at the end of mixing," which would suggest why there was a bigger difference in the moduli slopes after mixing than following proofing. The G'

and G" values for the defatted flour dough after mixing and proof was less sensitive to the frequency when compared to the control and the lipid added doughs. The defatted flour had higher G' and G" both after mixing and after proofing. This is evident in the frequency sweep graphs (Figures 3.6 and 3.7). This again, is most likely due to the strength of protein-protein interactions. Khatkar and Schofield (2002a) showed that gluten was less susceptible to changes in structure based on applied frequency compared to starch. Defatting and reconstitution studies of soft wheat flours used in cookies found that the starch congregated in "agglomerates and particles" following lipid removal, with the layer of protein covering the outside, preventing full hydration of the starch (Papantoniou et al 2004).

(a)

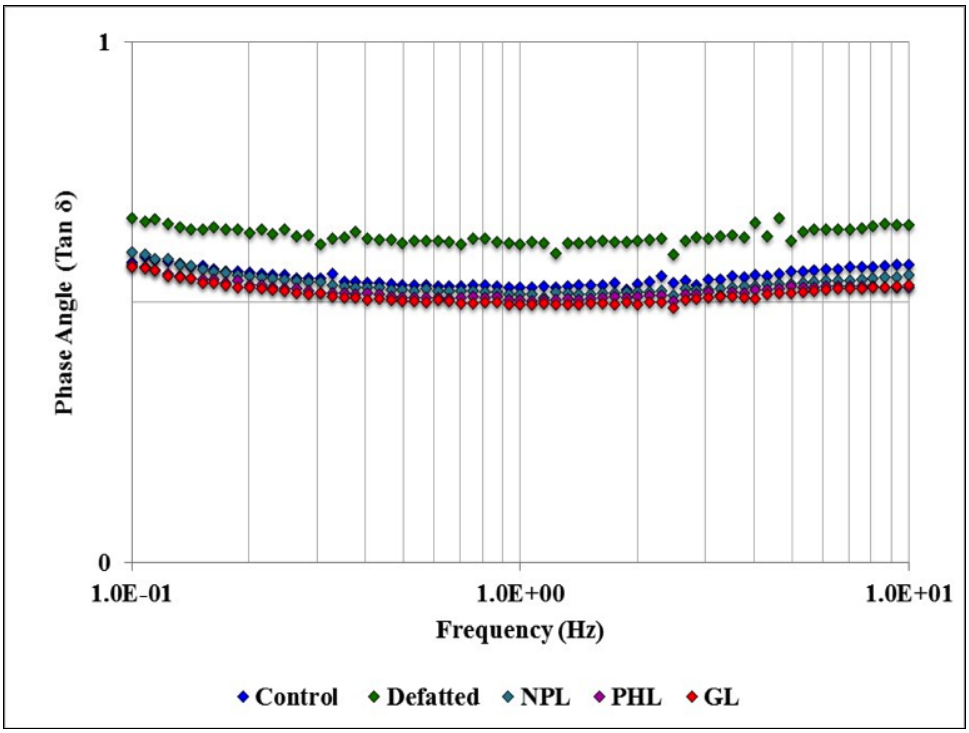

(b)

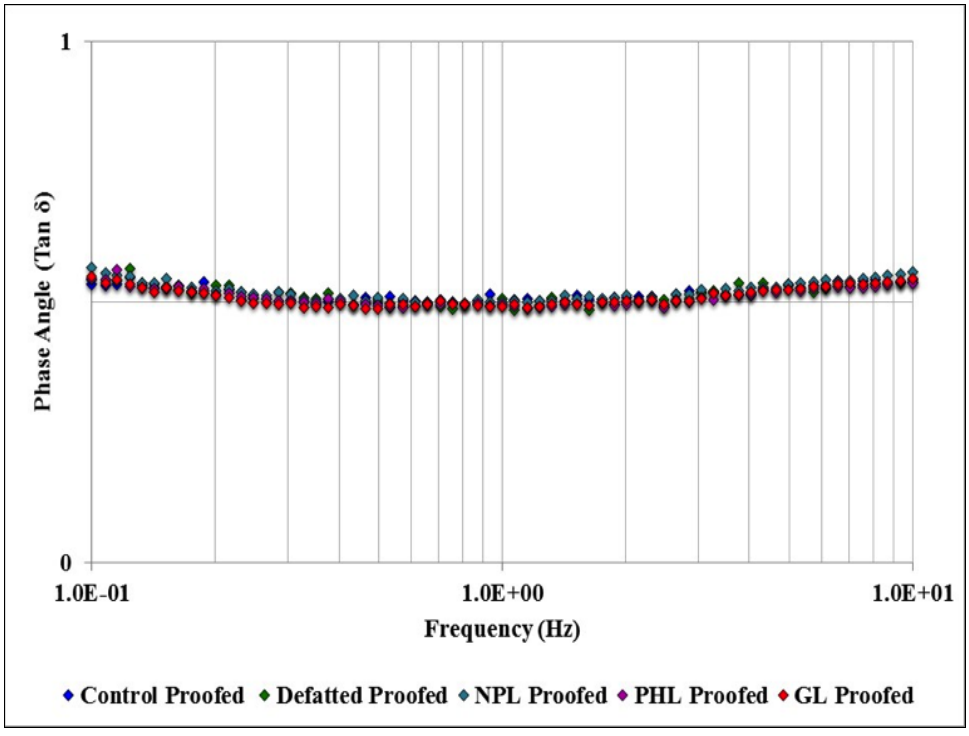

[a] Nonpolar (NPL), phospholipids (PHL), and glycolipids (GL); proofed (after proofing)

Figure 3.9. Phase angle (loss tangent) measurements (tan δ) for lipid treatment additions (a) after mixing (b) after proofing

The phase angle, or tan δ is the "ratio of the viscous and elastic response of samples tested (Singh and Singh 2013). The ratio between the two measurements show that when the sample has more elastic properties, the tan δ is less than 1 as compared to more viscous features, where the tan δ is greater than one (Khatkar and Schofield 2002a). For these specific lipid treatment results, there was a decrease in the tan δ curves with increasing frequency (Figure 3.9). The curves for both after mixing and after proofing data both fell below 1. This would signify more elastic or solid-like dough characteristics rather than liquid. Miller and Hoseney (1999) found similarities in gluten-starch systems where the tan δ curves fell below 1 for both high and low applied frequencies illustrating the elastic properties of the two components. There was little to no difference between the tan δ curves for the proofed dough while the after mixing defatted flour had a higher curve than the other samples. The difference in the defatted treatment as compared to the other samples is related to the increased storage modulus (G') as the tan δ is a ratio of both G' and G".

(a)

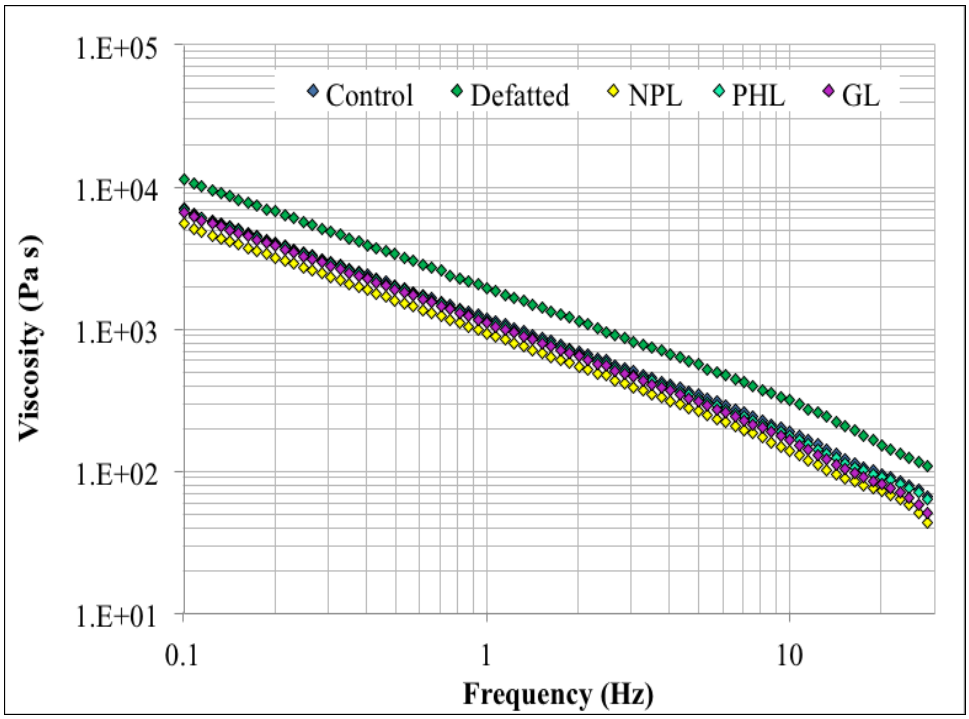

(b)

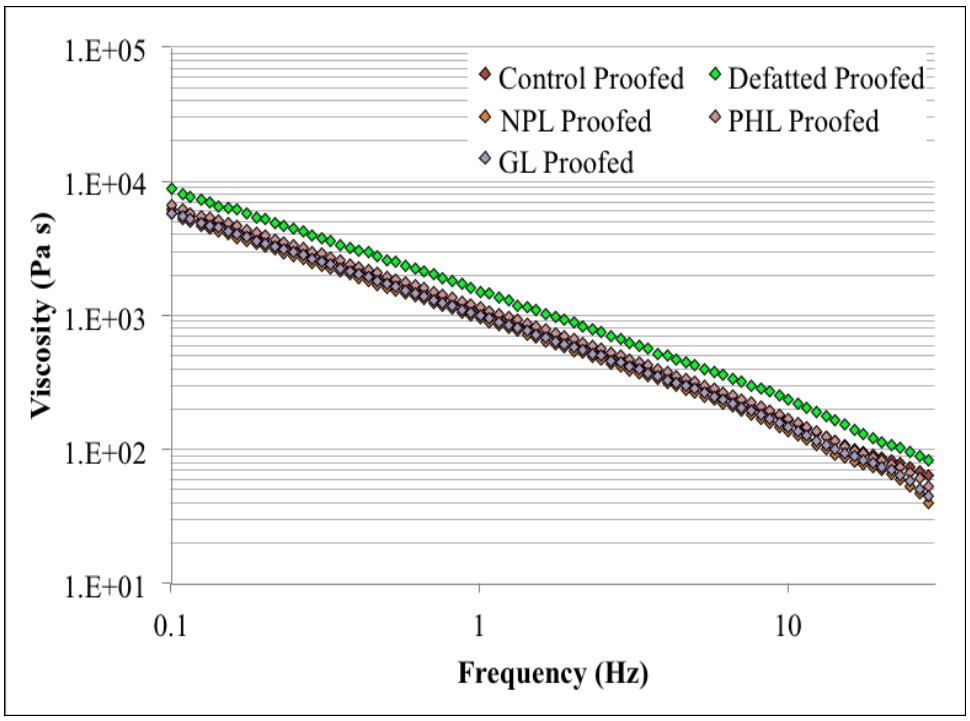

[a] Nonpolar (NPL), phospholipids (PHL), and glycolipids (GL)

Figure 3.10. Dependency of viscosity on frequency (a) after mixing and (b) after proofing

Changes in the viscosity (Figures 3.10) based on frequency showed a decrease in the viscosity as the frequency increased. This was seen for all treatments at both processing stages. The defatted flour had higher values after mixing than did the other lipid treatments. However, this trend wasn't seen for doughs after proofing. The proofed dough increased in stiffness as compared to the dough after mixing. This could be due to a strengthening effect from interactions and the formation of bonds between gluten and starch or other components in the system. Studies conducted by Lefebvre (2006) also showed a decrease in viscosity for starch samples with increased frequency. Besides having behavior that is nonlinear, dough demonstrates shear thinning or thixotropic properties (Weipert 1990). The dough is able to form complexes between starch particles creating a "continuous structure and this causes increases in the shear thinning (thixotropic) behavior of the dough" (Smith et al 1970). Complexes formed between starch granules create a "continuous structure and this causes increases in the shear thinning (thixotropic) behavior of the dough" (Smith et al 1970). The developments of starch-starch or starch-protein interactions have also been shown to cause decreases in the linearity of the curve at higher frequencies (Khatkar and Schofield 2002a).

3.3.2.3. Temperature sweep testing

The temperature sweep testing was performed between 25°C and 95°C, a range where dough, containing yeast, is converted to bread. In order to better understand the rheological properties of the dough under these conditions, it is imperative to first describe the baking process that is simulated. Following mixing, dough typically has a temperature of 27-30°C. During fermentation, the yeast has the highest amount of activity at 35-45°C, with an optimum at 35°C (Pyler and Gorton 2009). The ability for the yeast to produce CO_2 is reduced at a temperature near 43°C and then stops completely at 55°C (Cauvain 2012). Enzymatic activity within the dough, excluding alpha-amylase, will end at temperatures up to 60°C, and these enzymes will reduce the starch to dextrins or simple sugars (Pyler and Gorton 2009; Cauvain 2012). The highest enzymatic activity is between 60°C and 70°C (Pyler and Gorton 2009; Cauvain 2012). Between 50°C and 60°C the first onset of color due to Maillard browning and caramelization happens, with thickening of the crust structure and a reduction in its elasticity (Pyler and Gorton 2009). Increase in volume or oven-spring begins and starch gelatinization takes place between 55-60°C all the way up to 85°C (Pyler and Gorton 2009; Cauvain 2012). In addition, changes in protein (gluten) linkage at 90°C occur by the creation of disulfide bonds

(Delcour and Hoseney 2010). At 95°C, the dough loses all its viscous properties and exhibit its greatest elasticity (Delcour and Hoseney 2010).

Storage (G') and loss modulus (G") versus temperature curves are shown in Figure 3.11. The elastic modulus (G') curves decrease between 25°C and 75°C. However, the degree to which that occurs differently by treatment. The defatted and PHL samples had less temperature dependence compared to the GL, NPL, and the control. They showed the least loss in G'. The largest dip in the curves commenced at 55°C and lasted until ~75°C. Following this, G' values began to increase for the NPL, control, and GL samples. The increase in the PHL and defatted samples G' started at 65°C. The shapes of these modulus curves were similar to other tests conducted by Dreese et al (1988), Salvador et al (2004), and Agyare et al (2006). Dreese et al (1988) determined that the drop in viscosity was caused by the gelatinization of starch and "the magnitude of the change in G' was proportional to the amount of starch present in the dough." Salvador et al (2006) determined that following the drop and increase in G', the curves began to level off and reached the point where proteins begin to break down and the starch was fully gelatinized.

The curves also showed that the onset of starch gelatinization was earlier (lower temperature) for the defatted and PHL samples. This change was associated with the removal of lipids and the lower recovery of PHL extracted and re-added to the flour. Georgopoulos et al (2006) determined that the removal of lipids caused increase friction between the starch granules as well as decreased the gluten phase, thus increasing the speed of starch gelatinization. The NPL storage modulus (G') curve was most similar to the control while the GL curve fell in between the defatted and the control results. There was a concentration effect with the GL and NPL as there were more total NPL lipids fractionated out and added back compared to what was recovered by the total GL.

Due to the differences in type and level of lipids recovered in GL versus the NPL, the interactions with themselves, with starch, or with other compounds would cause changes the properties of the structural matrix. Tang and Copeland (2007) found that the chain length and amount of fatty acids were the limiting factor in creating starch-lipid interactions or lipid-lipid micelles and that these complexes would cause changes to the dough structure. At 75°C there was a sharp increase in the modulus for all treatments. Starch-lipid complexes that form during heating can alter the final viscosity of systems and the extent of this is dependent both on their

immiscibility in water and the amount of lipids present (Tang and Copeland 2007). In this study, each fraction (NPL, GL, and PHL) had varying concentrations of fatty acids at varying chain lengths. Some were longer chained lipids (MGDG or DGDG). This could cause them to react differently within the system. Consequently, there was an increase modulus due to lipids forming starch-lipid complexes, interacting with water, or forming lipid-lipid micelles. Overall, the control had the largest initial lipid concentration. For the loss modulus (G") the curve behavior was very similar to that of the storage modulus (G'). There was a decrease in the modulus starting at 25°C until 70°C, then a steep increase in the modulus following gelatinization. The magnitude of the G" slopes were slightly lower than those of G'. However, with the start of gelatinization and the increase of the moduli (70°C), the change was steeper than the G' curves. This would suggest that the gelatinizing starch produced more viscous-liquid behavior at this temperature most likely due to the shear thinning or thixotropic characteristics of the starch (Smith et al 1970).

The addition of NPL resulted in an additional peak in the G" curve (between 55°C and 65°C) following the start of gelatinization. This lipid fraction showed greater interaction with starch granules. Li et al (2004) found (through the use of confocal scanning laser microscopy) that NPL lipids were attached to starch at the granule surface in forms of "lipid droplets" which could cause changes between the gluten-starch and lipid-starch matrixes. In contrast, polar lipids in dough were associated more with glutenin at gas cell walls and the gliadin fraction in the bulk phase of the dough (Li et al 2004). Also various fatty acids undergo a melt between 45°C and 75°C (Reusch 2013), which could also provide explanation for the addition peaks on temperature sweep curves for lipid treatments.

(a)

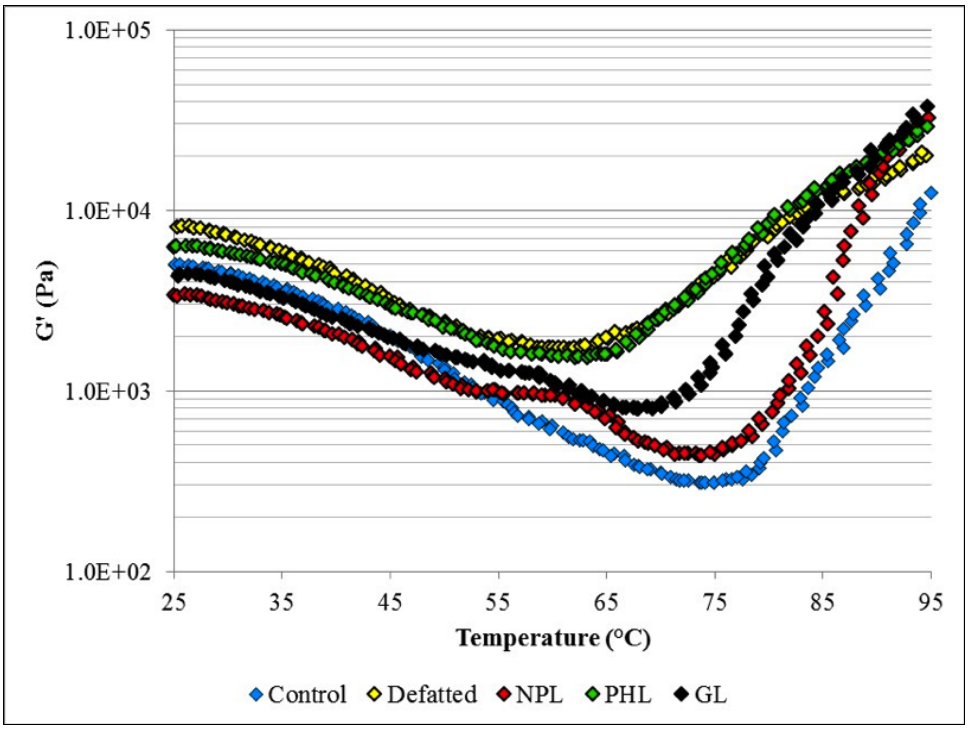

(b)

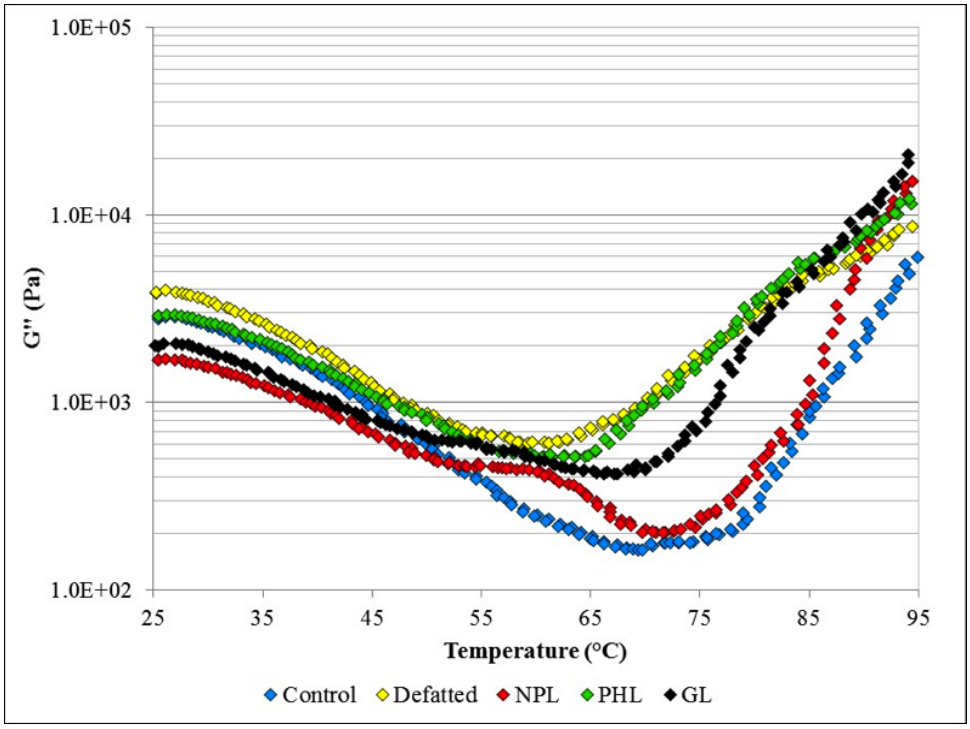

[a] Nonpolar (NPL), phospholipids (PHL), and glycolipids (GL)

Figure 3.11. Temperature sweep results for (a) storage (G') and (b) loss (G") moduli

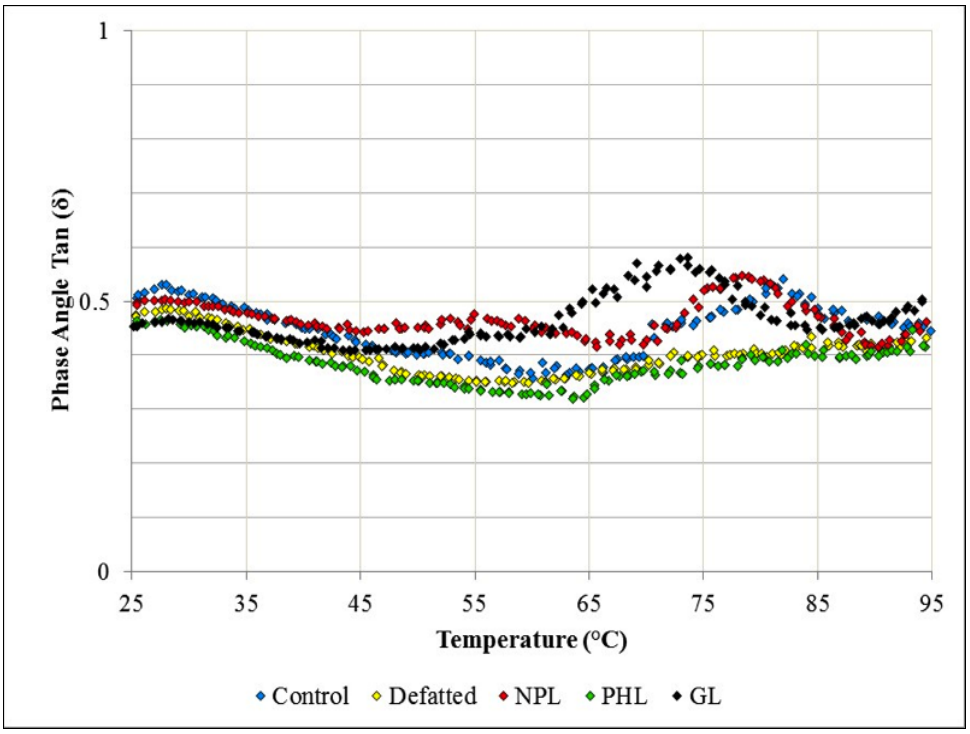

[a] Nonpolar (NPL), phospholipids (PHL), and glycolipids (GL)

Figure 3.12. Phase angle (tan δ) results for temperature sweeps of treatments with varying lipids

The phase angle (Figure 3.12) curves for the all treatments were below 1 indicating the dough had more elastic, solid-like characteristics. Between 65°C and 85°C, there was an increase in the curves for GL, NPL, and the control lines compared to the PHL and defatted samples. The GL curve showed a large peak in the curve starting at 57°C and drops again at 80°C. For the control and NPL, this similar curve increase was not seen until 70°C and decreased at 85°C. This was related to starch gelatinization and interactions between starch-lipids displaying more fluid-like properties. Changes in viscosity due to the addition of the lipid treatments are shown in Figure 3.12. The addition of the lipids caused changes in the gelatinization properties of the starch resulting in viscosity curves that were different for each treatment. The NPL addition showed viscosity behavior like the control, whereas the defatted, GL, and PHL did not. The NPL fractions showed to have the greatest affinity for starch as compared to the GL and PHL samples. Li et al (2004) found that GL and PHL lipid fractions formed both lipid-protein and lipid-starch

complexes. Following gelatinization starting at 55°C, the control had the highest drop in viscosity overall with a sharp increase again at 70°C. The defatted and PHL showed very little decrease in the viscosity following the earlier onset of gelatinzation (55°C), but then had an increase starting at 65°C. The GL viscosity curve fell between the defatted and the control having a decrease in the viscosity between 55°C and 65°C and an increase at 75°C. The viscosity curves also showed the same order and similar curve behavior as those found in both the storage (G') and loss (G") moduli.

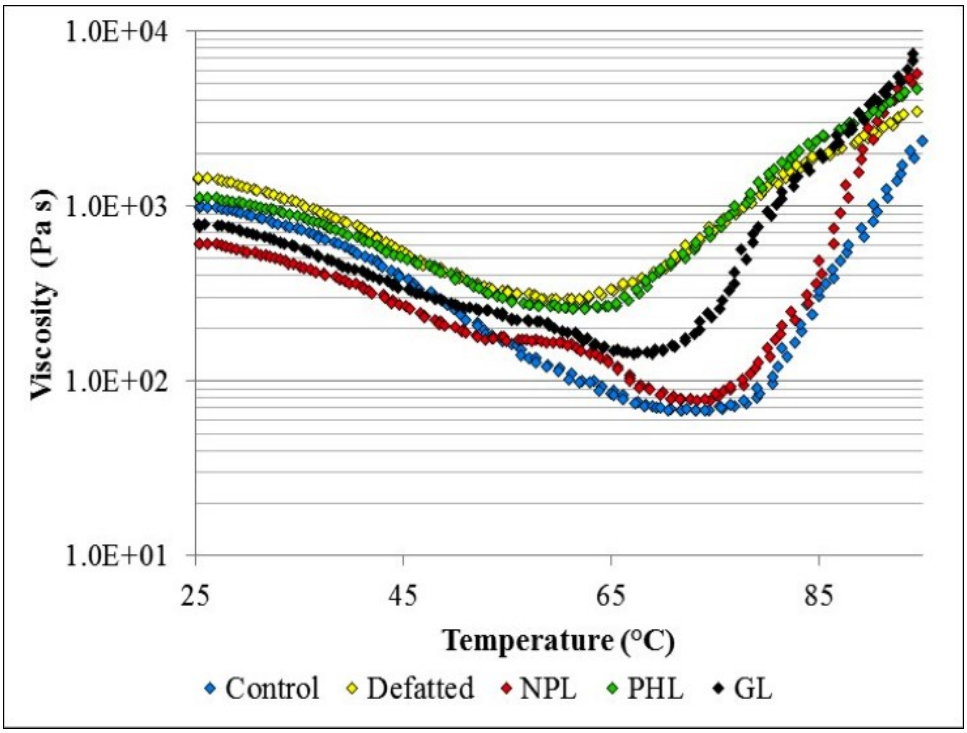

[a] Nonpolar (NPL), phospholipids (PHL), and glycolipids (GL)

Figure 3.13. Change in viscosity of lipid treatments as a function of temperature

3.3.3 Dough Rheology (large deformation)

3.3.3.1. Biaxial extension (Kieffer Rig testing)

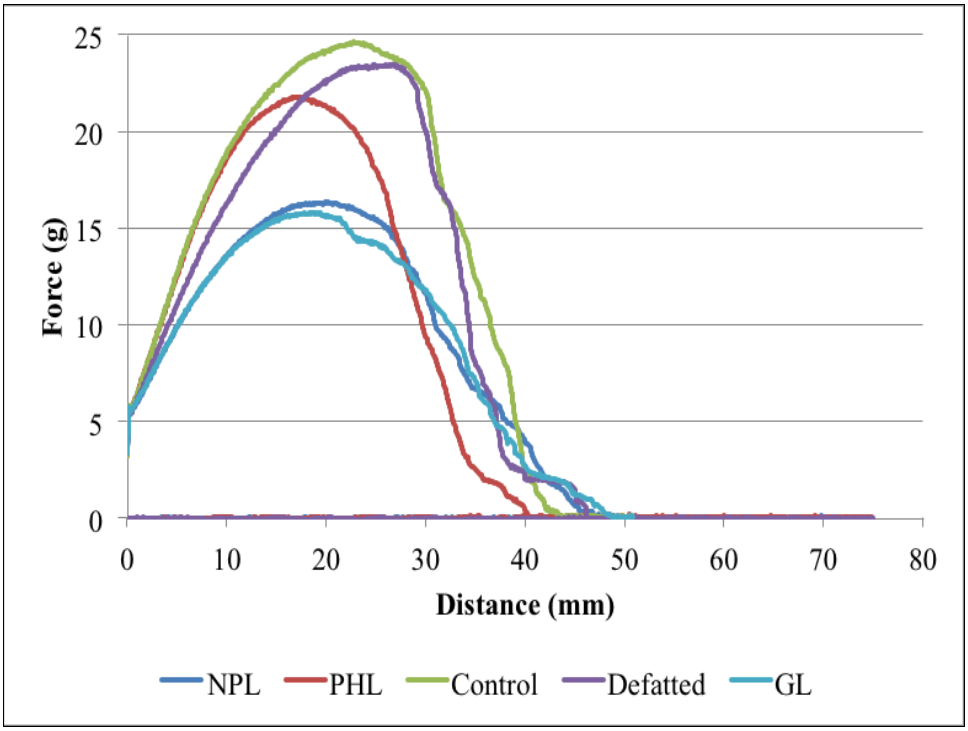

[a] Nonpolar (NPL), phospholipids (PHL), and glycolipids (GL)

Figure 3.14. Kieffer Rig (uniaxial) extensibility testing results for lipid treatments

Table 3.5 Kieffer Rig extensibility testing results for lipid treatments

Samples	**Force -R_{max} (g)**	**Distance- Ext_{max} (mm)**
Control	25.29[a] (4.89)	24.13[a] (4.78)
Defatted	25.59[a] (3.56)	25.73[a] (5.58)
NPL	15.73[b] (2.57)	22.00[ab] (4.84)
PHL	22.45[a] (3.34)	18.39[b] (3.33)
GL	16.75[b] (3.57)	22.77[ab] (4.90)

[a a] Nonpolar (NPL), phospholipids (PHL), and glycolipids (GL)
[b]Means in the same column with different letters are significantly different at a $p<0.05$; (n=90)
[b]Values in parenthesis indicate standard deviations

Large deformation testing is often used as means for evaluating changes that are related to extension and stretching as it is more representative of how the dough is treated during the bread making process. One of the most common extension tests is the Kieffer rig extensibility testing (large deformation), which gives uniaxial extensional measurements. Using uniaxial and biaxial testing, Sliwinski et al (2004b) found that gluten strength increased during extension primarly in the direction of the extension. Figure 3.14 shows the Kieffer Rig test results of dough containing varying lipid types and levels. The y-axis is resistance (including the R_{max} or the "peak force or resistance to extension") and the x-axis is the "distance of extension" (Ext_{max}) (Nash et al 2006). Dobraszczyk and Salmanowicz (2008) were able to link R_{max} values as a predictor of loaf volume. However, Ext_{max} was not a very good predictor. Tronsmo et al (2003), Dunnewind et al (2004), Sliwinski et al (2004b), and Dobraszczyk and Salmanowicz (2008) who also studied wheat flour and gluten using large deformation testing found similar extension/resistance curves shape results. Figure 3.14 shows that more force was needed to extend and break the control, defatted, and PHL dough samples while the NPL and GL samples required less. The max extension distance was significantly lower for the PHL than for the defatted and control reflecting a weakening effect perhaps because of fewer protein-protein interactions and more protein-PHL interactions. The reduction in max force for NPL and GL were much greater than any of the other treatments. Thus, the lipid presence caused the tension resistance to be reduced but not the extensibility of the dough.

Table 3.5 presents the force/distance measurements from the extensibility curves (Figure 3.14). The defatted flour dough required the most force (25.59 g) to break the dough, while NPL had the lowest (15.73 g). The control (25.29 g), PHL (22.45 g) and the defatted doughs had similar peak force measurements and were not significantly different than each other. The NPL (15.73 g) and GL (16.75 g) peak force were not significantly different. Dobraszczyk and Salmanowicz (2008) determined wheat flour dough force measurements to range from 8-30 g. However, distance measurements were higher in extensibility to failure for that study. Those results ranged between 50 mm and 95 mm. The force measurements in that particular study coincide with the results shown in this study while the extensibility measurements did not. The results in this study are much lower in extensibility ranging between 20 and 27 mm. This could be an indicator of the overall quality of the dough suggesting that this current flour was a poor baking flour or that the addition of yeast had a weakening effect on the dough. Yeast and

fermentation have been shown to weaken the overall strength of dough, which contributes to lower overall force measurments (Chin et al 2005). The GL and NPL reduced the strength of the dough. It may be that the gluten phase of the defatted flour was changed due to either the combination of lipid-protein or lipid-starch complexes formed during mixing.

The control (24.13 mm), defatted (25.73 mm), GL (22.77 mm) and NPL (22.00) treatments had the largest Ext_{max} and were not significantly different. The GL and PHL were not significantly different from the PHL (18.39 mm). The extensibility of the gluten proteins was weakened only by PHL. In conclusion, all dough extensibilities were approximately equal, but all the lipid treatments reduced the force for failure compared to the control or defatted flour. Thus, the addition of the lipids caused a reduction in the strength of the dough.

3.3.3.2. Strain Hardening

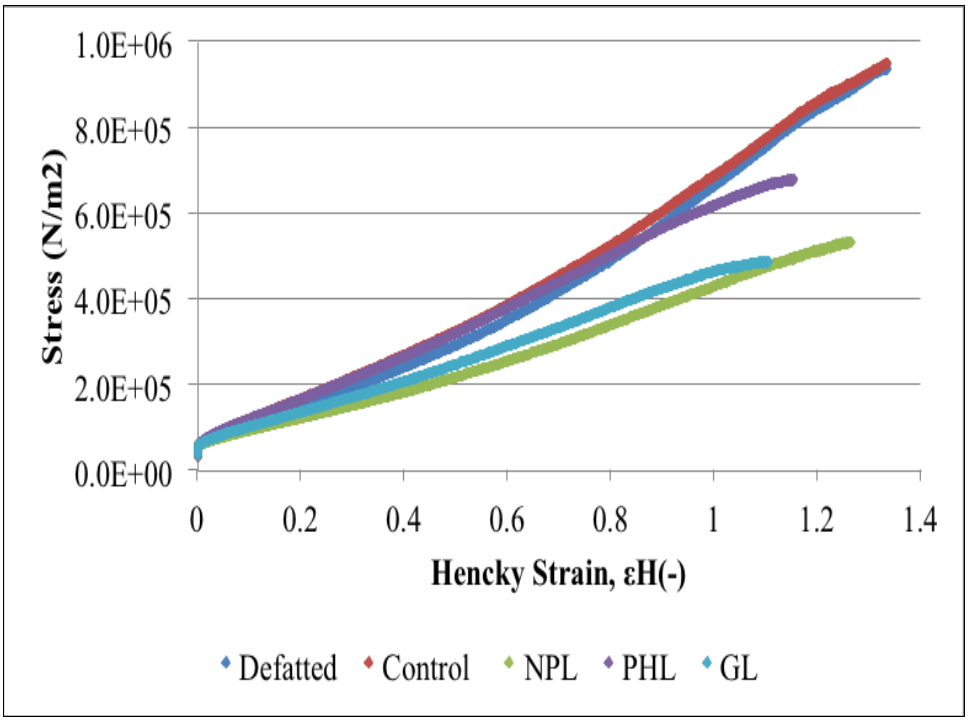

[a] Nonpolar (NPL), phospholipids (PHL), and glycolipids (GL)

Figure 3.15. Stress-strain curves used for determination of strain hardening behavior of doughs with varying lipid treatments

Table 3.6 Strain hardening measurements results for lipid treatments

Treatments	Fracture strain	Fracture stress (N/m^2)	Extensional stiffness (κ)	Strain hardening index(n)
Control	1.43[a] (0.13)	1,056,733.18[a] (169,586.56)	106,802.25[a] (17,651.05)	1.79[ab] (0.14)
Defatted	1.36[a] (0.12)	991,797.32[a] (156954.41)	95,997.64[ab] (8,184.43)	1.89[a] (0.12)
NPL	1.35[a] (0.20)	601,545.57[b] (149,346. 55)	84,657.67[b] (9,474.02)	1.61[b] (0.19)
PHL	1.15[b] (0.14)	713,589.50[b] (124,250.21)	99,871.29[a] (8,912.63)	1.95[a] (0.18)
GL	1.34[a] (0.22)	634,144.26[b] (128,087.79)	86,795.86[b] (11,216.78)	1.67[b] (0.24)

[a] Nonpolar (NPL), phospholipids (PHL), and glycolipids (GL)
[b]Means in the same column with different letters are significantly different at a $p<0.05$; (n=90)
[c]Values in parenthesis indicate standard deviations

From the uniaxial testing using the Kieffer rig, the conversion to biaxial testing was calculated to determine strain hardening following the work by Abang Zaidel et al (2007). The relationship between stress and Hencky strain can be determined by calculating strain hardening based off of the following equation (MacRitchie 2010):

$$\sigma = K\varepsilon^n$$

where σ is a representative measure of the stress, K is a constant value known as extensional stiffness, ε is Hencky strain and n the strain hardening factor (MacRitchie 2010). Higher values for n would signify more strain hardening and thus increased stability of the cell walls (MacRitchie 2010). A strain hardening number of (n) = 1 would be a linear curve, whereas a value of 2 corresponds to a more parabolic curve (Dobrasyzczyk and Robert 1994). If there is higher strain this will also affect the strain rate, as the strain will need to be greater for the cell walls to break down. Thus, the gas cell can undergo greater expansion before bursting (Dobrasyzczyk and Robert 1994).

Figure 3.15 illustrates the stress versus Hencky strain curves for the different lipid treatments. Both the control and defatted sample peaks were similar, indicating that these doughs had developed strong structural networks capable of holding and maintaining gas cells. It also

shows that there was minimal effect of chloroform extraction on the defatted sample's structural properties as compared to the control. The PHL curve had similarities to the defatted and control samples; however the lengh was shorter. The minimal differences between the defatted and PHL curves could be related to a concentration effect with the PHL addition being too small to manifest any differences. In contrast, both NPL and GL resulted in strain hardening at much lower stress and strain values than the control, defatted, and PHL samples. The GL treatment was slightly higher than the NPL but both treatments showed reduced ability to produce dough that had similar cell wall stability as the other three treatments. Table 3.6 contains the strain hardening measurements based off of the stress-strain curves (Fig. 3.15). These values included fracture stress, fracture strain, extensional stiffness (κ), and strain hardening (n). The fracture stress and the fracture strain are the highest two values before the dough fails from both the stress and Hencky strain.

The fracture (failure) strain was only significantly different for the PHL (1.15) while all the rest of the treatments fell between 1.35 and 1.43. Dobraszczyk and Roberts (1994) reported similar results for failure strain values for samples tested at varying water levels. In this current work, failure stress measurements were significantly higher for both the defatted (991,797 N/m^2) and the control (1,056,733 N/m^2) compared to NPL (601,546 N/m^2), PHL (713,590 N/m^2), and GL (634,144 N/m^2). The defatted and control samples' cell walls could withstand a higher applied stress (force per area) than the dough with the added lipids. The PHL and GL doughs had higher fracture stress values than did the NPL sample. However, all three samples manifested weakening on the cell wall strength. This would support the finding by Sroan and MacRitchie (2009) that it was a combination of not only lipids, but also of mixed monolayers that help with the overall support of gas cells.

The extensional stiffness (κ) was not significantly different between the NPL (84,658), GL (86, 796), and defatted samples (95,998). The control (106,802) and PHL (99,871) were significant from all the treatments except for the defatted. Typically, higher extensional stiffess is an indicator of a viscous or rigid dough (Chin et al 2005). The strain hardening values were lowest for both the NPL (1.61) and GL (1.67), but were not significantly different from the control (1.79). The defatted (1.89) and PHL (1.95) were significantly different from GL, NPL, and the control. All the strain hardening values were above 1 indicating that the added lipids did not reduce cell wall strength. Because none of the values were significantly different from the

control (only lower) both the NPL and GL could stabilize gas cells similar to the control. Both the defatted and PHL treatments had higher strain hardening values suggesting that the cell wall matrix was stronger and less susceptible to failure over time compared to the other treatments. This could be reflective of more protein-protein or starch-protein interactions within the samples due to the removal of lipids.

Sroan and MacRitchie (2009) also measured straining hardening of several soft and hard wheat doughs with varying polar and nonpolar lipid additions. The strain hardening values were higher for all those varieties than compared to this current study. However, their level of addition was much higher and the testing was done using biaxial methodology versus the uniaxial testing done in the current study. Their study also found higher strain hardening values for 60% NPL addition, comparable to the strain hardening index for their total lipid addition (Sroan and MacRitchie 2009). In comparison to these current results, there was lower values for the NPL and higher for the control. In contrast, Dobraszczyk and Roberts (1994) determined, from biaxial testing of flours with different water concentrations, strain hardening index results to be similar to those found in this current study.

3.3.4. Physical parameters of breads for XMT macro testing

The analytical baking results are shown in Table 3.7 for XMT macro testing. The whole loaf breads, made for analysis at Cargill, had no significant differences in proof heights. The control bread had the highest proof height at 6.84 cm, followed by PHL (6.81 cm), GL (6.75 cm), and NPL (6.70 cm). Because there were only small differences between the proof heights there was little to no influence of lipids. Loaf volumes (Table 3.7) were measured using rapeseed (volume) displacement following cooling. The control had the highest loaf volume at 754 cc, indicating that the flour used for baking was of poorer quality due to a lower volume measurement. This was significantly different from all the other treatments except the PHL (714 cc). PHL and GL (706 cc) were also not significantly different from one another while the NPL loaves had the lowest average loaf volume (644 cc). The specific volume, which takes into account the weight of the loaves, was also determined for each sample. Again, the control had the highest specific volume (5.24 cc/g), but in contrast to the loaf volume, the GL treatments (5.04 cc/g) were not different from the control. GL and PHL (4.93 cc/g) were not significant from one another. The NPL (4.56 cc/g) was also not significantly different from PHL loaves.

Table 3.7 Physical characteristics of whole loaf breads baked with different lipid treatments

Treatment	Proof Height (cm)	Loaf Volume (cc)	Loaf Specific Volume (cc/g)
Control	6.84[a] (0.37)	754.38[a] (36.98)	5.24[a] (0.25)
Nonpolar	6.70[a] (0.21)	643.75[b] (49.41)	4.56[b] (0.32)
Phospholipids	6.81[a] (0.18)	714.36[ac] (8.21)	4.93[bc] (0.12)
Glycolipids	6.75[a] (0.12)	705.63[c] (15.45)	5.04[ac] (0.09)

[a]Means in the same column with different letters are significantly different at a $p<0.05$; (n=24)
[b]Values in parenthesis indicate standard deviation

3.3.5. Physical parameters of breads for XMT micro testing

In addition to whole loaf testing, loaves were made from the control, defatted, and defatted flour that was reconstituted with 0.6%, 1.2%, and 2.5% NPL and 0.2%, 0.4%, and 0.6% PL. The PL fraction was the combination of PHL and GL. The PL addition was calculated from the amount of polar lipids extracted initially from the control flour sample used in this testing. Additionally, lipid concentrations were doubled and tripled. The highest concentration was chosen so as to not exceed the threshold to which the lipid addition could become detrimental to the final loaf volume (MacRichie and Gras 1973). The proof heights, loaf volume, and specific volume results are shown in Table 3.8.

Comparing the average proof heights of the control and the lipid treatments, the 2.5% NPL (7.31 cm) had the lowest proof height. This was only significantly different from the 0.6% NPL at (7.90 cm). Loaf volumes ranged between 690 cc and 830 cc with the control (799 cc) and the 0.6% PL (829 cc) having the highest volumes. Both 1.2% NPL (708 cc) and 2.5% NPL (694 cc) had the lowest volumes. The addition of higher amounts of NPL caused a decrease in volume while all the % PL increased with added concentration. The average specific volume decreased as the % NPL concentration increased. The control specific volumes fell in between the two lipid treatment additions at the varying concentrations.

Table 3.8. Average physical parameter measurements for center section breads baked with different lipid treatments

Treatments[a]	Proof Height (cm)	Loaf Volume (cc)	Loaf Specific Volume (cc/g)
Control	7.83[ab] (0.36)	799.44[ac] (20.83)	5.36[ab] (0.09)
NPL 0.6%	7.90[a] (0.11)	747.78[bc] (15.02)	5.09[b] (0.12)
NPL 1.2%	7.61[ab] (0.42)	707.78[b] (39.77)	4.83[b] (0.39)
NPL 2.5%	7.31[b] (0.49)	693.89[b] (57.05)	4.83[b] (0.42)
PL 0.2%	7.62[ab] (0.60)	756.11[ab] (93.13)	5.34[ab] (0.46)
PL 0.4%	7.73[ab] (0.38)	760.56[ab] (25.42)	5.25[b] (0.16)
PL 0.6%	7.79[ab] (0.23)	829.44[a](79.55)	5.84[a] (0.74)

[a] Nonpolar (NPL) and polar (PL)
[b]Means in the same column with different letters are significantly different at a $p<0.05$; (n=84)
[c]Values in parenthesis indicate standard deviations

3.3.6 Macrostructure analysis (C-Cell)

C-Cell analysis is a useful tool to determine changes in bread structure due to treatments that influence texture or sensorial characteristics of the final product. As provided by the C-Cell imaging guide, the following parameters and interpretation of these results are presented in Table 3.9. The raw images and values measured from the C-Cell for the whole loaf treatments are shown in Figure 3.16, and Table 3.10, respectively

Table 3.9 Structure parameters measured by C-Cell Imaging

Parameter	Definition[a]	Unit of measure
Slice area	Total area of a sample (reduced area measures typically correspond to reduced volumes)	Pixels (mm^2)
Number of cells	Number of distinctive cells found in the slice (larger #'s = finer cells)	No units
Number of holes	Number of holes in a slice (higher #'s = more holes)	No units
Area of cells	Area of cells as a percentage of slice area (greater % = open structure)	%
Area of holes	Area of holes as a percentage of slice area (greater % = larger sizes of holes)	%
Volume of holes	Total volume of all the holes in the slice combined (higher #'s = larger # or size of holes)	Pixels
Wall thickness	Avg. thickness of cell walls (larger #'s = thicker walls)	Pixels (mm)
Cell diameter	Avg. diameter of cells in the slice area (larger #'s = course, open structure)	Pixels (mm)
Cell elongation	Average length to width ratio of the cells-no influence of orientation of the cells (values closer to 1 = rounder cells)	No units

[a]Definitions adapted from the Baked Product Imaging System Analysis Guide, C-Cell Imaging (Calibre Control International, Ltd., Warrington, UK).

3.3.6.1. C-Cell macro XMT treatment analysis

The slice areas were significantly different between the samples. The NPL loaves had the lowest slice area (3744 mm^2) while the control had the largest (4380 mm^2). These differences in slice area were related to the differences in loaf volumes caused by the added lipid. However, the

number of cells was not found to be significantly different from one another (larger values indicating finer cells). The other parameters that were found to be different included area of cells, wall thickness, and cell diameter. For the area of cells, both the control (49.52%) and NPL (47.13%) where found to be significantly different from the PHL (48.40%), and GL (48.33%). These values were very close to 50%, which would be an indication of more open cell structure (overall higher volume).

Both the control (0.39 mm) and PHL (0.38 mm) had cell wall thicknesses that were significantly different from NPL (0.37 mm) and GL (0.37 mm). Thus, the control and PHL had slightly thicker cell walls. The cell diameter for the control (1.47 mm) was significantly higher than all the treatments. The NPL (1.24 mm) had the lowest. None of the cell elongation values were found to be significantly different from one another. These values were higher than 1 indicating less rounded cells and greater diversity in cell sizes. Sroan and MacRitchie (2009) found similar results (no differences in the number of cells), but cell diameters were different from one another due to the addition of polar and nonpolar lipids. Thus, the overall expansion and increase in loaf volume was more associated with the lipid treatments allowing for growth in the gas cell size rather than just being related to the number of cells (MacRitchie and Sroan 2009). Gandikota and MacRitchie (2005) determined that the dough ability to expand relied on the combination of the number of cells present and the matrix's ability to maintain those incorporated cells. The increase in the gas cell size for control, GL, and PHL sample would allow for more diverse cell size throughout the structure compared to NPL lipid addition. The NPL had smaller cell diameters, which inhibited expansion (Sroan and MacRitchie 2009). The higher the elongation the greater the stability during expansion and this would have an overall impact on the rheological properties of the dough (Gandikota and MacRitchie 2005). Because all the elongation values were similar to one another for all the treatments, lipid addition had little to no effect the strength of the cell walls.

A. Control B. NPL C. PHL D. GL

[a] Nonpolar (NPL), phospholipids (PHL), and glycolipids (GL)

Figure 3.16. C-Cell raw images of macro XMT samples with varying lipid treatments

Table 3.10. C-Cell analysis of macro XMT sample breads containing varying lipid treatments

Treatment	Slice Area (mm^2)	Number of Cells	Number of Holes	Area of Cells (%)	Area of Holes (%)	Volume of Holes	Wall Thickness (mm)	Cell Diameter (mm)	Cell Elongation
Control	4379.83[a]	3807.67[a]	3.00[a]	49.52[a]	1.39[a]	38.10[a]	0.39[a]	1.47[a]	1.72[a]
	(209.69)	(229.69)	(1.01)	(0.33)	(0.59)	(8.61)	(0.00)	(0.04)	(0.01)
NPL	3743.67[b]	3932.67[a]	3.28[a]	47.13[b]	2.08[a]	35.45[a]	0.37[b]	1.24[b]	1.72[a]
	(295.00)	(270.91)	(1.29)	(0.91)	(1.42)	(15.98)	(0.00)	(0.07)	(0.01)
PHL	4129.83[ac]	3977.17[a]	3.76[a]	48.40[c]	2.28 [a]	41.15[a]	0.38[c]	1.37[c]	1.71[a]
	(152.96)	(131.87)	(2.56)	(0.46)	(1.63)	(18.12)	(0.01)	(0.08)	(0.01)
GL	4046.00[bc]	3974.17[a]	4.05[a]	48.33[c]	3.05[a]	48.97[a]	0.37[bc]	1.31[bc]	1.70[a]
	(83.42)	(82.32)	(0.29)	(0.56)	(0.97)	(10.06)	(0.00)	(0.05)	(0.00)

[a] Nonpolar (NPL), phospholipids (PHL), and glycolipids (GL

[b]Means in the same column with different letters are significantly different at a $p<0.05$; (n=24)

[b]Values in parenthesis indicate standard deviations

3.3.6.2. C-Cell micro XMT treatment analysis

A. Control A. 0.6% NPL B. 1.2% NPL C. 2.5% NPL

A. 0.2% PL B. 0.4% PL C. 0.6% PL

[a] Nonpolar (NPL) and polar (PL)

Figure 3.17. C-Cell raw images of micro XMT sample slices for control, NPL (0.6%, 1.2%, 2.5%), and PL (0.2%, 0.4%, 0.6%) lipid additions

Table 3.11. C-Cell analysis of breads used for micro XMT analysis with varying lipid treatment additions

Treatment	Slice Area (mm^2)	Number of Cells	Number of Holes	Area of Cells (%)	Area of Holes (%)	Volume of Holes	Wall Thickness (mm)	Cell Diameter (mm)	Cell Elongation
Control	4130.33[ab]	3367.33[c]	4.11[a]	49.87[a]	3.79[a]	66.80[a]	0.40[a]	1.56[ab]	1.76[a]
	(91.66)	(108.56)	(1.52)	(0.23)	(0.42)	(5.09)	(0.00)	(0.04)	(0.05)
NPL 0.6%	3914.33[ab]	3603.33[bc]	2.80[a]	48.27[a]	2.18[a]	46.03[a]	0.38[ab]	1.37[ab]	1.74[a]
	(148.00)	(198.07)	(1.27)	(0.61)	(1.68)	(24.89)	(0.01)	(0.07)	(0.04)
NPL 1.2%	3664.33[b]	3264.33[c]	2.31[a]	48.97[a]	3.79[a]	64.90[a]	0.39[ab]	1.40[ab]	1.73[a]
	(287.79)	(93.55)	(0.99)	(0.50)	(3.78)	(41.00)	(0.01)	(0.06)	(0.04)
NPL 2.5%	3761.00[b]	3298.00[c]	3.42[a]	49.47[a]	2.63[a]	52.73[a]	0.39[ab]	1.46[ab]	1.76[a]
	(153.80)	(93.55)	(1.29)	(0.32)	(1.75)	(21.21)	(0.00)	(0.06)	(0.05)
PL 0.2%	4202.67[ab]	4062.33[a]	3.94[a]	48.93[a]	3.18[a]	53.40[a]	0.37[b]	1.32[b]	1.71[a]
	(146.85)	(77.02)	(0.29)	(0.64)	(1.87)	(21.83)	(0.01)	(0.05)	(0.05)
PL 0.4%	4091.33[ab]	4109.00[a]	2.52[a]	48.70[a]	1.77[a]	41.83[a]	0.37[b]	1.31[b]	1.70[a]
	(92.03)	(32.92)	(0.18)	(0.36)	(1.30)	(22.91)	(0.00)	(0.07)	(0.02)
PL 0.6%	4659.33[a]	3773.67[ab]	3.36[a]	50.27[a]	2.49[a]	54.70[a]	0.40[a]	1.63[a]	1.75[a]
	(686.07)	(106.10)	(1.66)	(1.62)	(1.99)	(22.42)	(0.02)	(0.23)	(0.03)

[a] Nonpolar (NPL) and polar (PL)

[b]Means in the same column with different letters are significantly different at a $p<0.05$; (n=21)

[b]Values in parenthesis indicate standard deviations

Figure 3.17 and Table 3.11 contain the C-Cell raw images of center sections and the value measurements of those breads. Slice area, number of cells, wall thickness, and cell diameter were signifcantly different between the treatments. The slice areas for the control, 0.2% PL, 0.4% PL, and 0.6% PL were larger than all the NPL treatments. Initially, the loaf volumes were also higher for the control and PL treatments than the NPL. The number of cells for the 0.2% PL (4602) and 0.4% PL (4109) were significantly different and higher than all the other treatments including the control. The cell wall thickness was significantly greater for both the control sample (0.40 mm) and 0.6% PL (0.40 mm) than for the 0.2% PL (0.37 mm) and 0.4% PL (0.37 mm) reflecting thicker overall cell walls. The average cell diameter of 0.6% PL (1.63 mm) was significantly higher than that of 0.2% PL (1.32 mm) and 0.4% PL (1.31 mm) while all the rest of the treatments fell between these two extremes, which was a more course, open structure. The control had the second highest average cell diameter at 1.56 mm. Again, no significant differences in cell elongation were seen between these added lipid treatments either, thus the cells were not as round and more diversified in shape.

3.3.7. Microstructure analysis of bread (X-ray microtomography)

X-ray microtomography (XMT) is a very useful tool to evaluate aerated cellular products as it helps to provide a better understanding of internal microstructure without compromising the sample (Falcone et al 2004; Lim and Barigou 2004: Falcone et al 2005; Babin et al 2006; Bellido et al 2006; Vlassenbroeck 2007; Besbes et al 2013: Cafarelli et al 2014b; Van Dyck et al 2014). Note that no direct comparison can be made between the macro XMT and the micro XMT results as sample sizes (whole loaf and center section-12 cm x 8 cm cube) and magnification ranges were different for each XMT instrument. The center section testing resolution was 15.5 μm while whole loaf testing was conducted at 61.4 μm resolution. The lower resolution for the center section work allowed the determination of the tiniest possible air cell or pore measurement within the VOI of the sample. However, this measurement is limited to that specific sample size. Due to the small sample size, the view of the entire loaf can't be evaluated without taking multiple images of the center section of the same loaf. In order to get the full loaf within the field view, the sample had to be moved farther away from the x-ray. This provided a better analysis of the cell and pore distribution in the whole sample, but some of the detail of the smaller cells was lost due to the distance from the x-ray source. Figure 3.18 shows the binary images of control samples for both micro and macro testing.

(a) 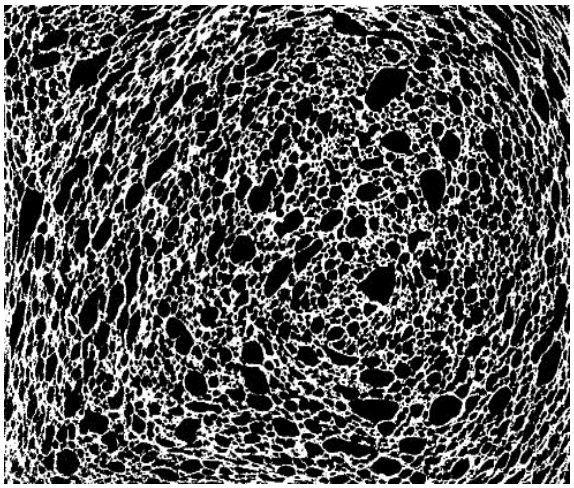 (b) 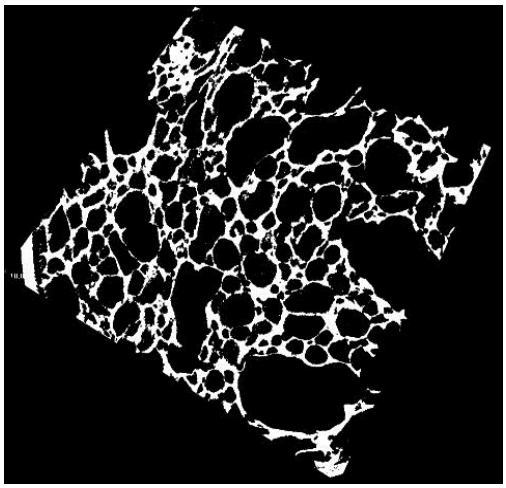

Figure 3.18. Binary images of the control sample for XMT macro (a) and micro (b) testing

3.3.7.1. XMT macro testing

Figure 3.18 shows whole loaf XMT measures of cell wall thickness, gas cell size, cumulative cell wall thickness and cumulative gas cell size. Cell wall thickness distribution ranged broadly with thicknesses between 100-700 μm. There was little to no difference between the wall thickness distributions (Fig. 3.18a) for the NPL, PHL, and GL with the distribution (~37-42%) at 368 μm. The control had no clear peak. Most of the values were between two sizes, 246 μm and 368 μm. The cumulative cell wall thickness distribution (Fig. 3.18b) showed little to no difference between the cumulative frequency for any of the treatment samples. Lipids had limited effect on the distribution of cell walls throughout the whole loaf.

Gas cell size curves (3.18c) showed a larger difference between the size distributions of the control and the three lipid treatments. The control curve peak was lower and broader than the NPL, PHL, and GL curves with fewer cells of 200 μm and 800 μm than GL, NPL, and PHL curves. The most frequent cell size was 400 μm for those lipid treatments. The control spread ranged between 0 μm and 790 μm, but had fewer cells between the 200 μm-400 μm. The GL and PHL had a slightly lower frequency of cells in the 390-400 μm range, but all the lipid treatments had the same distribution. The cumulative gas cell size distribution (Figure 3.18d) was shifted slightly to the right for the control loaf showing larger cell sizes in those samples as compared to the lipid treatments. The lipid additions appeared to have a greater influence on cell size than on cell wall thickness. This could be due to the lipids' effects on the gas cell expansion and is reflected in the loaf volume (Sroan and MacRitchie 2009).

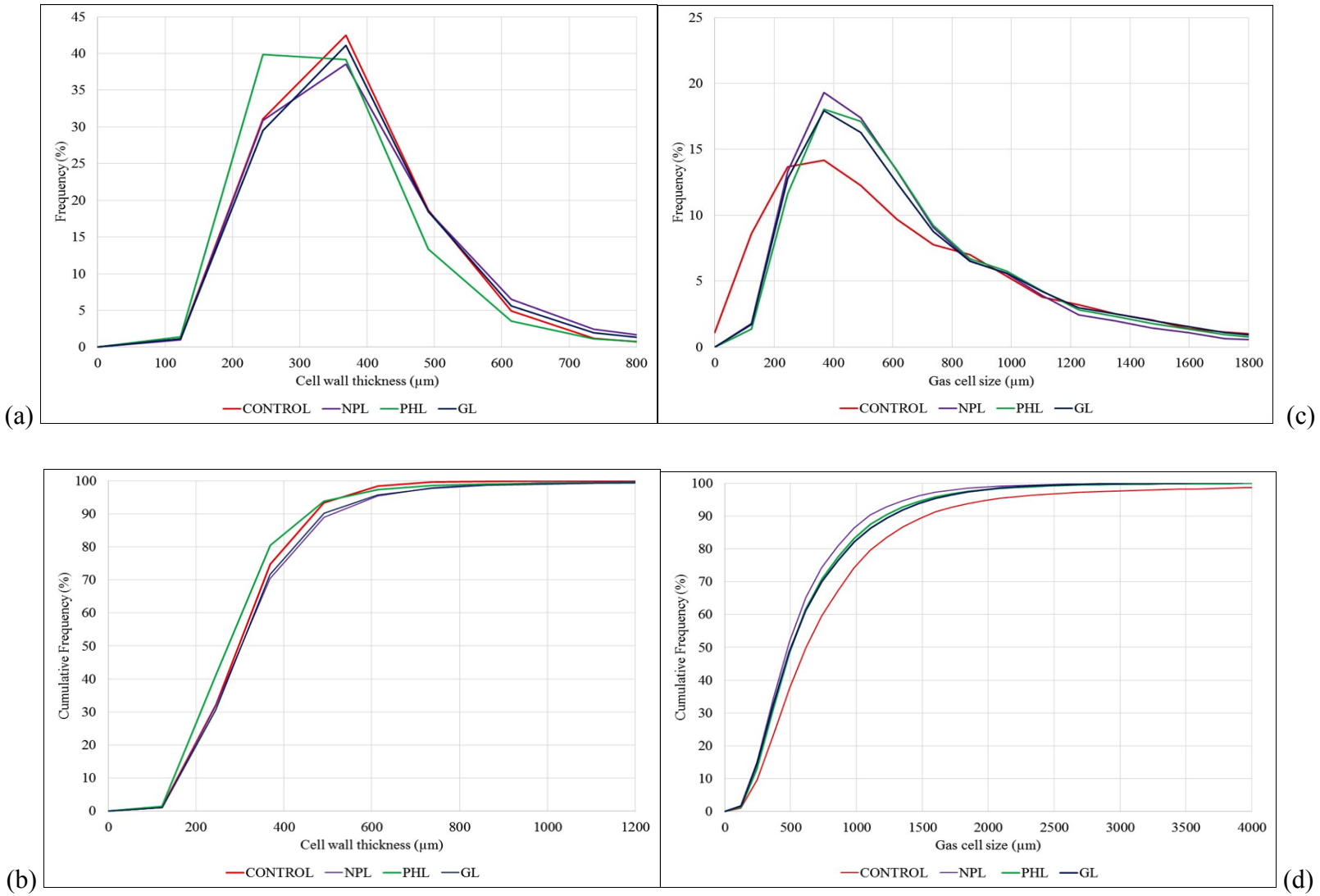

Figure 3.19 XMT loaf scans results for whole loaf samples for control, nonpolar (NPL), phospholipids (PHL), and glycolipids (GL) additions (a) cell wall thickness distribution, (b) cumulative cell wall thickness distribution, (c) gas cell size distribution, (d) cumulative gas cell size distribution.

Table 3.12 Macro XMT results for whole loaf breads containing varying lipid treatments

Treatments	Volume index (VOI) (um^3)	Solid volume (%)	Fragmentation index (1/µm)	Cell wall thickness (um)	Gas cell size (um)	Number of gas cells	Total porosity (%)
Control	1.57E14[a] (1.72E13)	42.37[a] (2.95)	-0.004 [a] (0.0002)	369.40[a] (22.67)	881.40[a] (24.10)	210540.80[a] (34711.89)	57.63[a] (2.95)
Nonpolar	1.28E14[a] (2.59E13)	51.45[b] (2.84)	-0.006[b] (0.0007)	389.75[a] (40.55)	648.68[b] (37.64)	74825.00[b] (45665.16)	50.24[b] (3.85)
Phospholipids	1.51E14[a] (6.40E12)	44.12[a] (3.83)	-0.005[ab] (0.0007)	359.37[a] (39.69)	699.85[b] (31.98)	118243.67[bc] (34823.08)	55.88[ab] (3.83)
Glycolipids	1.52E14[a] (2.45E13)	47.82[ab] (5.39)	-0.006[b] (0.0015)	394.22[a] (54.91)	700.34[b] (58.41)	169857.33[ac] (50700.87)	52.18[ab] (5.39)

[a]Means in the same column with different letters are significantly different at a $p<0.05$; (n=24)
[b]Values in parenthesis are standard deviations

Table 3.13 Gas cell size percentile distributions for whole loaf breads with added lipids

Treatments	25% (um)	50% (um)	75% (um)	95% (um)	Avg. gas cell size (um)
Control	392.95[a] (33.63)	650.83[a] (54.91)	1006.94[a] (33.63)	2112.11[a] (82.37)	881.40[a] (24.10)
Nonpolar	317.22[b] (25.07)	501.42[b] (25.07)	757.25[b] (50.13)	1412.17[b] (102.74)	648.68[b](37.64)
Phospholipids	337.69[ab] (51.37)	532.12[b] (31.71)	849.35[b] (71.78)	1562.67[b] (108.10)	699.85[b] (31.98)
Glycolipids	327.46[a] (31.71)	521.89[b] (51.37)	849.35[b] (81.61)	1575.90[b] (163.22)	700.34[b] (58.41)

[a]Means in the same column with different letters are significantly different at a $p<0.05$; (n=24)
[b]Values in parenthesis are standard deviations

XMT results for whole loaf samples are shown in Table 3.12. No significant differences were seen between the volume of interest (VOI) for any of the samples. The solid volume (%) within the VOI was significantly larger for the NPL samples (51.45%) than the control (42.37%) and PHL (44.12%). Curvature of the gas cells, determined from the fragmentation index found the control and all lipid treatments to be negative and very small in value. This indicated concavity with a connected pore structure. No significant differences were seen between the average cell wall thickness of any of the samples and the control. However, the average gas cell size (structure separation) measurements were significantly different. The control (881 μm) was significantly larger than all three treatments. The number of objects (amount of gas cells in a sample) was significantly higher for the control (210540) than for both NPL (74825) and PHL (118242), but not than the GL (16985). The combination of the reduction in the number of cells and the average gas cell size within the whole loaf, would suggest that the lipid treatments, specifically NPL influenced the abililty for the dough to stabilize and allow for expansion within the gas cells and this would be reflective in differences in volumes and specific volumes of the loaves. Finally, the total porosity of the control sample was higher (58%) than those of the NPL (50%), PHL (56%), and the GL (52%).

Table 3.13 contains the 25%, 50%, 75%, and 95% percentile values for all whole loaf treatments using data from the cumulative distribution graphs (Fig 3.18d). For every percentile range, there was difference in gas cell size between the control and the lipid treatments. The control had larger gas cells across each distribution. However, in the 25th percentile range, both the PHL (338 μm) and the GL (327 μm) were not significantly different from the control (393 μm) while the NPL (317 μm) was significantly different. At the higher percentile ranges (50%-95%), the control was significantly larger at each level. The average gas cell sizes of the samples fell between the 50th and the 75th percentile. The GL and PHL loaves had very similar percentile gas cell averages to one another throughout all ranges while the NPL had the smallest gas cells overall.

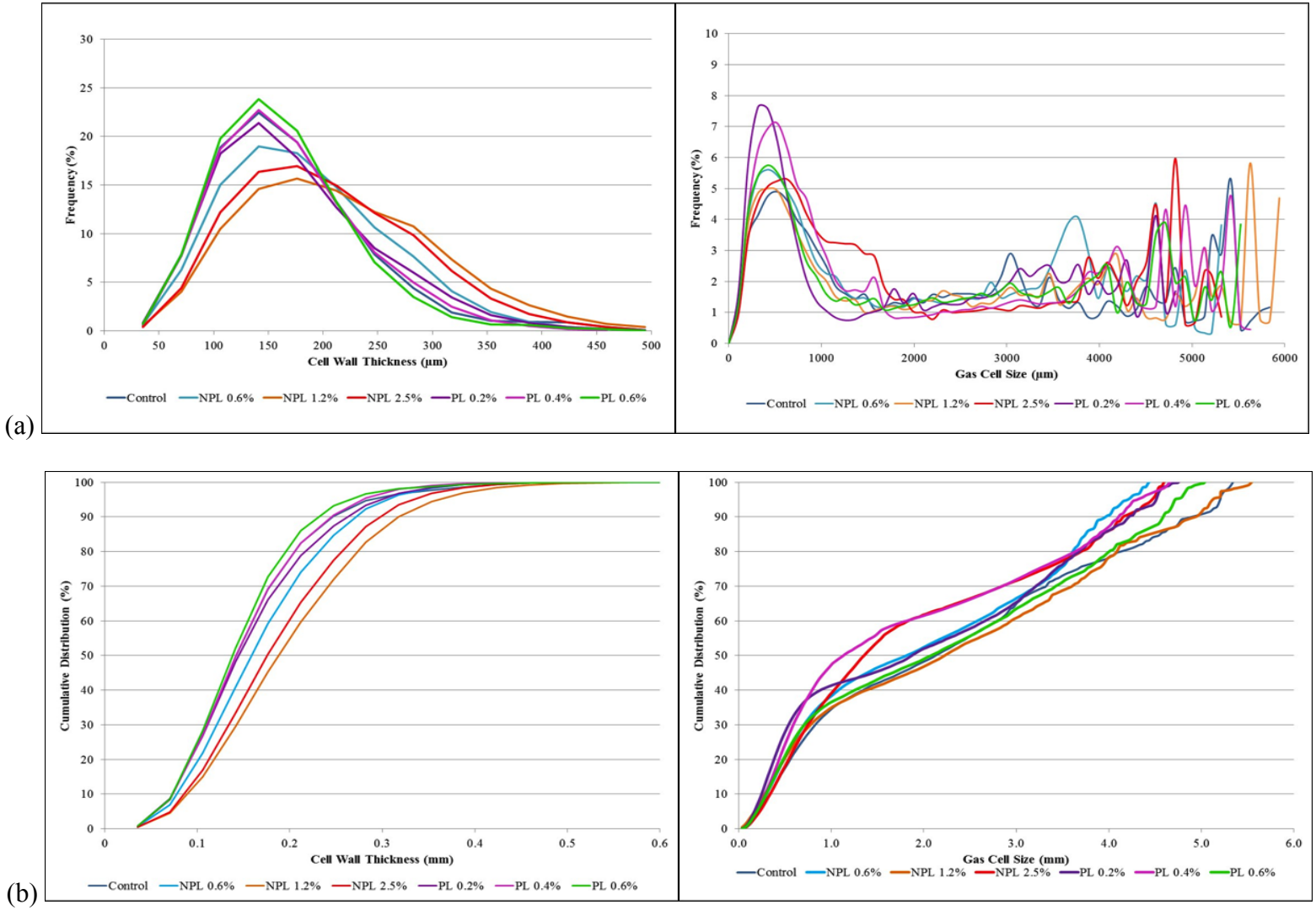

Figure 3.20. XMT scan results for center section of bread slice for control, 0.6, 1.4%, and 2.8% nonpolar (NPL) and 0.2%, 0.4%, and 0.6% polar (PL) (a) cell wall thickness distribution, (b) cumulative cell wall thickness distribution, (c) gas cell size distribution (d) cumulative gas cell size distribution.

3.3.7.2. XMT micro testing

Figure 3.19 contains the cell wall thickness distributions (a), cumulative cell wall thickness distributions (b), gas cell size distributions (c), and cumulative gas cell size distributions (d) for center section testing the control and varying levels of NPL and PL. The cell wall thickness distributions had thicknesses starting at 30 μm to 400 μm. All NPL concentrations caused the thickness spread to increase compared to the control sample. In contrast, the addition of PL caused difference from the control only at the varying levels. This trend is also seen in the cumulative cell wall thickness distribution curves where there was a shift to the right (thicker) in the curves of NPL as compared to the control and PL. The gas cell size distribution curves showed the highest percentage of cells were between 0 and 2000 μm. Both the 0.2% and 0.4% PL samples had the highest portion of their cells 1000 μm or less. The cumulative gas cell distribution curves were shifted more by the addition of 2.5% NPL and 0.4% PL as the frequency of smaller gas cells (1.0-2.0 mm) increased.

Table 3.14 presents XMT results for samples with varying levels of NPL and PL as well as the control. There were no significant differences between the VOI values or the percent object volumes for any of the treatments. Fragmentation measurements showed small, negative values, which suggested a connected, concave pore structure. There were significant differences between the average cell wall thickness as both 1.2% NPL (216 μm) and 2.5% NPL (204 μm) had increased thickness. The 0.6% PL (166 μm) had thickness close to that average cell wall of the control (166 μm). There were no significant differences in the average gas cell size in any of the samples. The 2.5% NPL (83020) had the highest number of gas cells and this was significantly different from all the treatments except for 0.6% PL (62005 μm). All the other number of gas cells were less than those two levels. Total porosity values were not significantly different from one another and ranged between 84% and 89%. Using cumulative gas cell distribution curve (Fig 3.19d) values were determined for 25^{th}, 50^{th}, 75^{th}, and 95^{th} percentile for all the treatments. They are compared in Table 3.15. None of the gas cell sizes were found to be significantly different from any of the samples at any of the percentile ranges.

Table 3.14. XMT results for center section breads containing varying lipid treatments

Treatment[a]	Volume index (VOI) (μm^3)	Solid volume (%)	Fragmentation index (1/µm)	Cell wall thickness (µm)	Gas cell size (µm)	Number of gas cells	Total porosity (%)
Control	2.89E12[a] (2.20E11)	12.07[a] (1.09)	-0.00194[ab] (0.00)	166.08[a] (6.38)	2288.08[a] (418.49)	36925.68[a] (6981.15)	87.93[a] (1.09)
NPL 0.6%	2.62E12[a] (2.70E11)	13.57[a] (1.43)	-0.00154[ab] (0.00)	185.56[ab] (3.72)	2072.75[a] (335.54)	48991.00[a] (123.12)	86.43[a] (1.43)
NPL 1.2%	2.84E12[a] (4.2E11)	15.21[a] (2.53)	-0.00278[a] (0.00)	216.16[b] (27.83)	2455.68[a] (533.40)	50246.00[a] (9176.86)	84.79[a] (2.53)
NPL 2.5%	2.41E12[a] (5.9E11)	14.24[a] (3.21)	-0.00130[ab] (0.00)	203.55[ab] (11.24)	2111.44[a] (1017.61)	36773.00[a] (8896.91)	85.76[a] (3.21)
PL 0.2%	2.58E12[a] (1.3E11)	13.87[a] (2.42)	0.00055[b] (0.00)	171.49[a] (23.67)	2016.95[a] (325.83)	83020.33[b] (13147.28)	86.13[a] (2.42)
PL 0.4%	2.34E12[a] (6.9E11)	13.36[a] (5.62)	-0.00053[b] (0.00)	174.98[ab] (4.79)	2109.87[a] (1182.73)	44570.67[a] (5564.29)	86.64[a] (5.62)
PL 0.6%	2.63E12[a] (3.0E11)	10.98[a] (2.62)	0.00277[ab] (0.00)	166.46[a] (6.25)	2312.65[a] (460.11)	62005.00[ab] (16213.52)	89.02[a] (2.62)

[a]Nonpolar (NPL) and polar (PL)
[b]Means in the same column with different letters are significantly different at $p<0.05$; (n=21)
[c]Values in parenthesis are standard deviations

Table 3.15 Gas cell size percentile distribution for center section breads at varying lipid treatments

Treatment	25% (µm)	50% (mm)	75% (µm)	95% (µm)	Avg. gas cell size (µm)
Control	678.02[a] (0.04)	2216.37[a] (0.40)	3766.12[a] (1.01)	5093.68[a] (0.51)	2288.08[a] (418.49)
NPL 0.6%	617.79[a] (0.06)	1888.69[a] (0.50)	3553.80[a] (0.54)	4342.22[a] (0.71)	2072.75[a] (335.54)
NPL 1.2%	682.52[a] (0.08)	2512.37[a] (0.68)	3895.06[a] (0.81)	5224.79 (1.03)	2455.68[a] (533.40)
NPL 2.5%	703.14[a] (0.15)	2154.68[a] (1.08)	3435.39[a] (1.88)	4181.44[a] (2.11)	2111.44[a] (1017.61)
PL 0.2%	454.39[a] (0.05)	1950.36[a] (0.65)	3490.80[a] (0.59)	4403.80[a] (0.39)	2016.95[a] (325.83)
PL 0.4%	619.95[a] (0.19)	2194.14[a] (1.37)	3385.42[a] (2.08)	4218.10[a] (2.28)	2109.87[a] (1182.73)
PL 0.6%	617.74[a] (0.14)	2247.12[a] (0.57)	3836.14[a] (0.77)	4931.18[a] (0.76)	2312.65[a] (460.11)

[a]Nonpolar (NPL) and polar (PL)
[b]Means in the same column with different letters are significantly different at $p<0.05$; (n=21)
[c]Values in parenthesis are standard deviations

3.4. Discussion

The changes in the visco-elastic properties of dough at small deformation are mostly associated with starch, protein, and water (Khatkar and Schofield 2002a). The addition of starch to gluten decreases G' promotes shear thinning behavior, and increases the elasticity of the sample (Smith et al 1970; Khatkar and Schofield 2002a, Song and Zheng 2007). Also the application of varying stress has shown to have a greater effect on starch and gluten than on gluten alone (Khatkar and Schofield 2002a). In general, starch is associated with "non-linearity" characteristics of the dough (Khatkar and Schofield 2002a). Protein's viscous and elastic behavior is directly linked to the glutenin to gliadin ratio (Song and Zheng 2007). Higher glutenin levels are correlated to measured elastic properties while gliadin is associated with the viscous characteristics. The increased levels of these combined fractions in flour will create stronger dough with improved shear viscosity (Song and Zheng 2007; Delcour and Hoseney 2007). Water also plays a role as it hydrates the system, fills in voids, and serves as a lubricator to reduce particle friction (Song and Zheng 2007).

In this study, Mixolab results showed that the addition of total lipids at both low and high concentrations had minimal effects on mixing behavior, protein weakening, and starch gelatinization. However, following gelatinization there was a difference between control and the other three test treatments in the applied torque needed for setback. The addition of total lipids-100g flour caused changes in the dough that reduced the torque. In contrast, the total lipids-200 g flour had higher torque values than did the control. The reduction in torque was likely due to the complexing of lipid chains with amylose or lipids with lipids, forming amylose-lipid complexes or the creation of lipid-lipid micelles (Tang and Copeland 2007). The amylose-lipids complexes formed slowed the onset of retrogradation. The complexing of lipids prevented amylose from recrystallizing, which is a main component cause of retrogradation. The control sample was lower than both defatted and total lipids-200 g addition as defatting alters the gluten phase and can strengthen the protein-protein interactions.

Stress sweep testing showed that increasing the applied stress caused a reduction in the moduli (G', G") for after mixing and proofing for all the lipid treatments with an LVR at 40 Pa. The defatted sample, however, was least affected by the applied stress at both processing stages.

The frequency sweep test showed that the moduli increased as the applied frequency increased. This would indicate that the dough exhibited elastic properties, which is often found in weaker flours containing higher starch content (Khatkar and Schofield 2002b). A larger change in the G' and G" for both the stress and frequency sweeps were seen after mixing than after proofing. Mixing allows for the creation, interaction, and bonding between polymers. It promotes the transfer and alignment of the lipids within the dough structure. Gerits et al (2015) found that in order for compounds such as lipids to have an influence on dough properties, these constituents must be present at the beginning of mixing. Papantoniou et al (2003) determined that lipid fractions have the greatest effect on cookie dough structure when present at mixing.

The increase in the G' moduli of the defatted sample during the frequency sweep was likely due to starch having more friction between the granules because of the defatting process. Georgopoulos et al (2006) determined that the initial size of the gluten structure was reduced due to lipid removal. This could allow for greater interaction between starch or protein molecules, thus increasing the G'. Due to the lipid removal, the defatted sample had more protein-protein interactions. Gómez et al (2011) found increased levels of S-S or disulfide bond linkages during over mixing of dough. This causes an increase in G' and decrease of tan δ, both associated with elastic properties of dough.

The lipid addition promoted the interaction of starch with the PHL, NPL, and GL reducing the moduli that wasn't seen with the defatted sample. The NPL fraction caused the biggest decrease in the G' and G" moduli of all the added treatments. The sample containing GL and PHL additions were characteristically more like the control as the chain links of the lipid structures were able to form complexes with proteins and starch. Wilde et al 1993 and Tang and Copeland 2007 found that lipids could interact with both starch and proteins. For the PHL treatment, there also was a concentration effect, as this sample was more similar to the defatted flour treatment. Because there was a lower concentration recovery from the extraction process, less of an influence of these lipids were seen.

Temperature sweep testing showed the greatest influence of starch as most of the differences between the treatments were across the temperature range of starch gelatinization. Initally, the G' of all the samples dropped during heating. PHL and the defatted flour were the least affected. For those two samples, starch gelatinization started earlier than did the other three treatments. These treatments had viscosity curves that were higher sooner than the other three

samples. Defatting and reconstitution studies of soft wheat flours used in cookies found that the starch existed as "agglomerates and particles" following lipid removal, with the layer of protein covering the outside, preventing full hydration of the starch (Papantoniou et al 2004). The binding of GL and NPL with starch slowed the onset of gelatinization making those samples similar to the control. The lipids also melted at temperatures between 45°C-65°C causing additional peaks in the curves for the GL and NPL samples. This facilitated starch-lipid complexation. There were also changes in viscosity (increased) for all treatments. However, the full gelatinization of starch occurred at a higher temperature for the NPL and control samples. The temperature of gelatinization was higher for GL addition than for defatted and PHL addition. However, there was a greater increase in viscosity at a lower temperature for the GL than the control and NPL addition. From the changes in gelatinization temperature and viscosity caused by GL, this would support the findings of Hoseney et al (1970) and Tang and Copeland (2007) that there was an interaction of GL with both starch and protein.

NPL addition caused the greatest changes to the characteristics of the dough. Samples conatining this fraction (NPL) had the lowest values for all rheological measurements. Because the behavior of the temperature sweep curves for the NPL resembled the control versus the defatted samples this would support the findings of Li et al (2004) who found that NPL was more associated with the starch than protein. NPL does not improve the loaf volume due to its inability to hold air cells as determined by MacRitchie and Gras (1973) because it does not form compressed monolayers at the interface. However, there still appeared to be an influence of the NPL on the overall rheological properties of the dough in contrast to the findings of Sroan et al (2009).

During proofing and baking, visco-elastic properties of dough change due to growing gas cells and experience biaxal response to the stresses and strains. Dough is an elastic film with the ability to expand/extend in response to increases in gas production because it undergoes uniaxial and biaxial extensions (Sliwinski et al 2004). Extension testing showed that the addition of all of the lipid fractions weakened the dough. The fracture force values were all reduced compared to the control and defatted samples. There was less effect on dough extension except for the PHL, which caused the extension values to be reduced. The decrease in extensibility curves and values was indication of reduced strength of the dough. This could be due to interactions of lipids with proteins, lipids with starch, or lipids with lipids as shown by Tang and Copeland (2007).

The stress fracture and the elastic properties are related to crumb structure and have a direct positive correlation with the thickness of cell walls (Falcone et al 2004). Cell wall thickness is affected by "mechanical" properties of the dough (Falcone et al 2004). The stress-strain measurements and strain hardening values in this current study were reduced by the presence of NPL, PHL, and GL. The control and defatted had the highest measured stress and strain values. The NPL continued to have lower values for all large deformation results except the fracture strain. PHL even though having reduced values, had similar fracture stress, extensional stiffness, and strain hardening index that closely resembled the control and defatted flours. The fracture strain was the lowest with PHL present, which was likely associated with the observed reduction in extensibility of the sample. Fracture stress values of the NPL samples were lowest, reflecting the least strength in the cell walls. This would decrease the ablity for gas cell expansion. GL and PHL showed more resistance to breaking and had higher fracture stresses. The NPL and GL resulted in reduced stiffness and loss of strain hardening. This suggests that these doughs wouldn't provide cell wall stability comparable to the control, defatted, or PHL samples. In the case of the defatted flour, the removal of lipids did not inhibit the dough's ability to expand because the gluten was still able to form a developed network and there were fewer interactions between polar lipids allowing for the development of more protein-protein interactions (Gan et al 1990; Paternotte et al 1994).

Gas cell expansion does not occur in the same way for each bubble; however, the cells initially start as spheres and then due to pressures gradually convert in to polyhedral shapes (Van Vliet et al 1992). These changes in the gas cell size and shape results in expansion of the bread loaf. These present results found no significant differences in proof heights of the whole loaf treatments. The control was larger in volume than all of the other treatments. Even though the volumes of the lipid containing treatments were reduced, the GL and PHL samples resulted in loaves with volumes that were larger than the NPL. MacRitchie and Gras (1973) found during their early work studying the function of lipids in bread baking, that nonpolar lipids were detrimental to loaf volumes. The results of the present study are in agreement with these earlier findings. It was also shown that the presence of polar lipids was beneficial to loaf volume, but the level of addition is critical for this enhancement to occur (MacRitchie and Gras 1973).

The center loaf volume testing showed that the addition of NPL and PL lipids did cause differences in the proof heights, suggesting a concentration effect of lipid addition. The largest

change was seen for the NPL; whereas, the PL didn't have as large of an influence. Differences in proof height were reflected in final product volumes. The higher levels of NPL caused reductions in loaf volume while PL addition caused increases in loaf volume to the point that the volumes were higher than those of the control.

These results were reflected in both C-Cell and XMT measurements. The C-Cell imaging of the whole loaf showed differences in the slice are, which was indicative of the changes in the overall volume of the samples. Both the NPL and GL were able to produce samples closer in size to the control than was the NPL. However, the number of cells within each loaf were not found to differ significantly. This indicated that all samples had finer cells than the control. Cell wall thickness was greater for the control than for any of the other treatments. This was also the case for cell diameters. The NPL loaves had thinner cell walls and the smallest cell diameters of all the treatments. Elongation values were larger than 1 for all the treatments suggesting that the gas cells were not limited to round shapes, but at a variety of sizes, thus better able to undergo greater expansion. When comparing the center loaf samples at varying lipid concentrations, the control and PL at all levels caused greater increases in slice area and number of cells than did the NPL. This again would be an indication of higher loaf volumes with larger ranges of finer cells for both the control and PL samples. Cell wall thickness was greatest for the control and 0.6% PL samples.

The whole loaf NPL, GL, and PHL samples had thicker cell walls than the control samples and a lower number gas cells. The GL and PHL samples had thickness values close to the control and NPL had the lowest values. These differences were linked to changes in the overall loaf volume as the GL and PHL allowed for cell expansion bringing them closer to the control. The NPL samples had more limited expansion, a larger solid matrix, and fewer gas cells. The loaves (NPL) produced were denser and smaller in volume. The addition of varying levels of each of the lipid resulted in a wider distribution of cell wall thicknesses and gas cell sizes. Higher cell thickness distributions for the NPL at all levels than with the PL addition.

The effect of NPL, GL, and PHL presence on the dough properties show that GL and PHL (which are the polar lipid) do influence the rheological properties of dough and the microstructure of bread, probably through their interactions with both starch and proteins. The PHL and GL can interact with both proteins and starch, which makes them more suited to move to stabilize gas cells and form amylose-lipid complexes. These lipids also can help to stabilize

gas cell walls, allowing for gas cell growth and expansion, thus providing support allowing for increase in loaf volume. This supports Gan et al (1990) and Sroan et al (2009) findings of the presence of a secondary liquid lamellae that helps to prevent coalescence of gas cells following the stretching of the gluten-starch matrix. Higher levels of PL lipids showed to have a greater influence on the structural matrix while NPL, on the other hand, was not able to provide stability to gas cells or prevent coalescence. The mechanism by which the polar lipids assist in stabilizing air cells is because of their ability to align themselves at the interface and surround gas cells. These lipids are most beneficial when the gluten-starch matrix begins to stretch and break down at the end of proofing and the beginning of baking (Gan et al 1990). This break down of the structure has been hypothesized as being caused by the over expansion due to internal pressures on the expanding gas cells (Gerits et al 2015).

3.5. Conclusion

The influence of native wheat lipid fractions on the rheological properties of dough and the microstructure of bread was affected by type of lipid and the interactions with other components in the structural matrix. The addition of all the lipid treatments weakend the dough, but rheological testing showed the dough exhibited greater elastic than viscous behavior. The addition of polar and nonpolar lipids showed interactions between both lipids and proteins and lipids and starch. This reduced the strength and increased the viscous properties of the dough as compared to the defatted samples. C-Cell imaging and XMT testing determined changes in the structural make-up and gas cell distribution as the polar lipid fractions had more positive influence on the loaf microstructure and volume as compared to the nonpolar lipids. The ability of the polar lipids to move to the interface, forming the secondary lamellae is beneficial part for promoting gas cell stability, improving and maintaining the crumb grain integrity, and providing overall, better quality bread. Even though lipids do have the capabilities to be surface active and maintain gas cells, their function is not limited to stabilize just gas cells, but also as contributors to visco-elastic properties of the dough.

3.6. References

AACC International. Approved Methods of Analysis, 11th Ed. Method 10-05.01. Guidelines for Measurement of Volume by Rapeseed Displacement. Approved October 17, 2001. AACC International: St. Paul, MN. http://dx.doi.org/10.1094/AACCIntMethod-10-05.01.

AACC International. Approved Methods of Analysis, 11th Ed. Method 10-10.03. Optimized Straight Dough Bread-making Method. Approved November 3, 1999. AACC International: St. Paul, MN. http://dx.doi.org/10.1094/AACCIntMethod-10-10.03.

AACC International. Approved Methods of Analysis, 11th Ed. Method 44-15.02. Moisture-Air Oven Method. Approved November 3, 1999. AACC International: St. Paul, MN. http://dx.doi.org/10.1094/AACCIntMethod-44-15.02.

AACC International. Approved Methods of Analysis, 11th Ed. Method 54-40.02. Mixograph Method. Approved November 3, 1999. AACC International: St. Paul, MN. http://dx.doi.org/10.1094/AACCIntMethod-54-40.02

AACC International. Approved Methods of Analysis, 11th Ed. Method 76-31.01. Determination of damaged starch-spectrophotometric method. Approved January 10, 2014. AACC International: St. Paul, MN. http://dx.doi.org/10.1094/AACCIntMethod-76-31.01.

AACC International. Approved Methods of Analysis, 11th Ed. Method 82-23.01. Table: Flour Weight to Give 100 g at 14% Moisture Basis. Approved November 3, 1999. AACC International: St. Paul, MN. http://dx.doi.org/10.1094/AACCIntMethod-82-23.01.

Abang Zaidel, D.N., Chin, N.L., Abdul Rahman, R., and Karim, R. 2008. Rheological characterisation of gluten from extensibilty measurement. J Food Eng. 86:549-556.

Agyare, K.K., Xiong, Y.L., Addo, K., and Akoh, C.C. 2004. Dynamic rheological and thermal properties of soft wheat flour dough containing structure lipid. J Food Sci. 69: E297-E302.

Alvarez-Jubete, L., Auty, M., Arendt, E.K., and Gallagher, E. 2010. Baking properties and microstructure of pseudocereal flours in gluten-free bread formulations. Euro Food Res Technol. 230: 437-445.

Autio, K., Flander, L., and Kinnunen, A., and Heinonen, R. 2001. Bread quality relationship with rheological measurements of wheat flour dough. Cereal Chem. 78: 654-657.

Babin, P., Della Valle, G., Chiron, H., Cloetens, P., Hoszowska, J., Pernot, P., Réquerre, Salvo, L., and Dendievel, R. 2006. Fast x-ray tomography analysis of bubble growth and foam setting during breadmaking. J Cereal Sci. 43: 393-397.

Besbes, E., Jury, V., Monteau, J.-Y., and Le Bail, A. 2013. Characterizing the cellular structure of bread crumb and crust as affected by heating rate using x-ray microtomography. J Food Eng. 115: 415-423.

Blazek, J., Gilbert, E.P., and Copeland, L. 2011. Effects of monoglycerides on pasting properties of wheat starch after repeated heating and cooling. J Cereal Sci. 54: 151-159.

Bonet, A., Blaszczak, W. and Rosell, C.M. 2006. Formation of homopolymers and heteropolymers between wheat flour and several protein sources by transglutaminase-catalyzed cross-linking. Cereal Chem.: 83: 665-662.

Cafarelli, B., Spada, A., Laverse, J., Lampignano, and Del Nobile, M.A. 2014a. An insight into the bread bubble structure: an x-ray microtomography approach. Food Res Int. 66: 180-185.

Cafarelli, B., Spada, A., Laverse, J., Lampignano, and Del Nobile, M.A. 2014b. X-ray microtomography and statistical analysis: tools to quantitatively classify bread microstructure. J. Food Eng. 124: 64-71.

Campos, D.T, Steffe, J.F., and NG, P.K.W. 1997. Rheological behavior of undeveloped and developed wheat dough. Cereal Chem. 74: 489-494.

Cauvain, S. 2012. Breadmaking: an overview. Pages 26-28 in: Breadmaking Improving Quality, 2nd Ed. S.P. Cauvain, ed. Woodhead Publishing Limited: Cambridge

Cauvain, S. 2013. Quality measures in baking. Cereal Food World. 58: 170-171.

C-Cell Imaging. 2014. Baked product imaging system analysis guide. Calibre Control International, Ltd: Warrington.

Chung, O.K., Pomeranz, Y., and Finney, K.F. 1982. Relation of polar lipid content to mixing requirement and loaf volume potential of hard red winter wheat flour. Cereal Chem. 59: 14-20.

Chung, O.K, Ohm, J-B., Ram, M.S., and Howitt, C.A. 2009. Wheat lipids. Pages 363-373 in: Wheat Chemistry and Technology, 4th Ed. K. Khan and P.R. Shewry, eds. AACC International, Inc.: St. Paul.

Chung, O.K. and Tsen, C.C. 1975. Changes in lipid binding and distribution during dough mixing. Cereal Chem. 52: 533-548.

Daftary, R.D., Pomeranz, Y., Shogren, M., and Finney, K.F. 1968. Functional bread-making properties of wheat flour lipids. 2. The role of flour lipid fractions in bread-making. Food Techn. 22: 79-82.

Delcour, J. A. and Hoseney, R.C. 2010. Principles of Cereal Science and Technology. AACC International, Inc.: St. Paul.

Dobraszczyk, B.J., and Roberts, C.A. 1994. Strain hardening and dough gas cell-wall failure in biaxial extension. J Cereal Sci. 20: 265-274.

Dobraszczyk, B.J., and Salmanowicz, B.P. 2008. Comparison of predictions of baking volume using large deformation rheological properties. J Cereal Sci. 47: 292-301.

Dreese, P.C., Faubion, J.M., and Hoseney, R.C. 1988. Dynamic rheological properties of flour, gluten, and gluten-starch doughs. I. temperature-dependent changes during heating. Cereal Chem. 65: 348-353.

Dunnewind, B., Sliwinski, E.L., Grolle, K., and Van Vliet, T. 2004. The Kieffer dough and gluten extensibility rig- an experimental evaluation. J. Text Stud. 34: 537-560.

Falcone, P.M., Baiano, A. Zanini, F., Mancini, L., Tromba, G. Montanari, F., and Del Nobile, M.A. 2004. A novel approach to the study of bread porous structure: Phase-contrast x-ray microtomography. J Food Sci. 69: E38-E43.

Falcone, P.M., Baiano, A. Zanini, F., Mancini, L., Tromba, G., Dreossi, F., G. Montanari, F., Scuor, N., and Del Nobile, M.A. 2005. Three-dimensional quantitative analysis of bread crumb by x-ray microtomography. J Food Sci. 70: E265-E272.

Faubion, J.M., and Hoseney, R.C. 1990. The viscoelastic properties of wheat flour dough. Pages: 57-59 in: Dough Rheology and Baked Product Texture. H. Faridi and J.M. Faubion, eds. Van Nostrand Reinhold: New York.

Finnie, S.M., Jeannotte, R., and Faubion, J.M. 2009. Quantitative characterization of polar lipids from wheat whole meal, flour, and starch. Cereal Chem. 86: 637-645.

Gan, Z., Angold, R.E., Williams, M.R., Ellis, P.R., Vaughan, J.G., and Galliard, T. 1990. The microstructure and gas retention of bread dough. J Cereal Sci. 12: 15-24.

Gan, Z., Ellis, P.R., and Schofield, J.D. 1995. Gas cell stabilisation and gas retention in wheat bread dough. J Cereal Sci. 21: 215-230.

Gandikota, S., and MacRitchie, F. 2005. Expansion capacity of doughs: methodology and applications. J Cereal Sci. 42:157-163.

Georgopoulos, T., Larsson, H., and Eliasson, A-C. 2004. A comparison of the rheological properties of wheat flour dough and its gluten prepared by ultracentrifugation. Food Hydrocolloids. 18: 143-151.

Georgopoulos, T., Larsson, H., and Eliasson, A-C. 2006. Influence of native lipids on the rheological properties of wheat flour dough and gluten. J Texture Stud. 37:49-62.

Gerits, L.R., Pareyt, B., and Delcour, J.A. 2013. Single run HPLC separation coupled to evaporate light scattering detection unravels wheat flour endogenous lipid redistribution during bread dough making. LWT-Food Sci Technol. 53: 426-433.

Gerits, L.R., Pareyt, B., and Delcour, J.A. 2014. A lipase base approach to studying the role of wheat lipids in bread making. Food Chem. 156: 190-196.

Gerits, L.R., Pareyt, B., Masure, H.G., and Delcour, J.A. 2015. Native and enzymatically modified wheat (*Triticum aestivum L.*) endogenous lipids in bread making: a focus on gas cell stabilization mechanisms. Food Chem. 172: 613-621

Gómez, A.V., Buchner, D., Tadini, C.C., Añón, M.C., and Puppo, M.C. 2013. Emulsifiers: effects on quality of fibre-enriched wheat bread. Food Bioprocess Technol 6: 11228-1239.

Hadnađev, M., Dapčević Hadnađev, T., Šimurina, O., and Filipčev, B. 2013. Empirical and fundamental rheological properties of wheat flour dough as affected by different climatic conditions. J Agr Sci Tech. 15: 1381-1391.

Hoseney, R.C., Finney, K.F., Pomeranz, Y., and Shogren, M.D. 1969. Functional (breadmaking) and biochemical properties of wheat flour components. V. role of total extractable lipids. Cereal Chem. 46: 606-613.

Hoseney, R.C., Finney, K.F., and Pomeranz, Y. 1970. Functional (breadmaking) and biochemical properties of wheat flour components. VI. gliadin-lipid-glutenin interactions in wheat gluten. Cereal Chem. 47: 135- 40.

Hoseney, R.C., Finney, K.F., and Shogren, M.D. 1972. Functional (breadmaking) and biochemical properties of wheat flour components. IX. replacing total free lipids with synthetic lipids. Cereal Chem. 49: 366-371.

Jekle, M., and Becker, T. 2015. Wheat dough microstructure: the relation between visual structure and mechanical behavior. Cr Rev Food Sci. 55: 369-382.

Keller, R.C.A., Orsel, R., and Hamer, R.J. 1997. Competitive adsorption behaviour of wheat flour components and emulsifiers at air-water interface. J Cereal Sci. 25: 175-183.

Khatkar, B.S., and Schofield, J.D. 2002a. Dynamic rheology of wheat flour dough. I. non-linear viscoelastic behaviour. J Sci Food Agric. 82: 827-829.

Khatkar, B.S., and Schofield, J.D. 2002b. Dynamic rheology of wheat flour dough. II. Assessment of dough strength and bread-making quality. J Sci Food Agric. 82: 823-826

Lefebvre, J. 2006. An outline of the non-linear viscoelastic behaviour of wheat flour dough in shear. Rheol Acta. 45: 525-538.

Létang, C., Piau, M., and Verdier, C. 1999. Characterization of wheat flour-water doughs. Part I: rheometry and microstructure. J Food Eng. 41: 121-132.

Li, W., Dobraszczyk, B.J., and Wilde, P.J. 2004. Surface properties and locations of gluten proteins and lipids revealed using confocal scanning laser microscopy in bread dough. J Cereal Sci. 39: 403-411.

Lim, K.S. and Barigou, M. 2004. X-ray micro-computed tomography of cellular food products. Food Res Int. 37:1001-1012.

Lodi, A. and Vodovotz, Y. 2008. Physical properties and water state changes during storage in soy bread with or without almond. Food Chem. 110: 554-561.

Macosko, C.W. 1994. Rheology Principles, Measurements, and Applications. VCH Publishers, Inc.: New York.

MacRitchie, F. 2010. Concepts in Cereal Chemistry. Taylor & Francis Group, LLC.: Boca Raton.

Miller, K.A., and Hoseney R.C. 1999. Dynamic rheological properties of wheat starch-gluten doughs. Cereal Chem. 76: 105-109.

MacRitchie, F., and Gras, P.W. 1973. The role of flour lipids in baking. Cereal Chem. 50:292-302.

MacRitchie, F. 1977. Flour lipids and their effects in baking. J Sci Food Agric. 28: 53-58.

Masi, P., Cavella, S., and Sepe, M. 1998. Characterization of dynamic viscoelastic behavior of wheat flour doughs at different moisture contents. Cereal Chem. 75: 429-432.

Melvin, M.A. 1979. The effect of extractable lipid on the viscosity characteristics of corn and wheat starches. J Sci Food Agric. 30: 731-738.

Miller, K.A., and Hoseney R.C. 1999. Dynamic rheological properties of wheat starch-gluten doughs. Cereal Chem. 76: 105-109.

Moreno-Atanasio, R., Williams, R.A., and Jia, X. 2010. Combing x-ray microtomography with computer simulation for analysis of granular porous materials. Particuology. 8:81-99.

Nash, D., Lanning, S.P., Fox, P., Martin, J.M., Blake, N.K., Souza, E., Graybosch, R.A., Giroux, M.J., and Talbert, L.E. 2006. Relationship of dough extensibility to dough strength in a spring wheat cross. Cereal Chem 83: 255-258.

Newberry, M.P., Phan-Thien, N., Larroque, O.R., Tanner, R.I., Larsen, N.G. 2002. Dynamic and elongation rheology of yeasted bread dough. Cereal Chem. 79: 874-879.

Ohm, J.B., and Chung, O.K. 2002. Relationship of free lipids with quality factors in hard winter wheat flours. Cereal Chem. 79: 274-278.

Papantoniou, E., Hammond, E.W., Scriven, F., Gordon, M.H., and Schofield, J.D. 2004. Effects of endogenous flour lipids on the quality of short-dough biscuits. J Sci Food Agric. 84: 1371-1380

Papantoniou, E., Hammond, E.W., Tsiami, A.A., Scriven, F., Gordon, M.H., and Schofield, J.D. 2003. Effects of endogenous flour lipids on the quality of semisweet biscuits. J Agric Food Chem: 51: 1057-1063.

Paternotte, T.A., Orsel, R., and Hamer. R.J. 1994. Dynamic interfacial behaviour of gliadin-diacylgalactosylglycerol (MGDG) films: possible implications for gas-cell stability in wheat flour doughs. J Cereal Sci. 19: 123-129.

Pomeranz, Y., Rubenthaler, G.L., Daftary, R.D., and Finney, K.F. 1966. Effects of lipids on bread baked from flour varying widely in bread-making potentialities. Food Technol. 20: 1225-1228.

Pyler, E.J., and Gorton, L.A. 2009. Baking Science & Technology, 4th Ed., Volume II: Formulation and Production: Sosland Publishing Co.: Kansas City.

Reusch, W. 2013. Lipids. http://www2.chemistry.msu.edu/faculty/reusch/VirtTxtJml/lipids.htm.

Salvador, A., Sanz, T., and Fiszman, S.M. 2006. Dynamic rheological characteristics of wheat-flour doughs. effect of adding NaCl, sucrose, and yeast. Food Hydrocolloid. 20: 780-786.

Singh, S., and Singh, N. 2013. Relationship of polymeric proteins and empirical dough rheology with dynamic rheology of dough and gluten from different wheat varieties. Food Hydrocolloid. 33: 342-248.

Skerritt, J.H., Hac, L., Bekes, F. 1999. Depolymerization of the glutenin macropolymers during dough mixing: I. changes in levels, molecular weight distribution, and overall composition. Cereal Chem. 76: 395-401.

Sliwinski, E.L., Kolster, P., and van Vliet, T. 2004a. Large deformation properties of wheat dough in uni- and biaxial extension. part I. flour dough. Rheol Acta. 43: 306-320.

Sliwinski, E.L., van der Hoef, F., Kolster, P., and van Vliet, T. 2004a. Large deformation properties of wheat dough in uni- and biaxial extension. part II. gluten dough. Rheol Acta. 43: 321-332.

Smith, J.R., Smith, T.L., Tschoegl, N.W. 1970. Rheological properties of wheat flour doughs. Rheol Acta. 9: 239-252.

Song, Y., and Zheng, Q. 2007. Dynamic rheological properties of wheat flour dough and proteins. Trends Food Sci Tech. 18: 132-138.

Sroan, B.S., Bean, S.R., and MacRitchie, F. 2009. Mechanism of gas cell stabilization in bread making. I. the primary gluten-starch matrix. J Cereal Sci. 49: 32-40.

Sroan, B.S., and MacRitchie, F. 2009. Mechanism of gas cell stabilization in bread making. II. the secondary liquid lamellae. J Cereal Sci. 49: 41-46.

Sun, H., Yan, S., Jiang, W., Li, G., MacRitchie, F. 2010. Contribution of lipid to physicochemical properties and Mantou-making quality of wheat flour. Food Chem. 121: 332-337.

Takahashi, S. and Seib, P. 1988. Paste and gel properties of prime corn and wheat starches with and without native lipids. Cereal Chem. 65: 474-483.

Tang, M.C. and Copeland, L. 2007. Analysis of complexes between lipids and wheat starch. Carbohyd Polym. 67: 80-85.

Tester, R.F., and Morrision, W.R. 1990. Swelling and gelatinization of cereal starches. I. effects of amylopectin, amylose, and lipids. Cereal Chem. 67: 551-557.

Trinh, L., Lowe, T., Campbell, G.M., Withers, P.J., and Martin, P.J. 2013. Bread dough aeration dynamics during pressure step-change mixer: studies by x-ray tomography, dough density and population balancing modeling. Chem Eng Sci. 101: 470-471.

Tronsmo, K.M., Magnus, E.M., Baardseth, P., Schofield, J.D., Aamodt, A., and Faergestad, E.M. 2003. Comparison of small and large deformation rheological properties of wheat dough and gluten. Cereal Chem. 80: 587-595.

Turbin-Orger, A., Della Valle, G., Doublier, J.L., Fameau, A.-L., Marze, S., Sauliner, L. 2015. Foaming and rheological properties of liquid phase extracted from wheat flour dough. Food Hydrocolloid. 43:114-124.

Upadhyay, R., Ghosal, D., Mehra, A. 2012. Characterization of bread dough: rheological properties and microstructure. J Food Eng. 109: 104-113.

Van Dyck, T., Verboven, P., Herremans, E., Defraeye, T., Van Campenhout, L., Wevers, M., Claes, J., Nicolaï, B. 2014. Characterisation of structural patterns in bread as evaluated by x-ray computer tomography. J Food Eng. 123: 67-77.

Van Vliet, T., Janssen, A.M., Bloksma, A.H., and Walstra, P. 1992. Strain hardening of dough as a requirement for gas retention. J Texture Stud. 23: 439-460.

Vlassenbroeck, J., Dierick, M., Masschaele, B., Cnudde, V., Van Hoorebeke, L., Jacobs, P. 2007. Software tools for quantification of x-ray microtomography at UGCT. Nucl Instrum Meth A. 580: 442-445.

Villarino, V.B., Jayasena, V., Coorey, R., Chakrabarti-Bell, S., and Johnson, S. 2014. The effects of bread-making process factors on Australian sweet lupin-wheat bread quality characteristics. Int J Food Sci Tech. 49: 2373-2381.

Watanabe, A., Yokomizo, K., and Eliasson, A-C. 2003. Effect of physical states of nonpolar lipids on rheology, ultracentrifugation, and microstructure of wheat flour dough. Cereal Chem. 80: 281-284.

Weipert, D. 1990. The benefits of basic rheometry in studying dough rheology. Cereal Chem. 67: 311-317.

Whitworth, M.B., Cauvain, S. P., and Cliffe, D. 2005. Measurement of bread cell structure by image analysis. Pages 193-198 in Using Cereal Science and Technology for the Benefit of Consumers. S.P. Cauvain, S.S. Salmon, and L.S. Young, eds. CRC Press LLC: Boca Raton.

Wilde, P.J., Clark, D.C., Marion, D. 1993. Influence of competitive adsorption of lysopalmitoylphosphotidylcholine on the functional properties of puroindoline, a lipid-binding protein isolated from wheat flour. J Agric Food Chem. 41: 1570-1576.

Watanabe, A., Yokomizo, K., and Eliasson, A-C. 2003. Effect of physical states of nonpolar lipids on rheology, ultracentrifugation, and microstructure of wheat flour dough. Cereal Chem. 80: 281-284.

Chapter 4 - The Effects of Varying Concentrations of Wheat Lipid Fractions on the Microstructure of Bread

4.1. Introduction

Bread quality is dependent on many characteristics including, color, flavor, texture, mouth-feel, size, and shape. Of these, loaf volume is crucial for consumer liking because it provides the structural basis, influences textural properties, and provides the basis for the internal crumb (Gan et al 1995). Bread can be best described as a sponge consisting of an internal phase of gas within a solid matrix of varying cell wall densities (Falcone et al 2004). Increase in dough and loaf volume is associated with the growth of individual air cells rather than an actual increase in the number of air cells (MacRitchie 1977). This in turn, affects the overall crumb grain, which is a result of the cell expansion and distribution in the dough matrix. The ability to maintain and stabilize gas cells within the internal structure of dough during the bread-making process makes wheat flour unique (Gan et al 1990). Overall, this combination of gas cells within the spongy, solid matrix constitutes the basis of the microstructure of the bread. The microstructure then can be fully characterized by features that include cell wall thickness, cell shape, crumb brightness, void fraction, and hardness of the crumb (Falcone et al 2004).

During bread baking, the dough is subjected to a series of manipulations (moulding and sheeting) that cause changes in size and distribution of the air cells (Sroan et al 2009). Much of dough's stability to this manipulation is associated with the gluten-starch matrix, which forms the backbone of the bread. It is this matrix that helps to create the physical barrier between air cells and prevents coalescence (Gan et al 1990). The proteins comprising gluten (glutenin and gliadin) are both "surface active" and can easily move to the gluten-starch matrix interface and help to stabilize and maintain expanding gas cells (Li et al 2004). Keller et al (1997) and Li et al (2004) determined that the gliadin fraction was the most "surface active" and was found at both the surface of the gas cell walls and in the "bulk phase" of the dough while glutenin was only found in the bulk phase. Because of the increased internal pressures during proofing and baking, the stability of the gas interface is only as strong as the amount of pressure that the compound (protein) at the highest concentration can withstand (Paternotte et al 1994).

It is well known that these gluten proteins form the backbone of the bread structure and are responsible for holding and maintaining air cells within the matrix and having the greatest influence on overall loaf volume (Chung et al 1980a; Delcour and Hoseney 2010). Although present in small amounts in the wheat kernel, native wheat lipids have also been shown to play a part in the stability of gas cells and loaf volume. Much research has been conducted and reviewed studying the influence of native wheat lipids on bread (Daftary et al 1968; Hoseney et al 1969; Hoseney et al 1970; Daniels et al 1971; Hoseney et al 1972; MacRitchie and Gras 1973; De Stefanis and Ponte 1976; Chung et al 1978; Chung et al 1980a; Chung et al 1980b; Chung et al 1982; Ohm and Chung 2002).

Lipids in wheat differ between varieties. Their effects on baking quality have been associated with the type of wheat and the environmental conditions under which they are grown (Chung et al 1980b). The lipids are found throughout the kernel with the highest concentration being the germ. However, the endosperm (flour) also contains small amounts of lipid and the level can be dependent on the milling yield and kernel hardness (MacRitchie 1977). There are differences in the classes of lipids in flour starting with total lipids encompassing all lipids including those connected to the starch granule matrix (Finnie et al 2009). The procedure for total lipid extraction induces starch granule swelling, which is necessary to remove internal lipids. Non-starch lipid extraction does not promote starch granule swelling. However, this technique is unable to remove the lipids that are associated with the starch granule (Finnie et al 2009). Wheat lipids can be further classified into free and bound fractions and the distinctions between these classes are based on the polarity of the solvents with which they can be extracted (Finnie et al 2009). Polar solvents such as isopropanol: water, extract bound lipid, which constitutes 0.6% of all lipids (Hoseney et al 1969; Hoseney et al 1970; Finnie et al 2009). The remaining 0.8% consists of free lipids. They are commonly extracted in nonpolar solvents such as hexane or petroleum ether (Hoseney et al 1969; Hoseney et al 1970; Finnie et al 2009).

During defatting and reconstitution studies of flour and lipids, MacRitchie (1977) found that adding low amounts (<0.1% by flour weight) of polar lipids caused a decrease in loaf volume while adding more restored the lost volume. This was explained as the lower levels of lipids added back prevented the protein from forming a complete layer on the surface of the interface that would allow it to provide stability (MacRitchie 1977; Patenotte et al 1994).

Techniques for fully understanding and interpreting the internal grain of bread and dough have been very limiting and usually require harsh sample preparation that can affect the integrity of the structure (Falcone et al 2004; Cafarelli et al 2014b). Typically, methods based on microscopy, light or electron, are the most common for evaluating the internal structure, but these techniques require harsh sample preparations through the use of chemicals or altering the sample by dehydration, gas removal, or even freezing (Falcone et al 2004). Another disadvantage to these techniques is the inability to look at more than one view of a sample (Cafarelli et al 2014b). Bread structure is anisotropic, having different air cell sizes, formations, connecting links, and alignments in different directions (Falcone et al 2005; Cafarelli et al 2014a). This makes the ability to view and understand the internal structure much more difficult, especially when the method is limited to one stationary image or view of a sample.

As an alternative to these methods, C-Cell imaging is used to determine and measure differences in quality of bread. This technique provides information on structural parameters of aerated food products by supplying information on crumb grain, slice area, cell wall thickness, and cell diameter (Cauvain 2013; Villarino et al 2014). C-Cell imaging utilizes a "monochrome framing camera" to take pictures of the sample using an internal lighting system that illuminates at lower angles from two directions inside a closed box to remove all other external lighting sources (Whitworth et al 2005) Light sources from the two different angles provide brightness contrast between the different components of the cell structure (Whitworth et al 2005). A two-dimensional (2D) image is captured by the camera and provides information on "cell wall thickness, size, position, and elongation of the cells" (Whitworth et al 2005)

In addition to C-Cell analysis, x-ray microtomography (XMT) is another technique that offers a non-invasive means to provide three-dimensional imaging through "x-ray attenuation based off of the changes of density within a sample" (Cafarelli et al 2014a; Cafarelli et al 20014b). The sample is analyzed by "x-ray projections that create 'cross-sectional images' as the sample is rotated creating a series of slices" that can be reconstructed into a 3-D image (Bellido et al 2006; Vlassenbroeck et al 2007; Cafarelli et al 2014b). These images provide a representation of the structure and air cell information of the whole analyzed sample. One of the benefits of this method of analysis is minimal sample preparation (Falcone et al 2005). The use of x-ray microtomography (XMT) as a tool to better understand internal microstructure is being heavily utilized in many areas of food research (Falcone et al 2004; Lim and Barigou 2004:

Falcone et al 2005; Babin et al 2006; Bellido et al 2006; Vlassenbroeck 2007; Besbes et al 2013: Cafarelli et al 2014b; Van Dyck et al 2014). In contrast to C-Cell imaging, the XMT shows differences between cell structures on a micro scale versus the C-Cell on a macro scale. The objective of this research was to evaluate the effects of lipid fractions (total, free, bound, nonpolar and polar), at varying concentrations, on internal crumb grain and gas cell distribution to determine their influences on the microstructure of bread.

4.2. Materials and Methods

4.2.1. Physical and chemical properties of flour

4.2.1.1 Flour

Kansas grown, hard red winter wheat was milled into straight grade flour at the Hal Ross Flour Mill at Kansas State University. The flour was produced at 73% extraction with a protein content of 10.36%, ash of 0.55%, and starch damage of 7.1% (AACCI Method 76-31.01) (AACCI 2014). Following milling, samples were collected into 50 lb bags and placed into -18°C freezer storage until utilized for analysis.

4.2.1.2. Moisture analysis

Moisture analysis was conducted on both control and defatted flours following AACCI method 44-15.02 (AACCI 1999). The moisture content for the control flour was determined to be 12.25% and for the defatted flour 8.76%.

4.2.1.3. Mixograph

Following moisture analysis flour absorption and mix time for the control and defatted flours were determined using the 35 g mixograph (AACCI Method 54-40.02) and Mixosmart software (National Manufacturing, Lincoln, NE) (AACCI 1999). The control flour was measured at 59%, 60%, 60.5%, and 62% absorption and the defatted flour was assessed at 59%, 62%, 64%, and 65% absorption (See Appendix A). Based on the mixograph curves, absorption and optimum mix time was evaluated during a practice bake to determine mixing times and water absorptions that would produce the best loaves for each flour treatment. The results from the practice bake were used for the actual treatment baking.

4.2.2. Defatting and reconstitution of lipids from flour

For the methodology and techniques for the defatting and reconsitituion of the varying lipid types from flour please refer Chapter 2.

4.2.3. Analytical baking

Flours were baked following AACCI method 10-10.03 (AACCI 1999). Modifications to the method included the exclusion of shortening to allow full evaluation of the influence of the lipid fractions on final product. Pup-loaves (100 g) were made containing control, defatted, reconstituted, free, bound, nonpolar, and polar lipids (flours were based on 14% moisture and weights for each treatment loaf were determined following AACCI method 82-23.01) (AACCI 1999). The procedure included a 90-minute fermentation using a 4 min baking schedule. The dough was fermented and proofed in a fermentation cabinet (National Manufacturing, Lincoln, NE) at 86°F (± 5°F) and 92-95% relative humidity. The dough underwent two punching steps using a double rolled sheeter (National Manufacturing, Lincoln, NE) first at 52 min and the second at 77 min. Following fermentation, dough was rounded using a moulder (National Manufacturing, Lincoln, NE), panned, and proofed for 39 min. Baking was for 24 min followed by cooling for 2.5 h. Volume was measured in accordance with AACCI method 10-05.01 (AACCI 2001). Following analysis and cooling, each pup-loaf was wrapped in Saran™ wrap, placed in a zip-lock bag and frozen at -18°C until needed for further analysis.

4.2.4. Bread macrostructure (C-Cell imaging)

Loaves were evaluated using C-Cell Imaging (Calibre Control International, Ltd, Warrington, UK). Each loaf was cut into 1.3 cm slices (±0.5 cm) using an electrical food slicer (Chef's Choice, Int., Colorado Springs, Co.). Every fifth slice from the base end with the break and shred facing upward was used for evaluation. Images were taken with the break and shred oriented to the left side. One slice from each loaf and three loaves from each treatment were imaged. Images were analyzed using C-Cell imaging software (C-Cell Version 2.0, Campden & Chorleywood Food Research Association Group, Gloucestershire, UK) accompaning the equipment. Parameters determined for each treatment included: slice area, number of cells, area of cells, area of holes, number of holes, volume of holes, cell wall thickness, and cell wall diameter.

4.2.5. Bread microstructure (x-ray microtomography)

X-ray microtomographic (XMT) analysis was conducted using Skyscan 1072 Micro-CT x-ray microtomograph (Skyscan, Belgium) for all treatments. Lipid types and levels included: control, defatted, 1.4% and 2.8% reconstituted (recon), 0.6%, 1.2%, 2.5% bound, 0.8%, 1.6%, 2.5% free, 0.6%, 1.2%, 2.5% nonpolar (NPL), 0.2%, 04%, 0.6% polar lipids (PL), which included both phospholipids (PHL) and glycolipids (GL). Three independent loaves from every treatment were tested using XMT. Each treatment series of loaves were removed from the freezer and with the Saran™ wrap still intact, allowed to set overnight in the retarder (4°C). Before XMT sampling the loaves were removed from the retarder (~40 min) and allowed to come to room temperature (25°C ±5) to reduce the effects of moisture evaporation during the scanning of the samples. Bread samples were sliced into 1.3 cm slices (±0.5 cm) using an electric food slicer (Chef's Choice, Int., Colorado Springs, Co.) and every fourth slice was used for testing. An 8 mm x 12 mm cube was cut from each slice and placed into a plastic tube with matching lid to prevent sample drying. The center section sample was securely mounted to the XMT base using a foam 13 mm two-sided adhesive disk. Once in the microtomograph, all samples were allowed to equilibrate within the chamber for 5 min. XMT measurements were done at 41 kV, 102 μA, 1.8 sec exposure, 15-16X magnification, stage position at 11.5 mm (±0.5), and resolution at 17 μm -18 μm. Sample reconstruction was conducted using NRecon (Version 1.6.3.3 Skyscan, Bruker MicroCT, Kontich, Belgium). The x-ray produced 206, 2-D cross-sectional images for each sample, which was used to reconstruct 3-D structures of the each treatment to determine quantitative values for air cell structure and distribution analysis. The assessment of the binary image and data analysis of the reconstructed sample was done with CTan (CT Analyzer, Version 1.10.1.0 Skyscan, Bruker MicroCT, Kontich, Belgium) and provided data that included: air cell size, cell wall thickness, air cell distribution, % total porosity, volume index (VOI), structure separation distribution, structure thickness distribution, and object volume.

4.2.6. Experimental design and statistical analysis

The experiment was setup as a completely randomized (CRD) one-way factorial design containing 16 lipid treatments made on 4 baking days. The treatments were randomly assigned to 4 different days, 3 loaves per treatment, 12 treatments per day with a total of 36 loaves made on

each bake day. Multivariate analysis (ANOVA) was conducted using SAS (Version 9.3, SAS Institute Inc., Cary, NC) with comparison between sample means using Tukey's least significant difference (LSD) testing at a confidence level of 95%.

4.3. Results

4.3.1 Physical and chemical properties of flour

4.3.1.1. Moisture analysis

The physical and chemical testing properties of both the defatted and control flours are shown in Table 4.1. The removal of lipids via chloroform extraction and the drying overnight caused the defatted flour to have lower moisture than the control. Papantoniou et al (2004) showed that defatted flour had an increased affinity for water caused by the reduction of polar lipid-protein reactions. The greater moisture loss, increased the water absorption needed for bread baking (64% vs 60.5%). The mixing time was also 30 sec shorter for the control flour at 3 min 30 sec compared to the defatted at 4 min.

Table 4.1. Physical and chemical characteristics of control and defatted flours

Parameters	Control	Defatted
Moisture content (%)	12.59	8.82
Absorption (%)[a]	60.5	64
Mix Time[a]	3.5 min	4 min

[a]Absorption and mix time were determined by mixograph testing and optimized during the baking process.

4.3.1.2. Mixograph

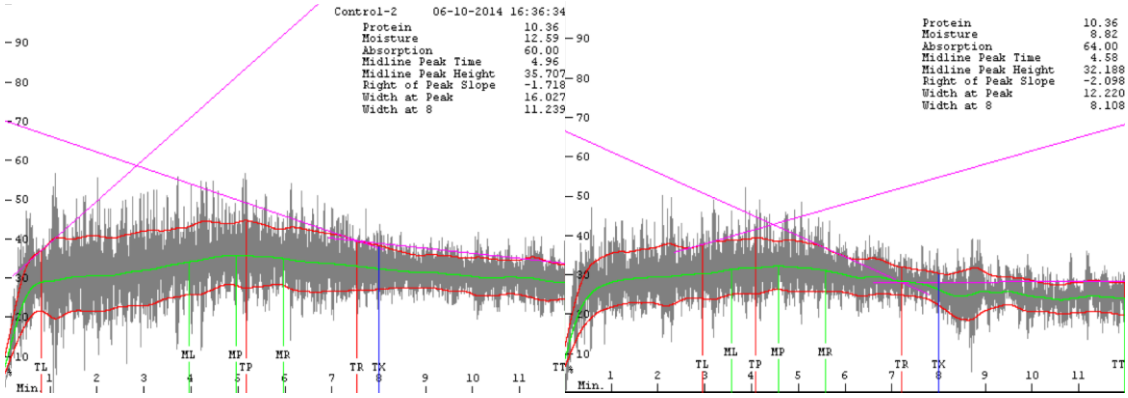

A. Control (60% abs) B. Defatted (64% abs)

Figure 4.1. Optimized mixograph results for sample flours used for testing

4.3.2. Physical properties of dough and bread

Proof heights, loaf volumes, and specific volumes (Table 4.2) were measured for each treatment and the average proof heights varied between 7.26 cm and 8.09 cm. The control average height was at 7.83 cm. Five of the treatment's average proof heights were higher than those of the control (0.6% bound, 1.2% bound, 2.5% bound, 0.8% free, 0.6% NPL) while all the rest were smaller. The loaf volumes varied over a wide range (between 690 cc and 970 cc). There were 7 treatment loaf volumes that were greater than the control: 0.6% bound, 1.2% bound, 2.5% bound, defatted, 0.6% PL, 1.4% reconstituted, and 2.8% reconstituted. The specific volumes, which included loaf weights as part of the calculation, also had the same results as the 7 treatments were greater than the control.

Table 4.2. Physical parameter measurements for breads baked with different lipid treatments

Treatment[a]	Proof Height (cm)	Loaf Volume (cc)	Loaf Specific Volume (cc/g)
Control	7.83^{bce} (0.36)	799.44^{bdf} (20.83)	5.36^{cdfg} (0.09)
Bound 0.6%	7.96^{bd} (0.10)	851.11^{b} (74.74)	5.91^{bd} (0.58)
Bound 1.2%	8.09^{b} (0.35)	969.44^{a} (58.33)	7.05^{a} (0.43)
Bound 2.5%	8.06^{bd} (0.27)	967.78^{a} (36.50)	7.08^{a} (0.29)
Defatted	7.82^{bce} (0.18)	810.56^{bdf} (40.03)	5.58^{befg} (0.19)
Free 0.8%	7.78^{ab} (0.20)	747.22^{cef} (33.27)	5.13^{ce} (0.17)
Free 1.6%	7.51^{ade} (0.21)	755.00^{cef} (21.36)	5.35^{cdfg} (0.23)
Free 2.5%	7.26^{a} (0.58)	742.22^{cd} (50.26)	5.35^{cdfg} (0.54)
NPL 0.6%	7.90^{bd} (0.11)	747.78^{cef} (15.02)	5.09^{ce} (0.12)
NPL 1.2%	7.61^{ab} (0.42)	707.78^{c} (39.77)	4.83^{c} (0.38)
NPL 2.5%	7.31^{ac} (0.49)	693.89^{c} (57.05)	4.83^{c} (0.42)
PL 0.2%	7.62^{ab} (0.60)	756.11^{cef} (93.13)	5.34^{cdfg} (0.46)
PL 0.4%	7.73^{ab} (0.38)	760.55^{cef} (25.42)	5.25^{cfg} (0.16)
PL 0.6%	7.79^{ab} (0.23)	829.44^{be} (79.55)	5.84^{bf} (0.74)
Recon 1.4%	7.67^{ab} (0.23)	822.50^{bdf} (32.84)	5.80^{bf} (0.27)
Recon 2.8%	7.51^{ade} (0.24)	852.22^{b} (34.11)	6.19^{b} (0.24)

[a]Nonpolar (NPL), polar (PL), and reconstituted (Recon)
[b]Means in the same column with different letters are significantly different at a $p<0.05$; (n=144)
[c]Values in parenthesis are standard deviations

4.3.3. Macrostructure analysis of breads containing varying lipids treatments (C-Cell)

Table 4.3 contains the results of C-Cell analysis of the lipid treatments added at varying concentrations (For definition of C-Cell terminology refer to Chapter 3, Table 3.9).. The parameters that were associated with loaf volume and gas cell distribution include: slice area, number of cells, area of cells, average cell wall thickness, average cell diameter, and cell elongation. The C-Cell results showed only the area of holes (%) and cell elongation to not be significantly different from the other lipid treatments The slice area, which is related to the overall loaf volume, had values starting with the smallest at 3664 mm^2 (1.2% NPL) to the largest area of 5278 mm^2 (1.2% bound). The control slice area fell in the middle at 4130 mm^2. Several of the loaves had slice area measurements lower than the control (~3600-4000 mm^2). These were mostly those loaves containing free and NPL lipid additions that also had lower loaf volumes. The treatments containing 0.6% bound, 1.2% bound, 2.5% bound, defatted, 0.6% PL, 1.4% recon, 2.8% recon all had slice area measurements that were greater than the control.

Significant differences were also found with the number of cells (2900-4300). The defatted (4287), 0.2% PL (4062), and 0.4% (4109) had the highest number of cell values of all the treatments. The control number of cells was 3367 and this was lower than 0.6%, 1.2%, and 2.5% bound lipid addition, 1.4% and 2.8% recon levels, and 0.6% NPL. The larger number of cell values correlate to finer cells in the slice, thus all the treatments above the control in this study had finer cells overall. Sroan and MacRitchie (2009) determined differences between the type and level of lipid additions for breads. For this current study, the addition of only polar lipids (0-200%) showed a decrease in the number of cells (2361 down to 1985) with increasing levels, except for 132% and 200% PL levels, which saw an increase in the number of cells (Sroan and MacRitchie 2009). This same trend occurred with the NPL lipid amounts (0-200%) as there was a decrease in the number of cells as the percentage of these lipids increased (Sroan and MacRitchie 2009).

The area of cells (%) were highest for 1.2% bound (51%), 2.5% bound (52%), 1.6% free (50%), 2.5% free (51%), 0.6%PL (50%), and 2.8% Recon (50%). All of these treatments had higher area of cells than the control (49.87%). The cell wall thickness values ranged between 0.37 mm and 0.42 mm. The 2.5% bound lipid loaves had the greatest average cell wall thickness

(0.42 mm), which was higher than the control (0.40 mm) while the defatted, 0.2% PL, and 0.4% PL had the lowest wall thickness (0.37 mm). Also, the 1.6% free, 2.5% free, and 0.6% PL had average cell wall thickness measurements that were the same as the control at 0.40 mm. All the other sample treatments fell below the control and above the lowest average thickness measurements of (0.37 mm). Pickett (2009) also found similar cell wall thickness ranges for the bread flour treatments tested (0.40-0.41 mm).

The addition of lipids caused differences between the average cell diameter measurements as the average diameter ranged between 1.31 mm and 1.76 mm. The defatted (1.31 mm) and 0.4% PL (1.31 mm) had the lowest values and 2.5% bound (1.76 mm) had the largest cell size. The control average cell diameter was at 1.56 mm, with 1.2% bound (1.74 mm), 2.5% bound (1.76 mm), 1.6% free (1.57 mm), 2.5% free (1.60 mm), and 0.6% PL (1.75 mm) having larger sizes. The measurement of elongation is "associated with greater tolerance to distortion before rupture," by the cell walls (Gandikota and MacRitchie 2005). The cell elongation measurements ranged between 1.60 and 1.76 and with no significant differences between them. These results were similar to Sroan and MacRitchie (2009) who also found elongation measurements to be between 1.60 and 1.70. In addition, the cell elongation had values higher than 1, indicating most of the cells were not strictly round and varied in sizes.

A. Control B. Defatted C. 1.4% Recon D. 2.8% Recon

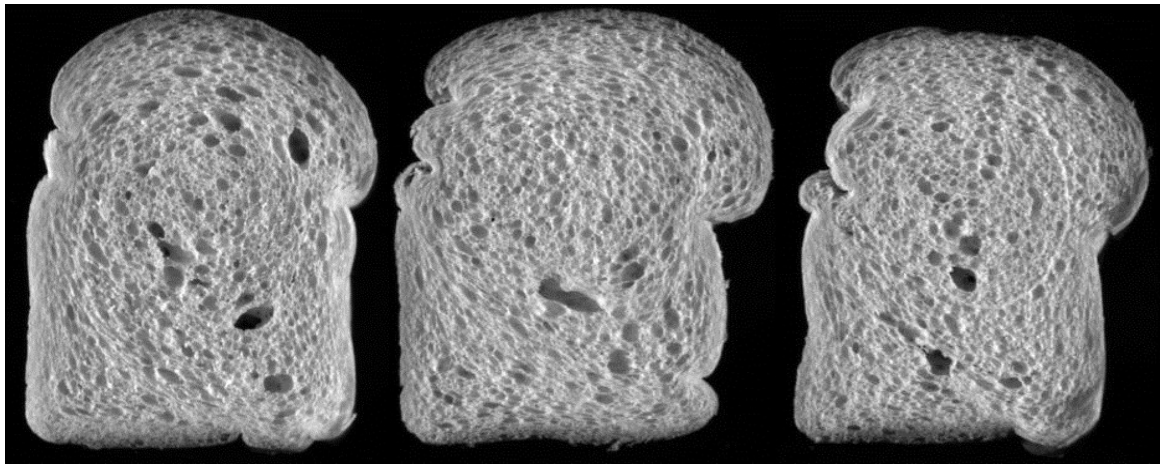

A. Bound 0.6% B. Bound 1.2% C. Bound 2.5%

Figure 4.2. C-Cell raw images of control, defatted, reconstituted (Recon) (1.4%, 2.8%), and bound (0.6%, 1.2%, 2.5%) lipid additions

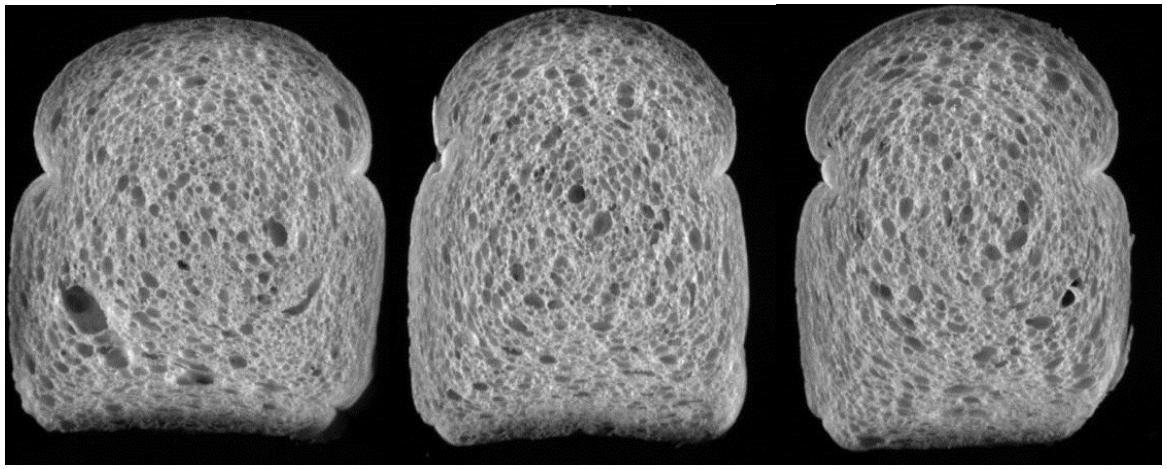

A. Free 0.8% B. Free 1.6% C. Free 2.5%

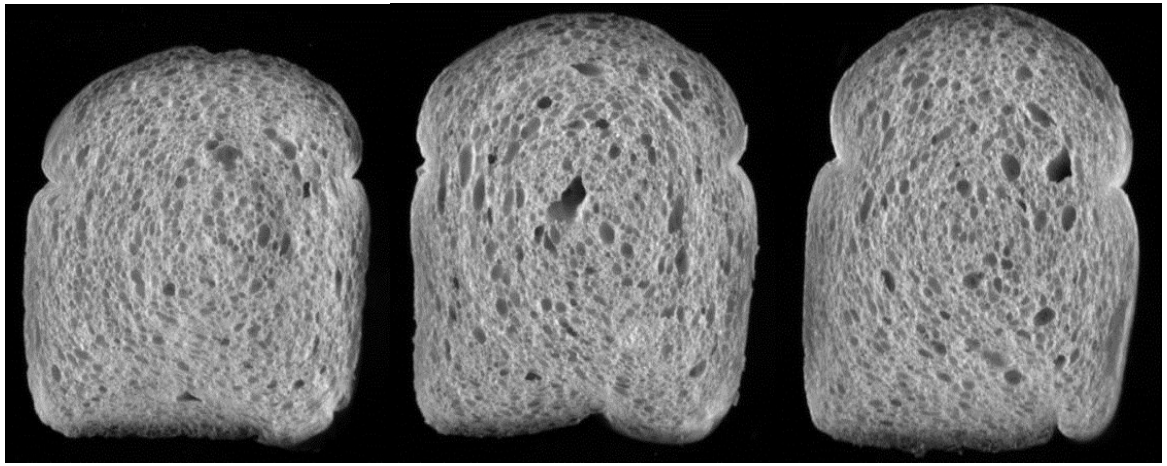

A. 0.6% NPL B. 1.2% NPL C. 2.5% NPL

Figure 4.3. C-Cell raw images of free (0.8%, 1.6%, 2.5%) and nonpolar (NPL) (0.6%, 1.2%, 2.5%) lipid additions

A. 0.2% PL B. 0.4% PL C. 0.6% PL

Figure 4.4. C-Cell raw images of polar (PL) (0.2%, 0.4%, 0.6%) lipid additions

Table 4.3. C-Cell analysis of breads containing varying lipid treatments

Treatment[a]	Slice Area (mm^2)	Number of Cells	Number of holes	Area of Cells (%)	Area of holes (%)	Volume of holes	Wall Thickness (mm)	Cell Diameter (mm)	Cell Elongation
Control	4130.33^{bc}	3367.33^{bg}	4.11^{ab}	49.87^{abcd}	3.79^{a}	66.80^{a}	0.40^{abd}	1.56^{abcde}	1.76^{a}
	(91.66)	(108.56)	(1.52)	(0.23)	(0.42)	(5.09)	(0.00)	(0.04)	(0.05)
Bound 0.6%	4266.00^{bc}	3766.67^{cefg}	1.79^{abc}	48.97^{bcd}	0.77^{a}	28.93^{ab}	0.39^{cd}	1.46^{bcde}	1.72^{a}
	(208.89)	(277.14)	(0.87)	(1.31)	(0.38)	(12.10)	(0.02)	(0.18)	(0.07)
Bound 1.2%	5278.00^{ab}	3817.67^{ag}	1.04^{bc}	51.14^{ab}	0.58^{a}	24.30^{ab}	0.41^{a}	1.74^{ab}	1.74^{a}
	(129.55)	(202.44)	(1.02)	(1.15)	(0.50)	(18.87)	(0.01)	(0.16)	(0.09)
Bound 2.5%	5131.33^{ab}	3601.00^{defg}	1.15^{abc}	51.74^{a}	0.65^{a}	27.83^{ab}	0.42^{ab}	1.76^{a}	1.71^{a}
	(187.40)	(206.16)	(1.03)	(0.21)	(0.51)	(16.16)	(0.00)	(0.01)	(0.02)
Defatted	4309.67^{bc}	4286.67^{a}	2.15^{abc}	48.51^{cd}	1.21^{a}	33.17^{ab}	0.37^{c}	1.31^{ce}	1.64^{a}
	(169.59)	(66.34)	(1.07)	(0.78)	(0.85)	(15.50)	(0.00)	(0.07)	(0.08)
Free 0.8%	3830.00^{c}	3360.67^{bg}	2.63^{abc}	49.04^{bcd}	2.21^{a}	50.60^{ab}	0.39^{cd}	1.45^{cde}	1.78^{a}
	(63.41)	(102.87)	(1.05)	(0.55)	(0.74)	(12.36)	(0.00)	(0.02)	(0.05)
Free 1.6%	3831.33^{c}	3063.67^{b}	0.89^{c}	50.05^{abcd}	0.52^{a}	18.97^{ab}	0.40^{abd}	1.57^{abcde}	1.78^{a}
	(122.66)	(140.30)	(1.12)	(0.46)	(0.74)	(17.72)	(0.00)	(0.08)	(0.04)
Free 2.5%	3838.33^{c}	2947.00^{b}	0.17^{c}	50.64^{abd}	0.08^{a}	7.00^{b}	0.40^{abd}	1.60^{abde}	1.74^{a}
	(327.13)	(212.45)	(0.20)	(0.15)	(0.11)	(4.94)	(0.00)	(0.04)	(0.07)
NPL 0.6%	3914.33^{c}	3603.33^{defg}	2.80^{abc}	48.27^{cd}	2.18^{a}	46.03^{ab}	0.38^{cd}	1.37^{cde}	1.74^{a}
	(148.00)	(198.07)	(1.27)	(0.61)	(1.68)	(24.89)	(0.01)	(0.07)	(0.04)

NPL 1.2%	3664.33[c]	3264.33[bd]	2.31[abc]	48.97[bcd]	3.79[a]	64.90[ab]	0.39[cd]	1.40[cde]	1.73[a]
	(287.79)	(258.09)	(0.99)	(0.50)	(3.78)	(41.00)	(0.01)	(0.06)	(0.04)
NPL 2.5%	3761.00[c]	3298.00[bf]	3.42[ab]	49.47[bcd]	2.63[a]	52.73[ab]	0.39[cd]	1.46[bcde]	1.76[a]
	(153.80)	(93.55)	(1.29)	(0.32)	(1.75)	(21.21)	(0.00)	(0.06)	(0.05)
PL 0.2%	4202.67[bc]	4062.33[ae]	3.94[b]	48.93[cd]	3.18[a]	53.40[ab]	0.37[c]	1.32[ce]	1.71[a]
	(146.85)	(77.02)	(0.29)	(0.64)	(1.87)	(21.83)	(0.01)	(0.05)	(0.05)
PL 0.4%	4091.33[bc]	4109.00[ac]	2.52[abc]	48.70[cd]	1.77[a]	41.83[ab]	0.37[c]	1.31[ce]	1.70[a]
	(92.03)	(32.92)	(0.18)	(0.36)	(1.30)	(22.91)	(0.00)	(0.07)	(0.02)
PL 0.6%	4659.33[ab]	3773.67[cefg]	3.36[ab]	50.27[abcd]	2.49[a]	54.70[ab]	0.40[abd]	1.63[abd]	1.75[a]
	(686.07)	(106.10)	(1.66)	(1.62)	(1.99)	(22.42)	(0.02)	(0.23)	(0.03)
Recon 1.4%	4361.00[bc]	3632.67[cdefg]	0.43[c]	49.93[abcd]	0.20[a]	10.43[ab]	0.39[bcd]	1.50[abcde]	1.70[a]
	(277.18)	(139.63)	(0.34)	(0.51)	(0.18)	(5.89)	(0.01)	(0.07)	(0.02)
Recon 2.8%	4815.67[ab]	3939.00[ae]	0.85[c]	50.37[abcd]	0.38[a]	21.77[ab]	0.39[bcd]	1.55[abcde]	1.72[a]
	(113.81)	(63.38)	(0.47)	(0.06)	(0.31)	(11.87)	(0.00)	(0.00)	(0.01)

[a] Nonpolar (NPL), polar (PL), and reconstituted (Recon)
[b]Means in the same column with different letters are significantly different at a $p<0.05$; (n=48)
[c]Values in parenthesis are standard deviations

4.3.4. Microstructure analysis of center pieces of bread containing varying lipids treatments (X-ray Microtomography)

The benefits of XMT analysis for aerated systems stem from its ability to view samples without compromising their integrity and creating 3-D images from the initial "projections." This is based off shadows, varying densities, and molecular weight of the tested sample (Moreno-Atanasio et al 2010). Utilizing an x-ray source, more specifically, an x-ray cone beam, the sample is rotated within the field of view of the beam where photons are either absorbed or pass through the sample, then gathered and collected by the detector. The rays returned to the detector are converted to a digital image (Moreno-Atanasio et al 2010). The projections can then be converted into a 3-D image using algorithms in the analysis software (Moreno-Atanasio et al 2010). Because bread is an open structure, the shape, size, and alignment of cells can be different from sample to sample or between types of bread. This microstructure influences overall crumb grain and texture (Cafarelli et al 2014; Van Dyck et al 2014). These changes in structure are caused during the breadmaking process, starting with mixing where air cells are incorporated, then fermentation by the growth of cell size, and finally where there is an increase in loaf size and cell wall separation when the bread sets (Besbes et al 2013).

The parameters measured from the reconstructed images include: volume of interest (VOI), solid volume, fragmentation index, cell wall thickness, gas cell size, number of gas cells, and total porosity. The "VOI" or volume of interest is determined from the series of "binary images," which eliminate undesirable background noise from the image (Van Dyck et al 2014). This value is the total area that was measured for each treatment. The rest of the measurements come from the area within the sample's VOI (Brubaker-MicroCT 2014). The object volume (%) is the "average percentage of solids occupied in the VOI " (Brubaker-MicroCT 2014). It constitutes the percentage of structure that is in the solid phase (Cafarelli et al 2014b). The fragmentation index is the degree of "concavity or convexity" of the cells. This is correlated to the connectivity (concavity) or the "isolated disconnection" (convexity) of the structure (Bruker-MicroCT 2014; Pickett 2009: Cafarelli et al 2014). The value of the fragmentation index can either be positive or negative. Smaller negative values are related to the connectivity (concavity) of sample and larger positive values related to discontinuities (convexity) (Cafarelli et al 2014). The structure thickness is a measure of the average cell wall thickness of the walls within the

region of interest (VOI) (Cafarelli et al 2014; Van Dyck et al 2014). Gas cell size is the average gas cell size found within the VOI (Cafarelli et al 2014). Number of objects measurement is the "total number of discreet binarised objects within the VOI where a discreet 3D object is a connected assemblage of solid (black) voxels fully surrounded on all sides in 3D by space (white) voxels" or simply stated, the number of gas cells (Bruker-MicroCT 2014). The total porosity is a percentage measure of all open and closed pores within the VOI (Bruker-MicroCT 2014; Van Dyck et al 2014).

Table 4.4. Structure parameters tested by X-ray microtomography

Parameter	Definition	Unit of measure
Volume index (VOI)	Volume of sample used in XMT testing	(μm^3)
Solid volume	Percentage volume of solid structure in the VOI	%
Fragmentation index	Measure of cell connectedness	(1/ μm)
Cell wall thickness	Average thickness of the cell walls	(μm)
Gas cell size	Average size of gas cells	(μm)
Number of gas cells	Amount of gas cells in the VOI	N/A
Total porosity	Percentage of void space within the VOI of the sample	%

In addition to the measurements listed above, gas cell size and cell wall thickness distributions from each tested sample were determined from the reconstructions and 3-D image analysis. Distribution curves for both gas cell size and cell wall thickness were plotted against the frequency (% appearance) at which specific cell wall thickness or gas cell sizes were found for each treatment. The gas cell size distributions were also converted to cumulative distribution curves to allow for determination of percentile measurements of gas cells at different frequencies (25%, 50%, 75%, and 95%).

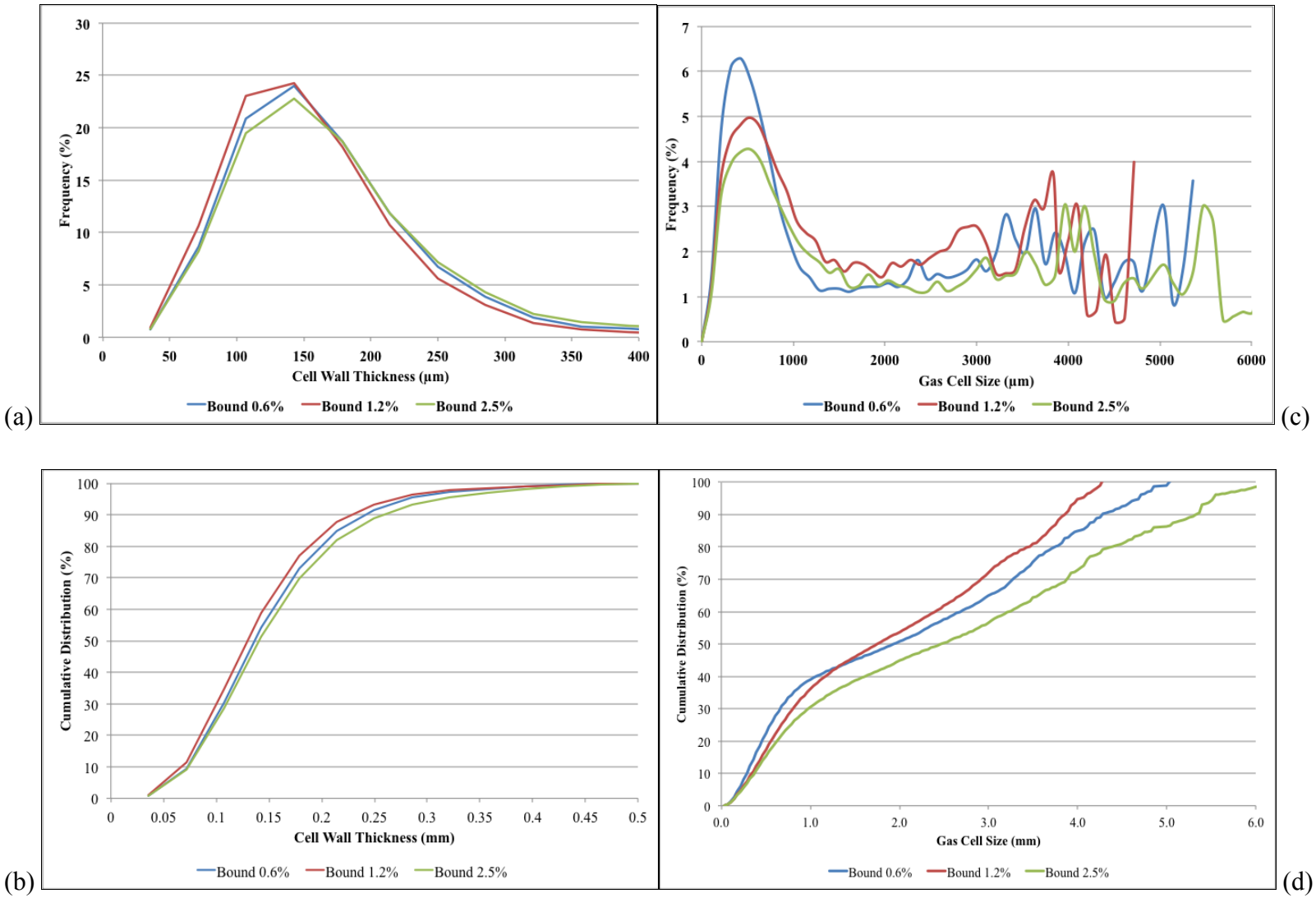

Figure 4.5. XMT scan results for center section of bread slice for bound samples at 0.6%, 1.2%, and 2.5% addition (a) cell wall thickness distribution, (b) cumulative cell wall thickness distribution, (c) gas cell size distribution (d) cumulative gas cell size distribution

Bound lipids were added 0.6%, 1.2%, and 2.5%. The bound lipids extracted from the flour contained 0.04g/200g flour or 0.02% polar lipids total in the sample fraction. Figure 4.5 shows the (a) cell wall thickness distribution, (b) cumulative cell wall thickness distribution, (c) gas cell size, and (d) cumulative gas cell size distribution as a function of frequency. Average cell wall thickness distributions were relatively similar for all treatments. All three curves had thickness ranges between 40 μm and 300 μm. The highest thickness frequency for all three treatments was 143 μm with 1.2% bound addition having the greatest percentage (24%) for that specific thickness. This was followed by the 0.6% addition at 24%, and 2.5% addition at 23%. Also, 1.2% bound had a higher frequency at 107 μm (23%). This trend wasn't seen with the other two samples. The cumulative cell wall thickness curve for bound lipid addition showed only a small shift in distributions for the average cell wall thickness with the greater amounts. At the higher concentrations, the curves moved to the right indicating an increase in the wall thickness. However, the bound lipid additions at 0.6% and 1.2% had slightly thinner walls than did the 2.5% bound. It is important to note that the shift in the distribution was very small for all three samples. Overall, the addition of bound lipids resulted in minimal differences in both the cell wall thickness and cumulative cell wall thickness distributions indicating there was little to no effect of bound lipid addition on altering the thickness of the cell walls.

The average gas cell size distribution curves for the three bound lipid additions showed tall, narrow peaks in the ranges of 0 μm to 1700 μm. This indicated that small gas cells were present in all three treatments. However, the highest concentration of bound lipids caused a decrease in the number of these smaller cells. Bound lipid addition at 0.6% had the highest frequency of cells (6.2%) at 428 μm while the 1.2% bound lipids had more gas cells of 518 μm at a lower frequency (5.0%). The 2.5% had the lowest peak percentage in this same small cell region with 4.3% being at a size of 536 μm. There was also a distribution of sizes that extended into the mid-range (2000-6000 μm), but these were all at a lower frequency than were the smaller cells. The average cumulative gas cell size curves shifted to the left with the addition of all levels of bound lipids to a larger population of cells below 1 mm in diameter. The 1.2% level also had a larger frequency of cells that were higher than 1.5 mm in diameter. The increased gas cell sizes would suggest either a larger number of cells were incorporated during mixing or these cells were able to undergo a greater amount of expansion, which would be reflective of an overall increased loaf volume.

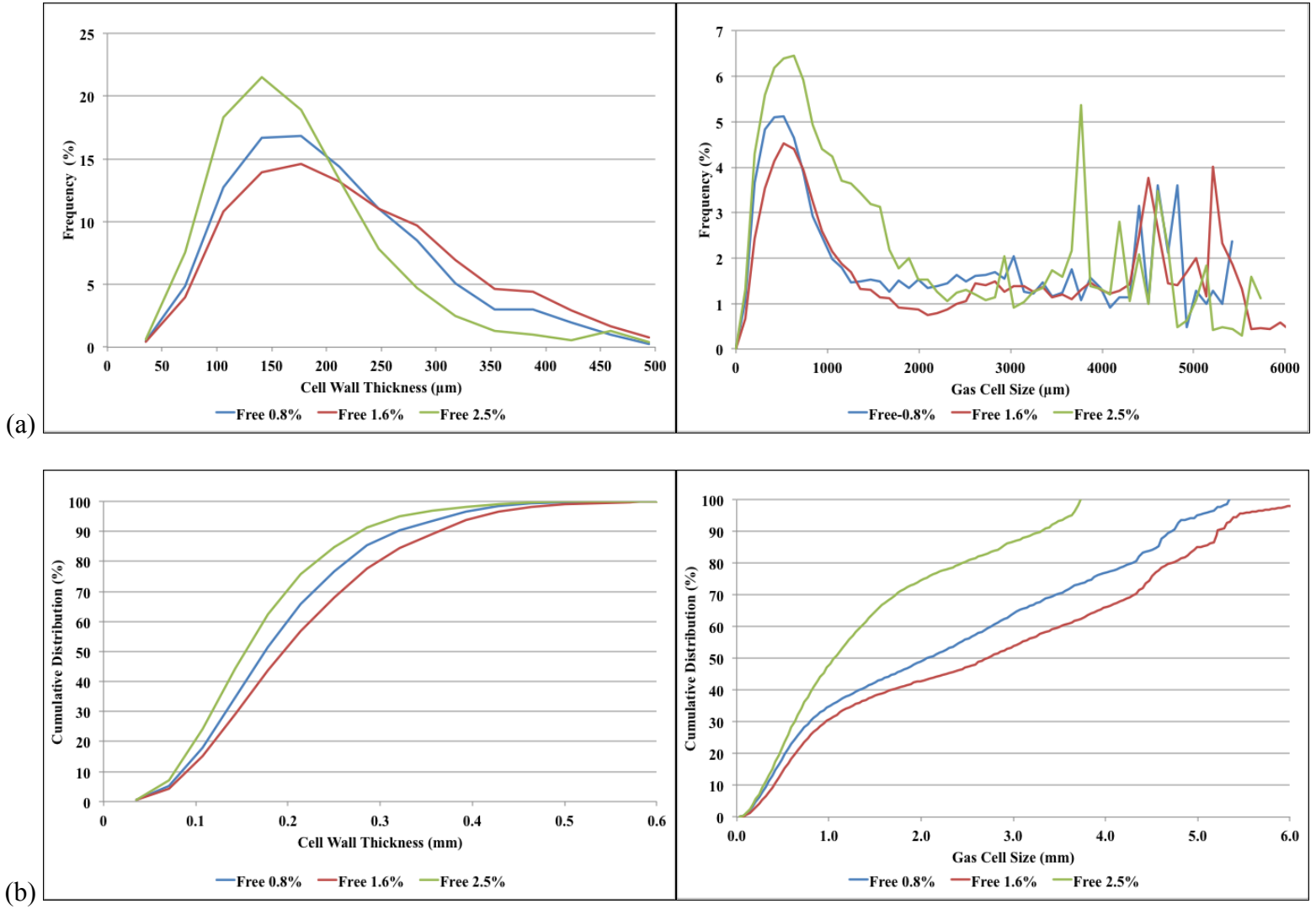

Figure 4.6. XMT scan results for center section of bread slice for free samples at 0.8%, 1.6%, and 2.5% addition (a) cell wall thickness distribution, (b) cumulative cell wall thickness distribution, (c) gas cell size distribution, (d) cumulative gas cell size distribution.

Free lipids at any addition level (Figure 4.6a) resulted in greater diversity in the average cell wall thickness measurements. Of the free lipid fraction, only 0.03 g/200g (0.01%) were polar lipids. The thickness distribution ranged between 40 μm and 450 μm and both the 0.8% and 1.6% treatment had a broader spread than did the 2.5% addition. Most of the 2.5% free were between 40 μm and 300 μm in thickness with a higher percentage (21.5%) of the distribution at 141.27 μm. The 0.8% and 1.6% treatment resulted in a greater shift with the values falling between 141 μm and 177 μm at a lower frequency. In this case, the addition of free lipids did cause a difference in the cell wall thickness. The loaves with the highest level of free lipid addition had the thinnest cell walls. Average cumulative cell wall thickness distributions for free lipid additions (Figure 4.6b) showed 2.5% free lipid addition to have the the thinnest cell walls. The other two samples' curves were shifted more to the right than the 2.5% curves, which indicates a higher frequency of thicker cell walls. A larger gap existed in the distribution starting at 50%, where the thickness values were 0.14 mm (free 2.5%), 0.17 mm (free 0.8%), and then 0.21 mm (1.6% free). The free lipid had a larger effect on cell wall thickness and this was dependent upon concentration.

A difference in gas cell size distribution was found between the levels of free lipid addition (Fig. 4.6c). The gas cell size showed the biggest spread between 0 μm and 2000 μm. The 2.5% free had the widest distribution of cells between 0 μm and 2000 μm, while lower levels of free resulted in a range between 0 μm and 1350 μm**.** There was also a large peak extending between 3500 and 4000 μm (specifically 3772 μm) with the 2.5% free. This was not seen with the other two treatments. The 2.5% free lipid addition had the highest frequency (6.4%) of cells at 524 μm and at 3772 μm (5.37%). In contrast, the highest frequency cell size (51%) for the 0.8% addition was at 419 μm and the 1.6% free addition (4.5%) at 524 μm. The 2.5% free lipid addition resulted in a wider range of gas cell sizes than the same fraction at lower inclusion levels. This suggested that the reduced level of polar lipids available to provide stability at the interface might have caused an increase in cell coalescence. The average cumulative gas cell size distribution shown in Figure 4.6d showed a considerable variation between the 2.5% free lipids and the other two lipid levels. The 2.5% free distribution was shifted much farther to the left than the other two samples indicating smaller cells. The biggest differences were seen beyond > 1.0 mm cell size as the frequency of the distribution between 1 mm and 4 mm was much higher than that of the lower levels of free lipid addition. At 50%, the cells for the 2.5% level fall below 1.0

mm in size as compared to sizes for 0.8% (1.9 mm) and (1.6%) (2.5 mm). Overall, the addition of triple the original amount of free lipids caused the distribution of the cells to become much smaller than the other two treatment samples indicating a reduction in the amount of cell coalescence.

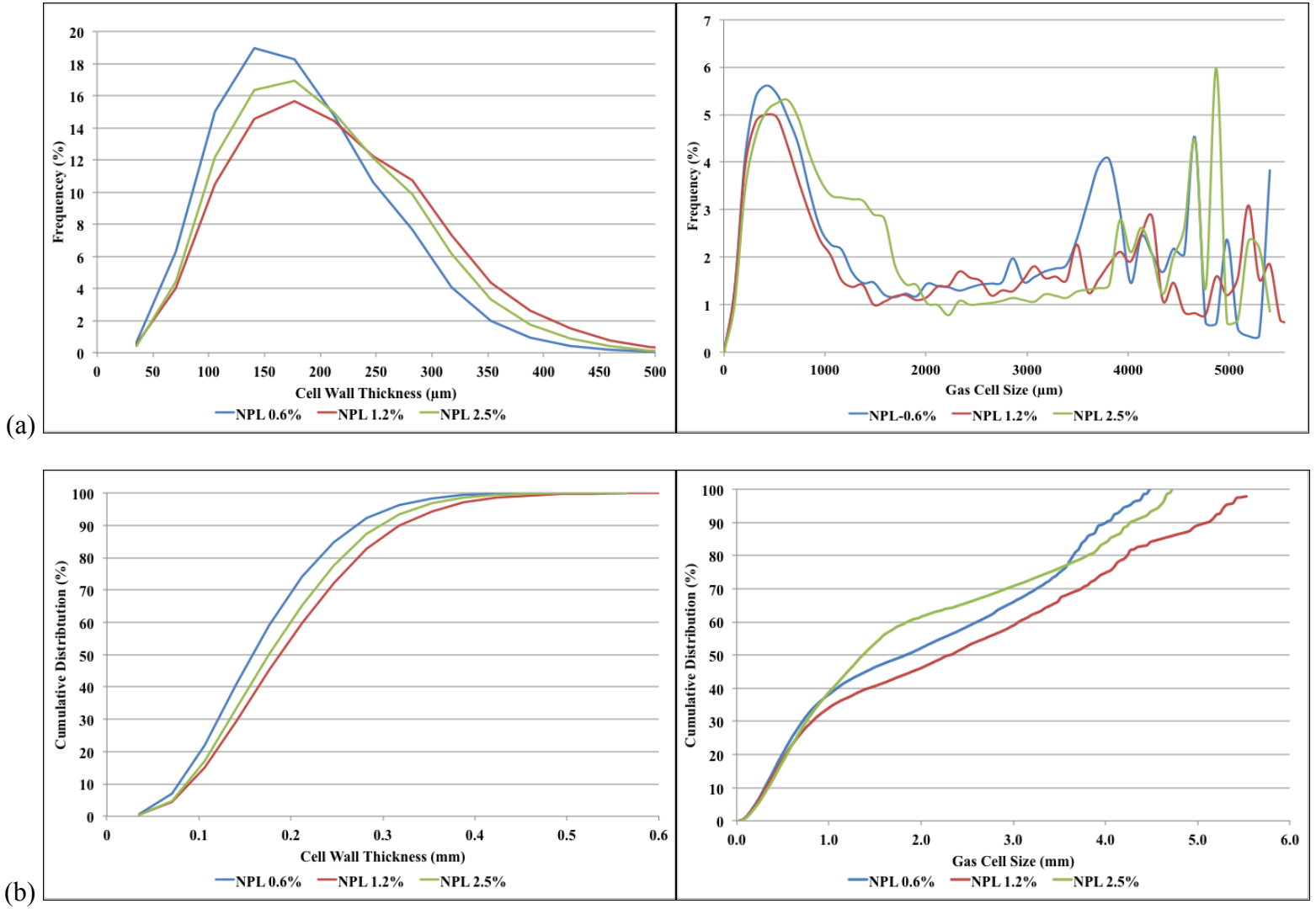

Figure 4.7. XMT scan results for center section of bread slice for nonpolar (NPL) samples at 0.6%, 1.2%, and 2.5% addition (a) cell wall thickness distribution, (b) cumulative cell wall thickness distribution, (c) gas cell size distribution, and (d) cumulative gas cell size distribution

The relationships between cell wall thickness distribution and gas cell size for the NPL additions (0.6%, 1.2%, and 2.5%) are shown in Figure 4.7. Cell wall thickness distributions were very broad with thicknesses between 40 μm and 400 μm. The 0.6% level had the smallest spread in the average cell thickness spread (40 μm-350 μm) with the highest frequency at 141 μm. The 1.2% and 2.5% NPL had the highest frequency (16% and 17%, respectively) at 177 μm cell wall thicknesses. The 1.2% and 2.5% samples had lower frequency distribution than the 0.6%, at a wider range (40-400 μm). For these treatments the cell walls were thicker indicating a higher concentration of solids in the samples. This in-turn, would show that a change in the overall volume was caused by a reduction in air cell entrapment or cell expansion. The NPL fractions are known to contain higher levels of free fatty acids, which are detrimental to loaf volumes as they are unable to support and stabilize gas cells similar to polar lipids (MacRitchie and Gras 1973). The average cumulative thickness distribution for NPL (Figure 4.7b) had thinner cell wall distribution for the 0.6% NPL than for the other two samples tested. Although the results only had small shifts between each distribution, the 1.2%, and 2.5% thickness distributions were closer to one another than the 0.6% NPL addition. Larger amounts of NPL caused a shift in the thickness distribution by creating breads with thicker cell walls. The addition of NPL reduced the dough's ability to entrapt air cells during mixing or allow for volume expansion over time.

The gas cell size distribution (Figure 4.7c) showed varying cell size frequencies that peaked between 0 μm and 2000 μm and again at 3500 μm to 5000 μm. The curve for the 2.5% had the greatest difference in frequencies between 1000 μm and 2000 μm while the lower two levels showed narrower peaks between 0 μm and 1500 μm. The 2.5% had the highest frequency of cells at 529.24 μm (5.2%) while the 0.6% (5.1%) and 1.2% (5.0%) had a larger frequency of cells at 424 μm. Also, all levels of the NPL had several cells that fell into the higher size regions between 3500-5000 μm. These peaks could be associated with one large cell causing an increase in the distribution at that size range or due to the deleterious effects of NPL not preventing coalescence over time. The increased level of NPL caused the widest spread in gas cell size distribution. The average cumulative gas cell size distribution (Figure 4.7d) illustrated that most the cell size distributions were relatively the same (30%) for the treatments as most of the cells were below 1.0 mm. Beyond 30%, there was a change in cell size for the lower level NPL addition. Lower levels of NPL had cells at larger diameters while the 2.5% NPL had a much

higher frequency of smaller cells. Thus, the expansion and size of the cells differed at the lower levels of NPL additions.

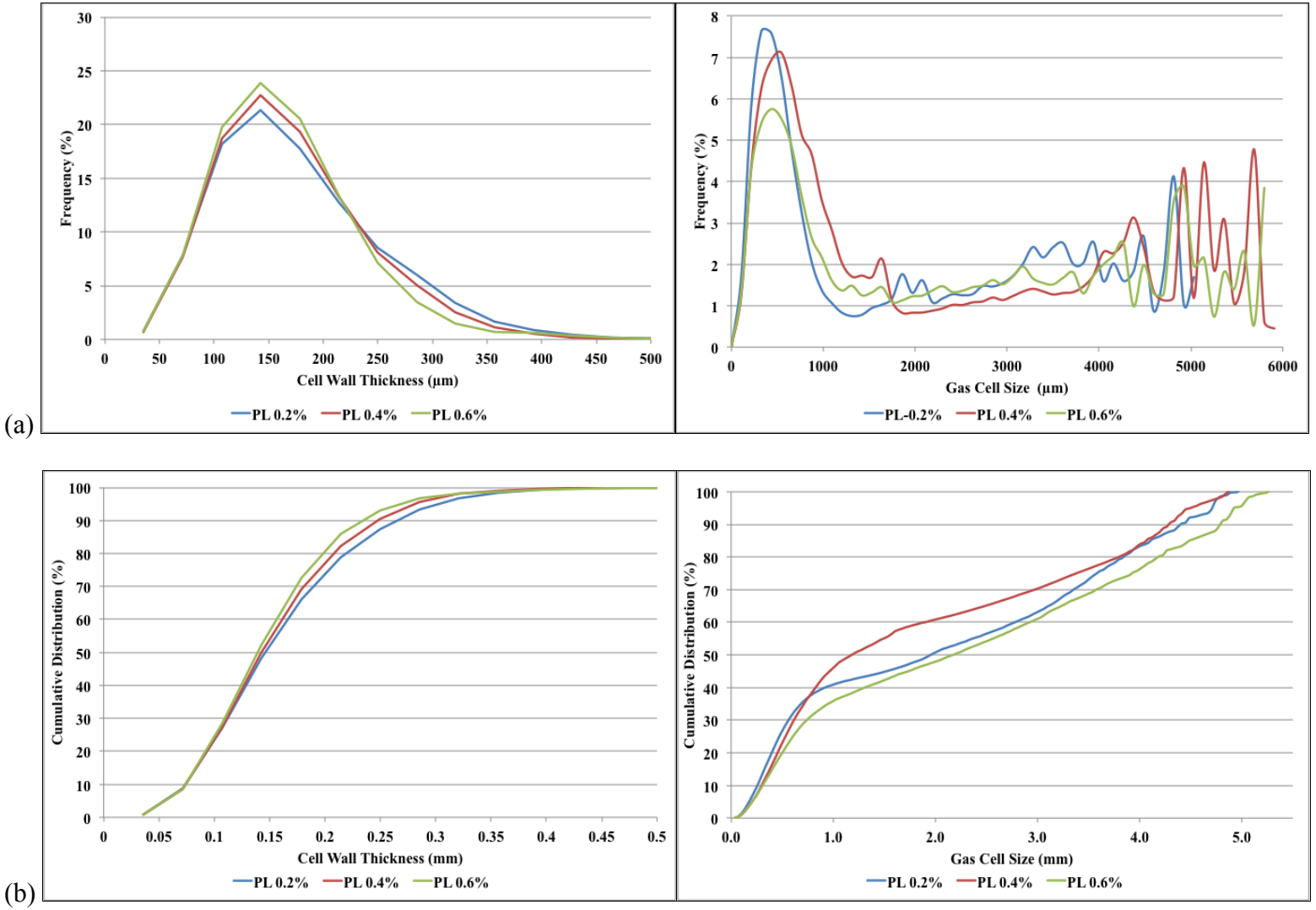

Figure 4.8. XMT scan results for center section of bread slice for polar (PL) samples at 0.2%, 0.4%, and 0.6% addition (a) cell wall thickness distribution, (b) cumulative cell wall thickness distribution, (c) gas cell size distribution, (d) cumulative gas cell size distribution

The PL addition caused very little change in the average cell wall thickness distributions and the average cumulative cell wall thickness distribution (Figure 4.8 a, b). The average cell thickness range for all three levels fell between 40 μm and 300 μm in thickness with all three treatments having the highest frequency at 143 μm. As the concentration of PL increased, there was a slight decrease in the frequency at 143 μm. The 0.6% PL samples contained the thinnest walls and the 0.2% PL addition the thickest. Most of the thickness fell below 0.15 mm and the separations between the curves only occurred between the samples once the thickness was greater than 0.2 mm.

The average gas cell size distribution curves (Figure 4.8 c) determined that most of the cell sizes were below 2000 μm but there was an evident shift between the cell size distributions between the levels of PL addition. The 0.2% had the thinnest peak with the highest peak height within the cell range of 0.0 μm and 1300 μm. The addition of 0.4% PL shifted the peak slightly to the right and widened the overall range of the cells to 1860 μm. There was also a drop in the peak height (5.8%) for the 0.6% PL peak where most of the cells were at 438 μm. For the 0.2% PL addition the largest number of cells (7.6%) were at 328 μm cell size and the 0.4% PL (7.1%) showed a shift to the right for the peak height to 547 μm size. There was also a higher frequency of cells in the 4000-6000 μm range, but as stated previously, this could be contributed to one or two larger cells causing the skewed distribution or there could be a series of large cells in the sample. This in the end would affect both the textural properties and the microstructure. From the average cumulative gas cell size distribution curve (Figure 4.8 d) the cell distribution was found to be larger for 0.2% and the 0.6% PL addition as the 0.4% PL had a smaller amount of cells between the 1.0 mm-3.0 mm. In comparison the 0.2% PL and 0.6% PL addition levels had cell sizes more similar to one another.

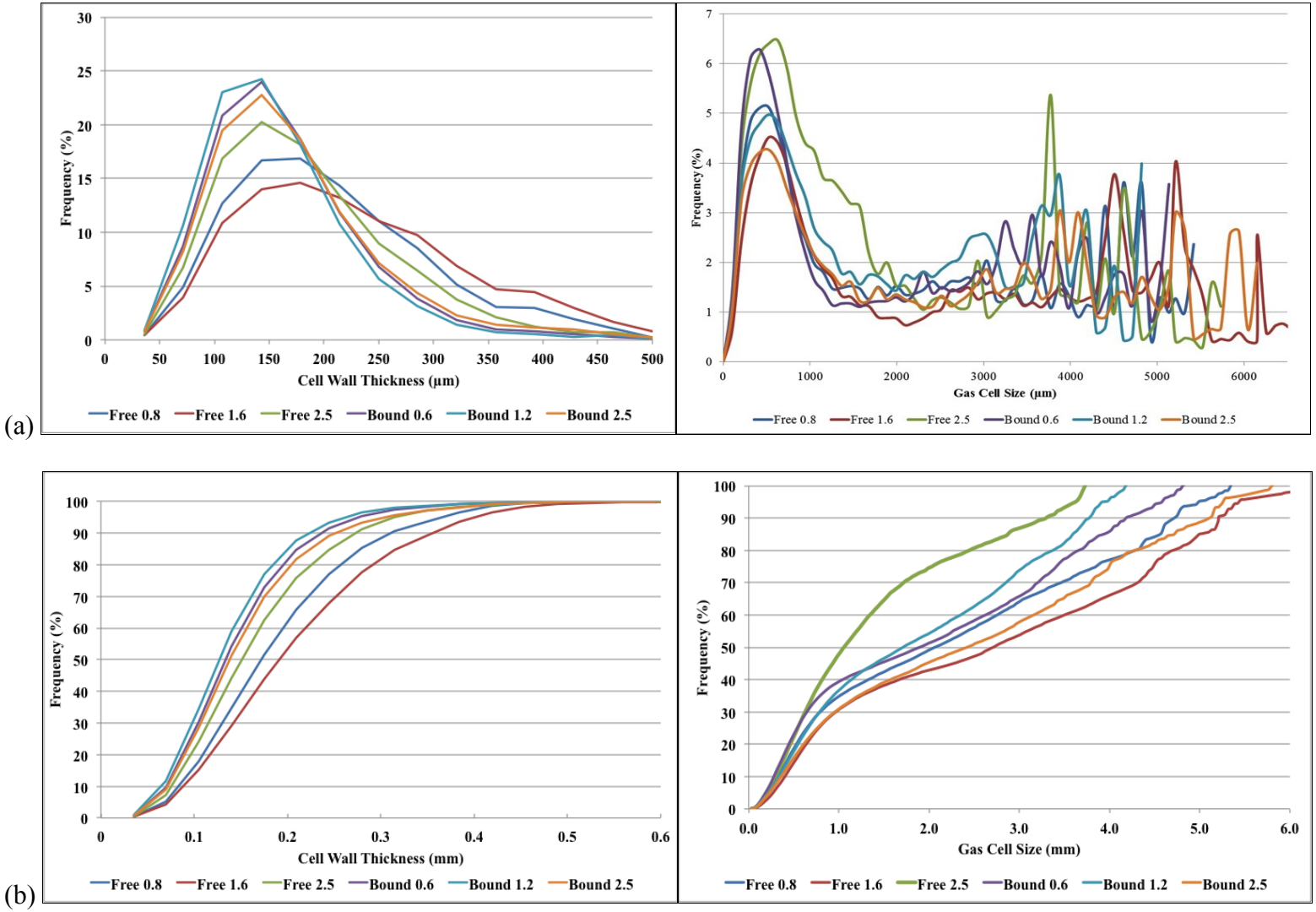

Figure 4.9. XMT scan results for center section of bread slice for free (0.8-2.5%) vs bound samples (0.6-2.5%) (a) cell wall thickness distribution, (b) cumulative cell wall thickness distribution, (c) gas cell size distribution, (d) cumulative gas cell size distribution.

The comparison of the free lipid concentrations versus bound lipid concentrations for cell wall thickness distribution, average cumulative cell wall distribution, gas cell size distribution, and average cumulative gas cell size distribution are shown in Figure 4.9 a-d. When comparing the average cell wall thickness distribution curves (Figure 4.9a), the range of thicknesses fell between 40 μm and 400 μm. All three bound lipid fractions showed narrower distributions (40 μm -300 μm) than the free as the spreads of those curves were wider. The maximum heights of each of the three bound treatments had a thickness value at 142.86 μm. The 2.5% free also had a peak height occur at 143 μm but this thickness was at a much lower frequency (20%). The peak area also widen (280 μm-357 μm) more than all the bound treatments. The 0.8% free and 1.6% free had a much broader spread in the distributions ranging from 50-392 μm and thus, the free samples had thicker cell walls than the bound lipid samples. Average cumulative cell wall thickness distribution (Figure 4.9b) showed a greater difference and spread between free samples as compared to the bound lipid treatment addition. Most of the cell wall thickness distributions for the bound lipid additions fell below 2.0 mm. The free lipids addition showed to have greater, overall thicknesses as the spacing between the curves were much bigger than the bound. This illustrated that the free bread loaves had thicker cells walls at all levels than the bound lipid loaves did.

For the gas cell size distribution (Figure 4.9c), most of the distribution for both the free and bound lipid addition fell between 0 μm and 1700 μm, with the exception of the 2.5% free. The 2.5% free had a large gas cell distributions ranging up to 2000 μm. Free lipid addition at 0.8% (5.1%) and 1.6% (4.5%) and bound lipid addition at 1.2% (5.0%) and 2.5% (4.3%) all had cell sizes with the highest peak distributions at 524 μm. The 0.6% bound had the highest peak distribution (6.3%) of gas cells at 419 μm and the 2.5% free at 629 μm (6.5%). For all treatments, there was also a large distribution of gas cells that ranged between 3000-6000 μm. At this distribution range, a greater amoung of larger cells were located throughout the loaf matrix with the various levels of lipid addition. Overall, the 2.5% free showed the widest gas cell size distribution, while most of the other treatment had a narrower curve spread made up of smaller cells. When looking at the cumulative gas cell size distributions (Figure 4.9d), all the treatments were relatively close to one another in size distribution while consisting of a mixture of sizes. This was the case for both free and bound, except for the 2.5% free lipid samples. This particular curve was more isolated due to a larger distribution of smaller cells.

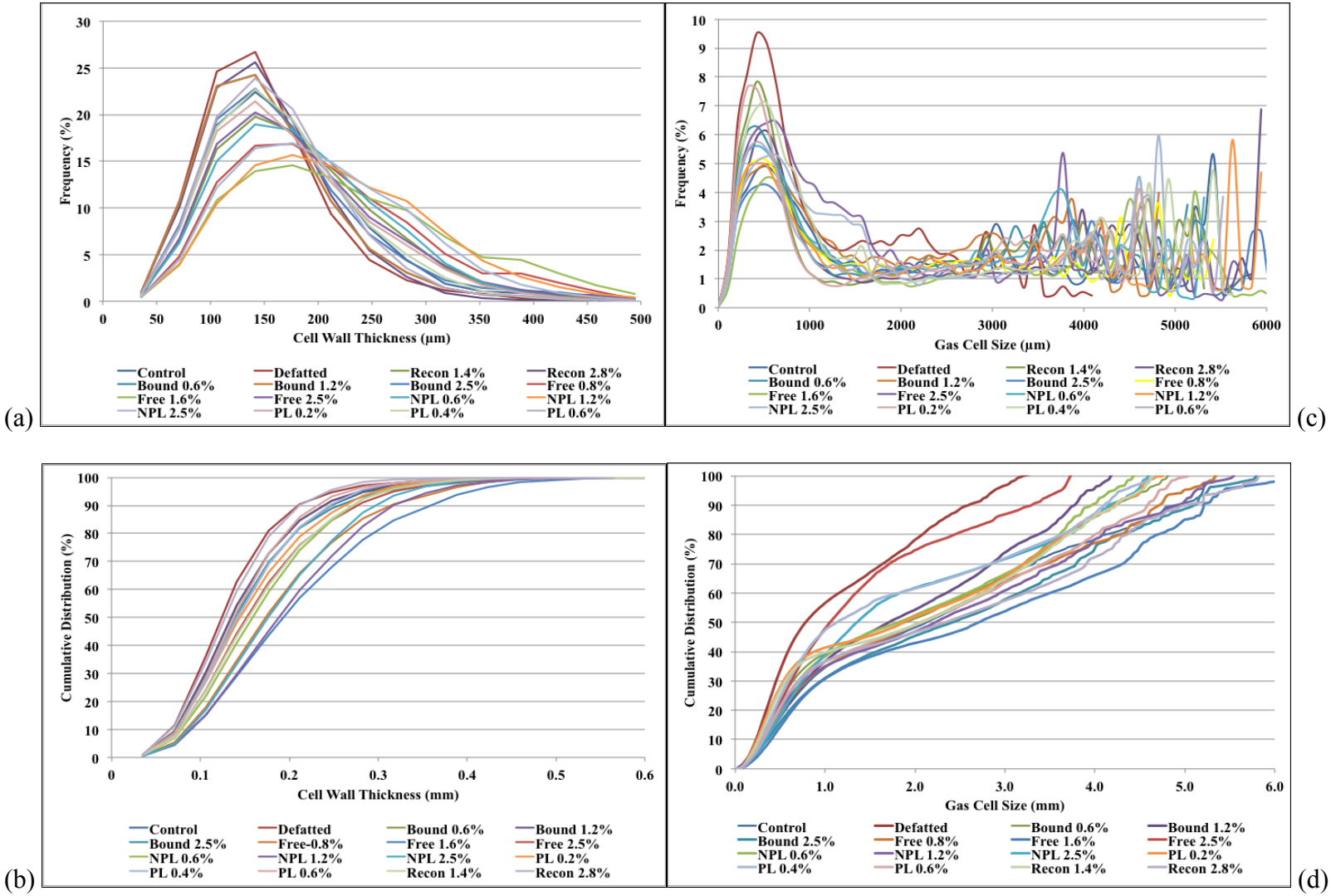

Figure 4.10. XMT scan results for center section of bread slice for all treatments at varying concentrations (a) cell wall thickness distribution, (b) cumulative cell wall thickness distribution, (c) gas cell size distribution, (d) cumulative gas cell size distribution.

The distribution curves for cell wall thickness and gas cell size for all lipid treatments at all concentrations are shown in Figure 4.10. The cell wall thickness distribution curves varied depending on the treatments with most of the curves falling between 0 μm and 300 μm. The 0.8% free, 1.6% free, 1.2% NPL, and 2.5% NPL curves were wider in distribution and extended outward from 0 μm to 400 μm. The control most frequent thickness fell in the middle of the other samples. The defatted, 2.8% recon, and 0.6%PL breads had greater frequencies at 141 μm thickness. The cumulative cell wall distribution showed similar trends. Most of the treatments fell close to the control with very limited shifts in the distributions. Again, 0.8% free, 1.6% free, 1.2% NPL, and 2.5% NPL had larger values reflecting thicker cell walls than all the other treatments. The defatted, 0.6% PL, and 2.8% recon loaves had the thinnest cell walls of all the samples (farthest left on the graph). The control, 1.2% bound, and 2.5% bound were the most similar to one another. Their distributions were at the lower end of the plot, closer to the defatted and 2.8% recon. In this case, a larger number of thicker cell walls could be signs of a more compacted cell structur and reduced volume.

The gas cell size distribution (Figure 4.10c) for all the lipid treatments existed in a narrower range of 0 μm -1000 μm. The 2.5% lipid addition of both the free and NPL had a large number of gas cells between 1000 μm and 2000 μm in size. The defatted sample had the highest peak (frequency 9.5%) at 419 μm followed by the 1.4% recon and 0.2% PL. The control, 1.2% bound, and 0.4% PL had shifts in the curve to 524 μm size while 2.5% NPL and 0.6% PL had the most gas cells at 629 μm. All the treatments were either equivalent in frequency or higher than the control except for 1.6% free and 2.5% bound. For all samples, excluding the defatted, there was also a group of cells between 4000 μm and 6000 μm. The cumulative gas cell size distribution curve also had diverse distribution of gas cell sizes throughout all the treatments. The control loaves size distribution fell almost directly in the middle with a large group of other lipid treatment being very close in distributions. The 2.5% free and defatted samples had the smallest overall gas cell size distribution On the other side, 1.6% free, 2.5% bound, and 2.8% reconstituted samples had greater gas cell size distributions than all the other treatments.

From the distribution curves, values for the eight parameters (VOI, object volume, fragmentation index, structure thickness, structure separation, number, and total porosity) are shown in Table 4.5. There were no significant differences between any of the VOI measurements for all treatments tested (2.19E12 μm^3 to 3.05E12 μm^3). The % solid volume also showed no

significant differences between any treatments. The 2.5% free and 2.5% NPL samples had the highest % solid volume (15%) and the 2.5% bound had the lowest percentage (9%). The NPL lipid addition had a greater amount of solids. The fragmentation index, which measures the connectivity of the sample, determined that all the samples had tightly connected structure as all the values were smaller than 1 (-0.00053-0.00315 1/μm). Some values were negative, which indicated concavity (highly connected). Cafaralli et al (2014) also found similar results (-0.001-0.003 1/μm) for fragmentation index for French bread samples analyzed with XMT.

The average cell wall thickness for each treatment sample was between 153 μm and 225 μm. The 1.6% free lipid addition had the highest average structure thickness at 225.12 μm while the defatted (154 μm) and the 1.2% bound (154 μm) samples had the lowest average structure thickness. The samples containing 1.2% NPL, 2.5% NPL, 0.8% free, and 1.6% free had average cell wall thicknesses between 200 μm and 225 μm. These results were bigger than the average thickness values determined for white pan bread by Falcone et al (2004) (28.3- 77.4 μm) and for a variety of breads tested by Primo-Martin et al (2010) (85-90 μm). In addition lower average cell wall thickness results were seen by Falcone et al (2005) (248-600 μm), Besbes et al (2013) (240 μm), Cafarelli et al (2014) (521-986 μm),and Van Dyck et al (2014) (170-190 μm).

The average gas cell size measurments ranged between 1590 μm and 2650 μm for the addition of lipids treatments, control, and defatted samples. There was no significant difference between the average gas cell size for any of the tested treatments. The 2.5% bound had the largest average cell size (2625 μm) and 2.5% free had the smallest size (1593 μm). These results were found to be higher than what were observed by Falcone et al (2005) (44 μm), Besbes et al (2013) (890 μm), and Cafarelli et al (2014) (375-450 μm). The number of gas cells differed between each sample treatment (36773-102661). Polar lipids added to bound, PL, and recon were significantly higher for the number of gas cells while the control, free, and NPL samples had the lowest. Total porosity measurements were found to not be significantly different for any of the tested treatments ranging between 84% and 91%. The sample with the lowest total porosity measurement was both the 2.5% free (85%) and 1.2 % NPL (85%). The highest total porosity was the 2.5% bound (91%). The total porosity results were very similar to those found by both, Primo-Martin et al (2010) (60-80%) and by Besbes et al (2013) (75-80%).

Table 4.5. XMT results for breads containing varying lipid treatments

Treatment	Volume index (VOI) (μm^3)	Solid volume (%)	Fragmentation index (1/µm)	Cell wall thickness (µm)	Gas cell size (µm)	Number of gas cells	Total porosity (%)
Control	2.89E12^{a} (2.20E11)	12.07^{a} (1.09)	-0.00194^{ab} (0.00)	166.08^{c} (6.38)	2288.08^{a} (418.49)	36925.68^{b} (6981.15)	87.93^{a} (1.09)
Bound 0.6%	3.05E12^{a} (5.62E11)	12.29^{a} (1.00)	-0.00054^{b} (0.00)	166.52^{c} (14.48)	2131.87^{a} (293.62)	67357.33^{ab} (15042.24)	87.72^{a} (1.00)
Bound 1.2%	2.60E12^{a} (2.01E11)	9.50^{a} (2.09)	0.00177^{ab} (0.00)	153.95^{c} (17.88)	1904.60^{a} (132.40)	57317.00^{ab} (10865.80)	90.50^{a} (2.09)
Bound 2.5%	2.80E12^{a} (9.09E11)	9.18^{a} (0.31)	-0.00082^{b} (0.00)	174.49^{bc} (25.61)	2625.24^{a} (519.49)	50027.33^{b} (2095.28)	90.82^{a} (0.31)
Defatted	2.19E12^{a} (2.16E11)	14.93^{a} (2.48)	-0.00059^{b} (0.00)	153.25^{c} (11.63)	1206.96^{a} (208.75)	63657.00^{ab} (9546.42)	85.07^{a} (2.48)
Free 0.8%	2.90E12^{a} (2.32E11)	13.67^{a} (1.23)	-0.00170^{ab} (0.00)	208.68^{ab} (15.52)	2372.15^{a} (522.73)	44550.68^{b} (32117. 82)	86.33^{a} (1.23)
Free 1.6%	3.01E12^{a} (1.16E11)	10.95^{a} (1.60)	0.00118^{ab} (0.00)	225.12^{ab} (27.46)	2772.84^{a} (324.48)	52703.33^{b} (17998.64)	89.05^{a} (1.60)
Free 2.5%	2.63E12^{a} (9.01E11)	15.21^{a} (2.44)	-0.00123^{ab} (0.00)	183.54^{abc} (14.11)	1593.01^{a} (857.55)	42727.33^{b} (11627.76)	84.79^{a} (2.53)
NPL 0.6%	2.62E12^{a} (2.68E11)	13.57^{a} (1.43)	-0.00154^{ab} (0.00)	185.56^{abc} (3.72)	2072.75^{a} (335.54)	48991.00^{b} (123.12)	86.43^{a} (1.43)
NPL 1.2%	2.84E12^{a} (4.17E11)	15.21^{a} (2.53)	-0.00278^{ab} (0.00)	216.16^{ab} (27.83)	2455.68^{a} (533.40)	50246.00^{b} (9176.86)	84.79^{a} (2.53)
NPL 2.5%	2.41E12^{a} (5.68E11)	14.24^{a} (3.21)	-0.00130^{ab} (0.00)	203.55^{ab} (11.24)	2111.44^{a} (1017.61)	36773.00^{b} (8896.91)	85.76^{a} (3.21)
PL 0.2%	2.58E12^{a} (1.31E11)	13.87^{a} (2.42)	0.00055^{b} (0.00)	171.49^{bc} (23.67)	2016.95^{a} (325.83)	83020.33^{ab} (13147.28)	86.13^{a} (2.42)

PL 0.4%	2.34E12[a]	13.36[a]	-0.00053[b]	174.98[bc]	2109.87[a]	44570.67[b]	86.64[a]
	(6.78E11)	(5.62)	(0.00)	(8.29)	(1182.73)	(5564.29)	(5.62)
PL 0.6%	2.63E12[a]	10.98[a]	0.00277[a]	166.46[bc]	2312.65[a]	62005.00[ab]	89.02[a]
	(3.00 E11)	(2.62)	(0.00)	(10.83)	(460.11)	(16213.52)	(2.62)
Recon 1.4%	2.51E12[a]	11.95[a]	0.00315[a]	179.39[abc]	2097.82[a]	102660.67[a]	88.05[a]
	(2.83E11)	(2.28)	(0.00)	(11.94)	(404.48)	(28291.01)	(2.28)
Recon 2.8%	2.66E12[a]	9.40[a]	0.00192[a]	157.89[a]	2589.90[a]	59073.67[a]	90.60[a]
	(8.66E11)	(0.76)	(0.00)	(6.55)	(181.44)	(5348.29)	(0.76)

[a a]Nonpolar (NPL), polar (PL), and reconstituted (Recon)
[b]Means in the same column with different letters are significantly different at a $p<0.05$; (n=48)
[c]Values in parenthesis are standard deviations

Table 4.5 contains the percentile values for 25%, 50%, 75%, and 95% markers from the cumulative distributions curves (see above graphs) for gas cell size. Significant differences between the air cell size distributions were only seen at the 25th percentile. From this data it shows that 25% of the total volume was made up of cells ranging between 421 μm and 812 μm. The control had an average size at 678 μm. The biggest differences were that 25% of the center section bread made from defatted flour had an average gas cell size of 421 μm, which was significantly different from the 1.6% free cell sizes (792 μm), and 2.5% bound (821 μm). All the other treatments at this percentile range fell in between the defatted and 2.5% bound. At the 95th percentile, the highest average gas cell was 5792 μm (2.8% recon) with all the other treatments being below this size. Between the 25^{th} percentile and 50^{th} percentile the cell size more than doubled for all treatments indicating an overall growth and varying range of cell sizes within the center section of the different breads tested. Less expansion in cell size was seen for both the 2.5% free and defatted samples as these treatments had the smallest gas cell size distribution at each percentile.

Table 4.6 Gas cell size percentile distributions for lipid treatments

Treatment	25% (µm)	50% (µm)	75% (µm)	95% (µm)	Avg. gas cell size (µm)
Control	678.02[ab] (43.02)	2216.37[a] (395.11)	3766.12[a] (1011.56)	5093.67[a] (506.19)	2288.08[a] (418.49)
Bound 0.6%	559.10[ab] (27.01)	2029.66[a] (370.52)	3546.71[a] (457.55)	3811.33[a] (916.59)	2131.87[a] (293.62)
Bound 1.2%	656.23[ab] (87.34)	1716.50[a] (42.11)	3122.36[a] (294.28)	4051.00[a] (388.27)	1904.60[a] (132.40)
Bound 2.5%	812.91[b] (174.94)	2582.70[a] (580.31)	4229.41[a] (801.26)	5623.13[a] (1136.57)	2625.24[a] (519.49)
Defatted	421.83[a] (33.69)	854.44[a] (155.96)	1922.27[a] (370.29)	3022.02[a] (489.92)	1206.96[a] (208.75)
Free 0.8%	743.02[ab] (281.73)	2212.71[a] (757.68)	3863.60[a] (941.40)	5168.03[a] (534.61)	2372.15[a] (522.73)
Free 1.6%	792.37[b] (66.87)	2847.31[a] (382.87)	4494.91[a] (523.40)	5846.29[a] (1018.09)	2772.84[a] (324.48)
Free 2.5%	559.40[ab] (37.66)	1476.10[a] (902.20)	2478.93[a] (1563.96)	2904.44[a] (1051.47)	1593.01[a] (857.55)
NPL 0.6%	617.79[ab] (63.64)	1888.69[a] (542.43)	3553.80[a] (503.29)	4342.22[a] (705.17)	2072.75[a] (335.54)
NPL 1.2%	682.52[ab] (809.91)	2512.37[a] (682.34)	3895.06[a] (81.53)	5224.79[a] (1032.72)	2455.68[a] (533.40)
NPL 2.5%	703.14[ab] (146.98)	2154.68[a] (1084.45)	3435.40[a] (1879.83)	4181.44[a] (2112.50)	2111.44[a] (1017.61)
PL 0.2%	454.39[ab] (54.10)	1950.04[a] (652.87)	3490.80[a] (589.62)	4403.80[a] (387.67)	2016.95[a] (325.83)
PL 0.4%	619.95[ab] (189.49)	2194.14[a] (1365.27)	3385.42[a] (2076.93)	4218.10[a] (2277.73)	44570.67[b] (5564.29)
PL 0.6%	617.74[ab] (137.91)	2247.12[a] (574.72)	3836.14[a] (767.16)	4931.18[a] (759.82)	62005.00[ab] (16213.52)
Recon 1.4%	484.92[ab] (112.18)	2129.41[a] (433.67)	3520.78[a] (698.99)	4487.66[a] (691.17)	102660.67[a] (28291.01)
Recon 2.8%	613.87[ab] (45.89)	2510.19[a] (337.37)	4357.90[a] (291.74)	5792.29[a] (515.84)	59073.67[a] (5348.29)

[a] Nonpolar (NPL), polar (PL), and reconstituted (Recon)
[b]Means in the same column with different letters are significantly different at a $p<0.05$; (n=48)
[c]Values in parenthesis are standard deviations

4.4. Discussion

The expansion of dough during the bread-making process is essential for a quality product as it contributes not only to the overall size of the loaf, but also in the development of crumb grain, mouth-feel, and the overall texture of the product (Cafarelli et al 2014b;Van Dyck et al 2014). Because of the porous nature of the crumb grain, the incorporation of air cells and expansion of the dough is crucial for the final product. This is essential for changing the foam into a sponge through the setting of the structure during baking (Cafarelli et al 2014b). The shape, size, positioning, and linkage between the cells can all differ (Cafarelli et al 2014a). Because air cells are only incorporated during mixing phase, the continuous expansion of the dough is solely based on the production of CO_2 from yeast, the doughs' ability to hold and retain the CO_2, the diffusion of gas into the incorporated air cells, and amount of gas cell coalescence (Cafarelli et al 2014a). Expansion is highly reflective of the dough's abililty to retain gas within the matrix (Moore and Hoseney 1986). The development of the bread typically occurs in the configuration of a "dome" and the small, incorporated air cells that start as "cylindrical" in shape will continue to expand over time and the cell shapes will change due to the expanding pore volume (Cafarelli 2014a).

From this study, seven of the tested treatments had loaf volumes that were close to or better than that of the control. These treatments included defatted, 0.6% bound, 1.2% bound, 2.5% bound, 0.6% PL, 1.4% reconstituted, and 2.8% reconstituted. All the other treatments had lower loaf volumes than the control. The lower loaf volumes indicated that these lipid fractions, at all concentration levels, had no improving effect on the loaf volume. MacRitchie and Gras (1973) found that nonpolar lipids were detrimental to loaf volumes and results found in this study are in agreement with these earlier findings. NPL fractions typically contain higher concentrations of free fatty acids that combine with amylose to form amylose-lipid complexes, preventing them from being surface active (Gerits et al 2014). The NPL showed an increases in cell wall thickness suggesting less expansion or more coalescence making the structure denser with a higher percentage of solids in the sample.

Comparing the 7 treatments, C-Cell analysis showed two factors that were related to higher loaf volumes: slice area and the number of cells. Slice area (mm^2), which is a measure of

the total area of the sample, was higher than the control for all 7 treatments. In addition, the number of cells were also larger than the control for all 7 treatments and this would be an indicator of a higher number of gas cells or a reduced amount of coalscence in each loaf. The XMT measurements that linked the samples with increased loaf volumes were the number of objects and total porosity. These had values that were very close to or larger than the control.

These common parameters for both XMT and C-Cell were both related to the incorporation of air cells that occurred during the mixing phase of the dough making process. The concentrations of polar lipids (specifically the glycolipids, MGDG and DGDG) known to be beneficial to loaf volume were higher in the six lipid treatments than in the NPL and free fractions (Daftary et al 1968; Chung et al 1982). From the lipid profiling analysis conducted at the KSU Lipidomics Research Center (refer to Chapter 2), the total lipids (recon) had the highest concentration of polar lipids (MGDG and DGDG) followed by the bound lipids, and the PL lipid fractions. MacRitchie and Gras (1973) determined that there was a concentration effect based on the amount of lipids added, which caused an increase in loaf volume. The key to maintaining and improving loaf volume is the dough's ability to allow for air cell incorporation during mixing and the holding and stabilizing of these cells over time.

In the case of the seven treatment flours, both proteins and polar lipids have surface active properties that allow them to move to the interface, hold, and stabilize air cells and both constituents are able to do this quite efficiently (Gan et al 1990). MacRitchie (1981) determined that moulding the dough caused changes in both cell size and the make-up of the interface. This in turn, allowed for the "desorable components to readily be forced out of the interface," producing a more stable film (MacRitchie 1981). In this current study, the increased concentrations of polar lipids found in these fractions could easily move to the interface due to the high quanities and their amphiphillic functional groups providing greater stability to the smaller gas cells and preventing coalscense. This in turn, would increase the volumes of these loaves as the cells are less mobile in the matrix and can easily undergo expansion. The increase in loaf volume is a function of the "stability of gas and this is related to changing the composition of protein-lipid film at the air-aqueous interface" (MacRitchie 1981).

The defatted flour resulted in a stronger structural network but did not affect the elongation of the cells measured by C-Cell, creating dough with a larger amount of smaller air cells with the greater ability to expand (Gandikota and MacRitchie 2005). The proteins and lipids

can stabilize gas cells either independently or synergistically. The increase in defatted volume compared to the control was likely associated with a greater amount of protein-protein interactions caused by the removal of the lipids. In this case, the linkage between the proteins provided the only support to gas cells due to no lipids being present to compete at the interface (Gandikota and MacRitchie 2005). If the polar lipid concentration is too low then this will limit their activity at the interface creating more protein-lipid interaction, which will hinder functionality (Gerits et al 2014). PL lipids added at the lower levels (0.2% and 0.4%) were not able to provide sufficient gas cell stability at the interface, but rather acted as a competitor to the proteins, reducing or impairing both component's ability to maintain cells and allow expansion, thus lowering the overall loaf volume.

The % bound and % PL additions had an improving effect. The higher levels of both fractions increased slice area, number of cells, number of objects, and total porosity values. The PL also caused the greatest changes in loaf volume and structure at 0.6% PL. MacRitchie and Gras (1973) determined that there was a threshold value for PL lipids and that a certain concentration had to be present before improvement could be seen in loaf volume. This, again, was due to competition with the proteins to move to the interface at the lower lipid concentrations in order to provide stability for the gas cells. Both of these treatments at all levels had cell wall thicknesses comparable to the control and were thinner than the NPL and free lipid addition. The solid volume was also less for bound and PL lipid additions indicating a greater percentage of air/gas rather than solids.

Free lipid addition at all concentrations didn't improve loaf volumes as compared to the control. This was associated with the amount of polar lipids found in the free fraction. This lipid fraction was lower in polar lipids, so even by doubling and tripling the level, the lipids weren't able to produce loaf volumes to levels equal to the control. However, shifts in the cell size distribution and wall thickness were greater for the 2.5% free addition. Hoseney et al (1969) found that the addition of free polar lipids was more beneficial to loaf volume than that of bound polar lipids alone. However, bound polar lipids have higher concentrations of MGDG and DGDG, the two glycolipids that have the greatest effect on gas cell stability (Pauly et al 2013). This may have been the same case for the free lipid addition at the lower concentrations. In addition, free fatty acids are more able to move into the free lipid fraction especially during the initial lipid extraction and this would have caused more deleterious effects to loaf volume (Gertis

et al 2014). C-Cell data found a reduced number of cells with a higher average cell diameter, which would suggest that the free lipids weren't as capable of stabilizing the gas cells over time, thus allowing for coalescence of gas cells.

As stated previously, mixing incorporates lipids and free fractions can become bound caused by the hydrophilic and hydrophilic attractions between polar lipids and gliadin and glutenin (Hoseney et al 1970; Gerits et al 2013). Gerits et al (2013) found that the process of mixing dough actually changed the distribution of polar and nonpolar lipids in the free lipid fraction making them become more bound. This was also seen for the polar lipids associated with the starch granules. They too were bound to the gluten. If the flour contained enough moisture, the mechanical action of mixing was not needed for free lipids to become bound (Gerits et al 2013).

The mechanism by which polar lipids assist in stabilizing air cells have been delineated by Gan et al (1990) as the formation of a secondary lipid lamellae made up of surface active compounds (i.e. polar lipids). They are able to align themselves at the interface and surround gas cells when the gluten-starch matrix begins to stretch and break down at the end of proofing and the beginning of baking. This break down of the structure has been hypothesized to be caused by the over expansion of gas cell and the internal pressure on the expanding cells (Gerits et al 2015). Sroan et al confirmed the presence of this secondary liquid lamellae as the secondary line of defense to prevent the coalescence of air cells following the stretching of the gluten-starch matrix (2009).

The polar lipids ability to reach the interface is associated with its capacity to form condensed monolayers that are able to pack easily and align the air cells (Sroan and MacRitchie 2009). This is opposed to NPL lipids, which can only form "expanded" monolayers that don't easily align at the interface (Sroan and MacRitchie 2009). The polar lipids that are able to form condensed monolayers are able to organize into "liquid-crystal phases" that create ordered crystalline structures called "hexagonal I mesophases" that are better suited for emulsification properties and stabilizing gas cells at the interface (Gertis et al 2014). In the case of lipid treatments tested here, the polar glycolipids (MGDG and DGDG) and phospholipids found in the bound, PL, and reconstituted fractions were more suited to align in this conformation.

4.4. Conclusion

The influence of varying lipid types and levels on the microstructure of bread was highly influenced by composition of polar lipids initially found in each lipid fraction, levels of lipids added to flour, and the number of air cells that were incorporated during mixing. Defatted, bound, reconstituted, and PL lipid treatments containing higher levels of polar lipid concentrations of MGDG and DGDG were shown to have the most positive effect on producing loaves that were comparable to or higher in loaf volume than the control. Varying levels of all lipids fractions tested did show differences in both cell wall thickness distributions and gas cell size on both a micro (XMT) and macro (C-Cell imaging) testing scale. The only correlation between lipid treatments at all levels and the control were found between loaf volume, concentration of polar lipids contained in each lipid type, number of gas cells, and porosity of each sample. The ability for polar lipids to move to the interface, forming the secondary lamellae, is beneficial for promoting gas cell stability and improving and maintaining crumb grain integrity. This in turn, provides an overall finer crumb texture, increased loaf volume, and better quality bread.

4.5. References

AACC International. Approved Methods of Analysis, 11th Ed. Method 10-05.01. Guidelines for Measurement of Volume by Rapeseed Displacement. Approved October 17, 2001. AACC International: St. Paul, MN. http://dx.doi.org/10.1094/AACCIntMethod-10-05.01.

AACC International. Approved Methods of Analysis, 11th Ed. Method 10-10.03. Optimized Straight Dough Bread-making Method. Approved November 3, 1999. AACC International: St. Paul, MN. http://dx.doi.org/10.1094/AACCIntMethod-10-10.03.

AACC International. Approved Methods of Analysis, 11th Ed. Method 44-15.02. Moisture-Air Oven Method. Approved November 3, 1999. AACC International: St. Paul, MN. http://dx.doi.org/10.1094/AACCIntMethod-44-15.02.

AACC International. Approved Methods of Analysis, 11th Ed. Method 54-40.02. Mixograph Method. Approved November 3, 1999. AACC International: St. Paul, MN. http://dx.doi.org/10.1094/AACCIntMethod-54-40.02

AACC International. Approved Methods of Analysis, 11th Ed. Method 76-31.01. Determination of damaged starch-spectrophotometric method. Approved January 10, 2014. AACC International: St. Paul, MN. http://dx.doi.org/10.1094/AACCIntMethod-76-31.01.

AACC International. Approved Methods of Analysis, 11th Ed. Method 82-23.01. Table: Flour Weight to Give 100 g at 14% Moisture Basis. Approved November 3, 1999. AACC International: St. Paul, MN. http://dx.doi.org/10.1094/AACCIntMethod-82-23.01.

Abang Zaidel, D.N., Chin, N.L., Abdul Rahman, R., and Karim, R. 2008. Rheological characterisation of gluten from extensibilty measurement. J Food Eng. 86:549-556.

Alvarez-Jubete, L., Auty, M., Arendt, E.K., and Gallagher, E. 2010. Baking properties and microstructure of pseudocereal flours in gluten-free bread formulations. Euro Food Res Technol. 230: 437-445.

Babin, P., Della Valle, G., Chiron, H., Cloetens, P., Hoszowska, J., Pernot, P., Réquerre, Salvo, L., and Dendievel, R. 2006. Fast x-ray tomography analysis of bubble growth and foam setting during breadmaking. J Cereal Sci. 43: 393-397.

Bellido, G.G., Scanlon, M.G., Page, J.H., and Hallgrimsson, B. 2006. The bubble size distribution in wheat flour dough. Food Res Int. 39:1058-1066.

Besbes, E., Jury, V., Monteau, J.-Y., and Le Bail, A. 2013. Characterizing the cellular structure of bread crumb and crust as affected by heating rate using x-ray microtomography. J Food Eng. 115: 415-423.

Bonet, A., Blaszczak, W. and Rosell, C.M. 2006. Formation of homopolymers and heteropolymers between wheat flour and several protein sources by transglutaminase-catalyzed cross-linking. Cereal Chem.: 83: 665-662.

Bruker-MicroCT. 2014. Morphometric parameters measured by Skyscan™ CT-analyzer software. http://www.skyscan.be/next/ctan03.pdf.

Cafarelli, B., Spada, A., Laverse, J., Lampignano, and Del Nobile, M.A. 2014a. An insight into the bread bubble structure: an x-ray microtomography approach. Food Res Int. 66:180-185.

Cafarelli, B., Spada, A., Laverse, J., Lampignano, and Del Nobile, M.A. 2014b. X-ray microtomography and statistical analysis: tools to quantitatively classify bread microstructure. J Food Eng. 124: 64-71.

Cauvain, S. 2013. Quality measures in baking. Cereal Food World. 58: 170-171.

C-Cell Imaging. 2014. Baked product imaging system analysis guide. Calibre Control International, Ltd: Warrington.

Chung, O.K., Pomeranz, Y., and Finney, K.F. 1978. Wheat flour lipids in breadmaking. Cereal Chem. 55: 598-618.

Chung, O.K., Pomeranz, Y., Shogren, M.D., Finney, K.F., and Howard, B.G. 1980a. Defatted and reconstituted wheat flours. VI. response to shortening addition and lipid removal in flours that vary in bread-making quality. Cereal Chem. 57: 111-117.

Chung, O.K., Pomeranz, Y., Jacobs, R.M., and Howard, B.G. 1980b. Lipid extraction conditions to differentiate among hard red winter wheats that vary in breadmaking. J Food Sci. 45: 1168-1174.

Chung, O.K., Pomeranz, Y., and Finney, K.F. 1982. Relation of polar lipid content to mixing requirement and loaf volume potential of hard red winter wheat flour. Cereal Chem. 59: 14-20.

Chung, O.K, Ohm, J-B., Ram, M.S., and Howitt, C.A. 2009. Wheat lipids. Pages 363-373 in: Wheat Chemistry and Technology, 4th Ed. K. Khan and P.R. Shewry, eds. AACC International, Inc.: St. Paul.

Chung, O.K. and Tsen, C.C. 1975. Changes in lipid binding and distribution during dough mixing. Cereal Chem. 52: 533-548.

Daftary, R.D., Pomeranz, Y., Shogren, M., and Finney, K.F. 1968. Functional bread-making properties of wheat flour lipids. 2. The role of flour lipid fractions in bread-making. Food Technol. 22: 79-82.

Daniels, N.W., Frazier, P.J., and Wood, P.S. 1971. Flour lipids and dough development. Bakers Dig. 45: 20-28.

Delcour, J. A. and Hoseney, R.C. 2010. Principles of Cereal Science and Technology. AACC International, Inc.: St. Paul.

De Stefanis, V.A. and Ponte, Jr., J.G. 1976. Studies on the breadmaking properties of wheat-flour nonpolar lipids. Cereal Chem. 53:636-642.

Falcone, P.M., Baiano, A. Zanini, F., Mancini, L., Tromba, G. Montanari, F., and Del Nobile, M.A. 2004. A novel approach to the study of bread porous structure: Phase-contrast x-ray microtomography. J Food Sci. 69: E38-E43.

Falcone, P.M., Baiano, A. Zanini, F., Mancini, L., Tromba, G., Dreossi, F., G. Montanari, F., Scuor, N., and Del Nobile, M.A. 2005. Three-dimensional quantitative analysis of bread crumb by x-ray microtomography. J Food Sci. 70: E265-E272.

Finnie, S.M., Jeannotte, R., and Faubion, J.M. 2009. Quantitative characterization of polar lipids from wheat whole meal, flour, and starch. Cereal Chem. 86: 637-645.

Gan, Z., Angold, R.E., Williams, M.R., Ellis, P.R., Vaughan, J.G., and Galliard, T. 1990. The microstructure and gas retention of bread dough. J Cereal Sci. 12: 15-24.

Gan, Z., Ellis, P.R., and Schofield, J.D. 1995. Gas cell stabilisation and gas retention in wheat bread dough. J Cereal Sci. 21: 215-230.

Gandikota, S., and MacRitchie, F. 2005. Expansion capacity of doughs: methodology and applications. J Cereal Sci. 42:157-163.

Gerits, L.R., Pareyt, B., and Delcour, J.A. 2013. Single run HPLC separation coupled to evaporate light scattering detection unravels wheat flour endogenous lipid redistribution during bread dough making. LWT-Food Sci Technol. 53: 426-433.

Gerits, L.R., Pareyt, B., and Delcour, J.A. 2014. A lipase base approach to studying the role of wheat lipids in bread making. Food Chem. 156: 190-196.

Gerits, L.R., Pareyt, B., and Delcour, J.A. 2015. Native and enzymatically modified (*Triticum aestivum L.*) endogenous lipids in bread making: a focus on gas cell stabilization mechanisms. Food Chem. 172: 613-621.

Hoseney, R.C., Finney, K.F., Pomeranz, Y., and Shogren, M.D. 1969. Functional (breadmaking) and biochemical properties of wheat flour components. V. role of total extractable lipids. Cereal Chem. 46: 606-613.

Hoseney, R.C., Finney, K.F., and Pomeranz, Y. 1970. Functional (breadmaking) and biochemical properties of wheat flour components. VI. gliadin-lipid-glutenin interactions in wheat gluten. Cereal Chem. 47: 135-140.

Hoseney, R.C., Finney, K.F., and Shogren, M.D. 1972. Functional (breadmaking) and biochemical properties of wheat flour components. IX. replacing total free lipids with synthetic lipids. Cereal Chem. 49: 366-371.

Keller, R.C.A., Orsel, R., and Hamer, R.J. 1997. Competitive adsorption behaviour of wheat flour components and emulsifiers at air-water interface. J Cereal Sci. 25: 175-183.

Li, W., Dobraszczyk, B.J., and Wilde, P.J. 2004. Surface properties and locations of gluten proteins and lipids revealed using confocal scanning laser microscopy in bread dough. J Cereal Sci. 39: 403-411.

Lim, K.S. and Barigou, M. 2004. X-ray micro-computed tomography of cellular food products. Food Res Int. 37:1001-1012.

Lodi, A. and Vodovotz, Y. 2008. Physical properties and water state changes during storage in soy bread with or without almond. Food Chem. 110: 554-561.

MacRitchie, F., and Gras, P.W. 1973. The role of flour lipids in baking. Cereal Chem. 50:292-302.

MacRitchie, F. 1977. Flour lipids and their effects in baking. J Sci Food Agric. 28: 53-58.

MacRitchie, F. 1981. Flour lipids: theoretical aspects and functional properties. Cereal Chem. 58: 156-158.

Melvin, M.A. 1979. The effect of extractable lipid on the viscosity characteristics of corn and wheat starches. J Sci Food Agric. 30: 731-738.

Moreno-Atanasio, R., Williams, R.A., and Jia, X. 2010. Combing x-ray microtomography with computer simulation for analysis of granular porous materials. Particuology. 8:81-99.

Moore, W.R. and Hoseney, R.C. 1986. Influence of shortening and surfactants on retention of carbon dioxide in bread dough. Cereal Chem. 63:67-70.

Newberry, M.P., Phan-Thien, N., Larroque, O.R., Tanner, R.I., Larsen, N.G. 2002. Dynamic and elongation rheology of yeasted bread dough. Cereal Chem. 79: 874-879.

Ohm, J.B., and Chung, O.K. 2002. Relationship of free lipids with quality factors in hard winter wheat flours. Cereal Chem. 79: 274-278.

Papantoniou, E., Hammond, E.W., Scriven, F., Gordon, M.H., and Schofield, J.D. 2004. Effects of endogenous flour lipids on the quality of short-dough biscuits. J Sci Food Agric. 84: 1371-1380

Paternotte, T.A., Orsel, R., and Hamer. R.J. 1994. Dynamic interfacial behaviour of gliadin-diacylgalactosylglycerol (MGDG) films: possible implications for gas-cell stability in wheat flour doughs. J Cereal Sci. 19: 123-129.

Pauly, A., Pareyt, B., Fierens, E., and Delcour, J.A. 2013. Wheat (*Triticum aestivum L.* and *T. turgidum L.* ssp. *Durum*) Kernel Hardness: I. current views on the role of puroindolines and polar lipids. Compr Rev Food Sci. 12: 413-426.

Pickett, M. M . 2009. Study of gas cell stability during breadmaking using x-ray microtomography and dough rheology. M.S. Thesis. Kansas State University.

Primo-Martín, C. van Dalen, G., Meinders, M.B.J., Don, A., Hamer, R.H., and van Vliet, T. 2010. Bread crispness and morphology can be controlled by proving conditions. Food Res Int. 43:207-217.

Pomeranz, Y., Rubenthaler, G.L., Daftary, R.D., and Finney, K.F. 1966. Effects of lipids on bread baked from flour varying widely in bread-making potentialities. Food Technol. 20: 1225-1228.

Sroan, B.S., Bean, S.R., and MacRitchie, F. 2009. Mechanism of gas cell stabilization in bread making. I. the primary gluten-starch matrix. J Cereal Sci. 49: 32-40.

Sroan, B.S., and MacRitchie, F. 2009. Mechanism of gas cell stabilization in bread making. II. the secondary liquid lamellae. J Cereal Sci. 49: 41-46.

Sun, H., Yan, S., Jiang, W., Li, G., MacRitchie, F. 2010. Contribution of lipid to physicochemical properties and Mantou-making quality of wheat flour. Food Chem. 121: 332-337.

Takahashi, S. and Seib, P. 1988. Paste and gel properties of prime corn and wheat starches with and without native lipids. Cereal Chem. 65: 474-483.

Tang, M.C. and Copeland, L. 2007. Analysis of complexes between lipids and wheat starch. Carbohyd Polym. 67: 80-85.

Tester, R.F., and Morrision, W.R. 1990. Swelling and gelatinization of cereal starches. I. effects of amylopectin, amylose, and lipids. Cereal Chem. 67: 551-557.

Trinh, L., Lowe, T., Campbell, G.M., Withers, P.J., and Martin, P.J. 2013. Bread dough aeration dynamics during pressure step-change mixer: studies by x-ray tomography, dough density and population balancing modeling. Chem Eng Sci. 101: 470-471.

Turbin-Orger, A., Della Valle, G., Doublier, J.L., Fameau, A.-L., Marze, S., Sauliner, L. 2015. Foaming and rheological properties of liquid phase extracted from wheat flour dough. Food Hydrocolloid. 43:114-124.

Upadhyay, R., Ghosal, D., Mehra, A. 2012. Characterization of bread dough: rheological properties and microstructure. J Food Eng. 109: 104-113.

Van Dyck, T., Verboven, P., Herremans, E., Defraeye, T., Van Campenhout, L., Wevers, M., Claes, J., Nicolaï, B. 2014. Characterisation of structural patterns in bread as evaluated by x-ray computer tomography. J Food Eng. 123: 67-77.

Vlassenbroeck, J., Dierick, M., Masschaele, B., Cnudde, V., Van Hoorebeke, L., Jacobs, P. 2007. Software tools for quantification of x-ray microtomography at UGCT. Nucl Instrum Meth A. 580: 442-445.

Vasanthan, T. and Hoover, R. 1992. Effect of defatting on starch structure and physicochemical properties. Food Chem. 45: 337-347.

Villarino, V.B., Jayasena, V., Coorey, R., Chakrabarti-Bell, S., and Johnson, S. 2014. The effects of bread-making process factors on Australian sweet lupin-wheat bread quality characteristics. Int J Food Sci Tech. 49: 2373-2381.

Whitworth, M.B., Cauvain, S. P., and Cliffe, D. 2005. Measurement of bread cell structure by image analysis. Pages 193-198 in Using Cereal Science and Technology for the Benefit of Consumers. S.P. Cauvain, S.S. Salmon, and L.S. Young, eds. CRC Press LLC: Boca Raton.

Wilde, P.J., Clark, D.C., Marion, D. 1993. Influence of competitive adsorption of lysopalmitoylphosphotidylcholine on the functional properties of puroindoline, a lipid-binding protein isolated from wheat flour. J Agric Food Chem. 41: 1570-1576.

Chapter 5 - Future Work

1. In this study, one flour variety was used for treatment testing, therefore for future studies, evaluating other types of flours ranging in strength (weak or strong) would help to broaden the understanding of the influence of lipids, especially on the microstructure and cell distribution.
2. The lipids were added to the dough and the final product was evaluated using XMT testing. Being that much of the mechanism for lipid functionality occurs after mixing, it would be beneficial to see the lipid influence and changes that occur in the dough during the stages of fermentation and proofing.
3. Due to the complexity and depth of the experimental design, not all lipid varations could be tested with all equipment, thus more testing on all types of lipid varieties should be included for future work. Adding the free and bound lipids to both, the dough and whole loaf XMT analysis and with oscillatory rheology testing should also be included in further studies.
4. For the extensional testing, varying the concentration of each lipid type would also provide a better understanding of how the level of addition influences strain hardening and cell wall strength.
5. In addition, changing the hook speed during extensional testing, would also help to provide more information about the large deformation performance of doughs containing the different lipids.

References

AACC International. Approved Methods of Analysis, 11th Ed. Method 10-05.01. Guidelines for Measurement of Volume by Rapeseed Displacement. Approved October 17, 1995. AACC International: St. Paul, MN. http://dx.doi.org/10.1094/AACCIntMethod-10-05.01.

AACC International. Approved Methods of Analysis, 11th Ed. Method 10-10.03. Optimized Straight Dough Bread-making Method. Approved November 3, 1995. AACC International: St. Paul, MN. http://dx.doi.org/10.1094/AACCIntMethod-10-10.03.

AACC International. Approved Methods of Analysis, 11th Ed. Method 44-15.02. Moisture-Air Oven Method. Approved October 30, 1975. AACC International: St. Paul, MN. http://dx.doi.org/10.1094/AACCIntMethod-44-15.02.

AACC International. Approved Methods of Analysis, 11th Ed. Method 54-40.02. Mixograph Method. Approved November 3, 1999. AACC International: St. Paul, MN. http://dx.doi.org/10.1094/AACCIntMethod-54-40.02

AACC International. Approved Methods of Analysis, 11th Ed. Method 76-31.01. Determination of damaged starch-spectrophotometric method. Approved November 8, 1995. AACC International: St. Paul, MN. http://dx.doi.org/10.1094/AACCIntMethod-76-31.01.

AACC International. Approved Methods of Analysis, 11th Ed. Method 82-23.01. Table: Flour Weight to Give 100 g at 14% Moisture Basis. Approved April 13, 1961. AACC International: St. Paul, MN. http://dx.doi.org/10.1094/AACCIntMethod-82-23.01.

AACC International. Approved Methods of Analysis, 11th Ed. Method 44-15.02. Moisture-Air Oven Method. Approved October 30, 1975. AACC International: St. Paul, MN. http://dx.doi.org/10.1094/AACCIntMethod-44-15.02.

AACC International. Approved Methods of Analysis, 11th Ed. Method 54-40.02. Mixograph Method. Approved November 3, 1999. AACC International: St. Paul, MN. http://dx.doi.org/10.1094/AACCIntMethod-54-40.02

AACC International. Approved Methods of Analysis, 11th Ed. Method 76-31.01. Determination of damaged starch-spectrophotometric method. Approved November 8, 1995. AACC International: St. Paul, MN. http://dx.doi.org/10.1094/AACCIntMethod-76-31.01.

AACC International. Approved Methods of Analysis, 11th Ed. Method 82-23.01. Table: Flour Weight to Give 100 g at 14% Moisture Basis. Approved April 13, 1961. AACC International: St. Paul, MN. http://dx.doi.org/10.1094/AACCIntMethod-82-23.01.

Abang Zaidel, D.N., Chin, D.N., Abdul Rahman, R., and Karim, R. 2008. Rheological characterisation of gluten from extensibility measurement. J Food Eng. 86:549-556

Agyare, K.K., Xiong, Y.L., Addo, K., and Akoh, C.C. 2004. Dynamic rheological and thermal properties of soft wheat flour dough containing structure lipid. J Food Sci. 69: E297-E302.

Alvarez-Jubete, L., Auty, M., Arendt, E.K. and Gallagher, E. 2010. Baking properties and microstructure of pseudocereal flours in gluten-free bread formulations. Euro Food Res Technol. 230: 437-445.

Autio, K., Flander, L., and Kinnunen, A., and Heinonen, R. 2001. Bread quality relationship with rheological measurements of wheat flour dough. Cereal Chem. 78: 654-657.

Babin, P., Della Valle, G., Chiron, H., Cloetens, P., Hoszowska, J., Pernot, P., Réquerre, L., Salvo, L., and Dendievel, R. 2006. Fast X-ray tomography analysis of bubble growth and foam setting during breadmaking. J Cereal Sci. 43: 393-397.

Baker J.C. 1941. The structure of the gas cell in bread dough. Cereal Chem. 18: 34-41.

Baker, J.C. and Mize, M.D. 1941. The origin of gas cells in bread dough. Cereal Chem. 18: 19-34.

Baker, J.C. and Mize, M.D. 1946. Gas occlusion during dough mixing. Cereal Chem. 23: 39-51.

Belderok, B. 2000. Part One: Developments in bread-making process. Pages. 42-43 in: Bread-making Quality of Wheat A Century of Breeding in Europe. D.A. Donner, Ed. Kluwer Academic Publishers: Dordrecht.

Bellido, G.G., Scanlon, M.G., Page, J.H., and Hallgrimsson, B. 2006. The bubble size distribution in wheat flour dough. Food Res. Int. 39:1058-1066.

Belton, P.S. 1999. Mini review: on the elasticity of wheat gluten. J Cereal Sci. 29:103-107.

Belton, P.S. 2005. New approaches to study molecular basis of the mechanical properties of gluten. J Cereal Sci. 41: 203-2011.

BeMiller, J.N. 2007. Carbohydrate Chemistry for Food Scientist. AACC International, Inc.: St. Paul.

Besbes E., Jury, V., Monteau, J.-Y., and Le Bail, A. 2013. Characterizing the cellular structure of bread crumb and crust affected by heating rate using X-ray microtomography. J Food Eng. 115: 415-423.

Blanshard, J.M.V. 1987. The significance of structure and function of the starch granules in baked products. Page 1 in: Chemistry and Physics of Baking. J.M.V. Blanshard, P.J. Frazier, and T. Galliard, eds. Royal Society of Chemistry: London.

Blazek, J. Gilbert, E.P., and Copeland, L. 2011. Effects of monoglycerides on pasting properties of wheat starch after repeated heating and cooling. J Cereal Sci. 54:151-159.

Bonet, A., Blaszczak, W. and Rosell, C.M. 2006. Formation of homopolymers and heteropolymers between wheat flour and several protein sources by transglutaminase-catalyzed cross-linking. Cereal Chem.: 83: 665-662.

Bruker-MicroCT. 2014. Morphometric parameters measured by Skyscan™ CT-analyzer software. http://www.skyscan.be/next/ctan03.pdf.

Cafarelli, B., Spada, A., Laverse, J., Lampignano, and Del Nobile, M.A. 2014a. An insight into the bread bubble structure: an x-ray microtomography approach. Food Res Int. 66: 180-185.

Cafarelli, B., Spada, A., Laverse, J., Lampignano, and Del Nobile, M.A. 2014b. X-ray microtomography and statistical analysis: tools to quantitatively classify bread microstructure. J. Food Eng. 124: 64-71.

Campos, D.T, Steffe, J.F., and NG, P.K.W. 1997. Rheological behavior of undeveloped and developed wheat dough. Cereal Chem. 74: 489-494.

Cauvain, S. 2012. Breadmaking: an overview. Pages 26-28 in: Breadmaking Improving Quality, 2nd Ed. S.P. Cauvain, ed. Woodhead Publishing Limited: Cambridge.

Cauvain, S. 2013. Quality measures in baking. Cereal Food World. 58: 170-171.

Carlson, T., Larsson, K., and Miezis, Y. 1978. Phase equilibria and structures in the aqueous system of wheat lipids. Cereal Chem. 55: 168-179.

Carlson, T.L-G., Larsson, K., Miezis, Y., and Poovarodom, S. 1979. Phase equilibria in aqueous system of wheat gluten lipids and in the aqueous salt system of wheat lipids. Cereal Chem. 56: 417-419.

Carr, N.O., Daniels, N.W.R., and Frazier, P.J. 1992. Lipid interactions in breadmaking. Cr Rev Food Sci. 31: 237-258.

Cauvain, S.P. 1998. Bread-the product. Pages 1-3 in: Technology of Breadmaking. S.P. Cauvain and L.S. Young, eds. Blackie Academic & Professional: New York.

C-Cell Imaging. 2014. Baked product imaging system analysis guide. Calibre Control International, Ltd: Warrington

Chung, O.K., Ohm, J-B., Ram, M.S., and Howitt, C.A. 2009. Wheat Lipids. Pages 363-373 in: Wheat Chemistry and Technology, 4th ed. K. Khan and P.R. Shewry, Eds. AACC International, Inc.: St. Paul.

Chung, O.K., Pomeranz, Y., and Finney, K.F. 1978. Wheat flour lipids in breadmaking. Cereal Chem. 55: 598-618.

Chung, O.K., Pomeranz, Y., and Finney, K.F. 1982. Relation of polar lipid content to mixing requirement and loaf volume potential of hard red winter wheat flours. Cereal Chem. 59: 14-20.

Chung, O.K., Pomeranz, Y., Finney, K.F., Hubbard, J.D., and Shogren, M.D. 1977a. Defatted and reconstituted wheat flours. I. Effects of solvent and soxhlet types on functional (breadmaking) properties. Cereal Chem. 54: 454-465.

Chung, O.K., Pomeranz, Y., Hwang, E.C., and Dikeman, E. 1979. Defatted and reconstituted wheat flours. IV. Effects of flour lipids on protein extractability from flours that vary in bread-making quality. 1979. Cereal Chem. 56: 220-226.

Chung, O.K., Pomeranz, Y., Finney, K.F., and Shogren, M.D. 1977b. Defatted and reconstituted wheat flours. II. Effects of solvent type and extracting conditions on flours varying in breadmaking quality. Cereal Chem. 54: 484-495.

Chung, O.K., Pomeranz, Y., Jacobs, R.M., and Howard, B.G. 1980a. Lipid extraction conditions differentiate among hard red winter wheats that vary in breadmaking. J Food Sci. 45: 1168-1174.

Chung, O.K., Pomeranz, Y., Shogren, M.D., Finney, K.F., and Howard B.G. 1980b. Defatted and reconstituted wheat flours. VI. response to shortening addition and lipid removal in flours that vary in bread-making quality. Cereal Chem. 57: 111-117.

Chung, O.K., Pomeranz, Y., Finney, K.F., Shogren, M.D., and Carville, D. 1980c. Defatted and reconstituted wheat flours. V. bread-making response to shortening of flour differentially defatted by varying solvent and temperature. Cereal Chem. 57: 106-110.

Chung, O.K., Shogren, M.D., Pomeranz, Y., and Finney, K.F. 1981. Defatted and reconstituted wheat flours. VII. the effect of 0-12% shortening (flour basis) in bread making. Cereal Chem. 58: 69-73.

Chung, O.K. and Tsen C.C. 1975. Changes in lipid binding and distribution during dough mixing. Cereal Chem. 52: 533-548.

Daftary R.D., Pomeranz, Y., Shogren, M., and Finney, K.F. 1968. Functional bread-making properties of wheat flour lipids. 2. the role of flour lipid fractions in bread-making. Food Technol. 22: 327-330.

Daniels, N.W., Frazier, P.J., and Wood, P.S. 1971. Flour lipids and dough development. Bakers Dig. 45: 20-28.

Daniels, N.W.R., Richmond, J.W., Eggitt, P.W.R., and Coppock, J.B.M. 1966. Studies on the lipids of flour. III. lipid binding in breadmaking. J Sci Food Agric. 17: 20-29.

Delcour, J.A. and Hoseney, R.C. 2010. Principles of Cereal Science and Technology, 3rd ed. AACC International, Inc.: St. Paul.

Department of Health and Human Services, Food and Drug Administration. 2013. Requirements for specific standardized bakery products. 21 CFR part 136. Fed. Regist. 63: 40135. 21CFR136.110.

De Stefanis, V.A. and Ponte, Jr., J.G. 1976. Studies on the breadmaking properties of wheat-flour nonpolar lipids. Cereal Chem. 53: 636-642.

Dobraszczyk, B.J. 2004. The physics of baking: rheological and polymer molecular structure-function relationships in breadmaking. J Non-Newtonian Fluid Mech. 124: 61-69.

Dobraszczyk, B.J., and Morgenstern, M.P. 2003. Rheology and the breadmaking process. J Cereal Sci. 38: 229-245.

Dobraszczyk, B.J., and Roberts, C.A. 1994. Strain hardening and dough gas cell-wall failure in biaxial extension. J Cereal Sci. 20: 265-274.

Dobraszczyk, B.J., and Salmanowicz, B.P. 2008. Comparison of predictions of baking volume using large deformation rheological properties. J Cereal Sci. 47: 292-301.

Dreese, P.C., Faubion, J.M., and Hoseney, R.C. 1988. Dynamic rheological properties of flour, gluten, and gluten-starch doughs. I. temperature-dependent changes during heating. Cereal Chem. 65: 348-353.

Dubreil, L., Compoint, J-P., and Marion, D. 1997. Interaction of puroindolines with wheat flour polar lipids determines their foaming properties. J Agric Food Chem. 45: 108-116

Dunnewind, B., Sliwinski, E.L., Grolle, K., and Van Vliet, T. 2004. The Kieffer dough and gluten extensibility rig- an experimental evaluation. J Text Stud. 34: 537-560.

Eliasson, A.-C., and Larsson, K. 1993. Cereals in Breadmaking A Molecular Colloidal Approach. Marcel Dekker, Inc.: New York.

Falcone, P.M., Baiano, A. Zanini, F., Mancini, L., Tromba, G. Montanari, F., and Del Nobile, M.A. 2004. A novel approach to the study of bread porous structure: Phase-contrast x-ray microtomography. J Food Sci. 69: E38-E43.

Falcone, P.M., Baiano, A. Zanini, F., Mancini, L., Tromba, Dreossi, F., G. Montanari, F., Scuor, N., and Del Nobile, M.A. 2005. Three-dimensional quantitative analysis of bread crumb by x-ray microtomography. J Food Sci. 70: E265-E272

Faubion, J.M., and Hoseney, R.C. 1990. The viscoelastic properties of wheat flour dough. Pages: 57-59 in: Dough Rheology and Baked Product Texture. H. Faridi and J.M. Faubion, eds. Van Nostrand Reinhold: New York.

Finnie, S.M.; Jeannotte, R.; and Faubion, J.M. 2009. Quantitative characterization of polar lipids from wheat whole meal, flour, and starch. Cereal Chem. 86: 637-645.

Finnie, S.M., Jeannotte, R., Morris, C.F., Giroux, M.J., and Faubion, J.M. 2010. Variation in polar lipids located on the surface of wheat starch. J Cereal Sci. 51: 73-80.

Finney, K.F., Pomeranz, Y., and Hoseney, R.C. 1976. Effect of solvent extractions on lipid composition, mixing time, and bread loaf volume. Cereal Chem. 53: 383-388.

Galliard, T., and Bowler, P. 1987. Morphology and composition of starch. Pages 71-72 in: Starch Properties and Potential. T. Galliard, ed. Society of Chemical Industry: Great Britain.

Gan, Z., Angold, R.E., Williams, M.R., Ellis, P.R., Vaughan, J.G., and Galliard, T. 1990. The microstructure and gas retention of bread dough. J Cereal Sci. 12: 15-24.

Gan, Z., Ellis, P.R., and Schofield, J.D. 1995. Gas cell stabilisation and gas retention in wheat bread dough. J Cereal Sci. 21: 215-230.

Gandikota, S., and MacRitchie, F. 2005. Expansion capacity of doughs: methodology and applications. J Cereal Sci. 42: 157-163.

Georgopoulos, T., Larsson, H., and Eliasson, A-C. 2004. A comparison of the rheological properties of wheat flour dough and its gluten prepared by ultracentrifugation. Food Hydrocolloids. 18: 143-151.

Georgopoulos, T., Larsson, H., and Eliasson, A-C. 2006. Influence of native lipids on the rheological properties of wheat flour dough and gluten. J Texture Stud. 37: 49-62

Gerits, L.R., Pareyt, B., and Delcour, J.A. 2013. Single run HPLC separation coupled to evaporate light scattering detection unravels wheat flour endogenous lipid redistribution during bread dough making. LWT-Food Sci Technol. 53: 426-433.

Gerits, L.R., Pareyt, B., and Delcour, J.A. 2014. A lipase base approach to studying the role of wheat lipids in bread making. Food Chem. 156: 190-196.

Gerits, L.R., Pareyt, B., and Delcour, J.A. 2015. Native and enzymatically modified (*Triticum aestivum L.*) endogenous lipids in bread making: a focus on gas cell stabilization mechanisms. Food Chem. 172: 613-621

Greenblatt, G.A., Bettge, A.D., and Morris, C.F. 1995. Relationship between endosperm texture and the occurrence of friabilin and bound polar lipids on wheat starch. Cereal Chem. 72: 172-176.

Gómez, A.V., Buchner, D., Tadini, C.C., Añón, M.C., and Puppo, M.C. 2013. Emulsifiers: effects on quality of fibre-enriched wheat bread. Food Bioprocess Technol 6: 11228-1239.

Hadnađev, M., Dapčević Hadnađev, T., Šimurina, O., and Filipčev, B. 2013. Empirical and fundamental rheological properties of wheat flour dough as affected by different climatic conditions. J Agr Sci Tech. 15: 1381-1391

Hamer, R.J., and Van Vliet, T. 2000. Understanding the structure and properties of gluten: an overview. Pages. 127-129 in: Wheat Gluten. P.R. Shewry and A.S. Tatham, eds. Royal Society of Chemistry: Cambridge.

Hoseney, R.C. 1984. Gas retention in bread doughs. Cereal Food World. 29: 305-308.

Hoseney, R.C. 1985. The mixing phenomenon. Cereal Food World. 30: 453- 457.

Hoseney, R.C., Finney, K.F., and Pomeranz, Y. 1969. Functional (breadmaking) and biochemical properties of wheat flour components. V. role of total extractable lipids. Cereal Chem. 46: 606-613.

Hoseney, R.C., Finney, K.F., and Pomeranz, Y. 1970. Functional (breadmaking) and biochemical properties of wheat flour components. VI. gliadin-lipid-glutenin interactions in wheat gluten. Cereal Chem. 47: 135-140.

Hoseney R.C., Finney, K.F., Pomeranz, Y., and Shogren, M.D. 1971. Functional and biochemical properties of wheat flour components. VIII. starch. Cereal Chem. 48: 191-201.

Hoseney, R.C., Finney, K.F., and Shogren, M.D. 1972. Functional (breadmaking) and biochemical properties of wheat flour components. IX. replacing total free lipids with synthetic lipids. Cereal Chem. 49: 366-371.

Jekle, M., and Becker, T. 2015. Wheat dough microstructure: the relation between visual structure and mechanical behavior. Cr Rev Food Sci. 55: 369-382.

Junge, R.C., and Hoseney, R.C. 1981a. A mechanism by which shortening and certain surfactants improve loaf volume in bread. Cereal Chem. 58: 408-412.

Junge, R.C., Hoseney, R.C., and Varriano-Marston, E. 1981b. Effect of surfactants on air incorporation in dough and the crumb grain of bread. Cereal Chem. 58: 338-342.

Keller, R.C.A., Orsel, R., and Hamer, R.J. 1997. Competitive adsorption behaviour of wheat flour components and emulsifiers at air-water interface. J Cereal Sci. 25: 175-183.

Khatkar, B.S., and Schofield, J.D. 2002a. Dynamic rheology of wheat flour dough. I. non-linear viscoelastic behaviour. J Sci Food Agric. 82: 827-829.

Khatkar, B.S., and Schofield, J.D. 2002b. Dynamic rheology of wheat flour dough. II. Assessment of dough strength and bread-making quality. J Sci Food Agric. 82: 823-826.

Lampignano, V., Mastromatteo, L.M., and Del Nobile, M.A. 2013. Microstructural, textural and sensorial properties of durum wheat bread as affected by yeast content. Food Res Int. 50: 369-376.

Larsson, H., and Eliasson, A-C. 1997. Influence of the starch granule surface on the rheological behaviour of wheat flour dough. J Texture Stud. 28: 487-501.

Lefebvre, J. 2006. An outline of the non-linear viscoelastic behaviour of wheat flour dough in shear. Rheol Acta. 45: 525-538.

Leissner, O. 1988. A comparison of the effect of different polymorphic forms of lipids in breadmaking. Cereal Chem. 65: 202-207.

Létang, C., Piau, M., and Verdier, C. 1999. Characterization of wheat flour-water doughs. Part I: rheometry and microstructure. J Food Eng. 41: 121-132.

Li, W., Dobraszczyk, B.J., and Wilde, P.J. 2004. Surface properties and locations of gluten proteins and lipids revealed using confocal scanning laser microscopy in bread dough. J Cereal Sci. 39: 403-411.

Lim, K.S. and Barigou, M. 2004. X-ray micro-computed tomography of cellular food products. Food Res Int. 37: 1001-1012.

Lodi, A. and Vodovotz, Y. 2008. Physical properties and water state changes during storage in soy bread with or without almond. Food Chem. 110: 554-561

Macosko, C.W. 1994. Rheology Principles, Measurements, and Applications. VCH Publishers, Inc.: New York.

MacRitchie, F., and Gras, P.W. 1973. The role of lipids in baking. Cereal Chem. 50: 292-302.

MacRitchie, F. 1976a. The liquid phase of dough and its role in baking. Cereal Chem. 53: 318-326.

MacRitchie, F. 1976b. Monolayer compression barrier in emulsion and foam stability. J Colloid Interf Sci. 56: 53-56.

MacRitchie, F. 1977. Flour lipids and their effects in baking. J Sci Food Agric. 28: 53-58.

MacRitchie, F. 1981. Flour lipids: theoretical aspects and functional properties. Cereal Chem. 58: 156-158

MacRitchie F. 2010. Concepts in Cereal Chemistry. Taylor and Francis Group, LLC.: Boca Raton.

Maire, E., Fazekas, A., Salvo, L., Dendievel, R., Youssef, S., Cloetens, P., and Letang, J.M. 2003. X-ray tomography applied to the characterization of cellular materials. Related finite element modeling problems. Compos Sci Technol. 63: 2431-2443.

Marion, D., Le Roux, C., Akoka, S., Tellier, C., and Gallant, D. 1987. Lipid-protein interactions in wheat gluten: a phosphorus nuclear magnetic resonance spectroscopy and freeze-fracture electron microscopy study. J Cereal Sci. 5: 101-115.

Masi, P., Cavella, S., and Sepe, M. 1998. Characterization of dynamic viscoelastic behavior of wheat flour doughs at different moisture contents. Cereal Chem. 75: 429-432.

Medcalf, D.G., Youngs, V.L., Gilles, K.A. 1968. Wheat Starches. II. effect of polar and nonpolar lipid fractions on pasting characteristics. Cereal Chem. 45: 88-95.

Melvin, M.A. 1979. The effect of extractable lipid on the viscosity characteristics of corn and wheat starches. J Sci Food Agric. 30: 731-738.

Mills, E.N.C., Wilde, P.J., Salt, L.J., and Skeggs, P. 2003. Bubbles formation and stabilization in bread dough. Food Bioprod Process. 81:189-193.

Miller, K.A., and Hoseney R.C. 1999. Dynamic rheological properties of wheat starch-gluten doughs. Cereal Chem. 76: 105-109

Moore, W.R. and Hoseney, R.C. 1986. Influence of shortening and surfactants on retention of carbon dioxide in bread dough. Cereal Chem. 63:67-70.

Moreno-Atanasio, R., Williams, R.A., and Jia, X. 2010. Combing x-ray microtomography with computer simulation for analysis of granular porous materials. Particuology. 8:81-99.

Morrision, W.R. 1988. Lipids in cereal starches: a review. J Cereal Sci. 8: 1-15.

Nash, D., Lanning, S.P., Fox, P., Martin, J.M., Blake, N.K., Souza, E., Graybosch, R.A., Giroux, M.J., and Talbert, L.E. 2006. Relationship of dough extensibility to dough strength in a spring wheat cross. Cereal Chem 83: 255-258.

Ohm, J.B., and Chung, O.K. 2002. Relationship of free lipids with quality factors in hard winter wheat flours. Cereal Chem. 79: 274-278.

Papantoniou, E., Hammond, E.W., Scriven, F., Gordon, M.H., and Schofield, J.D. 2004. Effects of endogenous flour lipids on the quality of short-dough biscuits. J Sci Food Agric. 84: 1371-1380.

Papantoniou, E., Hammond, E.W., Tsiami, A.A., Scriven, F., Gordon, M.H., and Schofield, J.D. 2003. Effects of endogenous flour lipids on the quality of semisweet biscuits. J Agric Food Chem: 51: 1057-1063

Pareyt, B., Finnie, S.M., Putseys, J.A., Delcour, J.A. 2011. Lipids in bread making: sources, interactions, and impact on bread quality. J Cereal Sci. 54: 266-279.

Paternotte, T.A., Orsel, R., and Hamer. R.J. 1994. Dynamic interfacial behaviour of gliadin-diacylgalactosylglycerol (MGDG) films: possible implications for gas-cell stability in wheat flour doughs. J Cereal Sci. 19: 123-129.

Pauly, A., Pareyt, B., Fierens, E., and Delcour, J.A. 2013. Wheat (*Triticum aestivum L.* and *T. turgidum L.* ssp. *Durum*) Kernel Hardness: I. current views on the role of puroindolines and polar lipids. Compr Rev Food Sci F. 12: 413-426.

Pickett, M. M . 2009. Study of gas cell stability during breadmaking using x-ray microtomography and dough rheology. M.S. Thesis. Kansas State University

Primo-Martin, C., Hamer, R.J., and H.J. de Jongh, H. 2006. Surface layer properties of dough liquor components: are they key parameters in gas retention in bread dough. Food Biophys. 1: 83-93.

Primo-Martin, C., van Nieuwenhuijzen, N.H., Hamer, R.J., and van Vliet, T. 2007. Crystallinity changes in wheat starch during the bread-making process: starch crystallinity in the bread crust. J Cereal Sci. 45: 219-226.

Pomeranz, Y. 1965. Polar vs. nonpolar wheat flour lipids in bread-making. Food Technol. 120-121.

Pomeranz, Y, Chung, O.K., and Robinson, R.J. 1966. The lipid composition of wheat flours varying widely in bread-making potentialities. J Am Oil Chem Society. 43: 45-48.

Pomeranz, Y. 1973. Interaction between glycolipids and wheat macromolecules in breadmaking. Page 153-188 in: Advances in Food Research Vol. 20. C.O. Chichester, ed. Academic Press, Inc.: New York.

Pomeranz, Y., Rubenthaler, G.L., Daftary, R.D., and Finney, K.F. 1966. Effects of lipids on bread baked from flour varying widely in bread-making potentialities. Food Technol. 20: 1225-1228

Pomeranz, Y., Shogren, M., and Finney, K.F. 1968. Functional bread-making properties of wheat flour lipids. 1. reconstitution studies and properties of defatted flours. Food Technol. 22: 324-327.

Ponte, Jr., J.G., and De Stefanis, V.A. 1969. Note on separation and baking properties of polar and nonpolar wheat flour lipids. Cereal Chem. 46: 325-329.

Ponte, Jr., J.G., and Baldwin, R.R. 1972. Studies on the lipid system of flour and dough. Bakers Dig. 46: 28-35.

Pyler, E.J., and Gorton, L.A. 2009. Baking Science & Technology, 4th Ed., Volume II: Formulation and Production: Sosland Publishing Co.: Kansas City.

Reusch, W. 2013. Lipids. http://www2.chemistry.msu.edu/faculty/reusch/VirtTxtJml/lipids.htm.

Sahi, S.S. 1994. Interfacial properties of the aqueous phases of wheat flour doughs. J Cereal Sci. 20: 119-127.

Salt, L.J., Wilde, P.J., George, D., Wellner, N., Skeggs, P.K., and Mills, E.N.C. 2006. Composition and surface properties of dough liquor. J Cereal Sci. 43: 284-292.

Salvador, A., Sanz, T., and Fiszman, S.M. 2006. Dynamic rheological characteristics of wheat-flour doughs. effect of adding NaCl, sucrose, and yeast. Food Hydrocolloid. 20: 780-786.

Salvo, L., Suéry, M., Marmottant, A., Limodin, N., Bernard, D. 2010. 3D imaging in material science: applications of x-ray tomography. CR Physique. 11: 641-649.

Schoch, T.J. 1965. Starch in bakery products. Bakers Dig. 39: 48-57.

Schofield, J.D. 1987. Flour protein: structure and functionality in baked products. Page 15 in: Chemistry and Physics of Baking. J.M.V. Blanshard, P.J. Frazier, and T. Galliard, eds. Royal Society of Chemistry: London.

Serna-Saldivar, S.O. 2010. Cereal Grains Properties, Processing, and Nutritional Attributes. Taylor & Francis Group, LLC.: Boca Raton.

Shah, P., Campbell, G.M., McKee, S.L., Rielly, C.D. 1998. Proving of bread dough: modeling the growth of individual bubbles. Food Bioprod Process. 76: 73-79.

Singh, H., and MacRitchie, F. 2001. Applications of polymer science properties of gluten. J Cereal Sci. 33: 231-243.

Singh, S., and Singh, N. 2013. Relationship of polymeric proteins and empirical dough rheology with dynamic rheology of dough and gluten from different wheat varieties. Food Hydrocolloid. 33: 342-248.

Skerritt, J.H., Hac, L., Bekes, F. 1999. Depolymerization of the glutenin macropolymers during dough mixing: I. changes in levels, molecular weight distribution, and overall composition. Cereal Chem. 76: 395-401.

Sliwinski, E.L., Kolster, P., and van Vliet, T. 2004a. Large deformation properties of wheat dough in uni- and biaxial extension. part I. flour dough. Rheol Acta. 43: 306-320.

Sliwinski, E.L., van der Hoef, F., Kolster, P., and van Vliet, T. 2004b. Large deformation properties of wheat dough in uni- and biaxial extension. part II. gluten dough. Rheol Acta. 43: 321-332.

Smith, J.R., Smith, T.L., Tschoegl, N.W. 1970. Rheological properties of wheat flour doughs. Rheol Acta. 9: 239-252.

Song, Y., and Zheng, Q. 2007. Dynamic rheological properties of wheat flour dough and proteins. Trends Food Sci Tech. 18: 132-138.

Sroan, B., Bean, S.R., and MacRitchie, F. 2009. Mechanism of gas cell stabilization in bread making. I. the primary gluten-starch matrix. J Cereal Sci. 49: 32-40.

Sroan B., and MacRitchie, F. 2009. Mechanism of gas cell stabilization in breadmaking. II. The secondary liquid lamellae. J Cereal Sci. 49: 41-46.

Stear, C.A. 1990. Handbook of Breadmaking Technology. Elsevier Science Publishers, LTD.: New York.

Sullivan, B. 1940. The function of the lipids in milling and baking. Cereal Chem. 17: 661- 668.

Sun, H., Yan, S., Jiang, W., Li, G., MacRitchie, F. 2010. Contribution of lipid to physicochemical properties and Mantou-making quality of wheat flour. Food Chem. 121: 332-337.

Takahashi, S. and Seib, P. 1988. Paste and gel properties of prime corn and wheat starches with and without native lipids. Cereal Chem. 65: 474-483.

Tang, M.C. and Copeland, L. 2007. Analysis of complexes between lipids and wheat starch. Carbohyd Polym. 67: 80-85.

Trinh, L., Lowe, T., Campbell, G.M., Withers, P.J., and Martin, P.J. 2013. Bread dough aeration dynamics during pressure step-change mixer: studies by x-ray tomography, dough density and population balancing modeling. Chem Eng Sci. 101: 470-471.

Tronsmo, K.M., Magnus, E.M., Baardseth, P., Schofield, J.D., Aamodt, A., and Faergestad, E.M. 2003. Comparison of small and large deformation rheological properties of wheat dough and gluten. Cereal Chem. 80: 587-595.

Turbin-Orger, A., Boller, E., Chaunier, L., Chiron, H., Della Valle, G., Réguerre, A.-L. 2012. Kinetics of bubble growth in wheat flour dough during proofing studied by computed x-ray micro-tomography. J Cereal Sci. 56: 676-683.

Upadhyay, R., Ghosal, D., Mehra, A. 2012. Characterization of bread dough: rheological properties and microstructure. J Food Eng. 109: 104-113.

Van Dyck, T., Verboven, P., Herremans, E., Defraeye, T., Van Campenhout, L., Wevers, M., Claes, J., Nicolaï, B. 2014. Characterisation of structural patterns in bread as evaluated by x-ray computer tomography. J Food Eng. 123: 67-77.

Van Vliet, T., Janssen, A.M., Bloksma, A.H., and Walstra, P. 1992. Strain hardening of dough as a requirement for gas retention. J Texture Stud. 23: 439-460.

Vlassenbroeck, J., Dierick, M., Masschaele, B., Cnudde, V., Van Hoorebeke, L., Jacobs, P. 2007. Software tools for quantification of x-ray microtomography at UGCT. Nucl Instrum Meth A. 580: 442-445.

Villarino, V.B., Jayasena, V., Coorey, R., Chakrabarti-Bell, S., and Johnson, S. 2014. The effects of bread-making process factors on Australian sweet lupin-wheat bread quality characteristics. Int J Food Sci Tech. 49: 2373-2381.

Wang, S., Austin, P., Bell, S. 2011. It's a maze: the pore structure of bread crumbs. J Cereal Sci. 54: 203-2010.

Watanabe, A., Yokomizo, K., and Eliasson, A-C. 2003. Effect of physical states of nonpolar lipids on rheology, ultracentrifugation, and microstructure of wheat flour dough. Cereal Chem. 80: 281-284.

Weipert, D. 1990. The benefits of basic rheometry in studying dough rheology. Cereal Chem. 67: 311-317.

Wilde, P.J., Clark, D.C., Marion, D. 1993. Influence of competitive adsorption of lysopalmitoylphosphotidylcholine on the functional properties of puroindoline, a lipid-binding protein isolated from wheat flour. J Agric Food Chem. 41: 1570-1576.

Whitworth, M.B., Cauvain, S. P., and Cliffe, D. 2005. Measurement of bread cell structure by image analysis. Pages 193-198 in Using Cereal Science and Technology for the Benefit of Consumers. S.P. Cauvain, S.S. Salmon, and L.S. Young, eds. CRC Press LLC: Boca Raton.

Xiao, S., Gao, W., Chen, Q-F., Chan, S-W., Zheng, S-X., Ma, J., Wang, W., Welti, R., and Chye, M-L. 2010. Overexpression of Arabidopsis Acyl-CoA binding protein ACBP3 promotes starvation-induced and age-dependent leaf senescence. The Plant Cell. 22: 1-20.

Yasui, T. 2012. Pleiotropic increases in free non-polar lipid, glycolipid and phospholipid contents in waxy bread wheat (*Triticum aestivum L.*) grain. J Sci Food Agric. 92: 2002-2007.

Zobel, H.F. 1988. Molecules to granules: a comprehensive starch review. Starch-Stärke. 40: 44-50.

Appendix A - Flour Mixographs

Figure 5.1 Mixograph curves for control flour

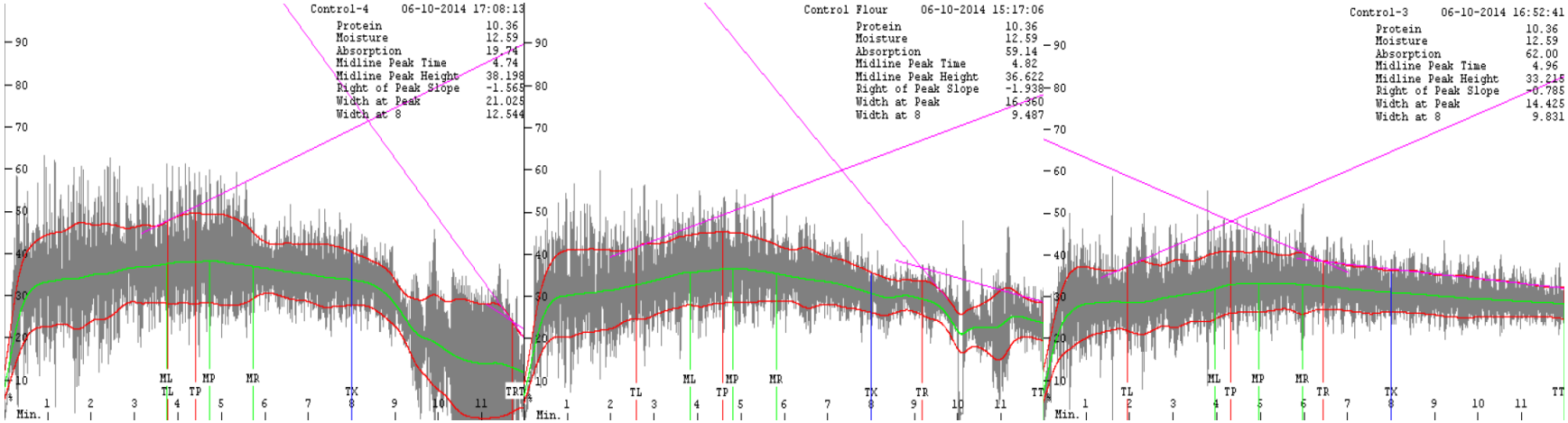

A. 58% Absorption B. 59% Absorption C. 62% Absorption

Figure 5.2 Mixograph curves for defatted flour

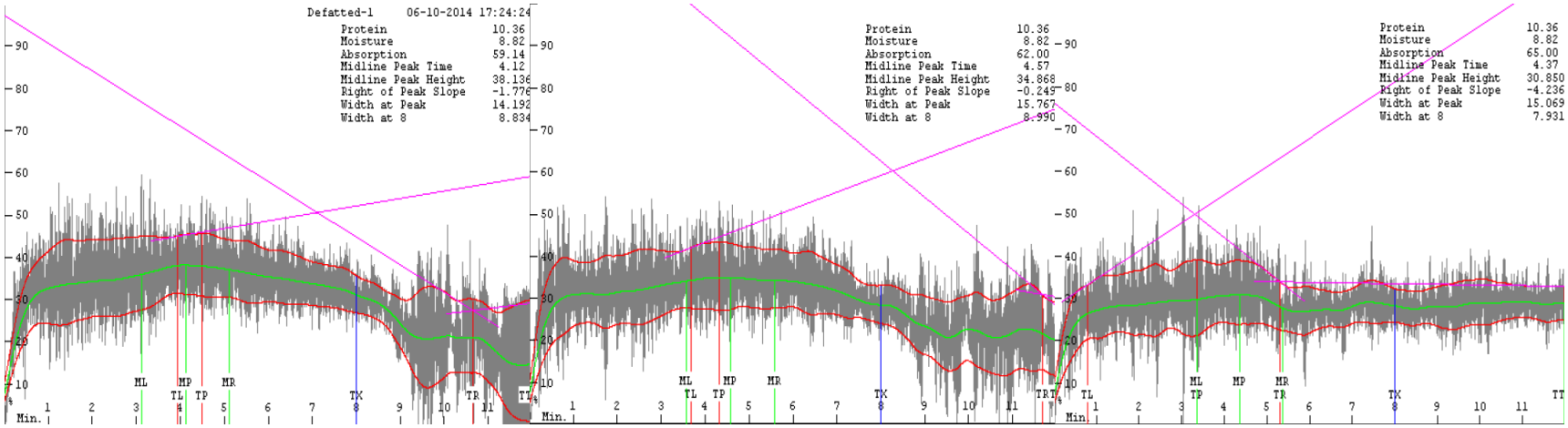

A. 59% Absorption B. 62% Absorption C. 65% Absorption

Appendix B - Compositional Analysis of Lipids in Control Flour

Table 5.1 Mean values for polar lipids found in control flour

Lipid Names	Polar Lipids (nmol/mg dry wt.)	Galactolipids (nmol/mg dry wt.)	Free Lipids (nmol/mg dry wt.)	Bound Lipids (nmol/mg dry wt.)	Total Lipids (nmol/mg dry wt.)
DGDG (34:6)	0.002	0.002	0.009	0.013	0.002
DGDG (34:5)	0.001	0.000	0.005	0.001	0.001
DGDG (34:4)	0.077	0.011	0.022	0.008	0.005
DGDG (34:3)	10.717	2.863	2.143	2.072	1.347
DGDG (34:2)	43.447	12.242	8.930	9.595	5.622
DGDG (34:1)	8.602	2.404	1.834	1.982	1.076
DGDG (36:6)	1.342	0.237	0.216	0.261	0.130
DGDG (36:5)	43.255	9.580	7.052	7.175	4.764
DGDG (36:4)	300.672	67.147	49.934	51.867	33.813
DGDG (36:3)	35.503	8.524	6.284	6.760	4.017
DGDG (36:2)	8.516	2.121	1.598	1.681	1.040
DGDG (36:1)	0.623	0.182	0.131	0.145	0.086
DGDG (38:6)	0.063	0.032	0.000	0.006	0.000
DGDG (38:5)	0.283	0.044	0.045	0.038	0.019
DGDG (38:4)	1.357	0.286	0.214	0.236	0.143
DGDG (38:3)	0.962	0.204	0.174	0.170	0.111
Total DGDG	**455.422**	**105.879**	**78.590**	**82.010**	**52.177**
MGDG (34:6)	0.000	0.000	0.024	0.009	0.000
MGDG (34:5)	0.019	0.000	0.010	0.007	0.006
MGDG (34:4)	0.225	0.003	0.018	0.007	0.013
MGDG (34:3)	4.906	0.081	0.527	0.245	0.312
MGDG (34:2)	15.407	0.291	1.584	0.803	0.936
MGDG (34:1)	2.629	0.041	0.260	0.152	0.175
MGDG (36:6)	1.750	0.006	0.190	0.123	0.112

MGDG (36:5)	70.489	1.101	7.158	3.531	4.182
MGDG (36:4)	627.146	10.436	64.354	32.385	37.622
MGDG (36:3)	66.259	1.162	7.315	3.556	4.281
MGDG (36:2)	6.076	0.099	0.622	0.335	0.362
MGDG (36:1)	0.428	0.001	0.049	0.034	0.044
MGDG (38:6)	0.012	0.000	0.000	0.011	0.035
MGDG (38:5)	0.205	0.005	0.005	0.019	0.036
MGDG (38:4)	0.861	0.000	0.086	0.044	0.036
MGDG (38:3)	0.859	0.001	0.076	0.045	0.047
Total MGDG	**797.269**	**13.227**	**82.276**	**41.305**	**48.198**
PG (32:1)	0.006	0.000	0.003	0.003	0.003
PG (32:0)	0.031	0.018	0.031	0.044	0.041
PG (34:4)	0.031	0.002	0.008	0.005	0.000
PG (34:3)	0.011	0.010	0.001	0.008	0.011
PG (34:2)	0.094	0.118	0.111	0.193	0.072
PG (34:1)	0.023	0.017	0.034	0.047	0.017
PG (34:0)	0.004	0.001	0.005	0.006	0.004
PG (36:6)	0.001	0.001	0.000	0.001	0.000
PG (36:5)	0.002	0.002	0.001	0.001	0.001
PG (36:4)	0.018	0.031	0.064	0.045	0.026
PG (36:3)	0.010	0.007	0.033	0.008	0.012
PG (36:2)	0.014	0.004	0.008	0.011	0.016
PG (36:1)	0.022	0.002	0.000	0.000	0.019
Total PG	**0.266**	**0.213**	**0.299**	**0.373**	**0.221**
LPG (16:1)	0.000	0.000	0.001	0.018	0.022
LPG (16:0)	0.253	0.005	0.113	0.179	0.021
LPG (18:3)	0.001	0.000	0.012	0.014	0.015
LPG (18:2)	0.237	0.054	0.203	0.217	0.059
LPG (18:1)	0.050	0.000	0.043	0.033	0.050
Total LPG	**0.541**	**0.059**	**0.371**	**0.462**	**0.167**
LPC (16:1)	0.001	0.000	0.003	0.011	0.002

LPC (16:0)	0.000	0.306	1.115	2.085	0.546
LPC (18:3)	0.000	0.014	0.032	0.111	0.018
LPC (18:2)	0.009	0.537	1.191	2.375	0.578
LPC (18:1)	0.000	0.075	0.210	0.409	0.116
LPC (18:0)	0.000	0.008	0.112	0.180	0.056
Total LPC	**0.010**	**0.938**	**2.663**	**5.171**	**1.316**
LPE (16:1)	0.000	0.000	0.000	0.000	0.000
LPE (16:0)	0.010	0.077	0.088	0.125	0.053
LPE (18:3)	0.000	0.001	0.000	0.008	0.002
LPE (18:2)	0.011	0.191	0.129	0.242	0.055
LPE (18:1)	0.000	0.023	0.025	0.033	0.014
Total LPE	**0.021**	**0.292**	**0.243**	**0.407**	**0.123**
PC (32:0)	0.000	0.126	0.214	0.189	0.126
PC (34:4)	0.000	0.001	0.007	0.011	0.005
PC (34:3)	0.000	0.331	0.296	0.306	0.178
PC (34:2)	0.015	6.784	6.294	5.165	3.598
PC (34:1)	0.000	1.477	1.564	1.427	0.981
PC (36:6)	0.000	0.010	0.014	0.029	0.012
PC (36:5)	0.000	0.606	0.416	0.455	0.256
PC (36:4)	0.103	7.149	5.535	4.785	3.273
PC (36:3)	0.016	3.479	2.653	2.531	1.574
PC (36:2)	0.000	0.892	0.832	0.716	0.493
PC (36:1)	0.000	0.056	0.130	0.105	0.066
PC (38:6)	0.000	0.000	0.003	0.015	0.001
PC (38:5)	0.000	0.000	0.009	0.011	0.002
PC (38:4)	0.000	0.005	0.035	0.028	0.013
PC (38:3)	0.000	0.051	0.090	0.082	0.051
PC (38:2)	0.025	0.021	0.033	0.121	0.024
PC (40:5)	0.000	0.000	0.006	0.007	0.001
PC (40:4)	0.000	0.000	0.001	0.002	0.000
PC (40:3)	0.000	0.000	0.005	0.004	0.002
PC (40:2)	0.000	0.016	0.017	0.016	0.009

Total PC	**0.158**	**21.007**	**18.156**	**16.003**	**10.663**
PE (32:3)	0.000	0.000	0.000	0.000	0.000
PE (32:2)	0.001	0.000	0.002	0.002	0.000
PE (32:1)	0.000	0.000	0.000	0.000	0.000
PE (32:0)	0.000	0.000	0.001	0.001	0.000
PE (34:4)	0.000	0.000	0.000	0.000	0.000
PE (34:3)	0.002	0.031	0.020	0.030	0.011
PE (34:2)	0.045	0.527	0.323	0.361	0.195
PE (34:1)	0.000	0.051	0.038	0.039	0.022
PE (36:6)	0.000	0.002	0.001	0.003	0.001
PE (36:5)	0.011	0.104	0.051	0.075	0.031
PE (36:4)	0.138	1.049	0.529	0.644	0.336
PE (36:3)	0.028	0.261	0.137	0.155	0.085
PE (36:2)	0.000	0.027	0.034	0.034	0.021
PE (36:1)	0.000	0.000	0.001	0.001	0.000
PE (38:6)	0.000	0.000	0.000	0.000	0.000
PE (38:5)	0.000	0.000	0.000	0.000	0.000
PE (38:4)	0.000	0.000	0.001	0.003	0.001
PE (38:3)	0.000	0.010	0.006	0.002	0.002
PE (40:3)	0.000	0.007	0.008	0.005	0.003
PE (40:2)	0.013	0.108	0.090	0.045	0.048
PE (42:4)	0.000	0.000	0.000	0.000	0.000
PE (42:3)	0.000	0.007	0.005	0.001	0.001
PE (42:2)	0.004	0.043	0.042	0.016	0.017
Total PE	**0.243**	**2.227**	**1.287**	**1.418**	**0.777**
PI (32:3)	0.000	0.000	0.000	0.000	0.000
PI (32:2)	0.003	0.000	0.002	0.002	0.000
PI (32:1)	0.027	0.001	0.002	0.004	0.000
PI (32:0)	0.006	0.000	0.039	0.008	0.009
PI (34:4)	0.001	0.000	0.001	0.000	0.000
PI (34:3)	0.014	0.005	0.041	0.112	0.015

PI (34:2)	0.169	0.110	0.404	1.437	0.153
PI (34:1)	0.154	0.028	0.056	0.151	0.012
PI (36:6)	0.001	0.000	0.001	0.000	0.003
PI (36:5)	0.002	0.002	0.034	0.047	0.010
PI (36:4)	0.044	0.026	0.242	0.358	0.089
PI (36:3)	0.019	0.009	0.120	0.145	0.039
PI (36:2)	0.029	0.000	0.052	0.054	0.008
PI (36:1)	0.015	0.003	0.002	0.002	0.001
Total PI	**0.485**	**0.185**	**0.996**	**2.321**	**0.340**
PS (34:4)	0.000	0.000	0.000	0.000	0.000
PS (34:3)	0.000	0.000	0.000	0.002	0.000
PS (34:2)	0.012	0.004	0.029	0.024	0.010
PS (34:1)	0.013	0.002	0.002	0.002	0.000
PS (36:6)	0.000	0.000	0.000	0.000	0.000
PS (36:5)	0.000	0.000	0.001	0.001	0.001
PS (36:4)	0.005	0.007	0.016	0.014	0.009
PS (36:3)	0.003	0.002	0.002	0.004	0.002
PS (36:2)	0.000	0.000	0.008	0.006	0.004
PS (36:1)	0.002	0.000	0.000	0.000	0.002
PS (38:6)	0.000	0.000	0.000	0.000	0.001
PS (38:5)	0.000	0.000	0.001	0.000	0.000
PS (38:4)	0.002	0.000	0.003	0.001	0.000
PS (38:3)	0.000	0.000	0.001	0.002	0.001
PS (38:2)	0.003	0.003	0.009	0.010	0.003
PS (38:1)	0.000	0.000	0.000	0.000	0.000
PS (40:4)	0.000	0.000	0.000	0.000	0.000
PS (40:3)	0.000	0.001	0.004	0.007	0.002
PS (40:2)	0.016	0.010	0.037	0.041	0.013
PS (40:1)	0.010	0.010	0.000	0.002	0.007
PS (42:4)	0.000	0.000	0.000	0.000	0.001
PS (42:3)	0.002	0.000	0.009	0.002	0.003
PS (42:2)	0.014	0.001	0.086	0.013	0.028
PS (42:1)	0.005	0.001	0.034	0.002	0.006

PS (44:3)	0.005	0.000	0.087	0.001	0.016
PS (44:2)	0.001	0.000	0.031	0.001	0.008
Total PS	**0.094**	**0.040**	**0.361**	**0.137**	**0.118**
PA (32:0)	0.003	0.000	0.010	0.008	0.006
PA (34:6)	0.001	0.000	0.000	0.000	0.000
PA (34:5)	0.000	0.000	0.000	0.000	0.000
PA (34:4)	0.000	0.000	0.000	0.000	0.000
PA (34:3)	0.022	0.000	0.058	0.057	0.026
PA (34:2)	0.306	0.034	0.681	0.704	0.359
PA (34:1)	0.068	0.001	0.128	0.118	0.070
PA (36:6)	0.001	0.001	0.002	0.003	0.002
PA (36:5)	0.050	0.001	0.103	0.117	0.052
PA (36:4)	0.450	0.084	0.841	0.933	0.443
PA (36:3)	0.154	0.019	0.301	0.305	0.163
PA (36:2)	0.033	0.005	0.077	0.074	0.046
Total PA	**1.089**	**0.145**	**2.201**	**2.319**	**1.169**
Total Polar Lipids	**1255.597**	**144.214**	**187.442**	**151.925**	**115.269**

[a]Monogalactosyldiglyceride (MGDG), digalactosyldiglyceride (DGDG), phosphatidylglycerols (PG), Lysophosphatidylglycerols (LPG), Lysophosphatidylcholines (LPC), Lysophosphatidylethanolamines (LPE), phosphatidylcholines (PC), phosphatidylethanolamines (PE), phosphatidylinositols (PI), phosphatidylserines (PS), and phosphatidic acid (PA)
[b] n=25